Ion-selective electrodes and optodes as tools for trace analysis of ions in environmentally and biologically important samples.

Lukasz Mendecki

Thesis submitted in partial fulfilment of the requirements of

Keele University

for the degree of Doctor of Philosophy

October 2016

Keele University

_____

SUBMISSION OF THESIS FOR A RESEARCH DEGREE

Part I. DECLARATION by the candidate for a research degree. To be bound in the thesis

Degree for which thesis being submitted   Doctor of Philosophy

Title of thesis   Ion-selective electrodes and optodes as tools for trace analysis of ions in environmentally and biologically important samples.

This thesis contains confidential information and is subject to the protocol set down for the submission and examination of such a thesis.

NO [please delete as appropriate; if YES the box in Declaration Part II should be completed]

Date of submission   07/07/2016   Original registration date   30/09/2013
(Date of submission must comply with Regulation 2D)

Name of candidate   Lukasz Mendecki

Research Institute Faculty of Natural Sciences   Name of Lead Supervisor Dr Aleksandar Radu

I certify that:

(a) The thesis being submitted for examination is my own account of my own research

(b) My research has been conducted ethically. Where relevant a letter from the approving body confirming that ethical approval has been given has been bound in the thesis as an Annex

(c) The data and results presented are the genuine data and results actually obtained by me during the conduct of the research

(d) Where I have drawn on the work, ideas and results of others this has been appropriately acknowledged in the thesis

(e) Where any collaboration has taken place with one or more other researchers, I have included within an 'Acknowledgments' section in the thesis a clear statement of their contributions, in line with the relevant statement in the Code of Practice (see Note overleaf).

(f) The greater portion of the work described in the thesis has been undertaken subsequent to my registration for the higher degree for which I am submitting for examination

(g) Where part of the work described in the thesis has previously been incorporated in another thesis submitted by me for a higher degree (if any), this has been identified and acknowledged in the thesis

(h) The thesis submitted is within the required word limit as specified in the Regulations

Total words in submitted thesis (including text and footnotes, but excluding references and appendices) 46056

Signature of candidate…………………………………   Date …………………

Note
Extract from Code of Practice: **If the research degree is set within a broader programme of work involving a group of investigators – particularly if this programme of work predates the candidate's registration – the candidate should provide an explicit statement (in an 'Acknowledgments' section) of the respective roles of the candidate and these other individuals in relevant aspects of the work reported in the thesis. For example, it should make clear, where relevant, the candidate's role in designing the study, developing data collection instruments, collecting primary data, analysing such data, and formulating conclusions from the analysis. Others involved in these aspects of the research should be named, and their contributions relative to that of the candidate should be specified (*this does not apply to the ordinary supervision, only if the supervisor or supervisory team has had greater than usual involvement*).**

_____

Abstract

Over the past decade, analytical chemists have been faced with a significant task to develop techniques and methodologies that are fully applicable to real-time sample analysis while significantly lowering per-sample and per-measurement costs. Such advancements are expected to make a great impact in many different fields ranging from environmental analysis to the health, security, and manufacturing industries.

Ion selective electrodes (ISEs) are a class of chemical sensors that in recent years went through a renaissance and showed excellent potential as tools for routine environmental monitoring and clinical analysis. They are cheap to manufacture, show excellent selectivity and sensitivity, are easily miniaturised and can be connected to simple communication devices. However, due to several limitations such as presence of transmembrane ion fluxes or plasticiser exudation, their full potential has not yet been utilised. This calls for improvements in materials and methodologies used for the preparation of ISEs.

Herein, significant improvements in lower detection limits of carbonate ISEs were achieved by conditioning the electrodes in the ionophore solution thus minimising/eliminating membrane ion fluxes. In addition, it was demonstrated that selectivity of ISEs can be enhanced by replacing traditional plasticisers with alternative materials such as ionic liquids (ILs). To further utilise the potential of ILs in ion sensing, 1,2,3-triazole based IL was covalently attached to the polymer backbone yielding a one component ISE. The inherent presence of iodide in the polymeric membrane reduced the need for conditioning thus allowing for direct determination of iodide in human urine samples. Similar approaches were undertaken to develop self-plasticised aluminium optical

sensors in which an initially water-soluble fluorophore was copolymerised with methacrylate-based monomer. This prevented its diffusion from the membrane into the aqueous phase. Low detection limit, high selectivity and the possibility of miniaturisation makes them potential candidates for developing aluminium sensors for clinical analysis.

This research demonstrates that by improving sensing methodologies as well as using novel materials for the preparation of ISEs and optical sensors, functional devices with excellent robustness, durability and reproducibility can be produced thus indicating yet unexplored avenues for further developments in sensing.

Acknowledgements

I am most grateful to my supervisor, Dr Aleksandar Radu, for his guidance, patience and support throughout the time of my doctoral research and most importantly for creating this amazing opportunity and trusting me with his research ideas. You have set an example of excellence as a researcher, mentor, instructor, and role model. Thank you for everything, as I would not be the same person as I am now without you.

I would also like to thank my second supervisor Dr Sergio Granados-Focil for his advice, expertise and moreover for having many fruitful and interesting conversations at Peppercorns. I would always have great memories associated with Clark.

Moreover, I would love to express my appreciation to all people from Keele University, Clark University and UCF who always helped and supported me throughout this amazing journey. A special thanks goes to Mike, Matt, Lena, Sean, Krista and Phil for their great friendship, constant and unlimited support and for helping me to stay sane. I could not have asked for more than what I got from you.

To my family, thank you for encouraging me in all of my pursuits and inspiring me to follow my dreams. I am especially grateful to my parents, who always believed in me and wanted the best for me, to my sister for always showing me where my place is and to my beloved girlfriend for always being there for me. I am also thankful to my grandma and Zuzia for providing a loving environment for me. I could not complete this journey without your support.

Papers directly resulting from the Doctoral Thesis:

[1]   Mendecki, L.; Fayose, T.; Stockmal, K. A.; Wei, J.; Granados-Focil, S.; McGraw, C. M.; Radu, A. *Anal. Chem.* **2015**, *87* (15), 7515–7518. - Robust and ultrasensitive polymer membrane-based carbonate-selective electrodes.

[2]   Mendecki, L.; Chen, X.; Callan, N.; Thompson, D. F.; Schazmann, B.; Granados-Focil, S.; Radu, A. *Anal. Chem.* **2016**, *88* (8), 4311–4317. - Simple, robust, and plasticizer-free iodide-selective sensor based on copolymerized triazole based ionic liquid.

[3]   Mendecki, L.; Callan, N.; Ahern, M.; Schazmann, B.; Radu, A. *Sensors.* **(In peer review) -** Influence of ionic liquids on the selectivity of ion exchange-based polymer membrane sensing layers.

[4]   Mendecki, L.; Granados-Focil, S.; Radu, A. *Anal. Chem.* **(In peer review) -** Lumogallion-based fluorescent sensor for aluminum (III) with ultra-low detection limits.

Papers indirectly resulting from the Doctoral Thesis:

[5]   Rich, M.; Mensah, S.T; Blanco-Martinez, E.; Calvo-Marzal, P.; Mendecki, L.; Radu, A.; Chumbimuni-Torres, K.Y. *Anal. Chem.* **(In peer review) -** Circumventing traditional conditioning protocols in polymer membrane-based ion-selective electrodes.

Patents

[1]   Sergio Granados-Focil, Aleksandar Radu, **Lukasz Mendecki**; US Patent No 62/319,895; Filing date 8th April 2016, ref#: CLK16-01P

VI

VII

VIII

List of Figures

List of Tables

List of Schemes

CHAPTER 1   An introduction to ion selective electrodes and optical sensors and their methods of characterisation.

1.1   Sensing devices and their modes of operation

The importance of sensors in life is unequivocal as they allow the perception of outside stimuli. Humans possess a multitude of senses with the senses of hearing, sight, smell, taste and touch are the most widely recognised. Each sense has its own function and helps people to perceive the world around them by obtaining both chemical and physical information about the surrounding environment. The same principles have been implemented during the design of 'physical' sensors. This gave rise to a large variety of sensors that can be used to measure the physical properties of an object such as temperature, pressure or electrical conductivity. This later stimulated the development of chemical sensors.[1] According to The International Union of Pure and Applied Chemistry (IUPAC) a chemical sensor is "A device that transforms chemical information, ranging from the concentration of a specific sample component to total composition analysis, into a useful analytical signal".[1]

The process of chemical sensing can be divided into three distinctive sections such as selective recognition, reversible signal transduction and transmission of the generated signal in the form of an electrical signal.[2] The schematic model of the sensing process is illustrated in Figure 1.1. Furthermore, chemical sensors can be categorised into five major groups (depending on the signal transduction): thermal, mechanical, magnetic, optical and electrical sensors.[3] The latter are by far the most studied types of chemical sensors.
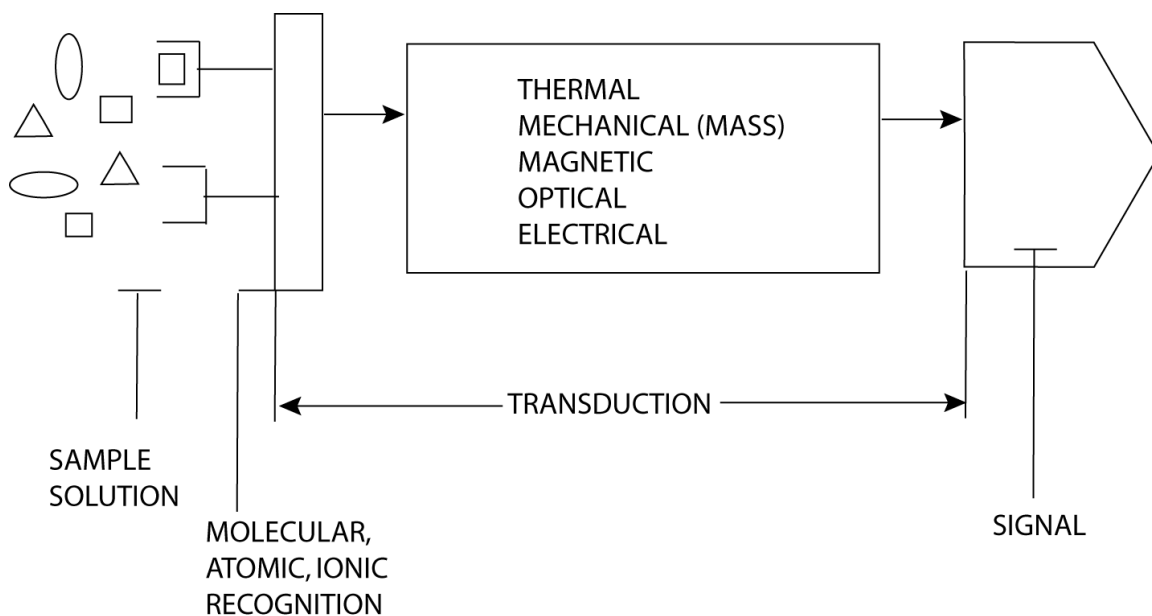
Figure 1.1 A schematic model showing the functioning of a chemical sensor.

Ionophore based sensor (IBS) is a well-studied class of chemical sensors that can exhibit either the electrochemical or optical transduction mechanism. The former group is often referred to as ion-selective electrodes (ISEs) while the latter as optical sensors or 'optodes'.

1.2 Ion selective electrodes

Ion selective electrodes are types of sensors that have been widely used in the field of chemical sensing as they offer a simple and convenient way of measuring changes in the activity of one or several ions in the investigated liquid or gas sample.[4] Any changes in the activity of ions are followed by a simultaneous change in the electrical potential that can be later recorded by a voltmeter. Schematic representation of an ISE measuring-cell assembly is demonstrated in Figure 1.2.
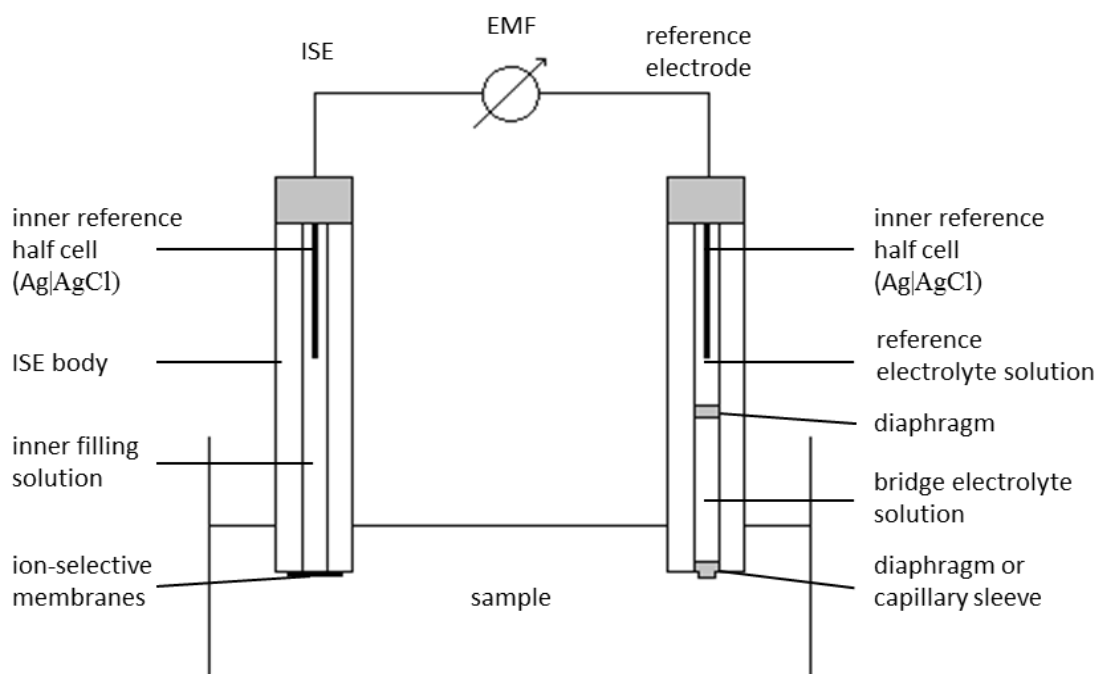
Ag | AgCl | KCl 1M | bridge electrolyte | sample ‖ membrane ‖ inner filling solution | AgCl

Figure 1.2 Schematic representation of the experimental setup in a conventional ion selective electrode measurement.

The history of ion selective electrodes can be traced back to the pioneering work carried out by Max Cremer in 1906.[5] He determined that the difference in the activity of hydrogen ions (H^+) between two solutions that are separated by a glass membrane can give rise to a membrane potential that is also known as an electromotive force (EMF). This relationship

was later explained by the Walther H Nernst. His findings indicated that at room temperature a 10 fold increase in the activity of measured ions is followed by an increase in the EMF of 59.2 mV/z_i.[6] This is illustrated by the following equation:

$$EMF = E° + \frac{2.303\ RT}{z_i F} \log a_i \qquad (1.1)$$

EMF corresponds to the electrical potential developed between the working and reference electrodes, $E°$ is a cell potential under standard conditions (273.15 K and 100 kPa), a_i is the activity of primary ions, z_i is the ionic charge of the ion i, F, R, T are the Faraday constant, the absolute temperature and the universal gas constant, respectively.

However, it was not until 1930s that the first glass pH electrode was manufactured.[7] This not only revolutionised the field of chemical sensing but also attracted more attention towards the development of ion selective electrodes. After the successful launch of the pH sensitive probes another class of ISEs was introduced to the chemical industry. The glass membranes that were treated as key elements of the ISEs were replaced with the crystalline compounds such as AgCl, Ag_2S or LaF_3. This gave rise to the first probes capable of measuring the concentration of fluoride and halide ions.[8] However, these ISEs only exhibit a good selectivity towards the ions that can penetrate and move between defect vacancies in the crystal lattice.[9] Therefore, the selectivity of membranes containing the crystalline materials remained rather limited. Furthermore, the ISEs with crystalline materials display large ionic resistance and therefore they may require further doping in order to increase

their conductivity. Fluoride selective electrodes are usually doped with europium (II) fluoride (EuF_2) to improve the response of the membrane by making it more conductive to the fluoride ions.[10]

The real breakthrough in the field of ion selective electrodes came with the discovery of the ionophore-based membranes.[11] An ionophore is better known as a chemical compound that binds and mediates transport of ions across the biological membranes.[12] Early days research carried out by Simon and Stefanac (1966) illustrated that certain antibiotics when used as doping agents can significantly enhance the transport of monovalent cations between the water-immiscible organic liquids.[13] These properties were later exploited during the design of ISEs containing an antibiotic e.g. valinomycin as an ion carrier. These electrodes exhibited high selectivity towards the potassium ions (K^+), therefore, allowing its measurements in various biological samples including blood and urine samples.[14] However, a more in-depth discussion on the role of ionophore in ISEs is given in Chapter 1 – Ionophore.

Previous studies identified that the performance of ISEs is mainly governed by the internal composition of a sensing membrane. Arguably, one of the most successful types of ISEs are polymer based membrane electrodes. Their main components include a polymer, a plasticiser, an ion exchanger and an ion carrier.[11] Each constituent plays a specific role in proper functioning of the membrane based ISEs. This is discussed in more details below:

1.2.1 Polymeric matrix

The main function of a polymeric matrix is to provide good mechanical stability to the membrane (resistance to the external pressure). The matrix also must be capable of dissolving all components of the membrane and ideally it should not contain any functional groups that may potentially interfere or reduce binding of ions of interest with the ionophore.[15] Poly(vinyl chloride) (PVC) is a common polymer used in the polymeric ion selective membranes.[16] However, due to inherently high rigidity of PVC, the addition of plasticiser is required to yield a more flexible and mechanically stable polymer (Chapter 1 – Plasticiser). Even though, PVC based membranes has been used in the field of ISEs for over 40 years, there are many issues associated with their use such as leaching of the plasticisers from the polymeric matrix.[17] In particular, ion selective field effect transistors (ISFETs) based on the PVC-plasticiser matrix suffered from very poor adhesion to the gate oxide layer thus shortening the lifetime of such devices.[18] Several alternative polymers has been already reported in the literature, however, many of them were rendered unsuitable for practical applications due to their incompatibility with the plasticisers that have been traditionally used for membrane preparation.[19,20]

This has sparked wide research interest in the synthesis of novel polymers that would demonstrate the appropriate functionality (response time, selectivity and sensitivity) without the need to add any external solvent mediators. Numerous plasticiser-free polymers such as polyurethanes,[21] polysiloxanes,[22] polythiophenes,[23] silicone rubber,[24] epoxyacrylates,[25] polyacrylates[26] and methacrylic-acrylic copolymers[27] have been synthesised and used as components for the preparation of ISEs with the latter being particularly attractive candidates as their physical and mechanical properties can be

selectively modified by simply choosing either different combinations of monomers or polymerisation routes or both.[27] Although, acrylic polymers can be used as substituents to the PVC based membranes, it is important to emphasise that such polymers also suffer from inherent disadvantages such as increased susceptibility to acid and base hydrolysis, poor tensile strength and increased tacticity.[19,20] Such characteristics often define the applicability of a sensor based on the acrylic polymeric architectures. Recently, the first use of sensing membranes based on methacrylic-acrylic polymer has been reported and the response characteristics of such membranes were evaluated in terms of their selectivity towards numerous cations and anions (cations: Mg^{2+}, Ca^{2+}, Na^+, Li^+, K^+; anions: ClO_4^-, NO_3^-, SCN^-).[28] Ionophore free membranes based on the methacrylic-acrylic copolymers displayed enhanced selectivity towards sodium ions over traditionally prepared ISEs (PVC plasticised with DOS or NPOE). The application of methacrylate based matrices was later significantly expanded to develop numerous potentiometric sensors, to create ion selective optodes and to be used solely as ion-exchanging membranes.[29–34] Modifications in physico-chemical properties of such copolymers also gave rise to a large group of ion selective membranes with reduced rate of trans-membrane ion diffusion, therefore suppressing ion fluxes and improving lower limits of detection.[29,33,35] This is discussed in more detail in Chapter 2.

The main characteristic that defines the functionality of methacrylic-acrylic polymers is their glass transition temperature as any variations in this parameter will directly influence mechanical properties of resulting polymers.[27,36] The glass transition temperature of copolymers can be estimated using the Flory-Fox equation (eq. 1.2) therefore allowing the

chemist to modulate physio-chemical characteristics of resultant polymers according to the research needs.[27]

$$\frac{1}{T_{g(Co)}} = \frac{w_1}{T_{g1}} + \frac{w_2}{T_{g2}} \qquad (1.2)$$

The parameter $T_{g(Co)}$ represents the glass transition temperature of the resultant copolymer; w_1 and w_2 are the weight fractions of first and second monomer respectively and T_{g1} and T_{g2} correspond to the glass transition temperature of homopolymers made from the monomer 1 and 2.

For the purpose of preparing ion selective membranes, it has been recommended to use polymers with a glass transition temperature lying within the range of -10°C to 10°C as such membranes often offer optimal mechanical properties.[37] For instance homopolymerised methyl methacrylate (PMMA, T_g = 105 °C) has been implemented as ISEs solid support but due to plasticiser incompatibility such membranes were rendered unsuitable for sensing purposes.[28] Similar observations were made for poly lauryl methacrylate (PLM, T_g = -65°C) where appropriate functionality could only be achieved with the addition of a plasticiser. However, such membranes still exhibited low mechanical stability and would not offer any advantages over the traditionally used polymers. As aforementioned, the individual homopolymers are often not suitable for making ion selective membranes, however a copolymer made of methyl methacrylate (MMA) and decyl methacrylate (DMA) or MMA and lauryl methacrylate (LMA) can be successfully

8

utilised as polymeric support.[33] LMA serves the function of internal plasticiser thus lowering the glass transition temperature of the polymer whereas the presence of methyl methacrylate improves the film-forming properties. Such copolymers are typically synthesised using free radical polymerisation (FRP) as this process is relatively immune to any impurities and can be carried out in bulk, emulsion, suspension or solution.[38]

Another major advantage of using copolymers as polymeric architecture is the lack of impurities that are often found in PVC. It is well established that the plasticised PVC membranes may contain inherently low concentrations of ionic sites (up to 6.0×10^{-5} mol L^{-1})[39] that have originated from the manufacturing process. These impurities are responsible for a small ionic conductivity of the membrane. It was even reported that the inherently present impurities can cause a cationic response even in the absence of ionophore or other added salts.[40] The overall ionic conductivity of plasticised PVC membranes is described by the following equation:

$$\sigma = \sum z_i e \, c_i \mu_i \qquad (1.3)$$

where $z_i e$ is the charge of species i, c_i is its volume concentration and μ_i represents ion mobility.

However, the ion selective membranes based on methacrylic-acrylic copolymers that do not contain ionophore and ionic sites (non-doped membranes) often display a very erratic

signal during potentiometric measurements and no response towards sample ions.[27–29] Since the response characteristics of ISEs will also vary with the glass transition temperature (harder membranes usually demonstrate lower diffusion coefficients), a range of polymers with varying transition temperatures are usually prepared and the resultant ion selective membranes are then analysed to find optimum composition for ion sensing purposes.[27,29]

In order to establish the percentage composition of the formed copolymer the peak intensity of a proton that is characteristic to a particular monomer unit is measured using nuclear magnetic resonance spectroscopy (NMR).[27,41] These parameters are later inserted in the following equation and the resultant monomer feed rations can be calculated.

$$F_A = \frac{\frac{1}{n}I(-CH_n)_A}{\frac{1}{n}I(-CH_n)_A + \frac{1}{n}I(-CH_n)_B} \qquad (1.4)$$

where F_A represents the mole fraction of monomer A in the resulting copolymer, n is number of protons within the specified functional group used for the calculations for example $-CH_n$, I is the peak intensity, and A and B correspond to polymer A and polymer B in the copolymer, respectively. The same equation can be used to determine composition of copolymers with more than two repeating units. For that purpose another $\frac{1}{n}(-CH_n)_X$ units need to be added in the denominator.

1.2.2 Plasticisers

Plasticisers are another important components used for the preparation of ion selective membranes. A plasticiser is usually added to the membrane in order to reduce the polymer glass transition temperature to below the ambient temperature. This changes the hard brittle polymer into softer and more flexible elastomer.[42] The addition of plasticiser strongly influences the physical and mechanical properties of the sensing membrane. Traditionally prepared plasticised PVC membranes contain approximately 100 to 200 parts per hundred resin (phr) of a plasticiser that corresponds to about 51% - 67% weight percent (% wt). Recently, it has been reported that membranes that contain less plasticiser retain their functionality and may even exhibit improved detection limits.[43] The presence of plasticisers also aids to dissolve other components of ISEs to produce a homogenous matrix.

Aside these functions, plasticisers used for the preparation of ion selective membranes can directly influence the chemical properties of ISEs (see Chapter 3). This is mainly caused by the differences in the polarity and therefore the dielectric constant values among various plasticisers, which have a direct influence on the ion-exchanging properties.[44] For instance, the dielectric constant of PVC ranges from 3 to 6 but when mixed with a suitable plasticiser it can significantly increase (Chapter 3). Similarly to the polymer, it is also desirable that the plasticiser does not interact with the targeted analyte for instance via complex formation. Some common types of plasticisers include bis(2-ethylhexyl) sebacate (DOS - A) or 2-nitrophenyl octyl ether (NPOE - B) as well as adipates and phthalates (Figure 1.3).
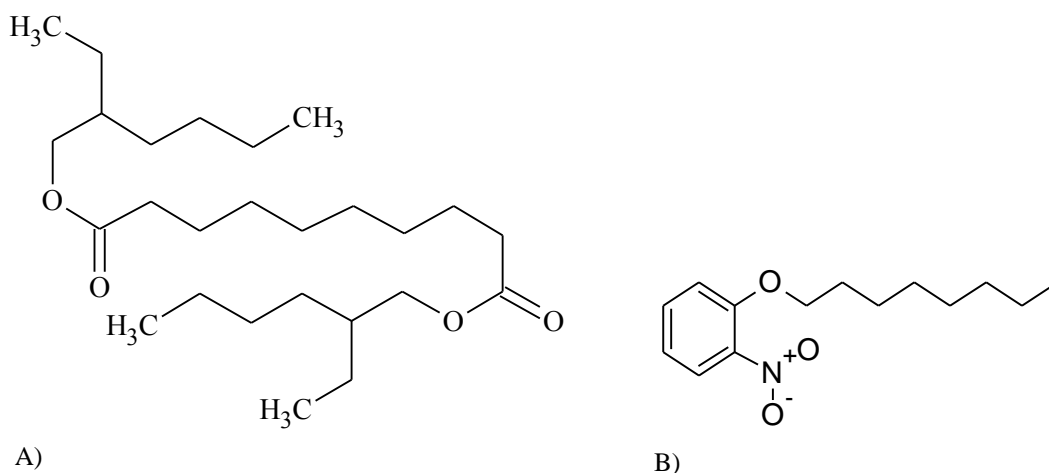
Figure 1.3 Structures of the two plasticisers DOS (Figure 1.3 A) and NPOE (Figure 1.3 B) that are commonly used as matrix solvents for ion sensing membranes.

It has been also reported that over time plasticisers have a tendency to evaporate, leach, migrate from the polymer matrix or undergo degradation. Leaching of the plasticiser especially from the PVC based membranes has a direct effect on the physio-chemical properties of sensing devices such as ISEs. This is expected to reduce the solubility of active components (ionophore and ionic sites) in the membrane bulk therefore resulting in an overall decrease in the selectivity and sensitivity of tested ISEs. Exudation of plasticiser also permanently reduces the lifetime of a sensor and may lead to very unstable responses and sample perturbations.[45] In the field of clinical analysis (*in vivo* measurements) such outcomes are even more harmful as it can stimulate a serious inflammatory response in the human body. For instance, phthalates, their metabolites and degradation products have been identified as potential endocrine disruptors.[46]

Recently, a new class of chemical compounds – ionic liquids (IL) has attracted rising interest due to their diversified range of applications (Figure 1.4).
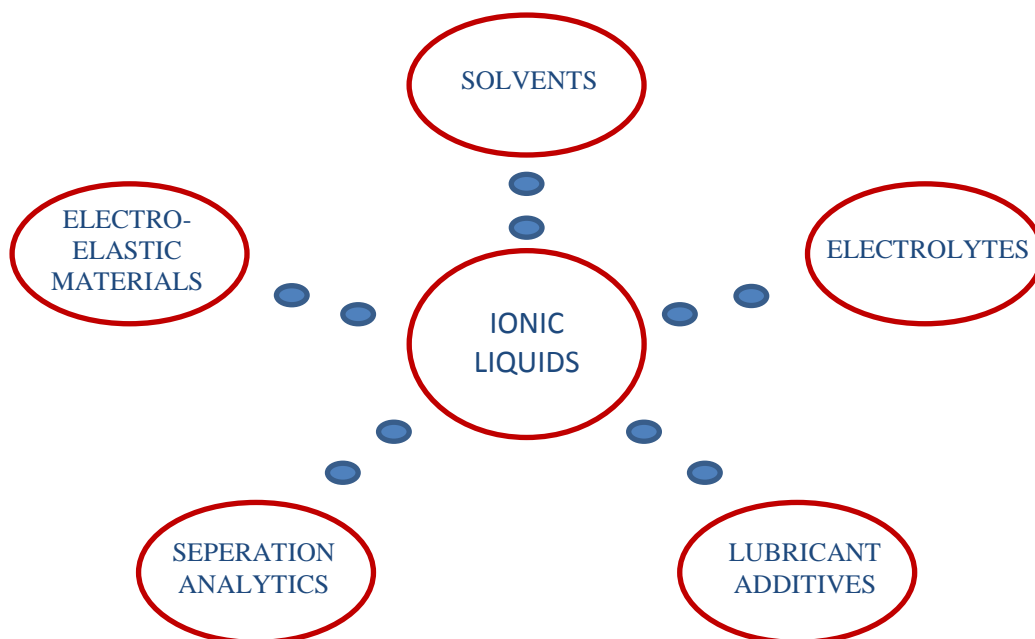
Figure 1.4 Potential applications of ILs

Figure 1.4 demonstrates that ILs possess a unique set of properties that make them viable candidates as materials for the preparation of ion selective membranes.[47] Moreover, by fine-tuning the structure, their physico-chemical properties can be tailor-designed to satisfy the specific application requirements. Their nature and characteristics along with the effects they induce on the properties of ISEs will be discussed in more details in Chapter 3. Since the plasticisers make up the largest component by weight of polymer based ion selective electrodes, it is crucial to enhance its stability/durability within the sensing membrane.

1.2.3 Lipophilic ion

One of the major roles of lipophilic ionic sites is to provide ion exchanging properties to the membrane. A lipophilic ionic exchanger is composed of a bulky lipophilic ion that due to its high energy of solvation is preferentially retained in the polymeric membrane and its

counter-ion that undergoes ion exchange with the ion of interest from the solution. For cation selective membrane, this process is demonstrated by the following equation:

$$A^+_{org}R^-_{org} + I^+_{aq} \rightarrow I^+_{org}R^-_{org} + A^+_{aq} \qquad (1.5)$$
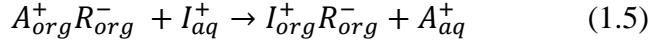
Partitioning of primary ion (I^+_{aq}) from aqueous solution into the membrane bulk results in its exchange with A^+_{org}. Whereas, anion R^-_{org} remains in the membrane thus rendering the membrane permselective while preserving the charge balance.

Sensing membranes that are doped with the lipophilic sites (ion exchangers) ensure proper functioning of the ISEs by maintaining the concentration of primary ions within the membrane at higher levels than the concentration of co-extracted ions.[48] It is also well known that the addition of known amount of lipophilic salts greatly enhances the selectivity, stability, reproducibility and response time of ISEs.

The most common types of lipophilic ions encountered in the literature are tetraalkyl ammonium salts for the anion-selective membranes and the derivatives of tetraphenyl borate for cation-selective ISEs.[6] It is noteworthy that some ionic sites are inherently present in the sensing membrane, as impurities coming from the polymer.[39] Although, ionic sites-free PVC based membranes can produce a potentiometric response, the concentration of these 'impurities' cannot be controlled and depends on the purification process during the synthesis of PVC polymers. Moreover, the ionic sites that are used in

ion selective membranes should exhibit high degree of lipophilicity to reduce or eliminate their mass diffusion in the direction of the sample. This process, if occurs, is known to cause severe deterioration of the electrode response eventually leading to complete loss of sensor functionality. Leaching of ion exchange sites have been also reported to have a direct influence on the response characteristics of ISEs for example its detection limits.[49] As the mass transport of ionic sites from the sensing layer takes place, the corresponding outward diffusion of primary ions is initiated in order to fulfil the electroneutrality requirement within the membrane bulk. This results in higher activity of analyte ions at the phase boundary and consequently will lead to worsening of lower detection limits. However, Bakker and Pretsch (1995) demonstrated that the presence of the ionophore may significantly reduce the rate of leaching of ion exchange sites due to ion-ionophore complex formation.[50]

To increase the overall hydrophobicity of ionic sites, alkylated or halogenated derivatives of tetraphenylborate salts such as tetra(p-tolyl)borates, tetrakis(4-chlorophenyl)borates, tetrakis(4-tert-butylphenyl)borates or tetrakis[3,5-bis(trifluoromethyl)phenyl]borates (TFPB) have been routinely used. Furthermore, these compounds demonstrate improved stability towards acid hydrolysis.[51] Even though, tetraphenylborate salts have found a widespread application in ISEs, the overall robustness of sensing devices based on the presence of this ion exchanger can be compromised as tetraphenylborates were reported to suffer from insufficient lipophilicity that led to severe leaching. They were also identified to be susceptible to oxidation and photodegradation.[52]

Recently, carboranes have been suggested as alternative materials to tetraphenylborate salts for the preparation of ISEs. The undecaiodinated and undecabrominated derivatives of carba-closo-dode-caborates exhibited improved selectivity and chemical stability over the TFPB ionic sites.[51] Despite the improvements in the performance of ISEs based on the presence of carboranes, their lack of commercial availability creates a significant obstacle to their widespread use. Another methodology that aims to reduce ionic sites leaching and to improve the lifetime and robustness of ISEs involves covalent attachment of the modified ion exchange sites to the polymer backbone. Several sensing membranes based on the presence of carboranes, tetraphenylborates and sulfonate methacrylic and acrylic derivatives have been already reported.[52–57] Such sensing devices demonstrated good response characteristics (Nernstian or near-Nernstian behaviour), adequate detection limits and required selectivity.

1.2.4 Ionophore

Polymer based ISEs that are only loaded with lipophilic ionic sites can exhibit Nernstian behaviour if exposed to sample ions where the selectivity will be defined by the lipophilicity of the ions found in the sample. However, the presence of ionophore (also referred as ion ligand or an ion carrier) has the main effect on the sensing properties of ISEs as it can define selectivity for a particular ion while omitting the relative lipophilicity of that ion.[58] The ionophore should ideally form reversible complexes with the targeted analyte as well as exhibit high selectivity towards the targeted ion in the presence of other interfering ions found in the sample.[59] Furthermore, the complex formation constant must be large enough to ensure that the primary ions are predominantly found in their complexed form within the membrane bulk. The complex formation constant can be derived from the equation (1.6)

$$i^z + nL \rightarrow iL_n^z \qquad (1.6)$$
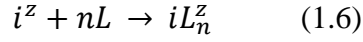
The parameter i refers to the ion of interest with the charge z, L is the ionophore, n corresponds to the stoichiometric complexing coefficient and iL_n^z describes the ion-ligand complex. Therefore, the complex formation constant (β_{iL_n}) can be defined as:

$$\beta_{iL_n} = \frac{[iL_n^z]}{[i^z][L]^n} \qquad (1.7)$$

It has been reported that complex formation constant for monovalent cations forming 1:1 complexes with the ionophore should range from 10^4 to 10^9 kg mol^{-1}.[6] The β_{iL_n} constant for divalent cations with 1:2 complex formation stoichiometry should lie in between 10^{15} and 10^{29} kg^2 mol^{-2}.[60]

The concentration of ionophore within the sensing membrane may vary depending on the sensor's application. However, it is recommended that for the 1:1 complex formation stoichiometry, the amount of the ionophore added is usually at twice the molar equivalent of the lipophilic ion exchange salts. This ensures that the analyte ions within the sensing membrane are only present in their complexed form.[48] Similarly to the other components used in ISEs, an ionophore must contain a substantial number of lipophilic groups in order to prevent its leaching from the membrane interface to the aqueous sample solution.

Leaching can significantly reduce the response of the ISEs with ionophore doped sensing membranes resulting in worsening of the detection limits where the rate of leaching is directly correlated to the lipophilicity of the membrane and the sample.[61]

There has been several reported studies on immobilising the ion chelator for enhanced performance and lifetime of the sensor.[53,62–64] This was typically achieved by either covalent attachment of long alkyl chains to the ionophore or by the direct immobilisation of the ionophore to the sensing membrane with the latter including copolymerisation of the ionophore with other monomers to produce a polymeric architecture,[65,66] covalent attachment of the ionophore to chemically modified PVC[62,67] and blending the PVC matrix with polymer-grafted ionophore.[65,68] Such modifications also led to improvements in the detection limits of ISEs and prevented formation of dimers within membranes doped with metalloporphyrins.[69]

1.2.5   Inert lipophilic ionic sites

On some occasions, ISEs can be doped with inert lipophilic ionic sites such as tetradodecylammonium tetrakis(4-chlorophenyl) borate to reduce the membrane resistance and consequently improve its electrical conductivity. They are typically comprised of both highly lipophilic cations and anions. In contrast to previously described ion exchange salts, they do not provide any ion-exchanging properties furthermore, it has been reported that the presence of inert lipophilic sites may lead to the increased selectivity of the sensing membrane to the divalent rather than monovalent ions as demonstrated by Nagele et al (1998).[70] This may be attributed to the changes in the activity coefficients in the organic phase. However, if the total concentration of ionic sites within the sensing membrane is too high, the overall performance of the electrode may be diminished.[71]

1.3 Response mechanism

The total electromotive force that is determined during the potentiometric measurements is considered as the sum of potential differences present at all interfaces of the electrochemical cell. Assuming that the potential difference developed at the membrane and inner filling solution interface is constant, its contribution can be added up to the other constant terms to give one sample independent potential ($E°$). Therefore, only two components are considered to be sample depended: a) the potential difference developed at the membrane interface (E_{mem}) and b) the liquid junction potential of the reference electrode (E_{ref}).[48] In its general form, the total EMF can be expressed as follows:

$$EMF = E_{const} + E_{mem} + E_{ref} \qquad (1.8)$$

The liquid junction potential is caused by the variation in the mobility of ions at the phase boundary between the bridge electrolyte of the reference electrode and the aqueous sample solution. However, it can be kept very small and sample independent by selecting a bridge electrolyte of a high concentration such as 1 M lithium acetate (LiOAc), potassium chloride (KCl) or ammonium nitrate (NH_4NO_3).[72] If required, the liquid junction potential can be calculated according to the Henderson formula (eq. 1.9).[73]

$$E_D = \frac{\sum z_i u_i(a_{i,ref} - a_{i,sol})}{\sum z_i^2 u_i(a_{i,ref} - a_{i,sol})} \; x \; \frac{RT}{F} \; x \; \frac{\sum z_i^2 u_i a_{i,sol}}{\sum z_i^2 u_i a_{i,ref}} \qquad (1.9)$$

z_i corresponds to the charge of the ion i, u_i is an absolute mobility of the ion i [cm^2 mol s^{-1} J^{-1}], $a_{i,ref}$ and $a_{i\,sol}$ are the activities of ion i in the bridge electrolyte solution of the reference electrode and in the sample solution respectively [mol L^{-1}].

Since the contribution of liquid junction potential can be minimised by altering the experimental conditions, the equation 1.8 can be simplified to:

$$EMF = E'_{const} + E_{mem} \qquad (1.10)$$

The membrane potential (E_{mem}) can be also defined as the sum of three separate constituents. They consist of: a) the potential difference at the phase boundary at the membrane/inner solution interface, b) the transmembrane potential difference, c) and the phase boundary potential at the membrane/sample interface. The phase boundary potential at the membrane and inner membrane interface is constant and therefore independent of the sample.[6]

The transmembrane potential is mainly caused by the diffusion of the electrolyte from parts of the membrane with higher concentration of the electrolyte to layers with lower concentration of the ionic species. However, the contribution of the transmembrane potential to the total EMF is very low and often can be ignored.[74] This is due to the homogenous distribution of the ions carrying opposite charges in the membrane (primary ion (+) and ion exchanger (-) for the cation permeable membranes). The phase boundary

potential occurs as a result of the charge separation at the interface between the organic phase and the aqueous phase. This is expressed by the following equation:

$$E_{PB} = \frac{RT}{z_I F} \ln k_I + \frac{RT}{z_I F} \ln \frac{a_{I(aq)}}{a_{I(mem)}} \qquad (1.11)$$

$a_{I(aq)}$ and $a_{I(mem)}$ correspond to the activity of the primary ions (uncomplexed), z_I is the charge carried by the primary ions present in the aqueous and organic media. The term k_I is the measure of lipophilicity of an ion. If combined with eq. 1.7, the same equation can be expressed as:

$$E_{PB} = E^0 + \frac{RT}{z_I F} \ln \frac{k_I \beta [L]_{org}^n a_{I\,(aq)}}{\gamma [IL_n]_{org}^{zI+}} \qquad (1.12)$$

k_I corresponds to the energy of phase transfer and accounts for energy of the transition of I from aqueous solution into the organic membrane. Since the following parameters are kept constant: k_I, β, $[L]_{org}^n$, and γ, they can be extracted to form E_0

$$E_{PB} = E^0 + \frac{RT}{z_I F} \ln \frac{a_{I\,(aq)}}{[IL_n]_{org}^{zI+}} \qquad (1.13)$$

if the activity of primary ions in the organic phase is kept constant, this equation is reduced to the well-known Nernst equation (1.1). The simplified mechanism of response for ISEs is shown in Figure 1.5.
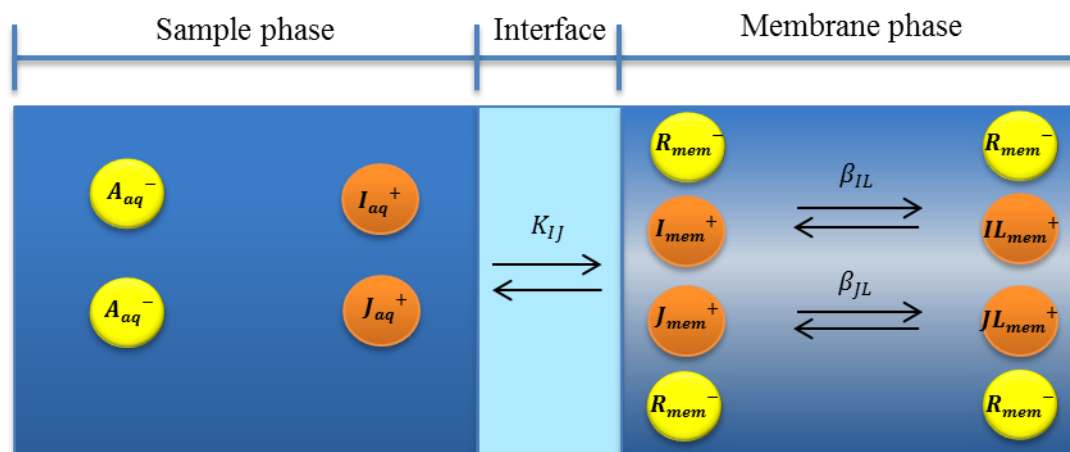
Figure 1.5 Schematic view of the equilibria that are involved when a cation-exchanger is placed in the aqueous sample solution. The term R^- represents the lipophilic ion exchanger and L is a cation selective ionophore. Symbols β_{IL} and β_{JL} are the formation constants of the IL^+ and JL^+ complexes where I^+ indicates the primary ions and J^+ are the interfering ionic species. K_{IJ} is the equilibrium constant for the exchange of I^+ and J^+ ions between aqueous and membrane phase.

1.3.1   Selectivity

Selectivity is an extremely important characteristic of a chemical sensor. It quantifies the preference of the analyte of choice over the other potentially interfering ion.[48] For liquid polymer membrane based ISEs, the extraction of interfering ions from the sample into the membrane phase is the main cause of selectivity degradation. The response of such electrodes can be predicted and determined from a vast number of parameters such as the thermodynamic constants, the complex formation constants of ion-ionophore pairs (within the membrane bulk) and the concentrations of both ionophore and ion exchanging salts.[75] Selectivity can be also described quantitatively by the selectivity coefficient K_{IJ}^{POT} that is a

direct function of the differences of the potentials generated by the presence of primary and interfering ions. This can be extrapolated to 1 M activity for these ions as demonstrated by the following equation:[76]

$$K_{IJ}^{POT} = \exp\left\{\frac{(E_J^0 - E_I^0)z_i F}{RT}\right\} \qquad (1.14)$$

True K_{IJ}^{POT} can be only obtained from adequate and unbiased potential measurements for each ion meaning that Nernstian response slopes are obtained for both interfering and primary ion.[77] This permits the determination of response functions of ISEs in mixed sample solutions.

Traditionally, the selectivity coefficient value is determined using either the separate solution method (SSM) or fixed interface method (FIM).[75] For each used ISE, both methods should produce identical results. The essence of SSM is that the potentiometric response of the membrane should be firstly measured in the solution of interfering ions (E_{J,a_J}) and then recorded in the primary ion solution (E_{I,a_I}). Under such conditions, tested ISEs are expected to produce Nernstian response to the interfering ions consequently making the determination of unbiased selectivity coefficients possible.

To obtain selectivity coefficients by FIM, the concentration of interfering ions is kept constant while the primary ion concentration is varied until there is no response to the

changing concentration of ions of interest – slope of the recorded calibration curve is $0.$[78]

For the determination of K_{IJ}^{POT}, the Nernstian response region is extrapolated to the EMF

for the activity of primary ions at its detection limits and the background interference.

The main equation that defines the relation between potentiometric selectivity coefficients

and the potential of ISEs measured in the presence of the interfering ions is known as the

Nicolsky-Eisenman equation:

$$EMF = E_I^0 + \frac{RT}{z_I F} \, ln\big(a_I(IJ) \, + \, \sum_{I \neq J} K_{IJ}^{POT} \times a_J(IJ)^{z_I/z_J}\big) \qquad (1.15)$$

The symbol (*IJ*) refers to the activity of ions in mixed solution. The above-mentioned

equation describes the behaviour of the electrode for separate and mixed solutions only

when the charges of primary and interfering ions are equal ($z_I = z_J$). However, if the

charges carried by the primary and interfering ions are not equal, only the linear ranges of

the response curve (determined either by the presence of primary ions or foreign ions) can

be used for the determination of unbiased selectivity coefficients. The response of

potentiometric ionophore-based membranes based on the phase boundary approach for

mixed ions, including monovalent and divalent ions is further defined by:[75]

$$EMF = E_I^0 + \frac{RT}{z_I F} ln\left(a_I(IJ) \, + \, \sum_{I \neq J} K_{IJ}^{POT} \times a_J(IJ)^{\frac{z_I}{z_J}}\right) - 1 \qquad (1.16)$$

Another, more intuitive approach was introduced by Gadzekpo and Christian (1984) which involved adding a specified activity of targeted ions to the reference solution and measuring the resultant membrane potential.[79] The same experiment is later repeated for the interfering ions (both reference solutions have to be identical) until the recorded potential matches membrane response from the experiment when the primary ions were added. The matched potential selectivity coefficient is then described by the ratio of primary ions to interfering ions.[80]

$$k_{IJ}^{POT} = \frac{a_I}{a_J} \qquad (1.17)$$

However, it is important to differentiate between the selectivity coefficients calculated from matched potential method and the ones obtained with Nicolsky-Eisenman equation. Since k_{IJ}^{POT} is directly influenced by the changes in experimental conditions, the selectivity coefficients determined with the matched potential method are not considered to be constant for the same tested electrode. Therefore, they do not represent the general characteristics of ISEs as opposed to K_{IJ}^{POT} that are regarded as true parameters that describe membranes response. Despite several limitations, the MPM has gained popularity among scientists as it directly reflects the experimental findings of ISEs in relevant samples even if some deviations from the expected (Nernstian) responses are observed.[81] Nevertheless, the selectivity parameters established with these two different approaches should not be directly compared but together can be regarded as useful tool for the characterisation of ISEs.

1.3.2   Limits of detection

In theory, ISEs are expected to display Nernstian behaviour at any given range of ion activity. However, as the upper and lower detection limits of the electrode are approached, the response starts to deviate from the expected (Nernstian) slope and electrode becomes less specific towards primary ions. According to IUPAC, both detection limits are found at the intersection of the two linear calibration curves (extrapolated) as demonstrated in Figure 1.6.[82]
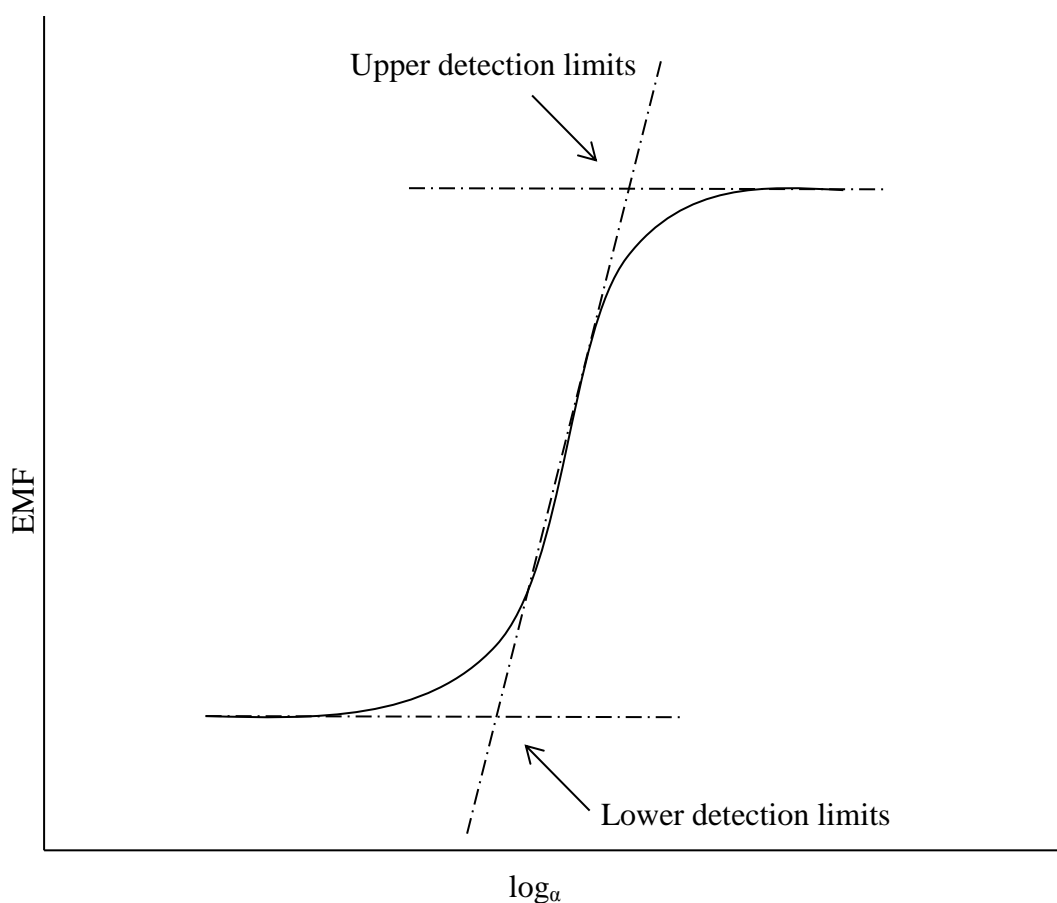
Figure 1.6 Schematic representation of how both lower and upper detection limits can be determined from potentiometric measurements.

The response of ISEs at high primary ion activity is predominantly governed by the co-extraction effects. This means that both primary ions and the interfering counter ions are being extracted from the sample solution into the membrane bulk leading to the overall decrease in membrane permselectivity, also referred to as the Donnan exclusion failure.[83] Such effect causes an increase in the concentration of primary ions in the membrane thus leading to the less than optimal response of the ISEs.

Lower limits of detection (LLOD) are approached when the electrode, at low primary ion activity, stops exhibiting Nernstian behaviour. Traditionally, LLODs are determined by two major factors:

- Interferences arising from the presence of competing (background) ions such as H^+ that are present in aqueous solution. This demonstrates that lower detection limits are directly influenced by the selectivity of the ISEs and therefore affected by the activity of background ions in the sample

$$log\ a_A(DL) = log(K_{IJ}^{pot} a_J(aq)^{z_A / z_J}) \qquad (1.18)$$

However, this thermodynamic explanation is not valid for membranes exhibiting high selectivity towards primary ions.

- Changes in the ion activity at the phase boundary (between sample and the electrode) caused by the membrane. These local perturbations are induced by the transmembrane ion fluxes that result in constant release of primary ions from the

27

membrane bulk into the sample. It gives rise to the non-zero primary ion activity at the phase boundary, disturbing the thermodynamic equilibrium.

For many years, it was considered that ion selective optodes based on the same sensitivity and selectivity defining elements showed much better limits of detection than their counterparts – ISEs. The major difference between the above-mentioned types of chemical sensors is the presence of inner filling solution in the liquid contact electrodes. It was approximated that a typical ion selective membrane used during potentiometric experiments contain a relatively high concentration ($\geq 1.0 \times 10^{-3}$ M) of primary ions, however, when the same membrane is put in the solution containing a very low concentration of primary ions ($\sim 1.0 \times 10^{-6}$ M) its response characteristics could be affected by the presence of transmembrane ion fluxes. The low activity of primary ions in the sample triggers the co-extraction of the inner electrolyte directly into the bulk of ion selective membrane.[84,85] This creates a concentration gradient across the sensing membrane and facilitates the primary ion net flux (diffusion) from the inner filling solution into the sample solution. These theoretical assumptions were later proved by scanning electrochemical microscopy experiments leading to new opportunities for the improvement of the detection limits of ISEs.[85,86]

The extraction of ions from the inner electrolyte solution and their transport across the sensing membrane give rise to a slightly elevated concentration of these ions (measured species) at the phase boundary between the sample and membrane bulk.[6] Therefore, the concentration of measured ions in the membrane does not longer correspond to the primary ion concentration at the phase boundary affecting (worsening) the lower detection limits of

ISEs. Further understanding of the zero current ion fluxes along with the development of new methodology for the determination of unbiased selectivity coefficients promoted the design of optimal ISEs and expanded their practical application in the ion sensing field. One of the major breakthrough in lowering LDLs was achieved when the inner filing solution of Pb^{2+} liquid contact electrodes with very small concentration of primary ions and relatively high activity of interfering ions was used to create a concentration gradient that induced the diffusion of primary ions from the sample towards the inner compartment (preventing them from leaching back into the sample).[85,87,88] However, in order to maintain the activity of primary ions in the inner filling solution constant, the presence of ion buffer (e.g. Na_2EDTA) was required – ion activity changes result in the potential change. This illustrates that even simple adjustments in the composition of inner filling solution such as lowering the primary ion concentration, introducing buffer solutions or adding chelating agents produced ISEs with the detection limits several order of magnitude lower than of the traditional ISEs.[85,87,89] For instance, Qin et al (2001) used a cation exchange resin in the inner filling solution to maintain the concentration of primary ions in the inner filling solution low and constant therefore reducing ion fluxes and improving lower detection limits.[90] The idea of suppressing ions fluxes was later utilised during the development of solid contact electrodes (SCEs).[90] This was achieved by removing the inner filling solution and applying the ion selective membrane directly on the electrical contact. However, the effects of such actions followed by the more detailed discussion regarding ion fluxes in solid contact electrodes are presented in Chapter 2.

SAMPLE MEMBRANE INNER SOLUTION

$[AL^-] = R^+_T$

A^-

A^-

δ_{PB} δ_{memb}

A)

SAMPLE MEMBRANE INNER SOLUTION

$[AL^-] = R^+_T + [X^+]$

A^-

$A^-_{PB} = A^-_{DL}$

R^+_T

A^-

B)

SAMPLE MEMBRANE

B^-

R^+_T

A^-

$[AL^-]$

$A^-_{PB} = A^-_{DL}$

$[BL^-]$

A^-

B^-

C)

SAMPLE MEMBRANE

R^+_T

B^-

A^-

$[AL^-]$

$[BL^-]$

A^-

D) B^-

$A^-_{PB} = A^-_{DL}$
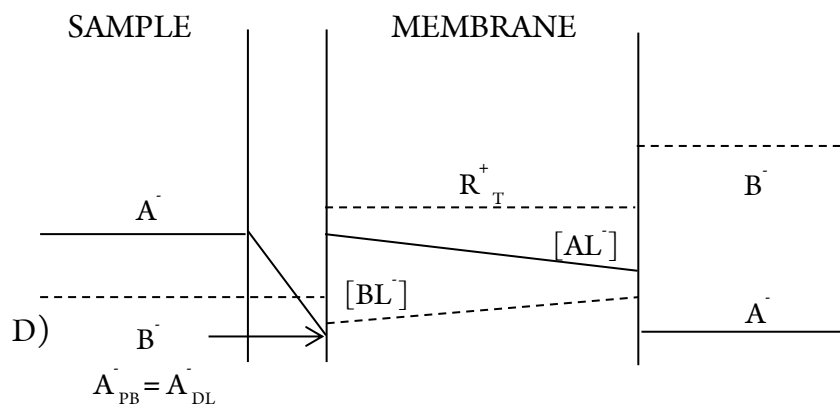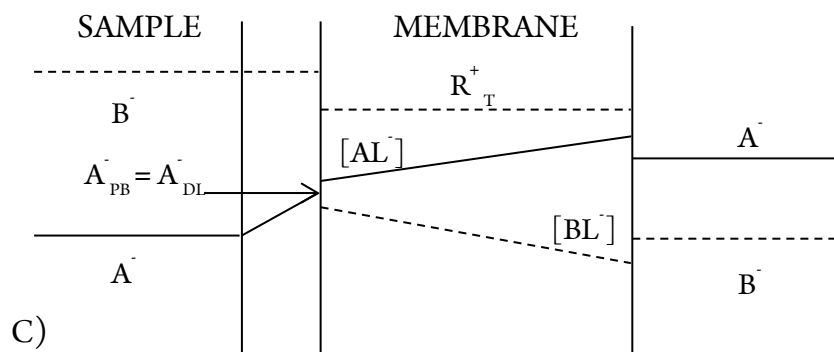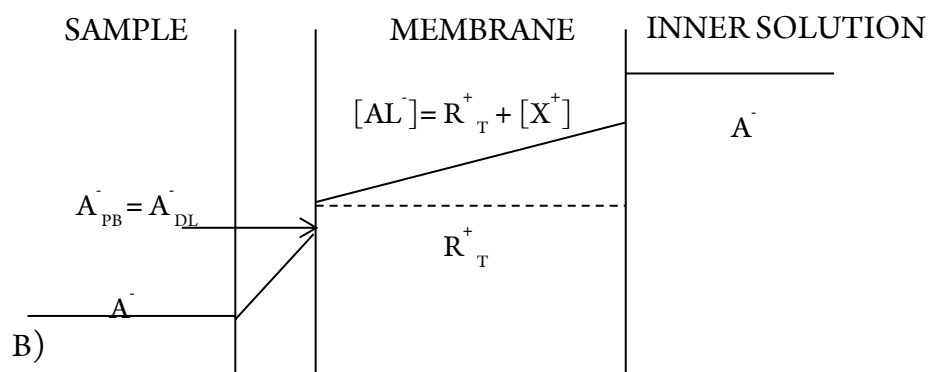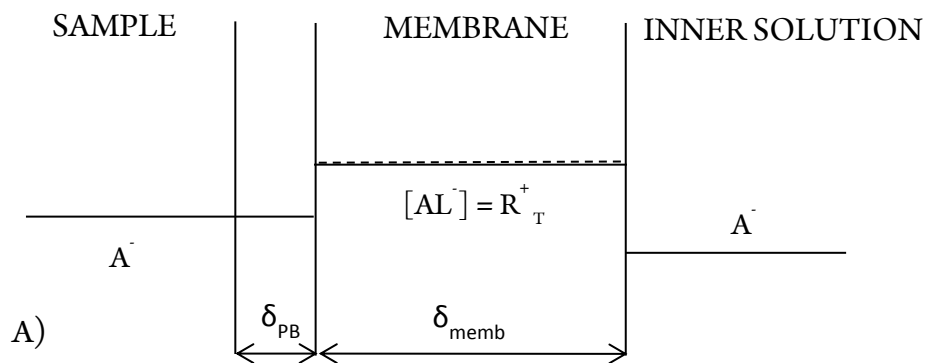
Figure 1.7 Schematic illustration of processes directly influencing lower detection limits of anion selective membranes containing lipophilic ion excluders (R^+_t) and ionophore (L) that can form complexes with both primary (A^-) and interfering (B^-) ions. Scheme (A) represents an idealised scenario where no transmembrane ion fluxes are present (δ_{memb} − membrane thickness), (B) relates to the mass diffusion of primary ion from the inner filling solution to the sample solution changing the local concentration of primary ions at the phase boundary (δ_{PB}). Schemes (C) and (D) demonstrate the concentration gradient induced by partial ion exchange at the sample and inner filling solution phase respectively.

For the more detailed study of ion fluxes in liquid contact electrodes, the recorded experimental EMF is defined by the phase boundary potential on both sides of the membrane (inner filling solution/membrane interface and sample/membrane phase boundary) as described in equation 1.19:[87]

$$EMF = E° + \frac{RT}{F} ln \frac{c_i [I^-]}{[IL^-]} - \frac{RT}{F} ln \frac{c_{i'} [I^-]'}{[IL^-]'} \qquad (1.19)$$

The symbols c_i and $[I^-]$ refer to the concentration of free primary ions in the sample solution and the membrane segment. The $[IL^-]$ corresponds to the concentration of ion-ionophore complex. Single prime describes parameters at the inner filling solution/membrane phase boundary, where no prime refers to the sample phase boundary.

In order to fulfil the criteria of the above presented model the following assumptions were made: (1) the concentration of charged species in the inner filling solution is buffered and therefore kept constant; (2) diffusion coefficients within each phase have the same magnitude (also kept constant) and are equal for all diffusing species in the membrane

bulk; (3) only two types of monovalent anions are present in the described system, which both form 1:1 complexes with the binding ligand (L); (4) only one type of cation (C^+) is present in the sample solution with its concentration being kept constant in both: the bulk of the sample and the diffusion (Nernstian) layer; the activity coefficient of each described species are close to unity and therefore their concentrations can be used for further calculations.

Such model illustrates that the optimal concentration of primary ions in the inner filling solution ($C_{I,is}^{opt}$) is dictated by the following processes: (1) leaching of the primary ions from the membrane when the $C_{I,is} > C_{I,is}^{opt}$ and (2) depletion of primary ions at the sample and membrane phase boundary when $C_{I,is} < C_{I,is}^{opt}$. Depletion is usually accompanied by the simultaneous release of the interfering ions that causes a sudden decrease in measured EMF (super-Nernstian behaviour).[87] Such response has been partially associated with the Hulanicki effect that typically takes place upon the contact of ion selective membrane with a targeted ion that is present in the sample at very low concentration – typically 1.0×10^{-6} M (primary ions are not initially present in the membrane bulk).[77,91,92] This induces an inward ion flux of primary ions into the ion selective membrane and results in the depletion of targeted ions in the Nernst diffusion layer at the sample-membrane phase boundary. Several approaches were suggested to supress or even fully eliminate the presence of super-Nernstian responses; some of which includes reducing the ionic strength within the membrane bulk[93] or introducing lipophilic particles into the surface of the membrane to minimise ion fluxes.[94] On the contrary, super-Nernstian response can be beneficial for continuous monitoring purposes or for end point determination during

potentiometric titrations as this potential change indicates when a critical concentration range is approached.[48,95,96]

1.4 Optodes

Another class of chemical sensors that utilises ionophores is that of optodes. In addition to the traditional ISEs, optode sensors typically contain a chromoionophore that exhibits a high selectivity towards the hydrogen ions (H^+).[11] The optode membranes, when introduced into a solution containing only a very small concentration of targeted ions, exhibit a colouration that is characteristic to the protonated form of a chromoionophore. A colour change is observed with an increasing concentration of an analyte ion and it is typically quantified by the means of fluorescence and absorption spectroscopy.[97] The development of given colouration can be attributed to the formation of ion-ligand complexes in the membrane bulk and a concurrent transfer of protons to the aqueous solution.[98] Therefore, the membrane develops the colour of the deprotonated chromoionophore, as demonstrated in the following equilibrium:

$$CH^+R^- + L + I^+_{(aq)} \rightleftarrows C + LI^+R^- + H^+_{(aq)} \qquad (1.20)$$
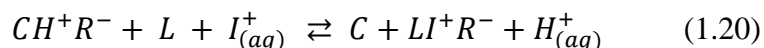
The parameter C is a chromoionophore, L is a ligand (ionophore) for targeted ion I^+, R^- is a lipophilic ion. This process illustrates (for cation selective membrane) that the optode response is not governed by the changes in the boundary potential at the sample/membrane interface but involves a total exchange of the ionic content between the membrane bulk and a surrounding solution. However, complete ion exchange results in a transmembrane mass transfer that may lengthen the response time of a sensor.[99,100] For polymeric membranes composed of the plasticised PVC, it is not uncommon that the response time towards the analyte of interest is in order of several hours. However, if the surface area of

34

the optode is increased, the mass transport from the solution is significantly accelerated giving rise to faster response times. This is especially pronounced when microspheres or nano-particles are used for example response times under 1 min were reported for the measurements of extracellular sodium.[101] Similarly, Xie et al (2014) demonstrated that miniaturised optodes can produce almost instantaneous responses to poly-ions such as protamine where the response time of traditional optical films were too long to reach a thermodynamic equilibrium.[102] Since ion selective optodes combine high selectivity of available ionophores with the ease of detection via optical signal measurements, their application within different scientific fields has been continuously rising.[103] Until recently only, the optode membranes have worked mainly under the conditions of thermodynamic equilibrium (passive mode).

1.4.1 Dynamic optodes

More recently, ion selective optodes based on the presence of stimuli-responsive materials have received a considerable attention[104] as full control of the ion exchange process between a sample and the sensing membrane during the optode operation and storage can be achieved. Shvarev (2006) reported that a photochemical acid generator (PGA) when incorporated into the sensing membrane matrix can influence the optode response towards the targeted ions.[105] Photogeneration of a hydrochloric acid (HCl) that was initiated during the membrane exposure to the ultraviolet (UV) radiation was proved to cause protonation of the chromoionophore. However, the degree of protonation decreased with the diffusion of HCl from the matrix interface into the aqueous solution. Even though, the optical sensors containing PGA could be successfully switched 'on' and 'off', their application remained largely limited due to the exhaustive nature of the PGAs (irreversible photolysis). In 2011, a research group led by Bakker noted that the photoinduced acidity change of the

indicator dye (spiropyran) might strongly influence the equilibrium conditions of an ion sensing membrane.[104] They observed that illumination of the spiropyran based membranes with both UV and visible light could induce large shifts in the pKa values inside the membrane (over six orders of magnitude). As the optical sensor was exposed to the UV radiation (λ - 365 nm), a chromoionophore was converted into a more basic form causing a diffusion of metal ions to the aqueous solution and a simultaneous uptake of the hydrogen ions into the membrane matrix. A reverse process was observed upon the illumination with a visible light (the excitation wavelength of 410 nm). However, the sensor was rendered inactive at very high pH (> 10). This can be attributed to the very low activity of H^+ at this high pH. Metal ions that are more abundantly present within the aqueous solution would enter the optode membrane and form complexes with the ionophore. As a consequence, an ejection of protons from the membrane matrix would occur (even in the presence of basic merocyanine). Although, a substantial drift from the expected response may occur at extremely low or high pH values, the spiropyran-based sensors are still suitable for performing measurements on the majority of biological and environmental samples. [98] A slightly different approach was taken by Xie et al (2012) during the design of chloride selective sensors.[106] They discovered that a hydrogen ion uptake that is governed by the presence of a chromoionophore (merocyanine) was accompanied by the simultaneous diffusion of chloride ions into the membrane bulk. Since then, several examples of optical sensors based on the presence of stimuli-activated materials have been reported, opening new avenues in the development of sensing devices.

1.4.2   Fluorescent indicators

Even though, the field of ion selective optodes offers almost unlimited options to modify the sensitivity and selectivity of the sensing mode for the given analyte, these optical

sensors often require the presence of several components that may possibly lead to longer and more thorough optimisations processes. Another class of optical detection methods relies on the presence of a complexing molecule that can selectively bind the analyte of interest and if irradiated with light of specific wavelength it can produce an optical signal in a form of fluorescence. Large number of either naturally occurring or chemically synthesised fluorescent dyes (fluorophores) exhibiting strong affinity towards various metal ions/molecules is available demonstrating their vast application across many scientific fields.[107] Fluorescence sensing materials can be also covalently linked to the recognition centre (ionophore) to produce an optically active ligand - fluoroionophore.[108,109] In this molecule, the recognition process is facilitated by the presence of the ionophore, where the response is later converted into a fluorescence signal by the perturbation in one of the following photoinduced processes: electron or charge transfer, energy transfer or either formation or loss of eximers or exciplexes.[110] The sensing mechanism of fluorescence sensors is typically based on the fluorescence quenching caused by the presence of a targeted analyte or sample-induced fluorescence in which the emitted signal is enhanced upon complex formation with the analyte.[111–114] The working range of fluorophore based sensors is predominantly defined by the affinity of the optical molecule for targeted species. Furthermore, the calibration of emission signal intensity on the concentration of the used sensors must be considered as the actual concentration of small-molecule sensors often cannot be controlled.[115] Signal rationing also better known as ratiometric detection and fluorescence lifetime imaging microscopy have been widely used for fluorescence ion detection as the performed measurements are independent of the sensor concentration.[116–119] The sensitivity of fluorescence based sensors is also dependent on the stability and brightness of the fluorophore used for sensing

membrane preparation. Bright fluorophores can be excited with the radiation of lower intensity and therefore they can be used at much lower concentrations than their counterparts. This is especially important if *in situ* measurements are performed as less photodamage to the living sample is induced. Stability of the fluorescent dye is also considered as crucial factor during the design of optical sensors as it defines the lifetime and dictates the robustness of the sensor. Repeated excitation and emission cycles can lead to the decay in fluorescence intensity (photobleaching) that may even cause photo-induced toxicity if living specimens are used. Another parameter that contributes to the sensitivity of fluorescence based optical sensors is the wavelength of radiation used for the excitation and emission of a fluorophore. If the investigated sample contains other species which can emit a fluorescent signal such as biomolecules then it may be difficult to distinguish between the background and real signals. Additionally, specimens in their excited state may react with molecular oxygen to produce free-radicals. This can produce severe photodamage to the sample/matrix.[120–123] Similarly to ion selective optodes, fluorescent dyes are entrapped within a polymeric matrix and can be used as optical films, microspheres or nano-particles. Also they carry a unique advantage over many other analytical tools as they do not require the presence of a separate reference device during the analytical measurements. Their response characteristics such as the response time also relies on the process of mass diffusion of the analyte from the aqueous phase into the optical sensor and can be varied as described in 'Optodes'. Recent advances in the fluorescence based sensors led to development of ultra-sensitive probes for instance for the uranyl ions determination with the detection limits reported at 1.0×10^{-11} M and excellent selectivity.[124] They have been also routinely employed for the detection of metal ions and organic molecules during *in vivo* and *in vitro* experiments.[125–129]

1.5 Electrochemical Impedance Spectroscopy (EIS) for determination of dielectric constants of ISEs

One of the fundamental laws describing the behaviour of electrical circuits is Ohm's law (eq. 1.21).[130]

$$V = IR \qquad (1.21)$$

Where, V is an electrical potential applied across the circuit in units of volts (V), I is the current that flows through the circuit in amperes (A) and R is the resistance of a circuit to the flow of electrical current in ohms (Ω). However, this relationship is only true if the investigated system behaves as an ideal resistor. In reality, electrical circuits exhibit more complex behaviour therefore the concept of resistance was replaced with another parameter − impedance. Impedance is defined as the measure of resistance to the flow of electric current without limitations of Ohm's law.[131] During an impedance measurement an AC perturbation signal is imposed to the electrochemical cell and the resulting current is measured. The excitation potential that is applied has to be small enough to ensure the pseudo-linear response of the cell. As a result, the current response to the AC potential will be a sin wave with the same frequency but with different amplitude and phase (Figure 1.8). The current-voltage response is later analysed by the frequency response analyser to provide information about the resistance, capacitance and inductance of the system at the particular frequency.[100]
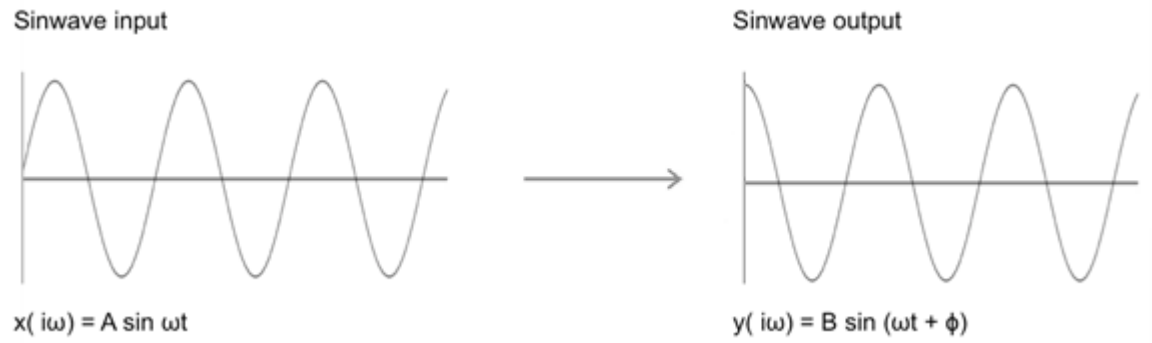
Figure 1.8 Sinusoidal current response in a linear system.

The applied potential when expressed as a function of time has a following form:

$$E_t = E_0 sin(\omega t) \qquad (1.22)$$

The parameter E_t is an excitation potential at time t, E_0 is the amplitude of the signal and ω is the radial frequency. As mentioned earlier, the corresponding current response (I_t) displays different amplitude (I_0) and is shifted in phase (ϕ). This is illustrated by the following equation:

$$I_t = I_0 sin(\omega t + \phi) \qquad (1.23)$$

Therefore, the total impedance of the investigated system can be defined as a ratio of input signal to output signal

$$Z = \frac{E_t}{I_t} = \frac{E_0 \sin(\omega t)}{I_0 \sin(\omega t + \phi)} \qquad (1.24)$$

The impedance can be also represented as a complex number as demonstrated by the equation 1.25:

$$Z = \frac{E}{I} = Z_0(cos\phi + isin\phi) \qquad (1.25)$$

For the graphic representation of impedance data, both the Cartesian and polar coordinates can be used. The plot of real part of the impedance - $ReZ(j\omega)$ versus the imaginary part of the impedance -$ImZ(j\omega)$ is named a Nyquist plot.[132] However, the main drawback of using the Nyquist diagram is that it does not provide information about the frequency at which the specific data point was collected. A Bode plot is a log-log plot of the magnitude $|Z(j\omega)|$ and phase (ϕ) of the impedance $Z(j\omega)$ as a function of the frequency of a sinusoidal excitation $(\omega \; or \; f = \; \omega/2\pi)$. In this case, the information about the frequency is available.[133] Unless otherwise specified, the Bode plot and Nyquist diagram will be referred as the impedance spectrum. Figure 1.9 gives an example of the same impedance function that is represented on the Nyquist plot (left) and Bode plot (right).
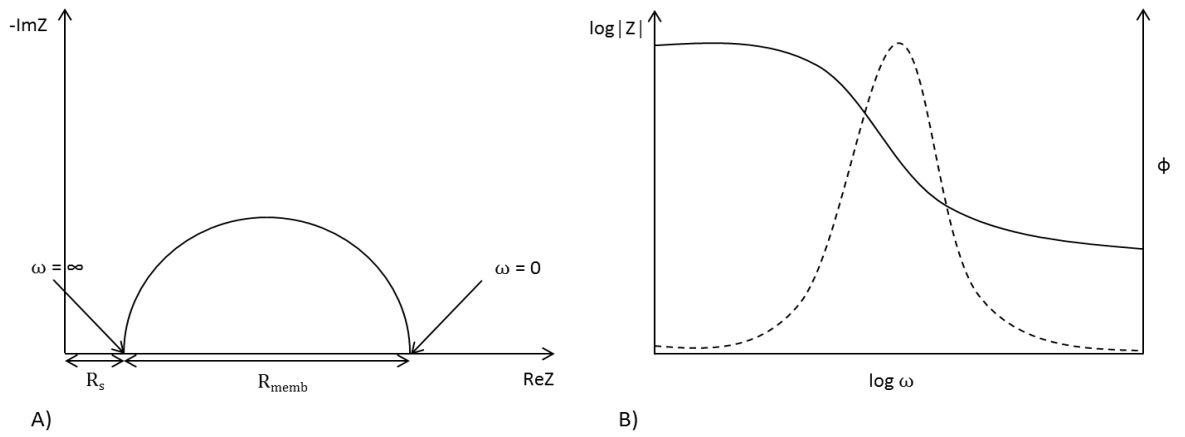
Figure 1.9 Complex plane impedance spectrum (Nyquist plot) − A, Bode diagram − B. High frequency data are presented on the left-hand side and the low frequency data are on the right side of the Nyquist plot. Whereas, the opposite trend is observed on the Bode plot (the left side shows low frequency data). On graph (B) the dashed line represents ϕ while the straight line is log|Z|. R_{memb} represents the resistance of the membrane and R_s is a resistance of the solution in which the sensing membrane is immersed.

In reality, the experimental EIS data are hardly ever found to produce the full semicircle with its midpoint on the real axis of the complexed plane as observed in Figure 1.9. However, two common perturbations can be distinguished, which presence may still yield partial semicircle in the complex plane: (1) the semicircle does not start at the origin point, either due to the presence of other semicircles at the high frequency data or if the resistance of background solution is not equal to zero ($R_s > 0$); (2) the centre of the resulting arc is shifted down below the real axis due to the presence of various elements that have been distributed in the membrane/electrode system. This results in the relaxation time being continuously distributed around a mean value.

Electrochemical impedance spectroscopy is a non-invasive technique that can be used to determine the physical and electrochemical properties of the investigated system. It has been already routinely employed during the characterisation of coatings, batteries, fuel

cells, etc.[134] Moreover, impedance spectroscopy has been applied for the characterisation of ion selective membranes.[26,134–136] EIS measurements performed on electron semiconductors and conductors usually involve the presence of redox-active species (Faradaic impedance). The measured impedance parameters give information about the electron transfer resistance, the capacitance of the double layer at the electrode/solution interface and diffusion of electroactive (redox-active) species in solution to/from the electrode surface.[133]

For the ISEs, impedance describes the diffusion of charged species (ions) across the membrane segment as well as their transport through the phase boundaries.[137] It is also a tool for the characterisation of time constants of individual processes occurring either in or at the membrane surface (including corrosion, adhesion of species, surface reactions).[138] This was also demonstrated by Radu et al (2010) where the EIS was used to differentiate between the ion selective membranes that have been exposed, prior the experiments, to the physical damage, biofouling or leaching of components.[139] In case of the ISEs, measured impedance is predominantly defined by the characteristics of a sensing membrane. This includes the total number of charged carriers, their type and mobility, rate of their transfer from the electrolyte into the membrane, adsorptions rate (if such reaction path is involved), the chemical and physical homogeneity (surface roughness and non-uniformly distributed properties of the irregular electrode surface contribute to the membrane impedance), type and location of surface ionic sites and adsorbed charges, and the rates of formation and recombination of charged moieties from lattice sites, complexes and ion pairs.[67,140]

43

Impedance measurements of ion selective membranes are usually carried out in symmetrical two, three or four electrode cells. The resulting complex impedance is not only dependent on the physico-chemical properties of the investigated ISEs but it is equally influenced by several other measurement conditions such as area of the membrane, temperature, concentration of the solution used for conditioning and measurements and humidity. Therefore, EIS experiments are typically performed in the concentrated electrolyte solutions at constant temperature with the area of working electrode and the membrane fragment being kept moderately large (diameter > 0.1 cm).

During equivalent circuit modelling the electrical system is considered to produce the same response to one that is obtained from the system measurements. Therefore, by selecting a model that reflects the investigated system (always made up from electrical circuit elements such as resistance, capacitance and inductance), information about different electrical and electrochemical elements can be derived. Unlike pure resistance, capacitive reactance (x_c) is a function of frequency as it imposes a phase shift between the excitation signals and output signals as shown in equation 1.26:[141]

$$x_c = \frac{1}{2\pi f C} \quad (1.26)$$

However, pure electrical elements are often not sufficient enough to describe the behaviour of the investigated system and therefore their combinations are commonly used for that purpose. The EIS spectrum with resistance and capacitance parameters coupled in parallel

are shown in Figure 1.9. The resultant plot is made of a semicircle that intersects the real axis at two data points: $\omega = \infty$ (high frequency) and $\omega = 0$ (low frequency data). The maximum is observed at $Z' = R_S + \frac{R}{2}$ where $Z'' = \frac{R}{2}$ occurs at the frequency of ω^p peak (where R is the diameter of the semicircle). Another, very important parameter of equivalent circuits is a time constant (τ) as it describes the relaxation time of the resistor-capacitator (RC) circuit. This also includes: the electrical conductivity, a mass and charge accumulation and the diffusion processes. If the diffusion of charged species across the membrane interface is very fast, only single arc (semicircle) that corresponds to the membrane bulk is observed on the Nyquist plot. The x-axis intercepts are then used to determine the resistance of the membrane and its surrounding solution as demonstrated in Figure 1.9. The capacitance of the membrane can be determined directly from the membrane resistance (eq. 1.27) or by the equivalent circuit fitting where C_g represents the geometric capacitance of the analysed membrane.

$$ C = \frac{1}{2\pi f_{max} R_{mem}} \qquad (1.27) $$

The parameter R_{mem} is the membrane resistance, C is a capacitance, f_{max} corresponds to the frequency at the maximum of the Nyquist plot. Several physico-chemical parameters such as surface charge, the dielectric constant and thickness of the membrane and the presence of background solution define this parameter. The doubling of membrane thickness would cause the overall capacitance to go down by half while the membrane resistance would double.[142] However, if the ion diffusion across the membrane interface is

slowed down, more than two semicircles can be observed.[136,142,143] The presence of first semicircle is usually attributed to the processes occurring within the membrane bulk, while the second arc (low frequency region) corresponds to the kinetic processes taking place at the sample/membrane interface. The extent of the second arc is determined by two major processes: slow, potential-depended mass diffusion of ions through the high resistance membrane layer (1) and slow, potential-depended charge transfer across membrane/solution interface (2). The relaxation frequencies corresponding to the material under investigation and the contact interface should differ by at least two orders of magnitude to achieve appropriate spectral resolution. If these conditions are not met and the relaxation frequencies of two different electro-active regions are close to each other, the Nyquist plot will adopt the shape of a depressed/distorted semicircle rather than give two well defined semicircles.[136] The kinetic process that contribute to the formation of a semicircle at low frequency data are described by following parameters: low frequency capacitance (C_{dl}) in parallel with surface layer resistance (R_{dl}).

However, if the diffusion of ions in the aqueous solution or ionic species in the membrane is slower than the kinetics of charge transfer at the membrane/solution interface, the resultant current during the impedance measurements starts being controlled by diffusion processes. On the Nyquist plot, it appears as a diagonal line at 45° angle to the real (Z) axis and is often referred as Warburg impedance. The magnitude of Warburg diffusion at high frequency data is relatively small since the distance for the diffusing species to travel is very short. At low frequencies, the same reactants must travel significantly farther, therefore increasing the contribution of Warburg impedance to the EIS spectra.

From a vast number of circuits used for data modelling, the Randles circuit is very common type used for the characterisation of ion selective membranes with EIS.[139] This model is defined by four major components: a solution resistance (R_1), a membrane resistance (R_2), a geometric capacitance (C) and Warburg diffusion (W) and it is further depicted in Figure 1.10.[137] However, the impedance data from polymer-membrane based sensors cannot always be explained using the above-mentioned circuit and often requires finding a different, more suitable model that describes the experimental findings.
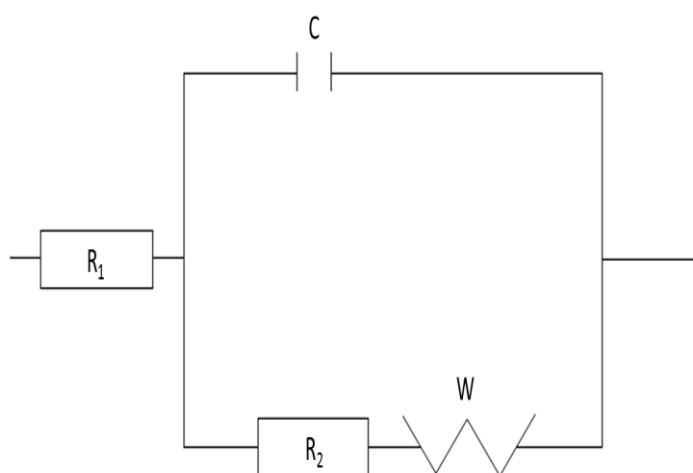
Figure 1.10 Equivalent circuit that can be used during the impedance measurements of ion selective membranes (Randles circuit).

1.5.1 EIS in the determination of dielectric constant

Another parameter that can be indirectly derived from the EIS measurements is the dielectric constant (the relative electrical permittivity). It can be calculated from the membrane bulk capacitance (and resistance) as demonstrated by the following equation:

$$C = \frac{\varepsilon_0 \varepsilon_r A}{d} \qquad (1.28)$$

C is a capacitance, ε_r is the relative electrical permittivity of the membrane, ε_0 is the relative permittivity of free space (electric constant), d is the membrane thickness also defined as the distance between two plates of a capacitor and A is the area of the membrane exposed to the aqueous solution.[144] Information about the dielectric constant of a material is important when designing a capacitor for the electrical circuits. In the field of ISEs, the dielectric constant is a useful measure of the polarity of the solvent and polymer and the ability of the investigated material/membrane to carry an electrical charge.[145] Therefore, the physico-chemical properties of the ion selective membranes are influenced by the changes in the dielectric constant of its components.

Several studies have illustrated that polarity of a plasticiser (dielectric constant) can strongly influence the selectivity and detection limits of the ISEs.[146] Ion selective membranes that are based on neutral carriers containing plasticisers with a low dielectric constant showed an enhanced selectivity towards the ions with low hydration energy. The opposite effect is observed if a plasticiser exhibits a high dielectric constant. Research carried out by Zahran et al (2014) demonstrated that anion selective membranes when plasticised with DOS ($\varepsilon_r \approx 4$) exhibited high selectivity towards the lipophilic ions whereas the same membranes containing 2-nitrophenyl octyl ether (NPOE) ($\varepsilon_r \approx 24$) were more selective to the chloride ions.[45] Further studies showed that PVC membranes might absorb some small amounts of water ($\varepsilon_r \approx 80.1$) when immersed in an aqueous solution subsequently resulting in an elevated dielectric constant of the membrane.[142] Since

the water uptake cannot be fully controlled and its degree may vary between membranes of the same composition, this can introduce a discrepancy between the measurements and therefore it can cause a variation in the ε_r values being citied in the literature. Similar observations were made by the research group lead by O'Rourke et al (2011).[144] They reported that EIS measurements carried out in the saturated solution of potassium chloride can give rise to higher values of the dielectric constants due to the penetration of a solvent and a salt into the membrane. These could explain the differences in the dielectric constant values observed for the PVC membranes tested by Armstrong et al (1988)[146] and O'Rourke et al (2011). A latter research group defined the A value as the surface area of the ion sensing membrane that was actually exposed to the aqueous solution. Whereas Armstrong et al (1988) used the geometrical area of the electrode as the value of A. This may provide a good explanation to the inconsistency between the obtained results since the dielectric constant value is dictated by the surface area of the sensing membrane. The application of EIS for the determination of dielectric constant of ion selective membranes is demonstrated in Chapter 3.

1.6 Ultraviolet and visible absorption and fluorescence spectroscopy

An in depth description of the science of ultraviolet and visible (UV/Vis) absorption spectrophotometry and fluorescence spectroscopy are described in detail by Harris in the book titled "Quantitative Chemical Analysis", Chapters 17 and 18 (2010). Some of the key points relevant for this Thesis have been adapted from this text.

Over a given range of wavelengths, every molecule absorbs, reflects or transmits electromagnetic radiation. UV/Vis absorption spectroscopy is an analytical technique that measures the reflection or absorbance characteristics of a given sample. The spectral region utilised in UV/Vis and fluorescence measurements often extends from the short wavelengths of the ultraviolet radiation (UV) through the visible region (Vis) of the spectrum reaching longer near infrared wavelengths (NIR). Therefore, this may be regarded as consisting of three spectral regions:

Table 1.1 Spectral range used during typical UV/Vis measurements.

Spectral region	Wavelength range
UV	190 nm – 380 nm
Vis	380 nm – 780 nm
NIR	780 nm – 1000 nm

Since this analytical tool can be applied to all chemical compounds that give rise to a measurement of absorbance across this defined, yet broad spectral range and as such, it is applicable to a wide array of scientific disciplines.

Qualitative analysis of studied compounds may be performed with the means of using a spectrophotometer as different molecules absorb radiation at different wavelengths. An absorption spectrum comprises of a number of absorption bands which correspond to structural properties (functional groups) within a particular chemical compound. However, this type of analysis is usually reserved for individual compounds as broad absorption bands and similar spectral characteristics of molecules may render it unsuitable to distinguish between various components in a mixture. In contrast, there are only few groups of compounds such as aromatic hydrocarbons that exhibit fluorescent properties. As no two compounds have exactly the same fluorescence characteristics (emission and excitation wavelengths), fluorometry is, therefore, considered as highly specific analytical tool.[147]

UV/Vis absorption spectroscopy has been routinely employed for the quantitative analysis of compounds based on their absorbance of electromagnetic radiation. Pioneering work in this area of research was carried out by French mathematician, Lambert which dates back to the XVIII century and was later followed by the German physicist, Beer. They related the attenuation of light to the properties of a sample through which the light was travelling. This is summarised by the equation:

$$A = c * \varepsilon * l \quad (1.29)$$

A corresponds to the absorption of the sample [Au], *c* is the concentration of the sample in the solution [mol/L], *l* refers to length of light path through the sample [cm], ε is the molar extinction coefficient [M^{-1} cm^{-1}]. Transmittance, *T*, is the ratio of transmitted radiation, *I*, of a sample to the incident radiation I_0 and can be defined as follows (eq. 1.30).

$$T = \frac{I}{I_0} \qquad (1.30)$$

Transmittance can be also expressed as the percentage of the amount of incident light transmitted through the sample.

$$T = \frac{I}{I_0} * 100 \quad (1.31)$$

Therefore, the amount of radiation transmitted through the analyte directly depends on the concentration of the sample of interest and on the path lengths (distance travelled by the monochromatic light) of the cuvette used for the spectroscopic measurements (Figure 1.11).
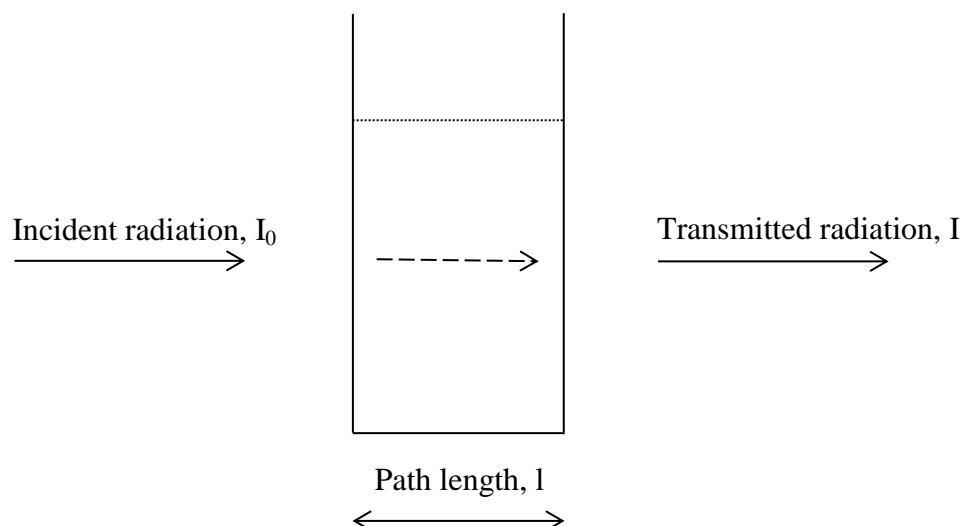
Figure 1.11 Schematic representation of how the transmittance of incident radiation, I_0, produced by a spectrophotometer, is affected by the concentration of the analyte, c and the distance it had to travel through the sample, l. Transmitted radiation is then collected by the detector.

The correlation described by Beer and Lambert has been routinely used for concentration determination of a pure analyte in a solution based on its absorbance providing that an accurate value of extinction coefficient is known. However, deviations from the linearity between the concentration and absorbance are sometimes encountered. Such limitations are the result of one or more following things: real limitations, instrumental factors or chemical factors.[148]

1) Real limitations involve:

   a) Only valid for diluted samples ($<$ 0.01 M)

   b) Absorption coefficient dependence on the refractive index of the medium

2) Chemical factors involve:

   a) Solvent effects including solute – solute and solute – solvent interactions

3) Instrumental deviations include:

   a) Effects of polychromatic radiation (as ε is specific to λ)

b) Stray light effects

Since the energy required to promote electrons from highest occupied molecular orbital (HOMO) to the lowest unoccupied molecular orbital (LUMO) has fixed value, the resulting absorption peaks corresponding to these electronic transitions should be sharp in nature (Figure 1.12). However, for each electronic level, a number of vibrational energy levels are available allowing further transition to occur and therefore significantly contributing towards band broadening.
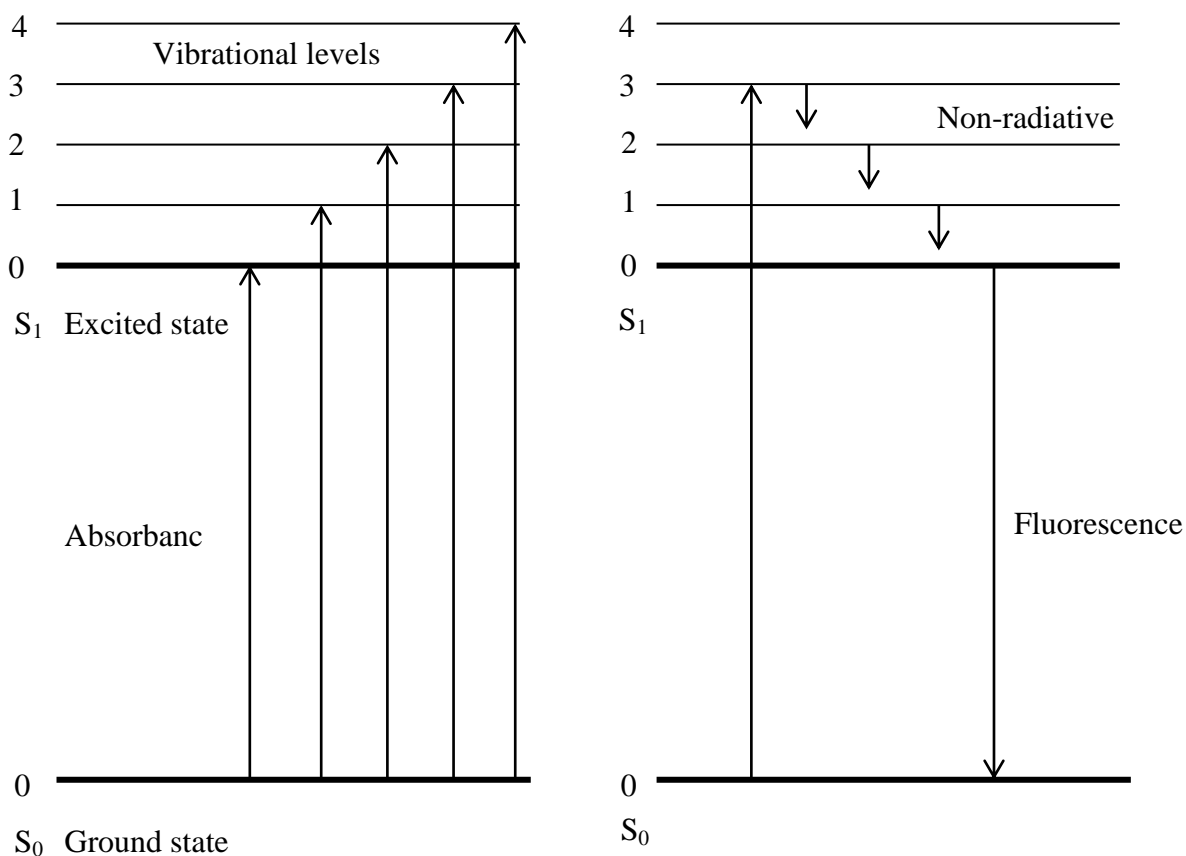
Figure 1.12 Simplified diagram of transitions occurring when the analyte is irradiated with a monochromatic light giving rise to absorption and fluorescence emission spectra.

After the required energy is provided to cause electronic transitions, the molecule can relax back to lower energy orbitals via several deactivation processes. Fluorescence emission is a type of radiative relaxation observed only if the excited species decay from the singlet electronic excited state to a permissible vibrational energy level in the ground state. Other relaxation processes involve: a) non-radiative deactivation; b) energy transfer between the excited state molecule, solvent or other specie present – often leads to fluorescence quenching; c) phosphorescence; d) change in the multiplicity of molecule due to spin reversal. However, as the molecule is promoted to the excited electronic state some of the energy used for the excitation is lost (energy dissipation). Therefore, the emission signal is always present at the lower energy region of the electromagnetic spectrum (longer wavelength). Absorption and fluorescence spectra are considered to be mirror images as similar energy gaps are observed for vibrational level in both ground and excited states of the molecule.
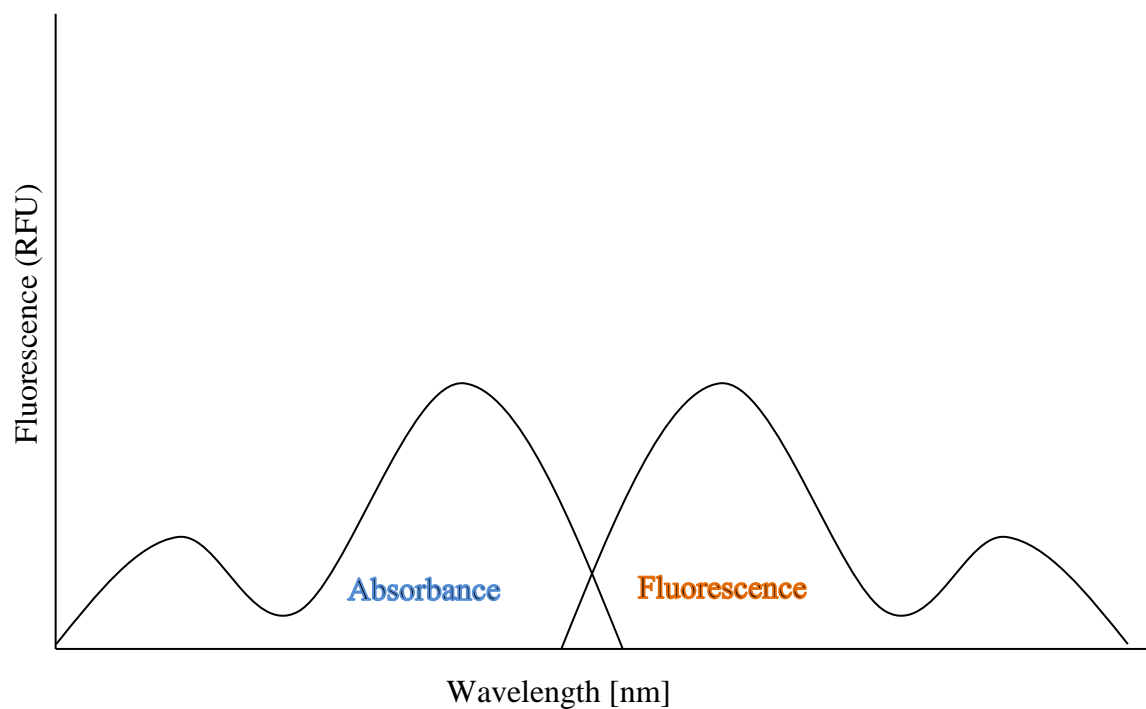
Figure 1.13 The relationship between absorbance and fluorescence spectra

In fluorescence spectroscopy the fraction of radiation absorbed by an analyte is independent of the intensity of the incident radiation and similarly to UV/Vis spectrophotometry is related to the concentration of the absorbing species by the Beer-Lambert equation as demonstrated:

$$\frac{I}{I_0} = e^{\epsilon c l} \qquad (1.32)$$

or expressed as:

$$\log_{10}\frac{I}{I_0} = \varepsilon * c * l \qquad (1.33)$$

The parameter $log_{10}\frac{I}{I_0}$ corresponds to the optical density of the sample. Fluorescence emission intensity of weakly absorbing specimens is related to the molecular extinction coefficient by the following equation:

$$F = I_0(2.303\varepsilon cl)\varphi_f \quad (1.34)$$

Therefore, the emitted fluorescence is directly proportional to the intensity of incident radiation. These equations demonstrate and explain the difference in sensitivity between the two techniques - fluorescence and UV/Vis absorption spectroscopy. Fluorometric measurements are predominantly limited by the intensity of the radiation supplied to excite the sample and the ability of the instrument to detect the low levels of radiation (reported LDLs reaching 1.0 x 10^{-12} M). Whereas, the sensitivity of UV/Vis spectrophotometry depends on the capability of the spectrometer to distinguish between the two nearly equal absorption signals (I and I_0). Reported detection limits for the UV/Vis spectroscopy rarely approach 1.0 x 10^{-8} M.[149] Despite numerous limitations of UV/Vis and fluorescence spectroscopy, both techniques are routinely employed for the characterisation of optical sensors as demonstrated in Chapter 5.[150]

1.7 Improvements in ion selective electrodes

Polymer based ISEs are better known as electrochemical sensors that respond to changes in the activity of certain charged species in the presence of other ions. Many studies have been already devised to improve the detection limits, selectivity and robustness of such sensors as well as to widen their field of applications. Among several methods proposed to achieve the above-mentioned purposes, three main groups can be distinguished:

Technical methodologies – research directed towards developing new methodologies and experimental approaches and towards gaining a closer and more in-depth understanding of response characteristics of ISEs. This involves optimisation and modification of sensing protocols/methodologies and sensor's design to produce more robust and durable devices.

Chemical methods – studies primarily aimed to design and synthesise new membrane materials with the purpose of overcoming limitations placed on the sensing processes by the presence of traditionally used membrane's components. This includes the use of novel polymers, plasticisers, ionophores etc. for the preparation of sensing devices to improve their sensing characteristics/performance.

Combined approaches – main focus is placed on utilising newly synthesised materials for the development of ISEs with further response enhancements arising from the improvements in the sensing methodology.

Intuitively modifications to polymer based ISEs appear to be relatively simple, however care has to be taken as modified electrodes have to retain the integrity and stability (mechanical properties), working range and response characteristics (selectivity and detection limits).

This work explores the above-mentioned avenues demonstrating how the performance of ion selective electrodes and optical sensors can be improved either by the application of new sensing methodologies or by the use of novel membrane components to produce applied sensing devices.

References

(1)   Hulanicki, A.; Glab, S.; Ingman, F. *Pure Appl. Chem.* **1991**, *63* (9).

(2)   Janata, J. *Principles of chemical sensors*, 2nd ed.; Springer: Dordrecht ; New York, 2009.

(3)   Sekhar, P.; Brosha, E.; Mukundan, R.; Garzon, F. *Interface* **2010**, *19* (4), 35–40.

(4)   Pretsch, E. *TrAC Trends Anal. Chem.* **2007**, *26* (1), 46–51.

(5)   Dole, M. *J. Chem. Educ.* **1980**, *57* (2), 134.

(6)   Bakker, E.; Bühlmann, P.; Pretsch, E. *Chem. Rev.* **1997**, *97* (8), 3083–3132.

(7)   Hines, W. G.; de Levie, R. *J. Chem. Educ.* **2010**, *87* (11), 1143–1153.

(8)   Morf, W. E. *The principles of ion-selective electrodes and of membrane transport: [Tab.]*; Studies in analytical chemistry; Elsevier: Amsterdam, 1981.

(9)   Brand, M. J. D.; Rechnitz, G. A. *Anal. Chem.* **1970**, *42* (4), 478–483.

(10)   Švarc-Gajić, J.; Stojanović, Z.; Vasiljević, I.; Kecojević, I. *J. Food Drug Anal.* **2013**, *21* (4), 384–389.

(11)   Bühlmann, P.; Chen, L. D. In *Supramolecular Chemistry*; Gale, P. A., Steed, J. W., Eds.; John Wiley & Sons, Ltd: Chichester, UK, 2012.

(12)   Lundblad, R. L. *Biochemistry and molecular biology compendium*, Rev. ed.; CRC Press/Taylor & Francis Group: Boca Raton, FL, 2007.

(13)   Stefanac, Z.; Simon, W. *Chimia* **1966**, *20* (12), 436–440.

(14)   Cattrall, R. W.; Tribuzio, S.; Freiser, H. *Anal. Chem.* **1974**, *46* (14), 2223–2224.

(15)   Moody, G. J.; Oke, R. B.; Thomas, J. D. R. *The Analyst* **1970**, *95* (1136), 910.

(16)   Armstrong, R. D.; Horvai, G. *Electrochimica Acta* **1990**, *35* (1), 1–7.

(17)   Paczosa-Bator, B.; Piech, R.; Lewenstam, A. *Talanta* **2010**, *81* (3), 1003–1009.

(18)   Abramova, N.; Bratov, A. *Sensors* **2009**, *9* (9), 7097–7110.

(19)   Rao, M. P. *J. Polym. Sci. Polym. Lett. Ed.* **1981**, *19* (3), 149–149.

(20)   Sandler, S. R.; Karo, W. *Polymer syntheses*, 2nd ed.; Organic chemistry; Academic
         Press: Boston, 1992.

(21)   Malinowska, E.; Niedziółka, J.; Meyerhoff, M. E. *Anal. Chim. Acta* **2001**, *432* (1),
         67–78.

(22)   Abu-Shawish, H. M.; Saadeh, S. M.; Hussien, A. R. *Talanta* **2008**, *76* (4), 941–
         948.

(23)   Akhtar, T.; Alam, M. *Sens. Lett.* **2014**, *12* (11), 1637–1644.

(24)   Tsujimura, Y.; Sunagawa, T.; Yokoyama, M.; Kimura, K. *The Analyst* **1996**, *121*
         (11), 1705.

(25)   Alexander, P. W.; Dimitrakopoulos, T.; Hibbert, D. B. *Electroanalysis* **1997**, *9*
         (11), 813–817.

(26)   Lisak, G.; Grygolowicz-Pawlak, E.; Mazurkiewicz, M.; Malinowska, E.; Sokalski,
         T.; Bobacka, J.; Lewenstam, A. *Microchim. Acta* **2009**, *164* (3–4), 293–297.

(27)   Heng, L. Y.; Hall, E. A. H. *Anal. Chim. Acta* **2000**, *403* (1–2), 77–89.

(28)   Qin, Y.; Peper, S.; Bakker, E. *Electroanalysis* **2002**, *14* (19–20), 1375–1381.

(29)   Heng, L. Y.; Toth, K.; Hall, E. A. H. *Talanta* **2004**, *63* (1), 73–87.

(30)   Heng, L. v; Chern, L. H.; Ahmad, M. *Sensors* **2002**, *2* (8), 339–346.

(31)   Heng, L. Y.; Fang, T. H.; Chern, L. H.; Ahmad, M. *Sensors* **2003**, *3* (4), 83–90.

(32)   Berrocal, M. J.; Johnson, R. D.; Badr, I. H. A.; Liu, M.; Gao, D.; Bachas, L. G.
         Anal. Chem. **2002**, *74* (15), 3644–3648.

(33)   Mendecki, L.; Fayose, T.; Stockmal, K. A.; Wei, J.; Granados-Focil, S.; McGraw,
         C. M.; Radu, A. *Anal. Chem.* **2015**, *87* (15), 7515–7518.

(34)   Michalska, A. J.; Appaih-Kusi, C.; Heng, L. Y.; Walkiewicz, S.; Hall, E. A. H. *Anal. Chem.* **2004**, *76* (7), 2031–2039.

(35)   Rubinova, N.; Chumbimuni-Torres, K.; Bakker, E. *Sens. Actuators B Chem.* **2006**, *121* (1), 135–141.

(36)   Heng, L. Y.; Hall, E. A. H. *Electroanalysis* **2000**, *12* (3), 187–193.

(37)   Malinowska, E.; Gawart, L.; Parzuchowski, P.; Rokicki, G.; Brzózka, Z. *Anal. Chim. Acta* **2000**, *421* (1), 93–101.

(38)   Braun, D. *Int. J. Polym. Sci.* **2009**, *2009*, 1–10.

(39)   Qin, Y.; Bakker, E. *Anal. Chem.* **2001**, *73* (17), 4262–4267.

(40)   Madou, M. J.; Morrison, S. R. *Chemical sensing with solid state devices*; Academic Press: Boston, 1989.

(41)   Brar, A. S.; Charan, S. *J. Polym. Sci. Part Polym. Chem.* **1996**, *34* (3), 333–339.

(42)   Daniels, P. H. *J. Vinyl Addit. Technol.* **2009**, *15* (4), 219–223.

(43)   Szigeti, Z.; Vigassy, T.; Bakker, E.; Pretsch, E. *Electroanalysis* **2006**, *18* (13–14), 1254–1265.

(44)   M., M. In *Recent Advances in Plasticizers*; Luqman, M., Ed.; InTech, 2012.

(45)   Zahran, E. M.; New, A.; Gavalas, V.; Bachas, L. G. *The Analyst* **2014**, *139* (4), 757–763.

(46)   Rahman, M.; Brazel, C. *Prog. Polym. Sci.* **2004**, *29* (12), 1223–1248.

(47)   Ghandi, K. *Green Sustain. Chem.* **2014**, *4* (1), 44–53.

(48)   Bakker, E. *Talanta* **2004**, *63* (1), 3–20.

(49)   Telting-Diaz, M.; Bakker, E. *Anal. Chem.* **2001**, *73* (22), 5582–5589.

(50)   Bakker, E.; Pretsch, E. *Anal. Chim. Acta* **1995**, *309* (1–3), 7–17.

(51) Peper, S.; Qin, Y.; Almond, P.; McKee, M.; Telting-Diaz, M.; Albrecht-Schmitt, T.; Bakker, E. *Anal. Chem.* **2003**, *75* (9), 2131–2139.

(52) Rosatzin, T.; Bakker, E.; Suzuki, K.; Simon, W. *Anal. Chim. Acta* **1993**, *280* (2), 197–208.

(53) Qin, Y.; Bakker, E. *Anal. Chem.* **2003**, *75* (21), 6002–6010.

(54) Ebdon, L.; Ellis, A. T.; Corfield, G. C. *The Analyst* **1982**, *107* (1272), 288.

(55) Ebdon, L.; Ellis, A. T.; Corfield, G. C. *The Analyst* **1979**, *104* (1241), 730.

(56) Reinhoudt, D. N.; Engbersen, J. F. J.; Brzozka, Z.; van der Vlekkert, H. H.; Honig, G. W. N.; Holterman, H. A. J.; Verkerk, U. H. *Anal. Chem.* **1994**, *66* (21), 3618–3623.

(57) Rosatzin, T.; Holy, P.; Seiler, K.; Rusterholz, B.; Simon, W. *Anal. Chem.* **1992**, *64* (18), 2029–2035.

(58) Johnson, R. D.; Bachas, L. G. *Anal. Bioanal. Chem.* **2003**, *376* (3), 328–341.

(59) Bühlmann, P.; Pretsch, E.; Bakker, E. *Chem. Rev.* **1998**, *98* (4), 1593–1688.

(60) Bakker, E.; Willer, M.; Lerchi, M.; Seiler, K.; Pretsch, E. *Anal. Chem.* **1994**, *66* (4), 516–521.

(61) Bühlmann, P.; Umezawa, Y.; Rondinini, S.; Vertova, A.; Pigliucci, A.; Bertesago, L. *Anal. Chem.* **2000**, *72* (8), 1843–1852.

(62) Daunert, S.; Bachas, L. G. *Anal. Chem.* **1990**, *62* (14), 1428–1431.

(63) Nooredeen, N. M.; Abd El-Ghaffar, M. A.; Darwish, W. M.; Elshereafy, E.; Radwan, A. A.; Abbas, M. N. *J. Solid State Electrochem.* **2015**, *19* (7), 2141–2154.

(64) Püntener, M.; Fibbioli, M.; Bakker, E.; Pretsch, E. *Electroanalysis* **2002**, *14* (19–20), 1329–1338.

(65)   Püntener, M.; Vigassy, T.; Baier, E.; Ceresa, A.; Pretsch, E. *Anal. Chim. Acta* **2004**, *503* (2), 187–194.

(66)   Nooredeen Abbas, M.; Radwan, A.-L. A.; Nawwar, G. A.; Zine, N.; Errachid, A. *Anal Methods* **2015**, *7* (3), 930–942.

(67)   Lindner, E.; Cosofret, V. V.; Kusy, R. P.; Buck, R. P.; Rosatzin, T.; Schaller, U.; Simon, W.; Jeney, J.; Tóth, K.; Pungor, E. *Talanta* **1993**, *40* (7), 957–967.

(68)   Cross, G. G.; Fyles, T. M.; Suresh, V. V. *Talanta* **1994**, *41* (9), 1589–1596.

(69)   Qin, Y.; Bakker, E. *Anal. Chem.* **2004**, *76* (15), 4379–4386.

(70)   Nägele, M.; Mi, Y.; Bakker, E.; Pretsch, E. *Anal. Chem.* **1998**, *70* (9), 1686–1691.

(71)   Oehme, M.; Simon, W. *Anal. Chim. Acta* **1976**, *86*, 21–25.

(72)   Newman, J. S.; Thomas-Alyea, K. E. *Electrochemical systems*, 3rd ed.; J. Wiley: Hoboken, N.J, 2004.

(73)   Morf, W. E. *Anal. Chem.* **1977**, *49* (6), 810–813.

(74)   Mikhelson, K. N.; Lewenstam, A.; Didina, S. E. *Electroanalysis* **1999**, *11* (10–11), 793–798.

(75)   Bakker, E.; Pretsch, E.; Bühlmann, P. *Anal. Chem.* **2000**, *72* (6), 1127–1133.

(76)   Umezawa, Y.; Umezawa, K.; Sato, H. *Pure Appl. Chem.* **1995**, *67* (3).

(77)   Bakker, E. *Anal. Chem.* **1997**, *69* (6), 1061–1069.

(78)   Mikhelson, K. N. *Ion-selective electrodes*; Lecture notes in chemistry; Springer: Berlin, 2013.

(79)   Gadzekpo, V. P. .; Christian, G. . *Anal. Chim. Acta* **1984**, *164*, 279–282.

(80)   Bakker, E.; Meruva, R. K.; Pretsch, E.; Meyerhoff, M. E. *Anal. Chem.* **1994**, *66* (19), 3021–3030.

(81) Tohda, K.; Dragoe, D.; Shibata, M.; Umezawa, Y. *Anal. Sci. Int. J. Jpn. Soc. Anal. Chem.* **2001**, *17* (6), 733–743.

(82) *IUPAC Compendium of Chemical Terminology: Gold Book*, 2.1.0.; Nič, M., Jirát, J., Košata, B., Jenkins, A., McNaught, A., Eds.; IUPAC: Research Triagle Park, NC, 2009.

(83) Yajima, S.; Tohda, K.; Bühlmann, P.; Umezawa, Y. *Anal. Chem.* **1997**, *69* (10), 1919–1924.

(84) Mathison, S.; Bakker, E. *Anal. Chem.* **1998**, *70* (2), 303–309.

(85) Sokalski, T.; Ceresa, A.; Zwickl, T.; Pretsch, E. *J. Am. Chem. Soc.* **1997**, *119* (46), 11347–11348.

(86) Gyurcsányi, R. E.; Pergel, É.; Nagy, R.; Kapui, I.; Thu Lan, B. T.; Tóth, K.; Bitter, I.; Lindner, E. *Anal. Chem.* **2001**, *73* (9), 2104–2111.

(87) Sokalski, T.; Ceresa, A.; Fibbioli, M.; Zwickl, T.; Bakker, E.; Pretsch, E. *Anal. Chem.* **1999**, *71* (6), 1210–1214.

(88) Ceresa, A.; Bakker, E.; Hattendorf, B.; Günther, D.; Pretsch, E. *Anal. Chem.* **2001**, *73* (2), 343–351.

(89) Qin, W.; Zwickl, T.; Pretsch, E. *Anal. Chem.* **2000**, *72* (14), 3236–3240.

(90) Chumbimuni-Torres, K. Y.; Rubinova, N.; Radu, A.; Kubota, L. T.; Bakker, E. *Anal. Chem.* **2006**, *78* (4), 1318–1322.

(91) Maj-Zurawska, M.; Sokalski, T.; Hulanicki, A. *Talanta* **1988**, *35* (4), 281–286.

(92) Peper, S.; Gonczy, C. *Int. J. Electrochem.* **2011**, *2011*, 1–8.

(93) Ceresa, A.; Sokalski, T.; Pretsch, E. *J. Electroanal. Chem.* **2001**, *501* (1–2), 70–76.

(94) Vigassy, T.; Gyurcsányi, R. E.; Pretsch, E. *Electroanalysis* **2003**, *15* (5–6), 375–382.

(95)   Peper, S.; Ceresa, A.; Bakker, E.; Pretsch, E. *Anal. Chem.* **2001**, *73* (15), 3768–3775.

(96)   Vigassy, T.; Morf, W. E.; Badertscher, M.; Ceresa, A.; de Rooij, N. F.; Pretsch, E. *Sens. Actuators B Chem.* **2001**, *76* (1–3), 477–482.

(97)   Gründler, P. *Chemical sensors an introduction for scientists and engineers*; Springer: Berlin; London, 2007.

(98)   Mistlberger, G.; Xie, X.; Pawlak, M.; Crespo, G. A.; Bakker, E. *Anal. Chem.* **2013**, *85* (5), 2983–2990.

(99)   Lerchi, M.; Bakker, E.; Rusterholz, B.; Simon, W. *Anal. Chem.* **1992**, *64* (14), 1534–1540.

(100)   Lerchi, M.; Reitter, E.; Simon, W.; Pretsch, E.; Chowdhury, D. A.; Kamata, S. *Anal. Chem.* **1994**, *66* (10), 1713–1717.

(101)   Balaconis, M. K.; Clark, H. A. *Anal. Chem.* **2012**, *84* (13), 5787–5793.

(102)   Xie, X.; Zhai, J.; Crespo, G. A.; Bakker, E. *Anal. Chem.* **2014**, *86* (17), 8770–8775.

(103)   Mistlberger, G.; Crespo, G. A.; Bakker, E. *Annu. Rev. Anal. Chem.* **2014**, *7* (1), 483–512.

(104)   Bakker, E.; Crespo, G.; Grygolowicz-Pawlak, E.; Mistlberger, G.; Pawlak, M.; Xie, X. *Chimia* **2011**, *65* (3), 141–149.

(105)   Shvarev, A. *J. Am. Chem. Soc.* **2006**, *128* (22), 7138–7139.

(106)   Xie, X.; Mistlberger, G.; Bakker, E. *J. Am. Chem. Soc.* **2012**, *134* (41), 16929–16932.

(107)   Watanabe, S. *Fluorophores: characterization, synthesis and applications*; Chemical engineering methods and technology; Nova Science Publishers, Inc: Hauppauge, New York, 2013.

(108) Shamsipur, M.; Alizadeh, K.; Hosseini, M.; Caltagirone, C.; Lippolis, V. *Sens. Actuators B Chem.* **2006**, *113* (2), 892–899.

(109) Aragoni, M. C.; Arca, M.; Bencini, A.; Blake, A. J.; Caltagirone, C.; De Filippo, G.; Devillanova, F. A.; Garau, A.; Gelbrich, T.; Hursthouse, M. B.; Isaia, F.; Lippolis, V.; Mameli, M.; Mariani, P.; Valtancoli, B.; Wilson, C. *Inorg. Chem.* **2007**, *46* (11), 4548–4559.

(110) Valeur, B. *Coord. Chem. Rev.* **2000**, *205* (1), 3–40.

(111) Ghosh, P.; Bharadwaj, P. K.; Roy, J.; Ghosh, S. *J. Am. Chem. Soc.* **1997**, *119* (49), 11903–11909.

(112) Ramachandram, B.; Samanta, A. *Chem. Commun.* **1997**, No. 11, 1037–1038.

(113) Sakamoto, H.; Ishikawa, J.; Nakao, S.; Wada, H. *Chem. Commun.* **2000**, No. 23, 2395–2396.

(114) Fabbrizzi, L.; Licchelli, M.; Pallavicini, P.; Sacchi, D.; Taglietti, A. *The Analyst* **1996**, *121* (12), 1763.

(115) Qian, X.; Xu, Z. *Chem Soc Rev* **2015**, *44* (14), 4487–4493.

(116) You, Y.; Lee, S.; Kim, T.; Ohkubo, K.; Chae, W.-S.; Fukuzumi, S.; Jhon, G.-J.; Nam, W.; Lippard, S. J. *J. Am. Chem. Soc.* **2011**, *133* (45), 18328–18342.

(117) Woo, H.; Cho, S.; Han, Y.; Chae, W.-S.; Ahn, D.-R.; You, Y.; Nam, W. *J. Am. Chem. Soc.* **2013**, *135* (12), 4771–4787.

(118) Carter, K. P.; Young, A. M.; Palmer, A. E. *Chem. Rev.* **2014**, *114* (8), 4564–4601.

(119) Domaille, D. W.; Que, E. L.; Chang, C. J. *Nat. Chem. Biol.* **2008**, *4* (3), 168–175.

(120) Hoebe, R. A.; Van Oven, C. H.; Gadella, T. W. J.; Dhonukshe, P. B.; Van Noorden, C. J. F.; Manders, E. M. M. *Nat. Biotechnol.* **2007**, *25* (2), 249–253.

(121) Grzelak, A.; Rychlik, B.; Bartosz, G. *Free Radic. Biol. Med.* **2001**, *30* (12), 1418–1425.

(122) Godley, B. F.; Shamsi, F. A.; Liang, F.-Q.; Jarrett, S. G.; Davies, S.; Boulton, M. *J. Biol. Chem.* **2005**, *280* (22), 21061–21066.

(123) Pattison, D. I.; Davies, M. J. *EXS* **2006**, No. 96, 131–157.

(124) Shamsipur, M.; Mohammadi, M.; Taherpour, A. (Arman); Garau, A.; Lippolis, V. *RSC Adv* **2015**, *5* (112), 92061–92070.

(125) Pickup, J. C.; Hussain, F.; Evans, N. D.; Rolinski, O. J.; Birch, D. J. S. *Biosens. Bioelectron.* **2005**, *20* (12), 2555–2565.

(126) Miao, Q.; Li, Q.; Yuan, Q.; Li, L.; Hai, Z.; Liu, S.; Liang, G. *Anal. Chem.* **2015**, *87* (6), 3460–3466.

(127) Saha, T.; Sengupta, A.; Hazra, P.; Talukdar, P. *Photochem Photobiol Sci* **2014**, *13* (10), 1427–1433.

(128) Jiang, Q.; Guo, Z.; Zhao, Y.; Wang, F.; Mao, L. *The Analyst* **2015**, *140* (1), 197–203.

(129) Kuo, S.-Y.; Li, H.-H.; Wu, P.-J.; Chen, C.-P.; Huang, Y.-C.; Chan, Y.-H. *Anal. Chem.* **2015**, *87* (9), 4765–4771.

(130) Ghosh, S. *Fundamentals of electrical and electronics engineering*; Prentice-Hall of India: New Delhi, 2003.

(131) *Impedance spectroscopy: theory, experiment, and applications*, 2nd ed.; Barsoukov, E., Macdonald, J. R., Eds.; Wiley-Interscience: Hoboken, N.J, 2005.

(132) Orazem, M. E.; Tribollet, B. *Electrochemical impedance spectroscopy*; The Electrochemical Society series; Wiley: Hoboken, N.J, 2008.

(133) Macdonald, J. R.; Johnson, W. B. In *Impedance Spectroscopy*; Barsoukov, E., Macdonald, J. R., Eds.; John Wiley & Sons, Inc.: Hoboken, NJ, USA, 2005; pp 1–26.

(134) Martinhon, P. T.; Carreño, J.; Sousa, C. R.; Barcia, O. E.; Mattos, O. R. *Electrochimica Acta* **2006**, *51* (15), 3022–3028.

(135) De Marco, R.; Jiang, Z.-T.; Pejcic, B.; van Riessen, A. *Electrochimica Acta* **2006**, *51* (23), 4886–4891.

(136) Toth, K.; Graf, E.; Horvai, G.; Pungor, E.; Buck, R. P. *Anal. Chem.* **1986**, *58* (13), 2741–2744.

(137) Mikhelson, K. N. *Chem. Anal.* **2006**, *51* (6), 853–867.

(138) De Marco, R.; Ng, A.; Panduwinata, D. *Electroanalysis* **2008**, *20* (3), 313–317.

(139) Radu, A.; Anastasova-Ivanova, S.; Paczosa-Bator, B.; Danielewski, M.; Bobacka, J.; Lewenstam, A.; Diamond, D. *Anal. Methods* **2010**, *2* (10), 1490.

(140) Buck, R. P. *Ion-Sel. Electrode Rev.* **1982**, *4*, 3–74.

(141) *Electrochemical dictionary*, 2., and extended ed.; Bard, A. J., Inzelt, G., Scholz, F., Eds.; Springer: Berlin, 2012.

(142) Horvai, G.; Graf, E.; Toth, K.; Pungor, E.; Buck, R. P. *Anal. Chem.* **1986**, *58* (13), 2735–2740.

(143) Ye, Q.; Vincze, A.; Horvai, G.; Leermakers, F. A. . *Electrochimica Acta* **1998**, *44* (1), 125–132.

(144) O'Rourke, M.; Duffy, N.; Marco, R. D.; Potter, I. *Membranes* **2011**, *1* (2), 132–148.

(145) Brown, W. H.; Iverson, B. L.; Anslyn, E. V.; Foote, C. S. *Organic chemistry*, 7th edition.; Wadsworth Cengage Learning: Australia ; Belmont, CA, 2014.

(146)   Armstrong, R. D.; Covington, A. K.; Proud, W. G. *J. Electroanal. Chem. Interfacial Electrochem.* **1988**, *257* (1–2), 155–160.

(147)   Harris, D. C. *Quantitative chemical analysis*, 8th ed.; W.H. Freeman and Co: New York, 2010.

(148)   Hollas, J. M. *Modern spectroscopy*, 3rd ed.; J. Wiley: Chichester ; New York, 1996.

(149)   Sharma, A.; Schulman, S. G. *Introduction to fluorescence spectroscopy*; Techniques in analytical chemistry series; Wiley: New York, 1999.

(150)   *Handbook of optical sensors*; Santos, J. L., Farahi, F., Eds.; CRC Press, Taylor & Francis Group: Boca Raton, FL, 2015.

CHAPTER 2 Robust and ultrasensitive polymer membrane-based carbonate-selective electrodes.

2.1 Introduction

In this chapter, modifications to the conditioning protocol that is required for the preparation of ISEs are proposed. This is expected to improve the individual sensing parameters of ISEs such as limits of detection and selectivity as well as to enhance their overall performance for the purpose of broadening their applications.

With the discovery of importance of transmembrane zero-current ion fluxes, major adjustments to the composition of inner filling solution of liquid contact electrodes were performed (see Chapter 1 - Sensitivity) resulting in the enhancement of lower detection limits and suppression of super-Nernstian responses.[1–5] Since these processes rely strongly on the alterations in the local ion concentration on the sample side of the membrane, modifications that prevent leaching of primary ions and sensing components (ionophore, ionic sites) from a membrane segment into the sample are expected to produce even better response characteristics. For example, it has been reported that the effective concentration of primary ions at the phase boundary can be changed by blocking the surface of a membrane with various surfactants (they regulate the release of primary ions from the membrane thus increasing the concentration of ion-ionophore complexes).[6]

More recently, scientists have focused on the use of solid contact electrodes (SCEs) as it was believed that the lack of inner filling solution will eliminate the presence of outward ion fluxes and thus offer large improvements in lower detection limits.[7] However, the performance of SCEs never matched the theoretical expectations. It was hypothesised that some impurities such as interfering ions can be extracted into the membrane subsequently triggering ion exchange at the phase boundary causing worsening of lower detection limits. Moreover, formation of a water layer at the metal-membrane interface may induce transmembrane ion fluxes resulting in LODs similar to liquid contact electrodes (LCEs) with optimised inner filling solution.[8] The above-mentioned degradation in the response of ISEs occurs since resulting water layer can serve as electrolyte reservoir that undergoes re-equilibration process each time the electrode is in contact with a sample of different composition.[8] This triggers ion transport and results in changes in the concentration of primary ions at the phase boundary (see Sensitivity, Chapter 1).

Furthermore, the ion to electron transduction in SCEs between the electrical conductor and ionically conducting ion selective membrane is poor (blocked interface) leading to significant potential instability.[7,9] Considerable efforts have been spent on the fabrication of hydrogel layers[10] and conductive polymers that could be inserted between the ion selective membrane and the underlying metal wire to suppress water layer formation and to provide a stable and reproducible electrode response. Especially, the application of conductive polymers such as poly(pyrrole),[11–14] poly(thiophene),[15] poly(3,4-ethylenedioxythiophene),[16] poly(indole)[17] and poly(aniline)[18,19] have gained widespread popularity within the field of SCEs as they provide sufficiently high redox capacitance

required to minimise the polarisability of the solid contact electrode.[20] This improves the process of the ion to electron transduction that takes place at the solid contact (eq. 2.1).[21]

$$M^+A^- + e^- \rightleftarrows M + A^- \qquad (2.1)$$
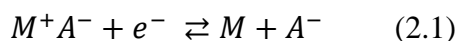
Where M^+ refers to a metal ion (e.g. Ag^+) or oxidised conducting polymer unit, e^- is an electron, M represents metal contact (e.g. Ag) or neutral conducting polymer unit, A^- is anion (e.g. Cl$^-$).

Typically, conductive polymers can be deposited onto the solid contact directly from the solution for instance via drop casting or by the means of electrochemical polymerisation of a large variety of monomers.[22] In the field of ISEs, conductive polymers can be used to enhance the ion to electron transduction where the characteristics of the sensing process are defined by the ion selective membrane.[14,23–25] If the conductive polymer can be dissolved in the same solvent as used for the preparation of ion selective membranes (e.g. dissolves ionic sites, ionophore and polymer), a single piece ISEs can be fabricated.[26] There have been also several reports demonstrating the functionality of conductive polymers in which the ion recognition components are covalently attached to the polymer backbone. However, to optimise the ion recognition and transduction processes, a very precise control of the electronic and ionic transport characteristics is required.[27]

Another approach to even further inhibit water layer formation and to increase the overall stability of ISEs involves the replacement of traditionally based PVC membranes with more hydrophobic, water repelling polymeric architectures, for instance - poly(methyl methacrylate) and poly(decyl methacrylate) or other methacrylic-acrylic copolymers.[28,29] Such modifications are very advantageous for the fabrication of robust and durable solid contact ISEs that can be further miniaturised for wide range of applications such as environmental monitoring and clinical analysis.

On many occasions, these above-mentioned strategies rely on tedious and sometimes lengthy preparatory protocols. While slopes and LDLs are normally stable for months, some small losses of LDLs of ~0.5-1 orders of magnitude are typically observed within the first week of electrode's shelf-life. These losses can be attributed to the re-establishment of small outward ion fluxes. Despite their simplicity, low cost, and ability to determine the bioavailable fraction of ions[25,30,31] the LDLs deterioration upon storage and the need for complex conditioning or preparation protocols have rendered them unreliable for in field applications. Notwithstanding the ISEs excellent potential for miniaturisation[32] their application in long-term analysis of small volumes (e.g. cells) is unsuitable due to outward ion fluxes compromising the integrity of the sample.

2.2 Carbonate determination

The widespread occurrence of carbonate species (CO_3^{2-}, HCO_3^- and CO_2) in environmental, industrial and clinical samples makes the determination of carbonate content an on-going area of interest. The latter is of particularly high importance as carbon dioxide species are present in the majority of body fluids and organs where they play a

crucial role in the acid-base and electrolyte balance in the human body.[33] Therefore, any changes in carbonate activity are often accompanied by changes in the concentration of other ions and pH. Since the human body pH is regulated by the pulmonary and renal mechanisms, the rapid and precise determination of carbonate compounds in biological fluids is highly important as it can indicate the malfunction of these processes.[34] Moreover, ever increasing concerns for ecological issues such as ocean acidification caused by the dissolution of carbon dioxide drive even further the need for more effective carbonate detection methods and selective and versatile sensors.[35–37] Numerous techniques including Fourier transform infrared spectroscopy (FTIR),[38,39] UV/Vis absorbance,[40] gas chromatography (GC),[41] passive acoustic emission[42] and potentiometric CO_2 gas sensors[43,44] have been proposed for the detection and quantification of carbonate species. However, the high operational and maintenance costs make the current approaches unsuitable for widespread point-of-care testing and on-site environmental analysis. This has created a demand for a fast, reliable, and portable analytical technique. Ion selective electrodes meet all of these requirements and, with recent development in solid-contact electrode manufacturing processes, are becoming increasingly common in health[45] and environmental[46] applications. However, the development of solid-contact electrodes with ultra-low detection limits and reproducible and stable standard potentials is still a great challenge.

So far the application of carbonate selective electrodes was rather limited due to the insufficient selectivity and sensitivity of these sensors. The first reported carbonate sensors were based on tri-fluoroacetyl-p-butylbenzene derivatives.[47,48] However, they suffered from the limited selectivity and sensitivity towards carbonate in the presence of salicylates,

perchlorates or thiocyanates. Several attempts were undertaken to improve selectivity by either optimising the effective concentration of membrane's components,[49] introducing the acceptor substituents at the para position of the phenyl ring of trifluoroacetophenone (TFA) based membranes,[50] increasing the pH[51] or adding extra layers that alkalise electrode surface.[52] Unfortunately, the interferences arising from the presence of chloride and salicylate anions still prevent the practical application of carbonate selective electrodes. Therefore, significant efforts are still being made to design a better sensor that demonstrates sufficient selectivity and sensitivity to carbonate species. In recent times, extensive research has been directed towards the design of new ion binding ligands that are based on pyrroles, guanidium or amides to improve the sensing process.[53,54] Especially, novel diamide receptors are of particular interest as they exhibit strong and selective binding to the anions due to their inherent flexibility (permits adjustments in the cavity size) and ability to form strong hydrogen bonds.[55] Despite significant improvements in the selectivity and detection limits, the synthesis of new materials can be challenging and requires all compounds to be characterised prior their practical use.

In this work a new methodology that aims to suppress or even fully eliminate outward ion fluxes (in the direction of the sample solution) has been developed thus offering large improvements in sensitivity and robustness of polymer membrane-based ion-selective electrodes. Such modifications led to the development of a chemical sensor with ultra-low detection limits and high selectivity for the detection of carbonate ions without any sample pre-concentration and/or instrumental signal enhancement.

2.3 Experimental

2.3.1 Materials

Tridodeclymethylamonium (TDMACl), ammonium ionophore I (nonactin), sodium tetrakis[3,5-bis(trifluoromethyl)phenyl]borate (NaTFPB) and sodium bicarbonate were purchased from Fluka. The synthesis of carbonate ionophore (diamide N,N1-bis(2,4-dinitrophenyl)isophthalohydrazide) was modified from Jain et al (2006).[55] and the synthesised ionophore was kindly provided by the research group led by Granados-Focil (Figure 2.1). All chemicals were of analytical reagent grade. Solutions of metal ions were prepared in ultra-pure water obtained with Pico Pure 3 water system. Working solutions of different activities were prepared by serial dilutions of a 0.1 M stock solution. DropSens Dual Carbon Screen-printed Electrodes (C1110) were purchased from Metrohm USA.
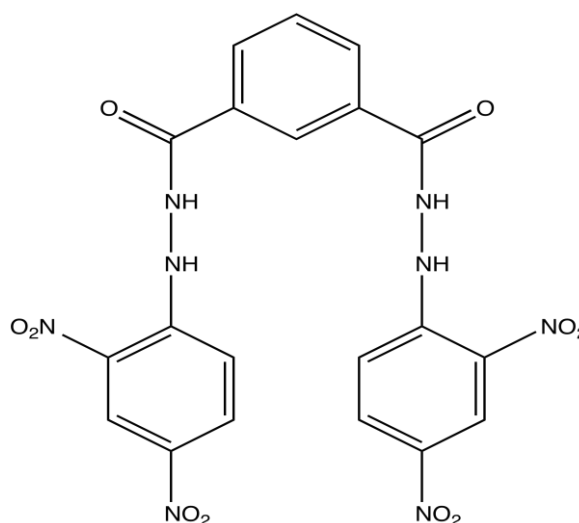
Figure 2.1 Chemical structure of the carbonate ionophore used in this study.

2.3.2 Preparation of copolymer D

Self-plasticised poly(lauryl methacrylate and methyl methacrylate) copolymer, also referred as copolymer D (63 mol % lauryl methacrylate (LMA), 37 mol % methyl-methacrylate (MMA) was synthesised via (0.1 eq) azobisisobutyronitrile (AIBN) initiated free radical polymerisation. LMA and MMA were firstly passed through a silica plug to remove an inhibitor. All reagents were then dissolved in tetrahydrofuran (THF) and run under reflux at 75°C for 24 h. Solvent was removed via rotary evaporation and the resulting copolymer was dissolved in dichloromethane (DCM) and reprecipitated from methanol. This was repeated until no traces of starting material were present in the resulting copolymer. ^{1}H NMR (200 MHz, CDCl$_3$, δ): δ 3.93 (br, 2H, COOCH$_2$), 3.59 (br, 3H, COOCH$_3$), 1.89 – 0.88 (m, COOCH$_2$(CH$_2$)$_{10}$CH$_3$).

2.3.3 Electrode preparation

The intermediate conducting layer composed of poly(3,4-ethylenedioxythiophene-2,5 diyl) (PEDOT) was electrochemically polymerised onto the solid contact electrodes (SCEs) by immersing the platforms into a solution of 0.2 M 3,4-ethylenedioxythiophene (EDOT), and 0.2 M tetrabutylammonium chloride in acetonitrile and using the SCE as a cathode and a graphite anode. Electropolymerisations were performed galvanostatically at 50 mA for 10 minutes using a Hewlett Packard E3630A potentiostat. (E3630A). The SCEs were left to dry for 24 h at room temperature and then placed in a room-temperature vacuum oven for 1 h before applying ion selective membranes.

2.3.4 Traditional carbonate sensing membranes

Traditional carbonate selective electrodes were prepared by dissolving carbonate ionophore (76 mmol/kg or 4% wt), TDMACl (11 mmol/kg or 1% wt) and copolymer D (95% wt) in 0.5 ml of THF. After the complete dissolution of all components the aliquot was drop cast onto the top of the PEDOT layer and left at room temperature to dry overnight. The following day, the carbonate selective electrodes were placed in 0.1 M solution of $NaHCO_3$ for 24 h. Note that pH of this solutions was ~8.4 resulting in ~10^{-3} M of CO_3^{2-}.

2.3.5 Ionophore-free carbonate sensing membranes

Ionophore-free membranes were prepared by dissolving the desired amount of TDMACl and copolymer D totalling 100 mg in 0.5 mL of THF. After the complete dissolution of all components the aliquot was drop cast onto the top of the PEDOT layer and left at room temperature to dry overnight. The following day, the carbonate selective electrodes were placed in 1 mg solution of carbonate ionophore in 0.5 mL THF and 20 mL ultra-pure water. Conditioning time was varied between 1 h and 24 h.

2.3.6 Preparation of optimised carbonate selective membranes

Optimised carbonate selective electrodes were prepared by dissolving carbonate ionophore (76 mmol/kg or 4% wt), TDMACl (11 mmol/kg or 1% wt) and copolymer (95% wt) in 0.5 ml of THF. After the complete dissolution of all components the aliquot was drop cast onto the top of the PEDOT layer and left at room temperature to dry overnight. The following day, the carbonate selective electrodes were placed in 1 mg solution of carbonate

ionophore in 0.5 mL THF and 20 mL ultra-pure water. Conditioning time was varied between 1 h and 24 h.

2.3.7 Preparation of ammonium and iodide selective electrodes

Traditional ammonium selective electrodes were prepared by dissolving 10 mmol/kg of ammonium ionophore, 5 mmol/kg of NaTFPB and PVC:DOS 33% : 66% wt in 1 ml THF. Iodide selective electrodes were prepared by dissolving 10 mmol/kg of iodide ionophore (mercuracarborand-3), 7.5 mmol/kg of TDMACl and the synthesised copolymer D (99% wt) in 1 ml of THF. After the complete dissolution of all components the aliquot was drop cast onto the top of the electrode and left at room temperature to dry overnight. The following day, the ammonium-selective and iodide-selective electrodes were placed for 24 h in 1.0×10^{-3} M solution of ammonium nitrate (NH_4NO_3) and potassium iodide (KI) respectively. The optimisation of the conditioning protocol was performed by placing electrodes in a solution of appropriate ionophore according to the protocol described above (1 mg solution of ionophore in 0.5 mL THF and 20 mL ultra-pure water for 24 h). The following day, electrodes were kept for 24 h in 1.0×10^{-5} M solutions of NH_4NO_3 and KI respectively.

2.3.8 Artificial seawater preparation

Artificial seawater (ASW) was prepared as proposed by Roy et al (1993),[56] with some modifications. Approximately 1 kg of distilled water was purged using $N_{2(g)}$ prior to salt addition. Table 2.1 demonstrates the molalities of each salt used for the preparation of ASW. The appropriate amounts of $MgCl_2$ and $CaCl_2$ were added from 1 M stock solutions of $MgCl_2 \cdot 6H_2O$ and anhydrous $CaCl_2$ respectively. All other salts were re-crystallised, oven dried overnight at 110°C, and added as solids. The seawater was adjusted to a known

dissolved inorganic carbon (DIC) of 2 mmol/kg using $NaHCO_3$. ASW was kept tightly sealed and covered with Parafilm to ensure no further dissolution of CO_2.

Table 2.1 The molalities of salts used for the preparation of artificial seawater for carbonate determination.

Salt	Molality (mol/kg)
NaCl	0.42764
Na_2SO_4	0.02927
KCl	0.01058
$MgCl_2$	0.05475
$CaCl_2$	0.01075
$NaHCO_3$	0.00200

2.3.9 Characterisation

Potentiometric responses were recorded with a Lawson Labs Inc. 16-channel EMF-16 interface (3217 Phoenixville Pike Malvern, PA 19355, USA) in a stirred solution using the Pinnacle Series H4403-2B as reference electrode. A glass VWR symphony 14002-780 Ag/AgCl pH electrode was used for pH measurements.

2.3.10 UV/Vis experiments

Ultraviolet-visible (UV/Vis) spectra were recorded using a Unicam UV500 double beam spectrophotometer (Unicam Instruments Ltd, UK). For monitoring of ionophore

partitioning into the membrane, carbonate specific ISEs were immersed in solution of ionophore as described above (1 mg solution of carbonate ionophore in 0.5 mL THF and 20 mL ultra-pure water) and diffusion of ionophore into the membrane was monitored using UV/Vis spectroscopy at 370 nm.

2.3.11 Selectivity

For selectivity measurements separate solution method was selected and the optimised carbonate selective membranes were prepared and applied onto the electrodes according to the protocol described in Chapter 2 - Preparation of optimised carbonate selective membranes. Each electrode was then left at room temperature to dry overnight. The following day, the carbonate selective membranes were placed in degassed solution of carbonate ionophore (1 mg) in ultra-pure water (20 mL) and THF (0.5 ml) and responses towards all ions were recorded according to separate solution method as described by Bakker.[57]

2.4 Results and discussion

Traditionally, during the preparation of ISEs, the ionophore is loaded into the membrane cocktail. Upon casting, drying, and conditioning, established ion fluxes can result in poisoned sample/membrane interface as illustrated in Figure 2.2A. This often results in a less than optimal performance of ISEs especially when ultra-sensitive measurements are performed. The approach proposed herein is analogous to the successful (but impractical) approach of using ion buffers in the sample to maintain low and constant ion activity at the sample/membrane interface.[58] This new methodology includes buffering the carbonate in the membrane side of the sample/membrane interface by using an excess of ionophore introduced from sample side. This involves a short (~60 min) conditioning of, in principle, dry electrode in the solution of ionophore. The lipophilic ionophore partitions into the membrane, which draws the carbonate ions from the aqueous side of sample/membrane interface into the membrane. This process recovers sample/membrane interface as illustrated in Figure 2.2B and consequently allows significant improvement of LDL.
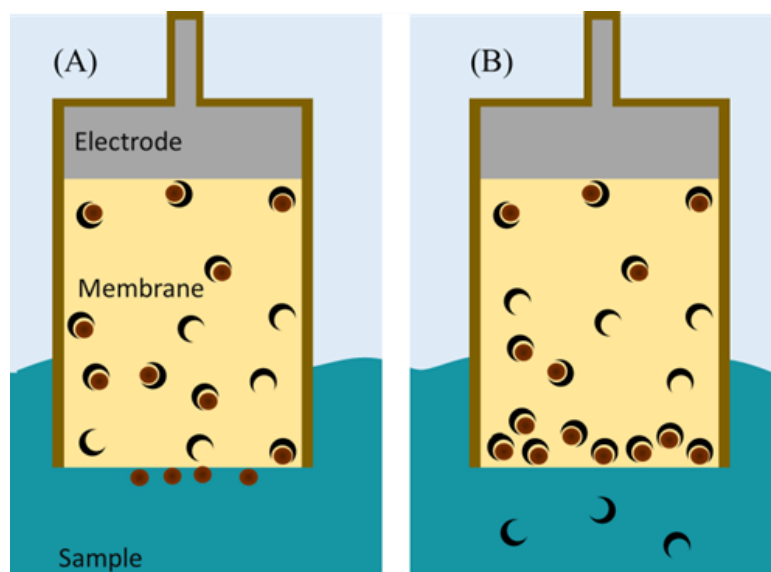
Figure 2.2 Schematic representation of state of ion-selective membranes after traditional conditioning (A) and after conditioning protocol suggested here (B). In the situation (A) the membrane is loaded with ionophore (black half-moons) followed by conditioning in the solution of primary ions (brown circles). Establishment of ion fluxes results in leaching of primary ions and their accumulation at the sample/membrane interface. In the situation (B), following the traditional conditioning the membrane is exposed to the solution of ionophore. It complexes ions at the sample/membrane interface and partitions in the membrane thus replenishing phase boundary.

In traditional solid-contact ISEs, outward ion fluxes are attributed to the ion exchange at the membrane-sample phase boundary as illustrated in Figure 2.3A and equation 2.2.

$$J^-_{aq,PB} + [AL^-]'_{org,PB} \rightarrow A^-_{aq,PB} + [JL^-]'_{org,PB} \qquad (2.2)$$
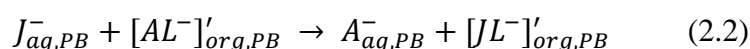
J^- and A^- represent interfering and primary ions respectively. $[AL^-]'$ is an analyte-ionophore complex at the phase boundary (PB) and $[JL^-]'$ is a complex of ionophore with an interfering ion. It can be hypothesised that the introduction of the ionophore (L) at the membrane-sample interphase will result in the complexation of diffused primary ions

according to equation 2.3: Due to the lipophilicity of ionophore, the [AL⁻]″ complex accumulates at the membrane side of the phase boundary and leads towards establishment of ion fluxes towards the bulk of the membrane as illustrated in Figure 2.3B.

$$A^-_{aq,PB} + L_{aq,PB} \rightarrow [AL^-]''_{org,PB} \qquad (2.3)$$

This step is achieved by conditioning the membrane in a solution of ionophore. The relatively low hydrophilicity of the ionophore promotes its diffusion from the conditioning solution into the membrane.

Note that the processes described in equations 2.2 and 2.3 occur at the same time and are mutually competitive. It is therefore expected that the concentration of carbonate ionophore within the membrane bulk is not uniform, as the majority of the ionophore will be deposited at the phase boundary at the membrane side. In an optimal case [AL⁻]' and [AL⁻]" are balanced leading towards the uniform concentration of [AL⁻] in the membrane and complete diminishing of ion fluxes (Figure 2.3C).

However, in non-optimised cases the dynamic process described in Figure 2.3B would have multifaceted consequences on the membrane response. For example:

1) Life-time - immediately after initial conditioning in solution of ionophore significant improvements in low detection limit (LDL) are expected due to the removal of primary ions from the sample side of sample/membrane interface. In the case in which

$[AL^-]'' \ll [AL^-]'$ eventual re-establishment of outward ion membrane fluxes is expected resulting in diminishing of improved LDLs. Initial concentration of ionophore in the membrane, ionophore partitioning coefficient and the diffusion coefficient of the ion-ionophore complex are expected to be determining factors for the practical usability of electrodes with improved LDLs.

2) Upper detection limit (UDL) - immediately after the conditioning of electrode in the solution of ionophore due to its complexation of free primary ions at the sample side of the sample/membrane phase boundary and the portioning of this complex into the membrane, the membrane side of phase boundary would be saturated with ion-ionophore complex. Depending on the concentration of primary ions at the sample side of phase boundary and the rate of partitioning of ion-ionophore complex into the membrane, the membrane side would have very limited (or even non-existent) concentration of free ionophore. In the situation in which there is no free ionophore the membrane response would exhibit Donnan failure (complete loss of response and/or response to counter ions).[59,60]

3) Selectivity - due to the extraction of additional amount of ionophore into the membrane the ionophore : ion-exchanger ratio (L:R) would be temporarily disturbed. Previous works have shown that there is an optimal L:R ratio that produces optimal selectivity.[61] The disturbance of the L:R ratio would very likely prevent from accurate determination of selectivity coefficients at least until the ion fluxes are completely equilibrated (Figure 2.3C). This difficulty to determine a theoretical parameter however is not expected to pose significant issue in practical applications. On the

contrary, removal of primary ion at the sample side of sample/membrane phase boundary in effect improves selectivity as evidenced by the improved LDL. Ion fluxes in part originate due to ion exchange between primary and interfering ions at the sample/membrane interface (which can be expressed as selectivity). The fact that leached primary ions are returned into the membrane implies reduced ion exchange with interfering ions thus improving the selectivity. It should be noted here that this improvement is expected to be temporary until the equilibration of fluxes as discussed above.
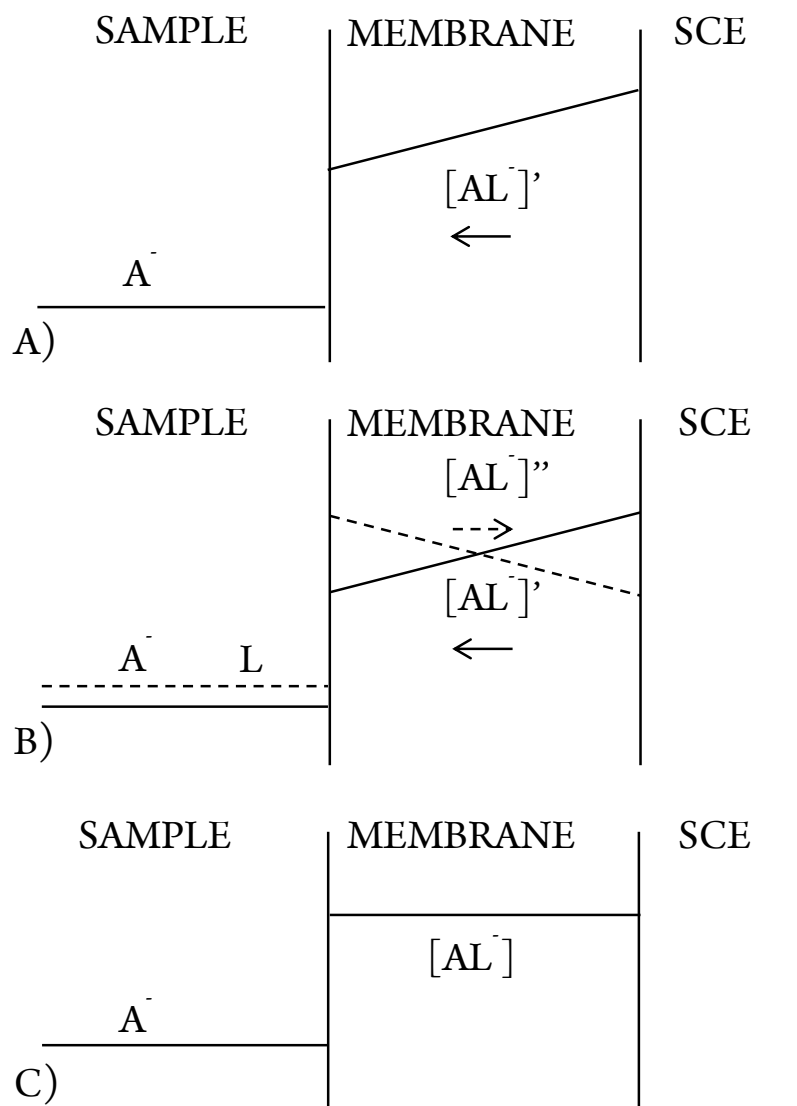
Figure 2.3 (A) Schematic illustration of how the exchange of analyte ions (A⁻) at the phase boundary results in ion fluxes of the ion-ionophore complex [AL⁻]' into the sample. (B) The addition of ionophore [L] to the conditioning solution facilitates complexation of analyte ions by the ionophore [AL⁻]" and triggers counter diffusion of the [AL⁻]" complexes from the sample into the membrane. This reduces or even fully eliminates ion fluxes (C). For the purpose of clarity, the fluxes of interfering ions have not been presented.

It is also reasonable to assume that the rate of inward diffusion of ion-ionophore complex will be a determining step in terms of sensor durability. That is why the traditional polymer matrix (PVC and plasticiser) was replaced by a lauryl methacrylate and methyl methacrylate copolymer backbone. Methacrylate-based copolymers exhibit significantly reduced diffusion coefficients of ion-ionophore complex in the membrane. It was also hypothesised that the presence of fresh ionophore at the membrane-sample phase boundary will complex primary ions that would otherwise leach into the sample resulting in significantly improved lower limits of detection.
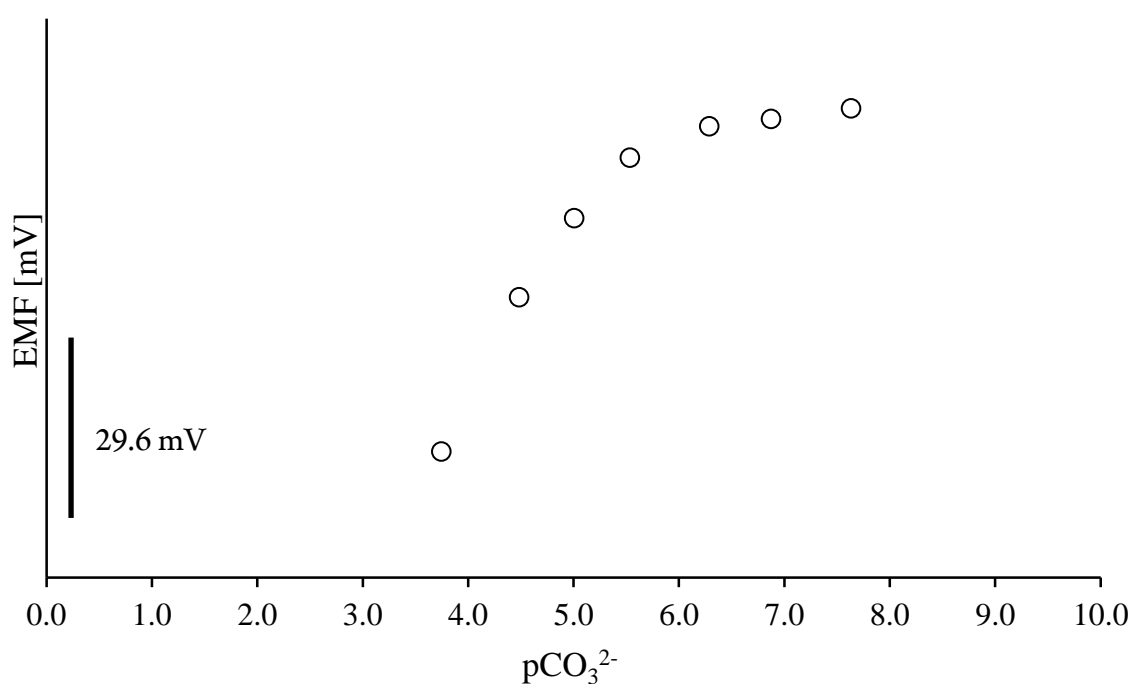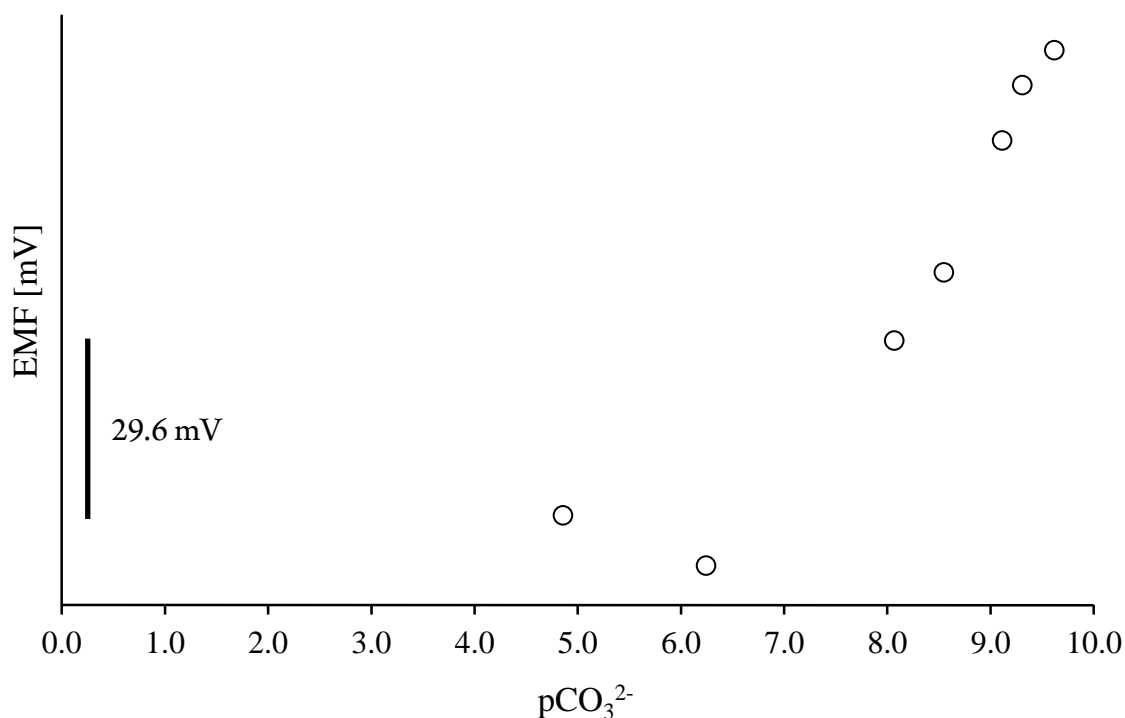
Figure 2.4 Calibration curves for the detection of carbonate with a traditional conditioning protocol (slope -27.1 mV/decade) (top) and with the new methodology proposed here (ionophore-free, slope -30.1 mV/decade) (bottom). It is apparent that conditioning of the ISEs in the solution of ionophore significantly enhances lower LODs.

The drastic difference in a response of the traditionally prepared ISEs versus the ionophore-free sensing membranes conditioned in the ionophore solution (Figure 2.4) could be explained by the enhanced suppression of outwards fluxes, thereby decreasing LOD to the ultra-low levels ($pCO_3^{2-} \sim 9.6$). However, from the data obtained in this study it was difficult to fully quantify and define lower detection limits, as even at very low activity of carbonate ions there was no breakdown in the response of ISEs. During each experiment ultra-pure water was used as a background solution to carry out the measurements of CO_3^{2-} prior the additions of sodium bicarbonate. The initial concentration of carbonate ions (LDL) was dictated by the amount of CO_2 dissolved (from the atmosphere) and the pH of background solution (5.8 ~ 6) as the speciation of carbonate

90

changes with the varying concentration of H^+ ions. This experimental approach did not allow for the measurements of lower carbonate concentrations than stated in this chapter. This illustrates the potential of proposed methodology to even further enhance LODs in the absence of experimental limitations.

The breakdown in potentiometric response at the upper detection end is most likely caused by the limited buffering capacity of the ISEs as no ionophore was introduced to the membrane during the preparation step (Figure 2.4 bottom). Traditionally, ISEs are loaded with the ionophore and ionic sites to prevent the co-extraction of ions of the opposite charge and to ensure full complexation of the primary ions. In this study, the concentration of diffused ionophore was observed to be significantly lower than the activity of ionic sites in the membrane as demonstrated in Figure 2.5.
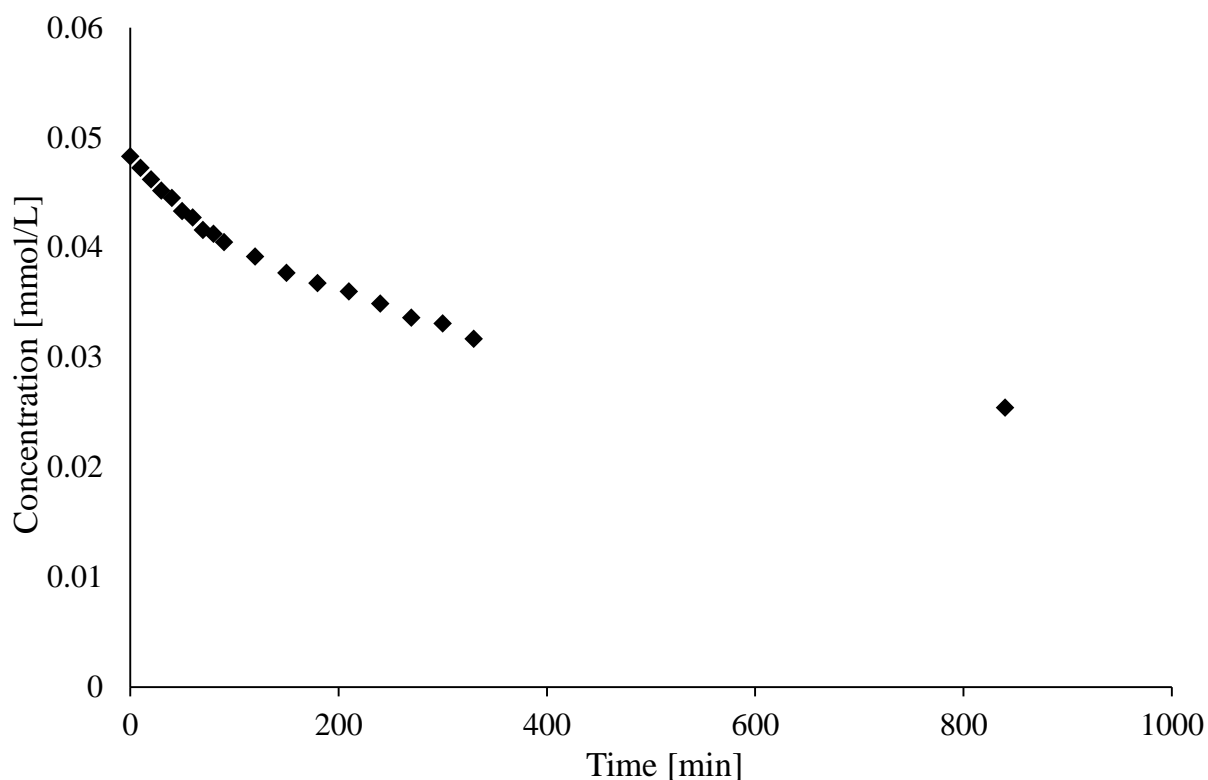
Figure 2.5 Decreasing concentration of the ionophore in the 4.83 x 10^{-5} M ionophore solution indicates its diffusion and deposition at the membrane bulk. This result indicates that ~50% of ionophore has partitioned into the membrane after ~60 min. As a confirmation of functionality of ISEs even after only 1 h conditioning in the solution of ionophore a large number of ISEs conditioned in this way show near-Nernstian slope and LDL in ppt levels as shown in Table 2.2.

The Nernstian response of such ISEs is perhaps counterintuitive since the ionophore concentration in the membrane should be higher than the concentration of ionic sites. Nevertheless, due to the slow diffusion of ionophore in the membrane, sufficient ionophore-ionic site concentration ratio is established locally at the membrane-sample interface. However, at high primary ion concentration in the sample bulk, the response of the ISEs is also dictated by the co-extraction effects. The extraction of counter ions from the sample into the membrane gives rise to non-Nernstian behaviour of the tested ISEs.

To expand the linear range of response and to improve upper detection limits, the concentration of ionic sites in the membrane bulk was decreased prior to the conditioning. Such optimisation resulted in the improvement of upper limits of detection (shift from -5.6 to -3.4) however, the observed response became significantly worse (17.3 mV per decade – Figure 2.6). This could be caused by the limited concentration of ionic sites in the membrane bulk as their substantial concentrations are required to demonstrate a Nernstian dependence on the analyte ion activity in the sample solution.
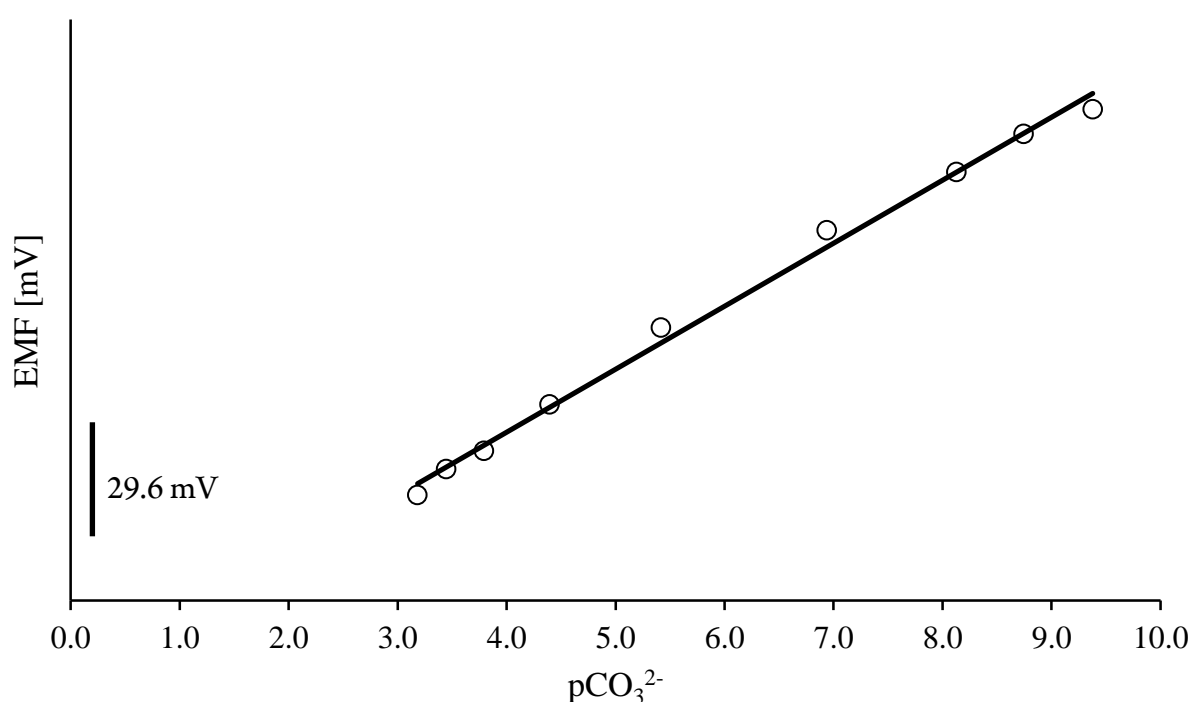
Figure 2.6 Non-Nernstian behaviour of the ionophore-free ISE containing 0.3% wt of ionic sites. Sensing membranes were conditioned for 24 h prior the measurements in the solution containing carbonate ionophore. The slope recorded for these ISEs was 17.3 ± 1.6 mV/decade with $R^2 = 0.99$.

The performance of traditionally made ISEs was later compared to one of the membranes loaded with the ionophore and ionic sites (4:1 ratio – mmol/kg) and conditioned in the carbonate ionophore solution. These ISEs showed near-Nernstian behaviour (27.4 mV per

decade) over a wide concentration ($pCO_3^{2-} = 3.3 - 9.6$) range with optimal LDL achieved under the given experimental conditions of $pCO_3 = 10.10$ (8×10^{-11} M or 5 ppt). This is demonstrated in Figure 2.7. The excess of ionophore ensures that the membrane exhibits its full buffering capacity preventing the extraction of counter ions from the sample. This indicates that ISEs doped with appropriate concentrations of the ion chelator and ionic sites give the most optimal performance. Note that the LDLs are here dictated by the speciation of CO_3^{2-} ion and its equilibrium with atmospheric CO_2. Traditionally, the LDLs of ISEs are dictated by the presence of interfering ions (selectivity) and determined from the typical curvilinear response curve. However, in this case, the curvilinear region is never observed.[62] This exciting observation implies that the fundamental LDLs for this system have not yet been measured and that with further system optimisation (e.g. preventing trace amounts of CO_3^{2-} through equilibrium with atmospheric CO_2), sub-ppt levels of CO_3^{2-} can possibly be determined.
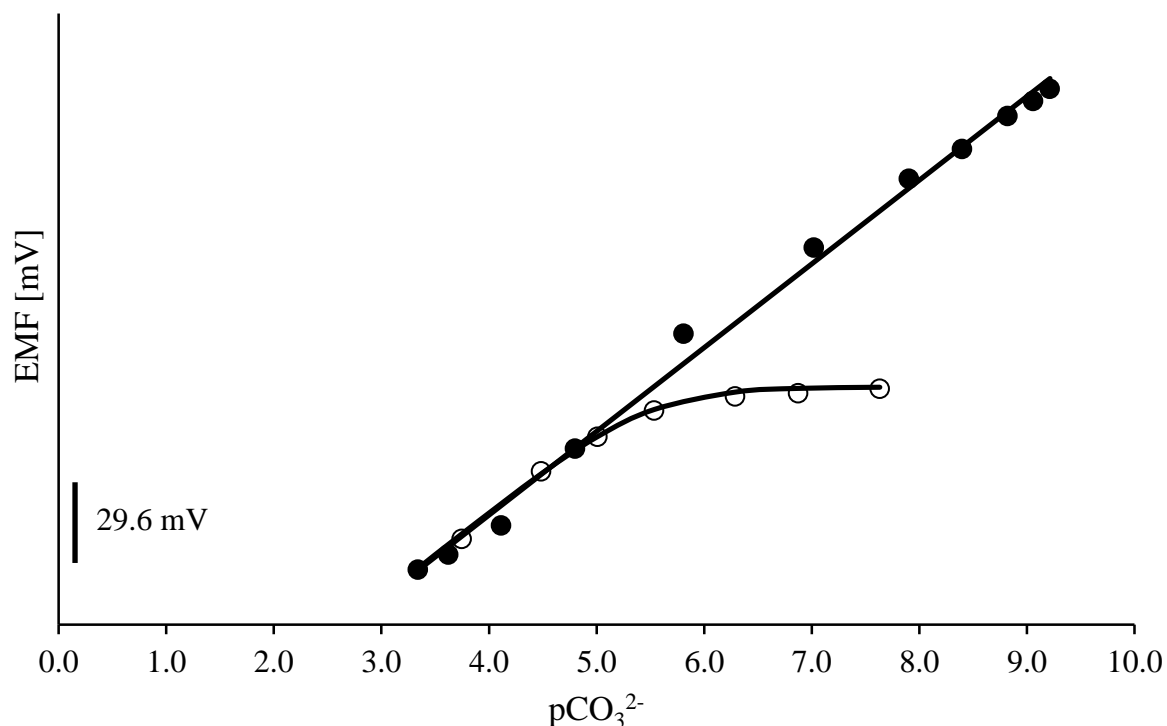
Figure 2.7 Response curves of CO_3^{2-} - selective electrodes prepared and conditioned in traditional fashion (open circles; slope = 27.1 mV/decade and LDL at pCO_3^{2-} (LDL) = 5.5), and using new methodology (closed circles). In the case of the latter the slope was 27.4 ± 1.4 mV/decade with R^2 = 0.99. Lower limits of detection are dictated by the speciation of CO_3^{2-} and is observed at pCO_3^{2-} = 9.6.

2.4.1 Selectivity of carbonate ISEs

Selectivity is an extremely important characteristic of a chemical sensor. It quantifies the preference for the chosen analyte over the other potentially interfering ions. However, limited selectivity of the ISEs can significantly influence the LDLs as demonstrated by the equation 1.18 in Chapter 1 - Limits of detection). This equation demonstrates that the smaller log K^{POT} the better LDLs. In the context of this work, the presence of strongly interfering ions (high log K^{POT}) promotes the ion exchange as described in the equilibrium shown in Figure 2.3A. Primary ions are being displaced by interfering ions, consequently the electrode stops responding to the analyte ions but still exhibits Nernstian behaviour to

the interferents. This can be used to measure minimal concentrations of interfering ions that would alter the electrode's response to primary ions and provide important information on the utility of the electrode in practical applications.

In an attempt to determine the selectivity of ISEs used, each sensor was exposed to the solution of ionophore and interfering ion as described in the experimental section. This was followed by recording the response curve for that particular ion. The slopes recorded for NO_3^-, SO_4^{2-} and Cl^- were -3.3 mV, -1.24 mV and -2.6 mV per decade respectively. The selectivity coefficient values for these set of ion sensing membranes could not be estimated as every electrode exhibited non-Nernstian behaviour and therefore did not meet the requirements defined by the Nikolsky-Eisenman equation.

A second set of optimised carbonate electrodes was prepared as described previously, but with a 24 h conditioning period in a solution containing carbonate ionophore (1 mg) and 20 mL of 1 M solution of selected interfering ions – (NO_3^-, SO_4^{2-} and Cl^-). The solutions were degassed under nitrogen for 30 min to remove any excess carbonate anions and to ensure that only interfering ions are present in the conditioning solutions. The following responses were obtained: -8.9 mV for NO_3^-, -12.8 mV for Cl^- and -7.4 mV for SO_4^{2-} (mV per decade) (Figure 2.8). Similarly, the interfering ions selected in this study did not produce Nernstian response at any given concentration and selectivity coefficient values could not be calculated from the experimental data. Multiple conditioning protocols were employed to ensure that the sensing membranes were exposed to the interfering ions only. However, a limited (non-Nernstian) response to the interfering ions remained unchanged throughout the experiments.
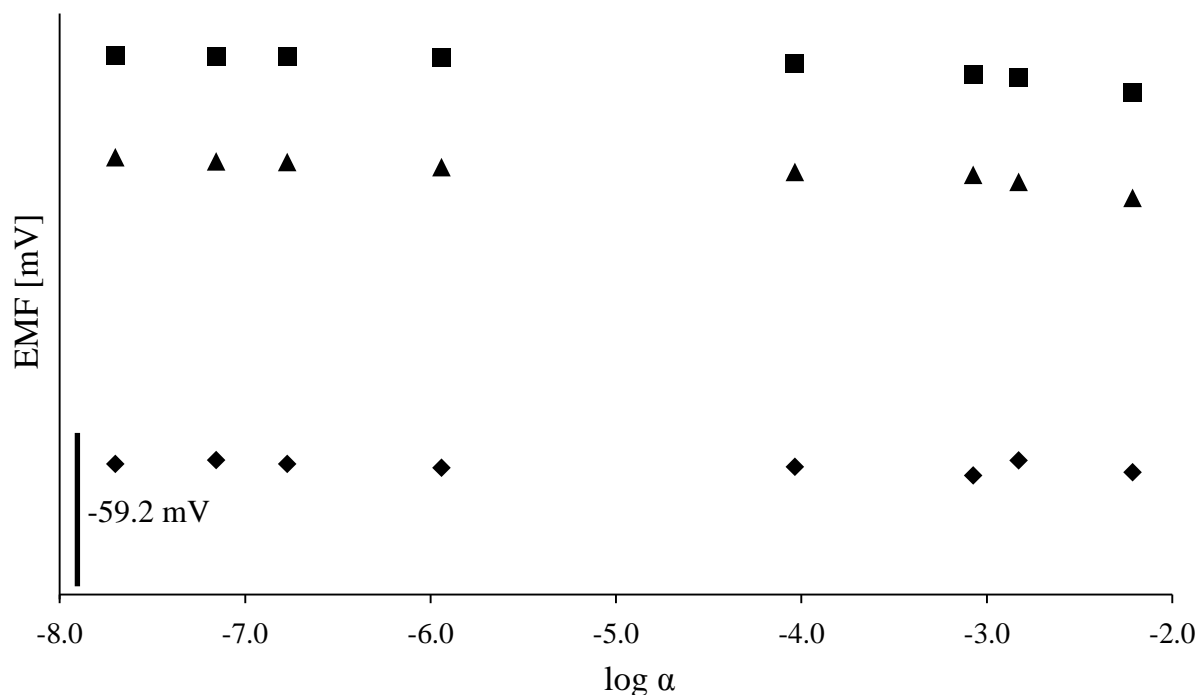
Figure 2.8 Potentiometric response of optimised carbonate selective electrodes for various metal anions: NO_3^- (diamonds; -8.9 mV per decade), Cl^- (triangles; -12.8 mV per decade) and SO_4^{2-} (squares; -7.4 mV per decade) obtained from selectivity measurements. In this case, the conditioning solution was degassed for 30 min prior to the experiment to reduce the activity of carbonate anions within the sample.

The severely sub-Nernstian responses for interfering ions is unexpected and very likely originates from the disturbance of L:R ratio as discussed above. In addition, it can be hypothesised that despite degassing of sample solution, the dissolution of atmospheric CO_2 into the membrane (due to drying in air for 24 hours) and/or in sample solution during the measurements results in the inevitable presence of CO_3^{2-} ions in both membrane and sample. Given the high CO_3^{2-} selectivity of ionophore, these minute concentrations may be sufficient to fully supress the response towards interfering ions thus disabling the possibility to quantify selectivity. Nevertheless, these results imply excellent potential for application at environmentally and biomedically relevant concentrations.

To determine the potentiometric behaviour of proposed sensors in complex media samples, ISEs with 4:1 ionophore to ionic sites ratio membrane composition and the new conditioning protocol were used in artificial seawater (adapted from Roy[56]). The measured response of carbonate selective electrode was near-Nernstian (26.9 ± 1.7 mV/decade) over a wide concentration range ($pCO_3^{2-} = 3.4 - 8.2$) and again exhibited ultra-low limits of detection (Figure 2.9).
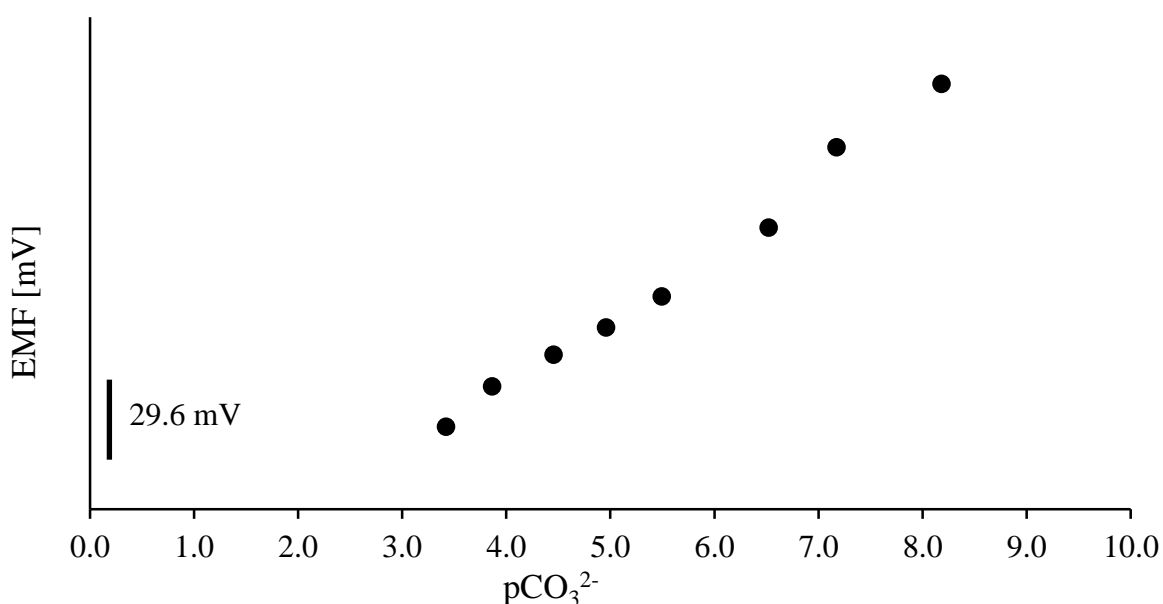
Figure 2.9 Response of the ion selective membrane loaded with the ionophore and ionic sites and conditioned in the ionophore solution for 24 h prior to the experiment. Artificial sea water was used as a background solution to determine if the resulting electrodes can retain their sensing properties in more complex sample.

2.4.2 Robustness of carbonate selective electrodes

Practical application has been a key driving force of this work and considerable efforts have been spent studying the robustness and reproducibility of response characteristics (slope and lower detection limits) of electrodes prepared using the new methodology. A vast number of electrodes (150+) including ionophore-free and membranes with pre-loaded

ionophore was prepared. They were tested immediately after preparation (without any other conditioning), followed by repetitions during several days, and/or after storage in air for up to several weeks. Near-Nernstian slopes at the response range of $pCO_3^{2-} > 8$ was observed in all cases (Table 2.2). Retention of the slope and impressive detection limits especially in the cases of already used ISEs that were later stored in air is an extremely important finding in terms of practical, in field application.

Table 2.2 Response ranges and slopes of selected ISEs.

Electrode category	Dry ISEs	Used ISEs	Optimised Electrodes
Measured range $[pCO_3^{2-}]$	9.6 – 4.1	8.9 – 6.9	10.0 - 3.50
Slope [mV/decade]	20.9 ± 0.8	20.5 ± 0.7	29.6 ± 0.4

In Table 2.2 the ISEs were divided in three main categories: a) Dry ISEs – representing the ionophore-free electrodes conditioned only in the solution of ionophore for 1 h, b) Used ISEs – representing Dry Electrodes that were used to record at least one calibration curve followed by the recording of next set of response after storage in air for ~2 weeks and c) Optimised Electrodes – representing fresh electrodes that were prepared as described above followed by their conditioning for at least 12 h in the solution of ionophore and recording response characteristics.

As the ionophore-free carbonate selective electrodes exhibited good functionality even after 1 h of conditioning in the ionophore solution, the proposed methodology was then

applied for the optimised carbonate electrodes to establish their response characteristics using the same timescale. Furthermore, the optimised ISEs were placed in conditioning solutions with varying amount of the ionophore dissolved (1 mg, 2 mg and 4 mg respectively) since the total concentration of the available ionophore may influence the time required for conditioning. In each case, the ion sensing membranes exhibited near-Nernstian responses to carbonate ion after 1 h of conditioning with the significant improvements in the experimental slope (27.8 ± 0.4 mV/decade for the optimised electrodes versus 20.9 ± 0.8 mV/decade for the dry electrodes) as shown in Table 2.3. The solubility of the ionophore in the homogenous mixture of THF and water dictated the total amount of the ionophore that could be used for the preparation of conditioning solution without the formation of a precipitate. For instance, if the amount of the dissolved carbonate ionophore exceeds 4 mg, an orange precipitate is formed in the solution. Since all tested electrodes exhibited near-theoretical response slopes, the solution containing 1 mg of the ionophore was chosen for further testing. These electrodes also carry the lowest risk of ionophore precipitation upon the exposure of THF to the atmosphere (e.g. loss due to solvent evaporation if the electrodes were stored in inappropriately sealed container). Further experiments are required to establish whether the same potentiometric behaviour would be obtained for the electrodes conditioned at lower ionophore concentrations or if the conditioning time was decreased. Nevertheless, these finding demonstrate that the potentiometric behaviour of carbonate selective electrodes can be significantly improved through the modifications in the conditioning protocol.

Table 2.3 Potentiometric behaviour (slopes and range) of carbonate selective ISEs.

Amount of the dissolved ionophore	1 mg	2 mg	4 mg
Measured range $[pCO_3^{2-}]$	9.7 – 4.0		
Slope [mV/decade]	27.8 ± 0.4	26.2 ± 0.3	26.7 ± 0.2

In Table 2.3 the optimised carbonate selective electrodes were divided into three categories based on the type of ionophore solution used for conditioning. 1 mg, 2 mg and 4 mg represent the amount of the ionophore dissolved in the same volume of organic and aqueous phase used for the preparation of conditioning solution as described in the Experimental section in Chapter 2. All electrodes were conditioned for 1 h prior the potentiometric measurements.

2.4.3 Ammonium and iodide determination

Herein, the validity of proposed methodology was demonstrated using CO_3^{2-} anion due to its tremendous clinical[33] and environmental importance[37,63,64] However, it could be hypothesised that the same conditioning protocol could be expanded to other ionophore based sensors with the promise of improving the detection limits for either cationic or anionic specimens. First and also the most intuitive approach was to test the response characteristics of the ISEs used for the determination of anionic species as they would most closely resemble previously described sensing process (anion determination). For that purpose, several iodide selective electrodes based on the presence of mercuracarborand-3

ionophore were prepared and conditioned according to traditional and proposed methodology. However, it is apparent that the solubility of the ionophore within the conditioning solution would dictate its final concentration in the resulting solution and therefore would directly influence the buffering capacity on the sample side of the membrane. The same concentration of the mercuracarborand-3 ionophore used for the preparation of the conditioning solution – 1 mg in 0.5 mL THF and 20 mL of ultra-pure water resulted in the formation of small white precipitate in the conditioning solution. This strongly indicates that some of the ionophore precipitated out of the solution as no salts/components other than stated in the Experimental section were used in this experiment.

Precipitate formation could arise due to either the evaporation of solvent (in this case THF); not sufficiently balanced ratio of the solvent used for the ionophore dissolution and water; or combination of both. However, each conditioning solution was kept in airtight containers that would prevent the release of THF to the atmosphere. One approach involves increasing the fraction of the organic phase in the homogenous mixture of water and THF to ensure that the ionophore is only found in the dissolved form. Also, the excess of THF would act as a solvent reservoir compensating for the loss of THF upon the exposure of the conditioning solution to air. Nevertheless, increasing the volume of the organic phase in the conditioning solution may lead to the deterioration of the potentiometric performance of the ISEs due to the: a) dissolution of ion sensing membrane from the solid contact; b) dissolution of the electrode's body that supports the sensing membrane (solid and liquid contact electrodes); c) combination of all factors. These may render liquid contact electrodes permanently unsuitable for further analytical

measurements as the dissolution of either the membrane components or supporting material would facilitate leakage of the inner filling solution from the internal compartment of the electrode into the conditioning solution. Even though, such modification carries the potential risk of damaging the membrane/sensor, very careful optimisation of this conditioning protocol (depending on the solubility of the ionophore in the organic phase) can result in the optimal concentration of the ionophore needed to buffer the sensing membrane. Another method to overcome the formation of precipitate relies on decreasing the concentration of ionophore in the conditioning solution. This would ensure that the mechanical stability of the sensing membrane is intact. However, if the concentration of ionophore is too small to provide optimal buffering capacity on the sample side of the membrane, only minimal changes in the response characteristics would be expected.

The advantage of using carbonate as a model ion in this study lies in its inherent presence within the conditioning solution due to the dissolution of carbon dioxide from the atmosphere. Therefore, the ion selective membrane is simultaneously exposed to the primary ions and the dissolved ionophore. This ensures that in one step the equilibrium within the membrane is established and allows the ionophore to diffuse towards the membrane phase.

To establish whether the proposed methodology can be applied for the determination of iodide, a three step conditioning protocol was utilised as described in the Experimental section - Preparation of ammonium and iodide selective electrodes. Firstly, the ion sensing membrane is placed in the solution of primary ions to ensure full equilibration. The same

electrode is then immersed in the ionophore solution to facilitate the diffusion of the ionophore and consequently its deposition at the sample/membrane interface. The rate of diffusion through the aqueous sample will depend on the mass of the ionophore and as for the carbonate ionophore it could not be monitored or quantified using optical spectroscopy. Therefore further studies are required to determine the optimum ionophore diffusion time to ensure full accumulation of the ionophore at the sample side of the membrane. Furthermore, the ISEs were placed in the solution of primary ions (lower concentration then initial) to minimise the occurrence of zero-current ion fluxes within the membrane.[3] The difference in the potentiometric response of the traditionally prepared ISEs (two conditioning steps) versus the ion selective membranes conditioned in the solution of the ionophore is demonstrated in Figure 2.10.
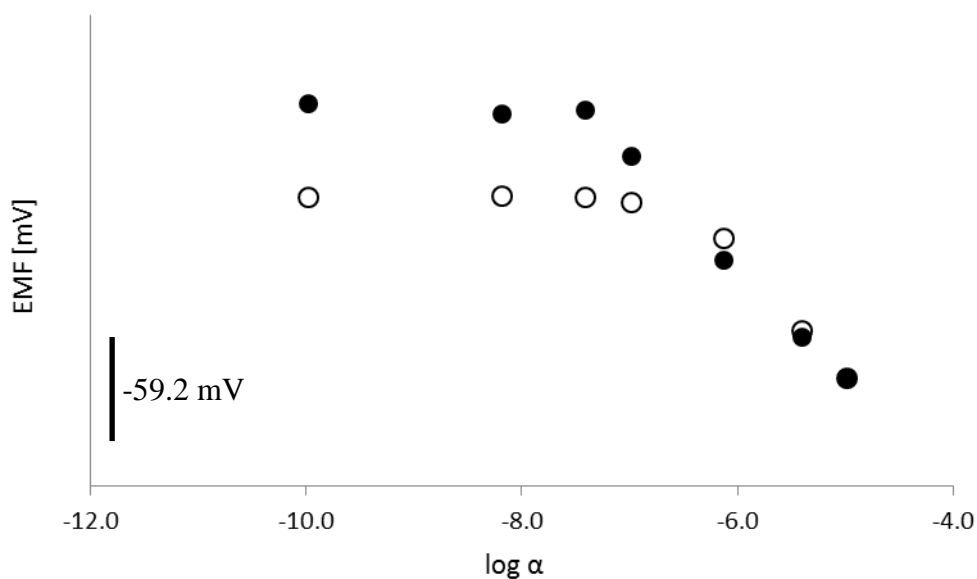
Figure 2.10 Calibration curves obtained for the detection of iodide with a traditional conditioning protocol (open circles, -60.1 ± 1.2 mV/decade, LOD = −6.6) and with the new methodology proposed here (black circles, -59.3 ± 2.0 mV/decade, LOD = −7.8). Over one order of magnitude improvement in LODs was observed for ISEs conditioned in the solution of iodide ionophore.

Even though, the observed detection limit from iodide measurements do not match lower limits of detection of carbonate selective electrodes, these findings strongly indicate that the same conditioning protocol can be expanded for other anionic species. The difference in the magnitude of the potentiometric response is most likely driven by the dissimilarity in physico-chemical properties of the ionophore (molecular weight, solubility, size etc.) used for the preparation of conditioning solution. The above-mentioned characteristics define the concentration of available ionophore in the solution and the time required for the ligand to diffuse through the sample to reach the outer surface of the sensing membrane. Therefore, a careful consideration of experimental conditions must be made to obtain the most optimum potentiometric response.

The same three step conditioning protocol was used during the preparation of ammonium selective electrodes (Experimental - Preparation of ammonium and iodide selective electrodes) to demonstrate the applicability of the proposed methodology for the determination of positively charged ions. Similarly, the ion sensing membranes prepared according to the new protocol demonstrated lower detection limits than the electrodes conditioned in the solution of primary ions only. The observed improvement in lower detection limits for ammonium selective electrodes is shown in Figure 2.11.
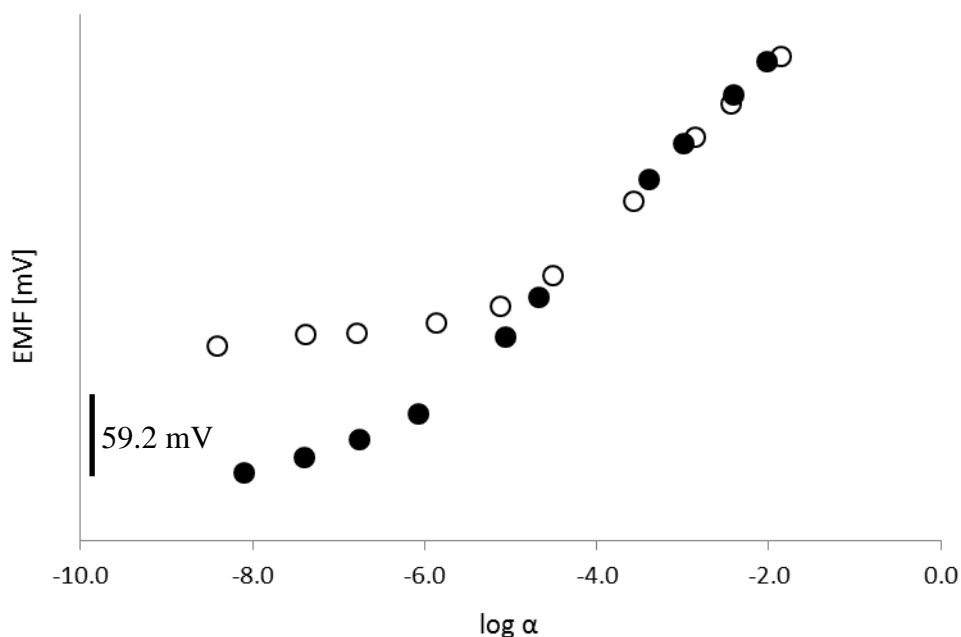
Figure 2.11 Response of the ammonium selective sensor with a traditional conditioning protocol (open circles, 57.5 ± 0.6 mV/decade, LOD = -5.5) and with the new methodology proposed here (black circles, 59.2 ± 2.2 mV/decade, LOD = -7.1). Over one order of magnitude improvement in LODs was observed for ISEs conditioned in the solution of ammonium ionophore.

These preliminary findings demonstrate that the proposed conditioning methodology can be utilised during the preparation of either cation or anion selective electrodes leading to ion sensing membranes with improved detection limits. Furthermore, even small enhancements in the response characteristics of ISEs at low analyte concentration can contribute significantly towards the development of applied chemical sensors. For instance, if the given ion sensing membrane exhibits detection limits just below the physiologically or environmentally relevant levels, the possibility of improving the LODs without the need to modify the composition of sensing membranes can be particularly attractive. Moreover, further optimisation of the proposed conditioning protocol may lead towards the development of ISEs with ultra-low detection limits.

2.5 Conclusions

This work describes a new, simple methodology for reducing/eliminating membrane ion fluxes thus achieving extremely low detection limits. The method was applied on carbonate selective electrodes, resulting in an improvement of the observed LDL by at least 4 orders of magnitude. The proposed ISEs exhibited near-Nernstian potentiometric responses to carbonate ions with a detection limit of 80 pmol L^{-1} (5 ppt) and were further utilised for direct determination of carbonate in seawater Furthermore, the sensors showed excellent robustness and durability at such low concentration ranges. Preliminary data indicates that the suggested methodology is general and can be applied for any number of cations and anions. Finally, this method eliminates a series of factors that, up until now were considered fundamentally limiting. The use if these ISEs in situations where either the sample has a strong influence on the electrode (trace level analysis in complex samples) or the electrode has strong influence on the sample (leaching of ions into the sample of ultra-small volume (e.g. cells)) has now become a real possibility.

References

(1)   Vigassy, T.; Gyurcsányi, R. E.; Pretsch, E. *Electroanalysis* **2003**, *15* (5–6), 375–382.

(2)   Ion, A. C.; Bakker, E.; Pretsch, E. *Anal. Chim. Acta* **2001**, *440* (2), 71–79.

(3)   Ceresa, A.; Bakker, E.; Hattendorf, B.; Günther, D.; Pretsch, E. *Anal. Chem.* **2001**, *73* (2), 343–351.

(4)   Sokalski, T.; Ceresa, A.; Fibbioli, M.; Zwickl, T.; Bakker, E.; Pretsch, E. *Anal. Chem.* **1999**, *71* (6), 1210–1214.

(5)   Qin, W.; Zwickl, T.; Pretsch, E. *Anal. Chem.* **2000**, *72* (14), 3236–3240.

(6)   Muslinkina, L.; Pretsch, E. *Electroanalysis* **2004**, *16* (19), 1569–1575.

(7)   Cattrall, R. W.; Freiser, H. *Anal. Chem.* **1971**, *43* (13), 1905–1906.

(8)   Fibbioli, M.; Morf, W. E.; Badertscher, M.; de Rooij, N. F.; Pretsch, E. *Electroanalysis* **2000**, *12* (16), 1286–1292.

(9)   Buck, R. P. *Anal. Chem.* **1976**, *48* (5), 23–39.

(10)   Lindner, E.; Cosofret, V. V.; Ufer, S.; Johnson, T. A.; Ash, R. B.; Nagle, H. T.; Neuman, M. R.; Buck, R. P. *Fresenius J. Anal. Chem. 346* (6), 584–588.

(11)   Zielińska, R.; Mulik, E.; Michalska, A.; Achmatowicz, S.; Maj-Żurawska, M. *Anal. Chim. Acta* **2002**, *451* (2), 243–249.

(12)   Gyurcsányi, R. E.; Nybäck, A.-S.; Ivaska, A.; Tóth, K.; Nagy, G. *The Analyst* **1998**, *123* (6), 1339–1344.

(13)   Michalska, A.; Hulanicki, A.; Lewenstam, A. *Microchem. J.* **1997**, *57* (1), 59–64.

(14)   Cadogan, A.; Gao, Z.; Lewenstam, A.; Ivaska, A.; Diamond, D. *Anal. Chem.* **1992**, *64* (21), 2496–2501.

(15)   Bobacka, J.; McCarrick, M.; Lewenstam, A.; Ivaska, A. *The Analyst* **1994**, *119* (9), 1985.

(16)   Bobacka, J.; Lahtinen, T.; Nordman, J.; Häggström, S.; Rissanen, K.; Lewenstam, A.; Ivaska, A. *Electroanalysis* **2001**, *13* (8–9), 723–726.

(17)   Pandey, P. C. *J. Electrochem. Soc.* **1998**, *145* (12), 4103.

(18)   Han, W.-S.; Park, M.-Y.; Chung, K.-C.; Cho, D.-H.; Hong, T.-K. *Anal. Sci.* **2000**, *16* (11), 1145–1149.

(19)   Lee, Y.-H.; Han, W.-S.; Lee, H.-J.; Ahn, S.-M.; Hong, T.-K. *J. Anal. Chem.* **2015**, *70* (5), 621–626.

(20)   Bobacka, J. *Anal. Chem.* **1999**, *71* (21), 4932–4937.

(21)   Bobacka, J.; Ivaska, A.; Lewenstam, A. *Electroanalysis* **2003**, *15* (5–6), 366–374.

(22)   Anastasova, S.; Radu, A.; Matzeu, G.; Zuliani, C.; Mattinen, U.; Bobacka, J.; Diamond, D. *Electrochimica Acta* **2012**, *73*, 93–97.

(23)   Mousavi, Z.; Granholm, K.; Sokalski, T.; Lewenstam, A. *The Analyst* **2013**, *138* (18), 5216.

(24)   Zuliani, C.; Matzeu, G.; Diamond, D. *Talanta* **2014**, *125*, 58–64.

(25)   McGraw, C. M.; Radu, T.; Radu, A.; Diamond, D. *Electroanalysis* **2008**, *20* (3), 340–346.

(26)   Bobacka, J.; Lindfors, T.; McCarrick, M.; Ivaska, A.; Lewenstam, A. *Anal. Chem.* **1995**, *67* (20), 3819–3823.

(27)   Bobacka, J. *Electroanalysis* **2006**, *18* (1), 7–18.

(28)   Heng, L. Y.; Hall, E. A. H. *Anal. Chim. Acta* **2000**, *403* (1–2), 77–89.

(29)   Qin, Y.; Bakker, E. *Anal. Chem.* **2003**, *75* (21), 6002–6010.

(30)   De Marco, R.; Clarke, G.; Pejcic, B. *Electroanalysis* **2007**, *19* (19–20), 1987–2001.

(31)   Radu, A.; Radu, T.; Mcgraw, C.; Dillingham, P.; Anastasova-Ivanova, S.; Diamond, D. *J. Serbian Chem. Soc.* **2013**, *78* (11), 1729–1761.

(32)   Messerli, M. A.; Kurtz, I.; Smith, P. J. S. *Anal. Bioanal. Chem.* **2008**, *390* (5), 1355–1359.

(33)   Kenneth D. McClatchey. *Clinical Laboratory Medicine*, 2nd ed.; Lippincott Williams and Wilkins: Philadelphia, 2002.

(34)   Gennari, F. J.; Weise, W. J. *Clin. J. Am. Soc. Nephrol.* **2008**, *3* (6), 1861–1868.

(35)   Ekstrom, J. A.; Suatoni, L.; Cooley, S. R.; Pendleton, L. H.; Waldbusser, G. G.; Cinner, J. E.; Ritter, J.; Langdon, C.; van Hooidonk, R.; Gledhill, D.; Wellman, K.; Beck, M. W.; Brander, L. M.; Rittschof, D.; Doherty, C.; Edwards, P. E. T.; Portela, R. *Nat. Clim. Change* **2015**, *5* (3), 207–214.

(36)   Orr, J. C.; Fabry, V. J.; Aumont, O.; Bopp, L.; Doney, S. C.; Feely, R. A.; Gnanadesikan, A.; Gruber, N.; Ishida, A.; Joos, F.; Key, R. M.; Lindsay, K.; Maier-Reimer, E.; Matear, R.; Monfray, P.; Mouchet, A.; Najjar, R. G.; Plattner, G.-K.; Rodgers, K. B.; Sabine, C. L.; Sarmiento, J. L.; Schlitzer, R.; Slater, R. D.; Totterdell, I. J.; Weirig, M.-F.; Yamanaka, Y.; Yool, A. *Nature* **2005**, *437* (7059), 681–686.

(37)   Hoegh-Guldberg, O.; Mumby, P. J.; Hooten, A. J.; Steneck, R. S.; Greenfield, P.; Gomez, E.; Harvell, C. D.; Sale, P. F.; Edwards, A. J.; Caldeira, K.; Knowlton, N.; Eakin, C. M.; Iglesias-Prieto, R.; Muthiga, N.; Bradbury, R. H.; Dubi, A.; Hatziolos, M. E. *Science* **2007**, *318* (5857), 1737–1742.

(38)   Pobiner, H. *Anal. Chem.* **1962**, *34* (7), 878–879.

(39)   Kaltin, S.; Haraldsson, C.; Anderson, L. G. *Mar. Chem.* **2005**, *96* (1–2), 53–60.

(40) Easley, R. A.; Patsavas, M. C.; Byrne, R. H.; Liu, X.; Feely, R. A.; Mathis, J. T. *Environ. Sci. Technol.* **2013**, 130110104920006.

(41) Hansen, T.; Gardeler, B.; Matthiessen, B. *Biogeosciences* **2013**, *10* (10), 6601–6608.

(42) Little, M. J.; Wentzell, P. D. *Anal. Chim. Acta* **1995**, *309* (1–3), 283–292.

(43) Severinghaus, J. W.; Bradley, A. F. *J. Appl. Physiol.* **1958**, *13* (3), 515–520.

(44) Chen, L. D.; Mandal, D.; Pozzi, G.; Gladysz, J. A.; Bühlmann, P. *J. Am. Chem. Soc.* **2011**, *133* (51), 20869–20877.

(45) Phillips, F.; Kaczor, K.; Gandhi, N.; Pendley, B.; Danish, R.; Neuman, M.; Toth, B.; Horvath, V.; Lindner, E. *Talanta* **2007**, *74* (2), 255–264.

(46) Guziński, M.; Lisak, G.; Sokalski, T.; Bobacka, J.; Ivaska, A.; Bocheńska, M.; Lewenstam, A. *Anal. Chem.* **2013**, *85* (3), 1555–1561.

(47) Meyerhoff, M. E.; Pretsch, E.; Welti, D. H.; Simon, W. *Anal. Chem.* **1987**, *59* (1), 144–150.

(48) Sokalski, T.; Paradowski, D.; Ostaszewska, J.; Maj-?urawska, M.; Mieczkowski, J.; Lewenstam, A.; Hulanicki, A. *The Analyst* **1996**, *121* (2), 133.

(49) Scott, W. J.; Chapoteau, E.; Kumar, A. *Clin. Chem.* **1986**, *32* (1 Pt 1), 137–141.

(50) Makarychev-Mikhailov, S.; Legin, A.; Mortensen, J.; Levitchev, S.; Vlasov, Y. *The Analyst* **2004**, *129* (3), 213–218.

(51) Greenberg, J. A.; Meyerhoff, M. E. *Anal. Chim. Acta* **1982**, *141* (0), 57–64.

(52) Lee, K. S.; Shin, J. H.; Han, S. H.; Cha, G. S.; Shin, D. S.; Kim, H. D. *Anal. Chem.* **1993**, *65* (21), 3151–3155.

(53) Beer, P. D.; Hayes, E. J. *35 Years Synth. Anion Recept. Chem. 1968-2003* **2003**, *240* (1–2), 167–189.

(54)   Sessler, J. L.; Camiolo, S.; Gale, P. A. *35 Years Synth. Anion Recept. Chem. 1968-2003* **2003**, *240* (1–2), 17–55.

(55)   Jain, A. K.; Gupta, V. K.; Raisoni, J. R. *Electrochimica Acta* **2006**, *52* (3), 951–957.

(56)   Roy, R. N.; Roy, L. N.; Vogel, K. M.; Porter-Moore, C.; Pearson, T.; Good, C. E.; Millero, F. J.; Campbell, D. M. *Mar. Phys. Chem. - Mem. Contrib. Made Field Dr Ricardo Pytkowicz* **1993**, *44* (2–4), 249–267.

(57)   Bakker, E. *Anal. Chem.* **1997**, *69* (6), 1061–1069.

(58)   Schefer, U.; Ammann, D.; Pretsch, E.; Oesch, U.; Simon, W. *Anal. Chem.* **1986**, *58* (11), 2282–2285.

(59)   Boles, J. H.; Buck, R. P. *Anal. Chem.* **1973**, *45* (12), 2057–2062.

(60)   Xie, X.; Zhai, J.; Bakker, E. *J. Am. Chem. Soc.* **2014**, *136* (47), 16465–16468.

(61)   Meier, P. C.; Morf, W. E.; Läubli, M.; Simon, W. *Anal. Chim. Acta* **1984**, *156*, 1–8.

(62)   Dillingham, P. W.; Radu, T.; Diamond, D.; Radu, A.; McGraw, C. M. *Electroanalysis* **2012**, *24* (2), 316–324.

(63)   de Beer, D.; Bissett, A.; de Wit, R.; Jonkers, H.; Köhler-Rink, S.; Nam, H.; Kim, B. H.; Eickert, G.; Grinstain, M. *Limnol. Oceanogr. Methods* **2008**, *6* (10), 532–541.

(64)   Han, C.; Cai, W.-J.; Wang, Y.; Ye, Y. *J. Oceanogr.* **2014**, *70* (5), 425–433.

CHAPTER 3   Influence of ionic liquids on the selectivity of ion exchange-based polymer membrane sensing layers.

3.1   Ion-exchange membranes

Ion exchange-based membranes are utilised in many types of chemical sensors. For example, spectroelectrochemical sensors utilise polymeric polyelectrolyte films as the first mode of selectivity that facilitate the selective extraction and pre-concentration of analyte from the sample. This is then followed by ion transport to the optically transparent electrode where the electrochemical and optical signals are measured.[1–3] 'Electronic tongues' are sensors that utilise a number of low selective membranes in conjunction with advanced mathematical procedures for signal processing and analyte detection.[4] Ion selective electrodes (ISEs) based on the use of a polymeric membrane rely on the addition of a highly selective ligand typically referred to as an ionophore to facilitate the selective extraction and binding of target analyte.[5,6] This approach greatly enhances the selectivity of the membrane for the specific analyte and allows development of sensitive, portable and inexpensive sensors for selective determination of the activity of ions in aqueous solutions.[7,8]

Ion exchange-based membranes are typically composed of plasticised polymers with the addition of an ion exchange salt. The latter are typically salts that contain a highly lipophilic ion which enables exchange of only its hydrophilic counter-ion with ions of the same charge from the sample thus rendering the membrane permselective. When there are

no other complexes formed, the selectivity of sensing layers is based on the energy transfer of ions from the aqueous phase to the organic membrane[9] and therefore it is strongly influenced by both the lipophilicity of a targeted ion and the internal composition of a sensing membrane. In this case the selectivity follows the well-established Hofmeister series ($ClO_4^- > SCN^- > I^- > NO_3^- > Br^- > Cl^- > HCO_3^- > SO_4^{2-} > HPO_4^{2-}$).[10]

This sequence shows that the most lipophilic anions are preferentially extracted from the sample into the PVC based membrane, whereas the transfer of very hydrophilic ions such as sulphates, phosphates and ferrocyanides into the ionophore-free membrane is energetically most unfavourable due to large hydration energy. Among several proposed approaches to invert the Hofmeister sequence, the most common is to introduce a selective ionophore that reduces phase transfer energy and facilitates the ion transfer into the membrane matrix.[11] Other strategies for modulating membrane selectivity involve the utilisation of different materials used for the preparation of ion-exchange membranes such as lipophilic ion exchange salt or indeed the matrix itself. Additionally, it has been reported that the extraction of hydrophilic anions may be facilitated if the difference in the dielectric constant (ε) between the sample water and the membrane phase is reduced.[12] As the plasticiser usually comprises over fifty percent of the polymeric membrane, its physico-chemical properties would dictate the dielectric constant of the ISEs and consequently influence the ion-exchanging properties. Therefore, the focus of this study is placed on the potential use of ionic liquids as membrane solvating media.

Room temperature ionic liquids (RTIL) are molten salts exclusively composed of ions that exist in a liquid state at ambient temperature. They are mainly defined by the weak coordination characteristics between the ionic moieties owing to the presence of large cation and smaller charge delocalised anion.[13] Therefore, this leads to a very low tendency of RTILs to crystallise due to the dissymmetry of the cation and flexibility of anion. One of the pioneering examples of RTIL is formed by the combination of a 1-ethyl-3-methylimidazolium (EMI) cation and N,N-bis(trifluoromethane)sulphonamide (TFSI) anion.[14] This attempt gave rise to a liquid with very high ionic conductivity and improved stability to the decomposition at high vacuum pressure reaching up to 300-400°C. The almost non-measurable vapour pressure, low toxicity, high ionic mobility, large electrochemical window and very good electrical conductivity have led to their diverse applications in chemical sciences.[15] Among the above-mentioned properties, the negligible volatility of RTILs and consequently the possibility for their future re-use characterised them as 'green recyclable solvents'. However, more recent studies indicated that several ILs can impart toxicity to living organisms such as through enzyme inhibition and may pose serious environmental threats to the aquatic and terrestrial ecosystems.[16] Even though, RTILs are still routinely used in chemical synthesis,[17] biocatalytic transformations,[18,19] electrochemistry,[20,21] and analytical science.[22,23] Since ionic liquids can undergo almost unlimited structural variations (via cation and anion modifications),[24] their characteristics can be optimised for a specific target application.[25] Therefore, several different kinds of salts can be used to design ILs including imidazolium, pyrrolidinium and quaternary ammonium salts as cationic species and bis(trifluoromethanesulphonyl)imide, bis(fluorosulphonyl)imide and hexafluorophosphate as anions.[14] Moreover, on the basis of

their chemical composition RTILs can be further subdivided into three distinctive classes such as protic, aprotic and zwitterionic (Figure 3.1).
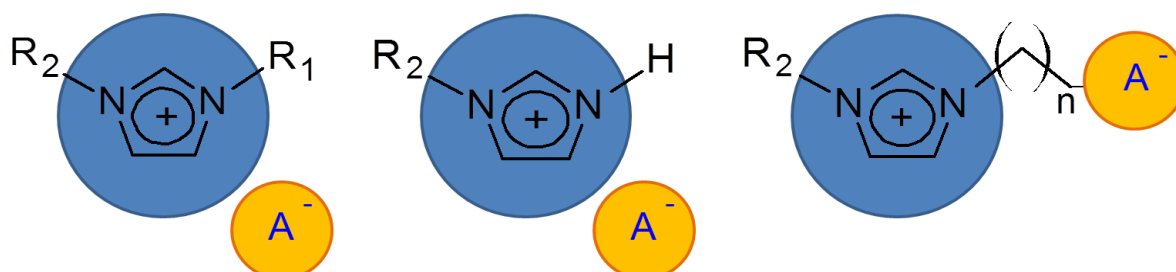
Figure 3.1 Three distinctive classes of RTILs: aprotic ILs with their primary application in lithium batteries and superconductors (left); protic ILs are found, for instance, in fuel cells (centre); zwitterionic ILs are suitable for the preparation of ionic liquid based membranes (right).

The interest in RTILs is growing very quickly in separation science due to their unique properties such as varying polarity and low volatility which are associated with non-polar and ionic interactions[26]. Additionally, the presence of different functional groups attached to the surface of the stationary phase promotes further extraction of the target analyte resulting in improved chromatographic performance.[27] Therefore, RTILs have excellent potential for utilisation in ion exchange-based membranes as extraction solvents[28] for modulating their selectivity.

Recently, RTILs have been employed as alternative materials to the particular components of ion selective membranes. In the pioneering work carried out by Coll et al (2005) the ion sensing membranes were doped with 1-butyl-3-methylimidazolium hexafluorophosphate IL yielding ISEs with improved response towards sulphate anions. This was attributed to the increase in the dielectric constant of the sensing membranes due to the presence of the

selected RTIL.[9] Since then, ILs has been used as cation excluders,[9,29,30] ionophores[31] or plasticisers[32] in the field of ISEs. For instance, Shvedene and co-workers (2006) demonstrated that bistrifluoromethanesulfonimidate salts of 1-butyl-2,3-dimethylimidazolium and dodecylethyldiphenylphosphonium may serve the function of plasticisers for the poly(methyl methacrylate) and PVC polymer based membranes.[32] Wardak and Lenik (2013) showed that imidazolium based ILs can be introduced into the ion sensing membrane to simultaneously act as transducer media (stabilise the electrode potential) and to reduce the resistance of the membrane.[33] This demonstrates that large structural complexity of RTILs provides enormous potential for the development of ion exchange-based membranes whose selectivity can be finely tuned via doping the membrane with RTILs. However, at the same time it puts pressure to perform systematic studies that will lead towards a full understanding of the role of RTILs in modulation of selectivity of ion exchange-based membranes.

In this study a wide range of RTILs based on trihexyl(tetradecyl)phosphonium [$P_{6,6,6,14}$] cation was used in order to investigate the hypothesis that RTILs can change the selectivity characteristics of sensing membranes if they are utilised as polymeric plasticisers. In industrial applications phosphonium-based RTILs offer superior properties over nitrogen containing ILs (e.g. imidazolium based ILs) ones due to their large availability and low cost.[34] In this study, it is also relevant that phosphonium-based ionic liquids serve as a suitable solvent/plasticiser for polymeric membranes made of PVC that is traditionally used for the preparation of ion-exchange membranes.[25,35] It is well known that the dielectric constant is one of the key solvent properties that defines polarity of the studied

solvent and therefore it is expected that the structural variation (more specifically presence of the anion) between selected IL would result in further polarity changes.[36]

Herein, the potentiometric response and selectivity coefficients for a range of anions using ionophore-free polymeric membranes plasticised with ILs are determined. The selectivity coefficients were compared with the ones obtained with membranes using traditional solvent mediators and/or their mixtures with ILs. Selectivity coefficients were evaluated for the determination of iodide ion which has been selected as a model ion in this study, in part due to its significance in clinical medicine.[37] The biological importance of iodide along with the techniques and methods that are routinely employed for its determination are discussed in more detail in Chapter 4.

3.2 Experimental

3.2.1 Materials

Poly(vinyl) chloride (PVC) was of a selectophore grade and purchased from Sigma Aldrich, UK. Bis(2-ethylhexyl) sebacate (DOS) (Fluka), 2-nitrophenyl octyl ether (NPOE) (Fluka), tetradodecylammonium chloride (TDAMCl) (Aldrich) were used for fabrication of ionophore free membranes.

Ionic liquids such as trihexyl(tetradecyl)phosphonium dicyanamide $[P_{6,6,6,14}][DCA^-]$, trihexyl(tetradecyl)phosphonium bis(trifluoromethylsulfonyl)amide $[P_{6,6,6,14}][TFMS^-]$, trihexyl(tetradecyl)phosphonium chloride $[P_{6,6,6,14}][Cl^-]$, trihexyl(tetradecyl)phosphonium dodecylbenzenesulfonate $[P_{6,6,6,14}][DBS^-]$, trihexyl(tetradecyl)phosphonium methanesulfonate $[P_{6,6,6,14}][MS^-]$ were purchased from Strem Chemicals and had purities >95%. The $[P_{6,6,6,14}][MO^-]$, trihexyl(tetradecyl)phosphonium methylorange was generously donated by the group of Prof Diamond, (Dublin City University, Ireland).

All other chemicals were of the analytical reagent grade. Solutions of metal ions were prepared in ultra-pure water obtained with a Pico Pure 3 water system. Working solutions of different activities were prepared by serial dilutions of a 0.1 M stock solution.
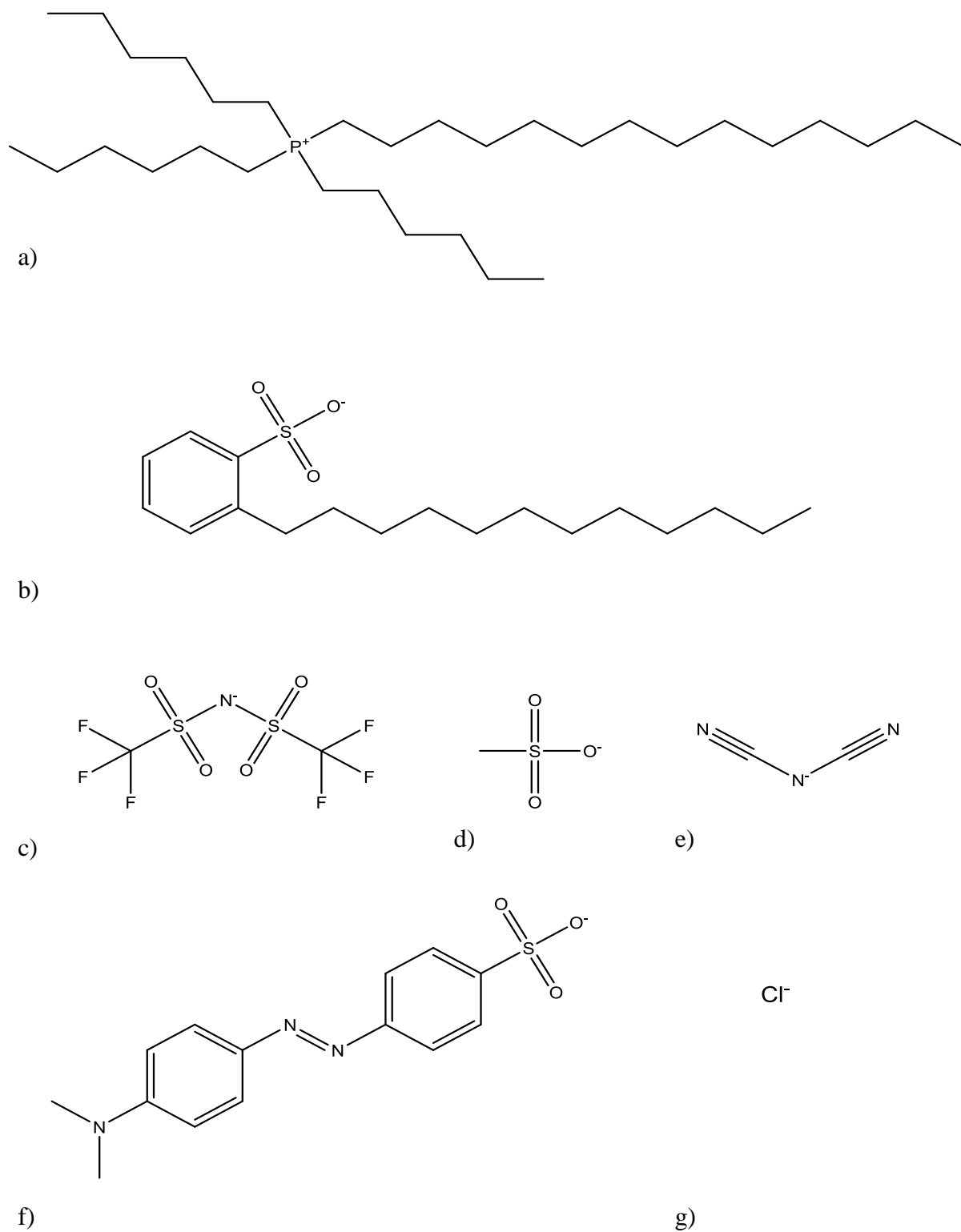
Figure 3.2 RTILs used for the preparation of ion-exchange membranes; a) trihexyl(tetradecyl)phosphonium cation; b) dodecylbenzenesulfonate anion; c) bis(trifluoromethylsulfonyl)amide anion; d) methanesulfonate anion; e) dicyanamide anion; f) methyl orange anion and g) chloride anion.

3.2.2 Preparation of ion-exchange membranes

Solid contact probes consisted of four independent gold wires (Sigma Aldrich, UK) embedded within the non-conducting polyurethane resin/polymer (Figure 3.3). Ionophore-free membranes were prepared by dissolving TDAMCl (1% wt), PVC (33% wt) and desired plasticiser or RTIL in 0.5 mL of THF. For measurements using electrochemical impedance spectroscopy (EIS) the aliquot was also drop cast onto the top of solid contact electrodes (gold contact) and left at room temperature to dry overnight. The same conditioning protocol was utilised as during the preparation of ion selective membranes.

For potentiometric measurements a solution of POT (1.0×10^{-3} M of monomer in chloroform) was applied onto the same, as stated above, solid contact electrodes and left at room temperature to dry. This was followed by drop casting the aliquot of membrane cocktail which was then left at room temperature to dry overnight. Similarly, the ISEs were conditioned for 24 h at 0.1 M solution of $CaCl_2$.
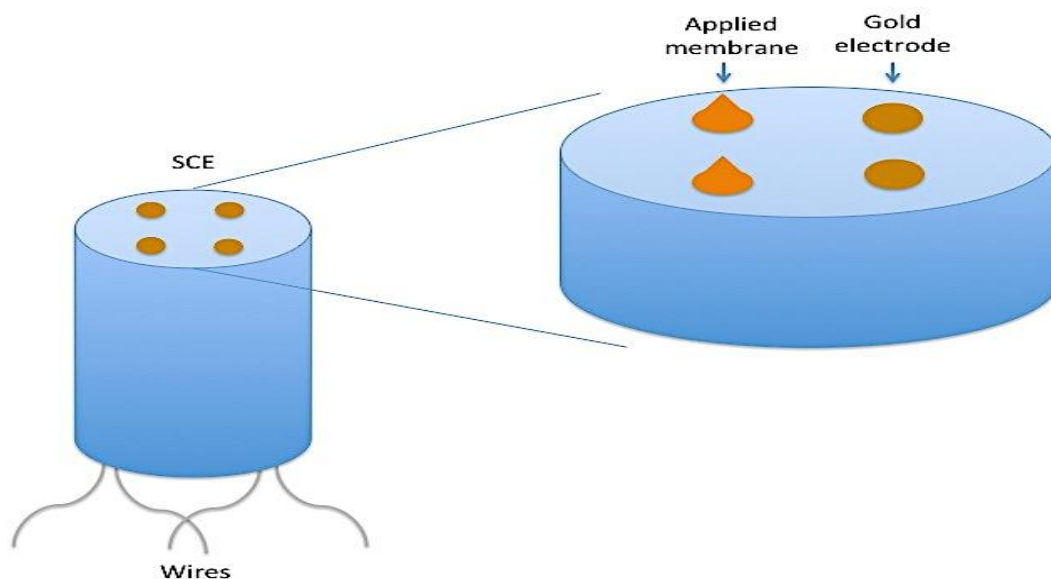
Figure 3.3 Schematic representation of a solid contact electrode (SCE) used in this study.

3.2.3 EMF measurements

Potentiometric responses were recorded with a Lawson Labs Inc. 16-channel EMF-16 interface (3217 Phoenixville Pike Malvern, PA 19355, USA) in a stirred solution against a double-junction Ag|AgCl|sat. KCl|1M LiOAc reference electrode (Fluka).

3.2.4 Electrochemical impedance spectroscopy measurements

Impedance measurements were performed by using an Ivium Technologies CompactStat Impedance Analyser coupled to a Himux XR 8 channel electrochemical multiplexer (Ivium Technologies). The EIS measurements were performed as described earlier.[38] Briefly, EIS spectra were collected using amplitude of 0.1 V and a frequency range of 100 kHz to 25 Hz. A conventional three electrode set-up was used in this study using platinum auxiliary electrode and a silver-silver chloride electrode as the reference. Each measurement was carried out in 0.1 M solutions of metal salts at room temperature. All impedance spectra

were fitted to equivalent circuits using the IviumStat software version 2.0. All measurements were done in at least triplicates. This allowed determination of resistance and capacitance components. The latter was relevant for further calculations. Dielectric constants were calculated as proposed by O'Rourke[39] using the equation 1.27 in Chapter 1 - EIS in the determination of dielectric constant. Membrane thicknesses were measured 5 times using digital micrometer and then averaged prior to the determination of the dielectric constant.

As the recorded impedance for ion-exchange membranes plasticised with the room temperature ionic liquids was very low, it was necessary to minimise the effects of the charge transfer resistance and solution resistance of the internal reference electrode on the overall measured impedance. In this study, the saturated solution of potassium chloride was used to minimise/eliminates the contribution of above-mentioned resistances for the internal Ag/AgCl reference electrode.

3.2.5   Selectivity measurements

For selectivity experiments separate solution method was used and the potentiometric responses of tested ISEs were recorded according to the protocol proposed by Bakker.[40] Upon conditioning in 0.1 M $CaCl_2$ solution the electrode response was determined for each of the chosen interfering anion separately in the following order: $Fe(CN)_6^{4-}$, SO_4^{2-}, OH^-, Br^-, NO_3^-, $HCrO_4^-$, SCN^-, ClO_4^-, Cl^- prior to the determination of the response to iodide.

3.3 Results and discussion

3.3.1 Role of ionic liquids in ISEs

Prior to embarking on the determination of selectivity coefficients, the attention was focused on the determination of the role of ILs in ion-exchange polymer based membranes. In other words, the determination whether the IL-based matrix exhibits only-nonspecific interactions with ion of choice as is the case of traditional plasticisers was carried out. It can be hypothesised that if ILs demonstrate a specific interaction (association) with the ion of choice (in other words behave as ionophore) the occurrence of so called Donna exclusion failure should be observed.[41]

Due to the potentially strong interaction of IL and I⁻, as the ion of choice in this study, it's partitioning into the membrane would be enhanced relative to a simple inert matrix. This would result in the situation where the amount of extracted analyte ion would exceed the one dictated by the amount of ion exchanger thus leading to co-extraction of counter-ion (K^+) in order to preserve electroneutrality of the membrane. Consequentially, deviation from Nernstian response would be observed. In extreme cases the response could be completely reversed and electrode would become selective to counter-ion.[42,43] Observation of Donnan failure can be observed in solutions containing high concentration of ion of interest thus allowing observation of upper detection limit.[43] Figure 3.4 demonstrates responses of IL-based electrodes to iodide. Some deviation from Nernstian slopes is indeed observed but only in the case of membranes ILs based on [DBS⁻] and [DCA⁻]. Intuitively, it could be expected that the effect would be reduced with reducing the amount of ILs to 50%. Indeed this is observed in membrane containing [DBS⁻] while it completely

disappears in the membrane based on [DCA⁻]. Potential reasons for observation of Donnan failure are discussed later in this chapter. Overall, it can be concluded that almost no studied ILs exhibit specific interactions with ion of choice and therefore, are suitable for use as plasticisers in ion-exchange membranes.
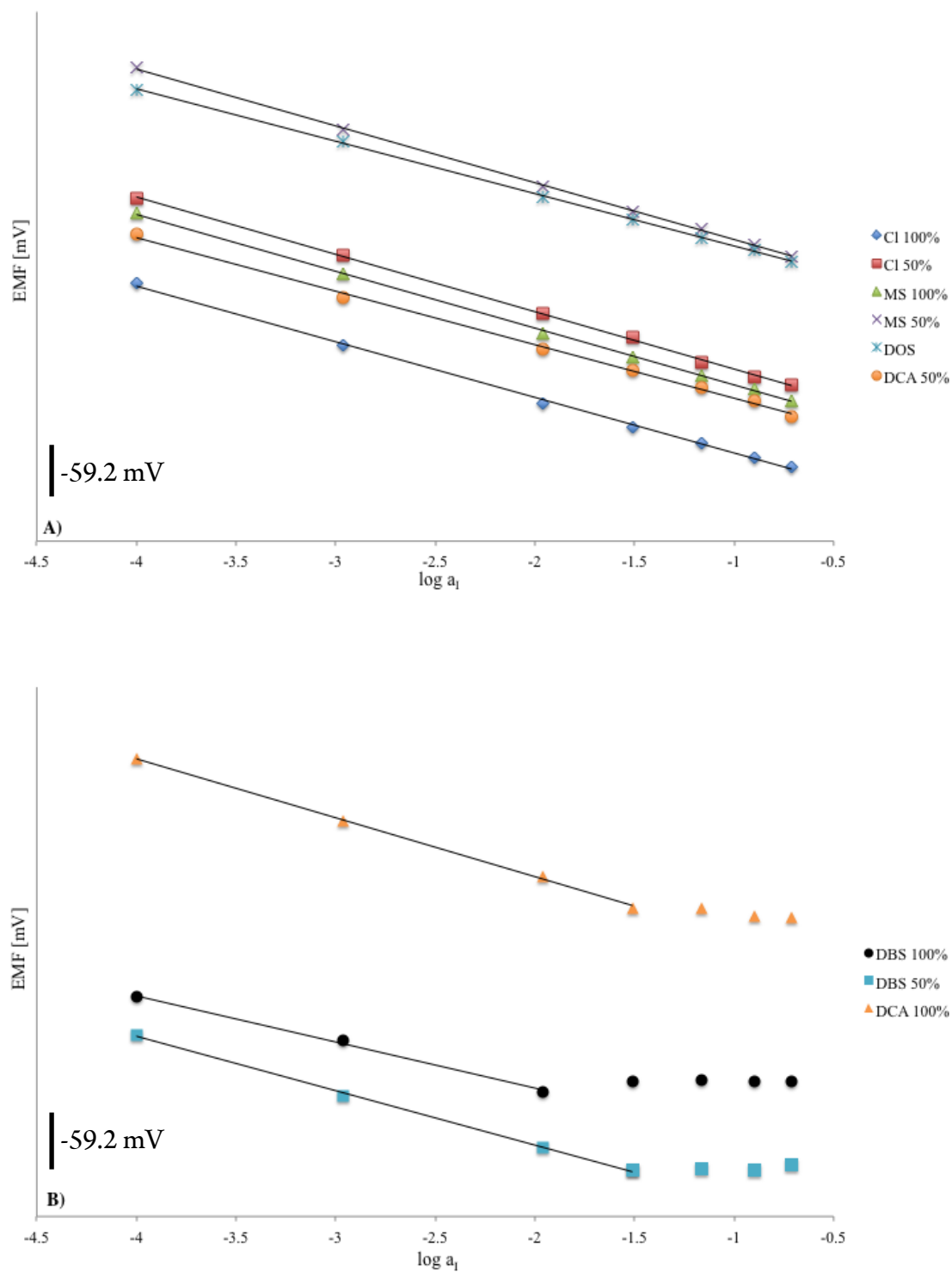
Figure 3.4 Potentiometric slopes recorded for ion-exchange membranes plasticised with selected RTIL. A) potentiometric responses of IL-based electrodes that do not show Donnan exclusion failure. B) responses of electrodes based on [DCA⁻] and [DBS⁻] exhibiting Donnan failure.

3.3.2 Ion-exchange membranes

In contrast to traditionally prepared ion selective membranes used for decades in potentiometric measurements, ionic liquid based ISEs display significantly different physico-chemical properties. For instance, they may demonstrate varying selectivity characteristics that do not always follow the well-established Hofmeister order. It can be hypothesised that very high ionic content arising from the presence of IL within the polymeric matrix may contribute to the overall increase in the polarity of the ion exchange membrane (higher dielectric constant). As a result, the extraction of more hydrophilic anions from the aqueous solution into the organic phase is facilitated. Since ISEs routinely employed in potentiometry usually contain more than 50% of a plasticiser, their replacement with more ionic species significantly reduces the resistance and capacitance, as demonstrated by a low impedance response (Figure 3.5). The frequency dispersion in the recorded EIS spectrum of the inset in Figure 3.5 resembles a compressed semicircle. Roughened surface of the used electrode has been previously indicated to cause the dispersion in measured frequency in EIS experiments of polymeric membranes, however in the context of this study the frequency dispersion could be caused by the presence of polymer and plasticiser domains (chemical inhomogeneity within the membrane bulk). Moreover, the non-ideal shape of Nyquist plot may be also attributed to the local differences in the thickness of the casted membrane. As the solvent used for the preparation of ion-exchange membranes evaporates into the atmosphere, the outer side of the polymeric film was reported to be more irregular (rougher) if compared to the surface contacting the electrode. On some occasion, the thickness of polymeric membranes either plasticised with conventional solvent mediators or ILs varied across the casted film by approximately 5%. This could give rise to the frequency dispersion in the recorded EIS

spectrum. For that purpose, a constant phase element parameter was introduced during modelling of impedance data to produce the unbiased capacitance and dielectric constant. Furthermore, the EIS measurements of ion selective membranes can display inductive behaviour indicating a resistance to phase change to the frequency scanning of the investigated ISE.[39] If such behaviour is observed, the determination of dielectric constant should be avoided as it may introduce a significant bias into the results.
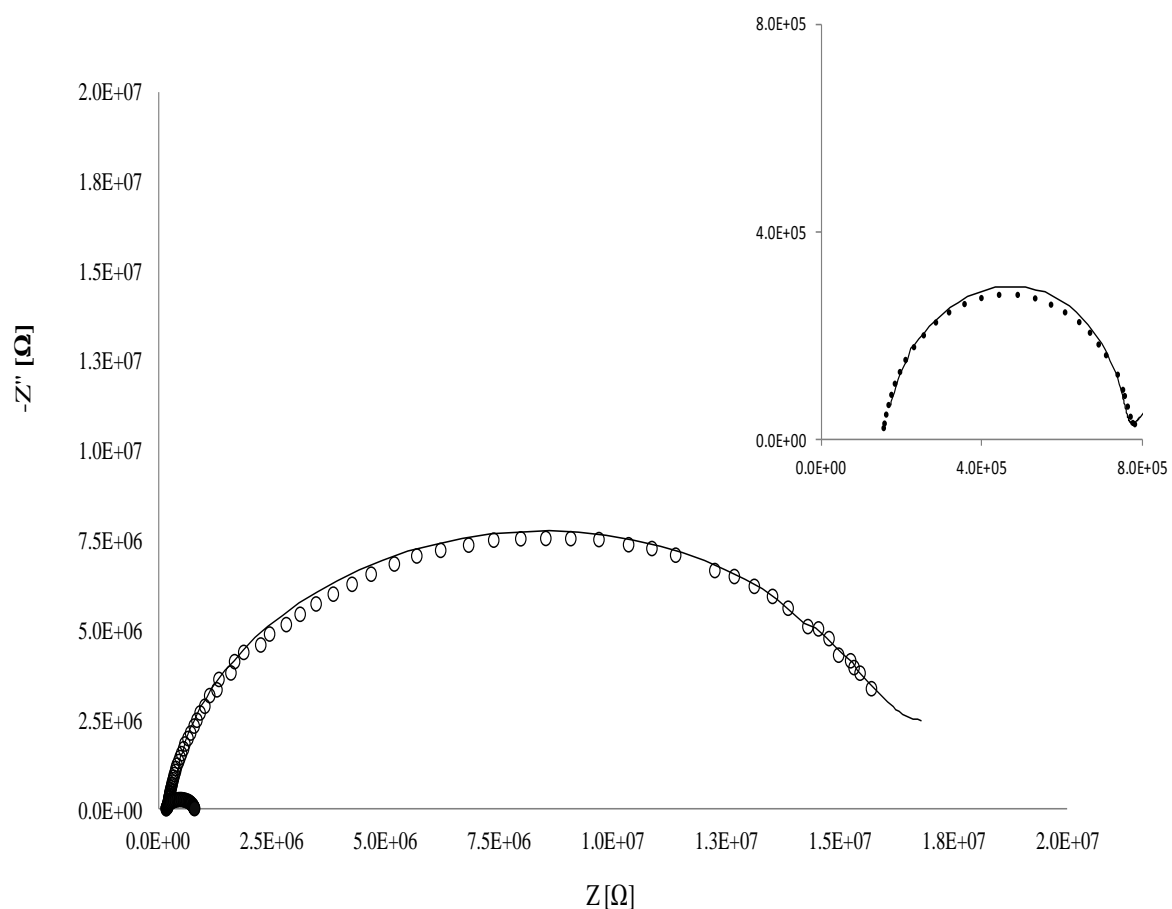
Figure 3.5 Impedance spectra of the ionophore free membranes plasticised either with DOS (open circles) and [P$_{6,6,6,14}$][DBS$^-$] ionic liquid (closed circles) and their corresponding fitting results with the equivalent circuits (straight line). The inset in the upper section of the figure illustrates the Nyquist plot of [DBS$^-$] based membranes. The line is a fit to the   It can be observed that the presence of ionic liquids decreases membrane's resistance by the factor of about 20.

The majority of the polymeric membranes investigated in this study, with the exception of the [DBS⁻], DOS and NPOE plasticised ISEs, showed extremely low resistances, which unfortunately could not be accurately quantified. These results imply a very ionic nature of tested membranes and therefore excessively high dielectric values. On the contrary, both membranes containing traditional plasticisers displayed much higher resistance with the NPOE based sensors being more conductive than those plasticised with DOS. This can be explained by the more polar nature of NPOE as evidenced by the values of dielectric constant measured. These findings are further summarised in Table 3.1.

Table 3.1 Dielectric constants calculated for ion-exchange membranes plasticised entirely with either traditional plasticisers or ionic liquids. Since all IL based membranes contained the same form of a cation - [$P_{6,6,6,14}$], for the simplicity of data presentation, only their corresponding anions are listed.

PVC membrane composition	Dielectric constant
33% PVC, 66% DOS	13.5 ± 1.0
33% PVC, 66% NPOE	23.6 ± 0.5
33% PVC, 66% [DBS⁻]	40.0 ± 0.4
33% PVC, 66% [DCA⁻], [Cl⁻], [TFMS⁻], [MS⁻], [MO⁻]	N/A

To validate whether the highly ionic nature of the investigated electrodes had a direct influence on the selectivity of ISEs, the potentiometric response of each membrane was measured. Three electrodes of each type were prepared and their working characteristics in the separate solutions of various anions ($Fe(CN)_6^{4-}$, SO_4^{2-}, OH^-, Br^-, NO_3^-, $HCrO_4^-$, SCN^-, ClO_4^-, Cl^- and I^-) were evaluated. All electrodes responded with theoretical Nernstian or near-Nernstian slopes upon adding known concentrations of interfering anions to the

sample solution with ultrapure water as background. Every studied membrane responded rapidly (Chapter 3 – Response time) to changes in the concentration of background ions, producing a stable signal. Short term stabilities were also evaluated from the potentiometric data. The gradual change in the response of tested ISEs (EMF vs time) provided information about the electrodes short term stability, with values not exceeding 0.2 mV min^{-1}. These obtained results are promising for practical applications.

3.3.3 Response time

The response time of tested ion-exchange membranes was determined via pipetting the concentrated standard solution of selected ions into a stirred aqueous solution and the resulting changes in the EMF response were recorded. The time for the electrode to respond towards the changing concentration of ions was measured from the moment when both the reference electrode and ion-exchange membranes were placed into the sample solution at which the activity of determined ions is changed to the first instant ($\Delta E/\Delta t = 0.4$ mV/min).[44] It has been previously reported that the response time of ISEs depends on the concentration of primary ions in the sample solution and it is longer in more diluted solutions. The longest response time recorded in this study was 12 seconds for [P$_{6,6,6,14}$][MS$^-$] plasticised membranes in 1.0×10^{-5} M solution of selected ions. The remaining ion-exchange membranes plasticised with RTILs and traditional plasticisers exhibited maximum response time of 10 seconds for the same concentration of ionic species. As the concentration of the solution was increased to approximately 1.0×10^{-3} M the response time of each electrode was reduced to 6-7 seconds. The response time recorded for each ion-exchange membrane was independent of the type of anion (salt) used during potentiometric measurements.

3.3.4 Selectivity of ion-exchange membranes

On several occasions, ion-exchange membranes plasticised with ILs exhibited the selectivity that is characteristic to the Hofmeister sequence with its magnitude deviating significantly from the ISEs prepared with traditional plasticisers. It was especially apparent that the most lipophilic membranes (containing DOS) favoured the extraction of ClO_4^- over iodide ions by about three orders of magnitude while the same ion was less preferentially extracted when more polar membranes were used – $\log K^{POT} = 2.5$ for NPOE and between 1.7 to 0.7 for IL based ISEs. As suggested earlier, the resulting increase in polarity may be accounted to the high content of IL moieties within the membrane segment. Their presence decreases the overall lipophilicity of the membrane and minimises the energy barrier for more hydrophilic ions to cross the phase boundary interface. These findings are strongly supported by the EIS data presented earlier in Table 3.1.

Polymeric membranes with low dielectric constant values (plasticised with DOS) favoured extraction of less hydrated ions such as perchlorates or thiocyanates, however when the overall hydrophilicity of these electrodes was increased (higher ε) the selective response towards these anions approached those of more hydrophilic ions (ε - DOS < NPOE < IL based membranes). The difference in polarity between investigated IL based membranes could not be calculated from the EIS measurements as the resistance of majority of these electrodes was too small to determine the geometric capacitance of the membranes and consequently it could not be used to calculate the dielectric constants. Moreover, ion-exchange membranes plasticised with the $[P_{6,6,6,14}][MS^-]$ showed an inductive behaviour (Figure 3.6). The determination of dielectric constants from such membranes was not

carried out in order to minimise experimental bias and therefore such values were only calculated from well-defined semicircles as illustrated in Figure 3.5. The inductive behaviour during EIS measurements has been previously attributed to the problems associated with wiring, instrument or electrodes. However, to reassure the reproducibility of the impedance measurements, the same experimental setup was used throughout the experiment and each selected ion-exchange membrane was tested at least three times. Since, only polymeric membranes prepared with [MS⁻] RTIL demonstrated the above-mentioned inductive behaviour, it could be hypothesised that such response characteristic is solely unique for this particular ion-exchange membrane. Furthermore, inductive behaviour has been ascribed to the formation of a surface layer (e.g. adsorption of species on the nickel surface)[45] or fouling. In light of these findings the presence of inductive loop in Figure 3.6 cannot be fully explained.

Even though, the polarity of each membrane could not be quantified, the capacitive behaviour indicates extremely polar (ionic) nature of investigated samples as reported by O'Rourke[39] and therefore it supports the findings from the performed potentiometric experiments.
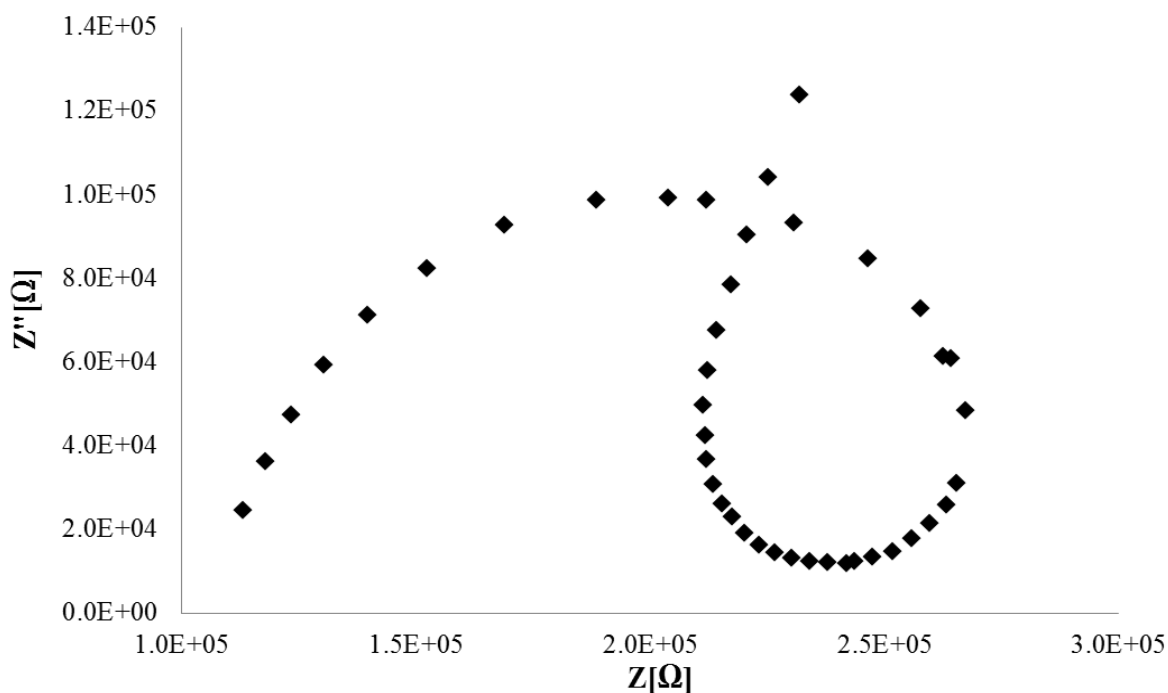
Figure 3.6 Inductive behaviour of the ion selective membrane plasticised fully with [MS⁻] ionic liquid.

Interestingly, out of several tested IL based membranes only those plasticised with [P$_{6,6,6,14}$][DBS⁻] produced responses that allowed for the quantification of dielectric constant values. Dodecylbenzenesulfonate anions have previously been demonstrated to form micellar aggregates in aqueous solution if the critical micelle concentration (CMC) is reached.[46] It could be hypothesised that [DBS⁻] anions at very high concentrations such as those used during the preparation of ISEs may form reversed micellar aggregates. It has been recently reported that ionic liquid moieties may be arranged within the membrane during the impedance measurements in order to reduce the ion charge density.[47] The self-aggregation behaviour of RTILs in aqueous solutions was investigated in the literature by means of mass spectrometry,[47] ¹H NMR[48] and fluorescence spectroscopy.[49] It was found that the tendency of ILs to form aggregates strongly depends on the structural properties of given ILs such as the length of alkyl chains and the type of counter-ions and aromatic rings

133

used to make up the molecule as well as their interactions with the surrounding media.[50] For instance, 1-butyl-3-methylimidazolium tetrafluoroborate [BMIM][BF$_4$] IL moieties assemble to form larger aggregates in solvent of decreasing polarity to minimise the charge density within the ions.[47] Preliminary studies indicated that the presence of larger anions in this case [DBS$^-$] may reduce the need of charge delocalisation by forming ionic liquid aggregates. Agglomerates formation can result in the decline of the number of ionic carriers and therefore give rise to the elevated resistance and lower ionic conductivity. Research carried out by Dorbirtz et al (2005) showed that this effect is even more pronounced at high concentrations of ionic liquids.[47] These results are in good agreements with findings from this study where both ionic liquids contribute over 66% towards the total mass of the membrane and therefore fulfil the requirements for aggregates formation. This would lead to a decrease in the number of ionic species present in the membrane and subsequently result in larger resistance of the sensing membrane. The proposed linear reverse micelle arrangement is demonstrated in Figure 3.7. Interestingly, ion selective membranes plasticised with a 1:1 mixture of DOS and [DBS$^-$] ionic liquid displayed a significantly higher dielectric constant (Table 3.2) than membranes containing pure IL as a plasticiser. Since the overall concentration of [DBS$^-$] anions was reduced, it is possible that the CMC was not reached and therefore what may appear to be counterintuitive, more ionic species (carrying charge) were present in the ion-exchange membrane. With the increasing concentration of DOS (2:1 ratio), the dielectric constant of such membranes was observed to be much lower as the more lipophilic character of that plasticiser would start dominating and defining membrane characteristics. This is illustrated in Table 3.2.
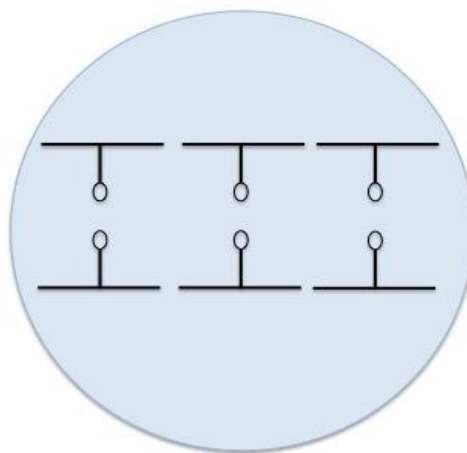
Figure 3.7 Proposed charge density stabilisation of [DBS⁻] in thin PVC based membrane via the formation of aggregates. Reverse micelles of [DBS⁻] are formed within the polymeric matrix (which also occurs at high concentrations of [DBS⁻]).

Table 3.2 Dielectric constants of [P$_{6,6,6,14}$][DBS⁻] based membranes obtained from EIS measurements.

PVC membrane composition	Dielectric constant
33% PVC, 66% DBS⁻	40.0 ± 2.1
33% PVC, 50% DOS and 50% DBS⁻	312.4 ± 8.3
33% PVC, 66% DOS and 33% DBS⁻	48.1 ± 1.8

Further potentiometric experiments revealed that the majority of IL based ISEs favoured extraction of ions with small hydration radii as predicted by the ion-exchange theory. On most occasions, the perchlorate and thiocyanate anions were favoured over better-hydrated

ions such as bromide or chloride. It has been reported that a ClO_4^- ion is usually preferred by approximately 4.5 – 5 orders of magnitude over Cl^- ions,[51] however, much smaller differences (approximately 1 order of magnitude) were observed for membranes plasticised entirely with $[P_{6,6,6,14}][MO^-]$ ionic liquid (Figure 3.8). The same membrane demonstrated a very narrow selectivity range (small differences in the selectivity coefficient values) indicating a relatively non-selective nature of this membrane. Such membranes that exhibit a non-selective response have been already indicated as potential candidates for the separation science detectors[52] and for the analysis of abundant hydrophilic anions in the presence of more lipophilic interfering ions. Interestingly, the same membrane started exhibiting a more selective response towards lipophilic ions when the same IL was mixed with DOS at 1:1 ratio (Figure 3.9). This shows that with an addition of a more lipophilic plasticiser the response characteristics can be reversed providing extra functionality to the membrane.

Figure 3.8 Logarithmic value of selectivity coefficients of iodide (I⁻) versus noted interfering ion (A⁻) obtained by using the separate solution method and utilising noted plasticiser as solvent mediators. The dotted line indicates log $K^{POT}_{I,I}$ thus equalling zero.

As is illustrated in Figure 3.8, several IL based sensors displayed selectivity deviations from the Hofmeister sequence. Depending on the specific IL based membrane, some hydrophilic ions were preferentially extracted into the membrane bulk over the more lipophilic anions. For example, the extraction of chloride anions in [TFMS⁻] and [DBS⁻] based membranes appears to be less energetically favourable than the extraction of sulphate or bromide ions. Whereas, sensing membranes containing [MO⁻] moieties responded preferentially to the nitrate ions rather than ClO₄⁻ anions. Moreover, most of the ISEs favoured extraction of nitrate ions over hydrogen chromate ions as predicted by the ion-exchange theory with the exception of membranes containing [MS⁻] species that showed more selective response towards the hydrogen chromate ions. The majority of

membranes exhibited a very limited (unselective) response to ferrocyanide anions due to the high hydration energy of this ion. However, the ISEs plasticised with $[P_{6,6,6,14}][DCA^-]$, $[DBS^-]$ and $[MS^-]$ favoured the diffusion of $Fe(CN)_6^{4-}$ from the sample into the membrane bulk over the extraction of less hydrophilic sulphate anions.

Table 3.3 Selectivity coefficients values (log K^{POT}) calculated for the ion selective membranes that were fully plasticised with either traditional solvent mediators such as DOS and NPOE or $[P_{6,6,6,14}]$ based ionic liquids.

Anion / Type	DOS	NPOE	[DBS⁻]	[Cl⁻]	[TFMS⁻]	[DCA⁻]	[MS⁻]	[MO⁻]
ClO_4^-	2.71 ± 0.04	2.42 ± 0.11	1.35 ± 0.26	1.24 ± 0.05	1.79 ± 0.03	1.25 ± 0.02	1.22 ± 0.06	1.20 ± 0.11
SCN^-	1.63 ± 0.10	1.05 ± 0.10	-0.52 ± 0.05	0.58 ± 0.09	1.06 ± 0.13	0.37 ± 0.09	-0.35 ± 0.06	2.33 ± 0.04
NO_3^-	0.25 ± 0.03	-0.49 ± 0.00	-0.62 ± 0.08	-0.27 ± 0.08	0.49 ± 0.03	-0.61 ± 0.09	-1.21 ± 0.07	0.45 ± 0.03
$HCrO_4^-$	-0.86 ± 0.16	-1.29 ± 0.13	-0.67 ± 0.06	-0.79 ± 0.07	-0.70 ± 0.05	-0.87 ± 0.01	-0.78 ± 0.15	-1.90 ± 0.06
OH^-	-0.93 ± 0.04	-2.00 ± 0.06	-4.05 ± 0.13	-0.90 ± 0.11	-2.33 ± 0.02	-4.16 ± 0.09	-4.80 ± 0.09	-0.53 ± 013
Br^-	-1.63 ± 0.02	-2.05 ± 0.01	-1.30 ± 0.03	-1.42 ± 0.07	-1.94 ± 0.12	-1.26 ± 0.04	-1.57 ± 0.04	-0.86 ± 0.01
Cl^-	-1.90 ± 0.08	-3.22 ± 0.02	-3.59 ± 0.01	-0.46 ± 0.01	-2.58 ± 0.01	-2.22 ± 0.13	-3.48 ± 0.01	0.04 ± 0.01
$Fe(CN)_6^{4-}$	-3.67 ± 0.06	-4.43 ± 0.01	-3.33 ± 0.06	-3.50 ± 0.13	-3.63 ± 0.05	-3.44 ± 0.11	-3.54 ± 0.06	-3.36 ± 0.10
SO_4^{2-}	-3.21 ± 0.01	-2.33 ± 0.00	-3.49 ± 0.12	-2.71 ± 0.01	-2.51 ± 0.03	-4.17 ± 0.01	-4.48 ± 0.01	-1.93 ± 0.02

Table 3.4 Experimental slopes (mV/decade) obtained during potentiometric measurements for ion selective membranes entirely plasticised with ionic liquids or traditional plasticisers.

Anion / Type	DOS	NPOE	[DBS⁻]	[Cl⁻]	[TFMS⁻]	[DCA⁻]	[MS⁻]	[MO⁻]
ClO_4^-	-66.8 ± 3.2	-67.7 ± 2.2	-66.9 ± 4.3	-57.7 ± 0.6	-55.0 ± 6.2	-65.6 ± 1.0	-80.8 ±1.2	-89.6 ± 3.8
SCN^-	-57.5 ± 1.6	-54.4 ± 1.5	-64.6 ± 1.7	-45.9 ± 0.7	-50.8 ± 3.0	-54.1 ± 2.0	-63.1 ± 3.3	-35.1 ± 2.0
I^-	-65.9 ± 2.7	-54.8 ± 1.1	-60.2 ± 5.0	-56.9 ± 5.6	-56.9 ± 5.3	-53.4 ± 5.8	-58.4 ± 5.1	-68.7 ± 1.0
NO_3^-	-65.3 ± 3.2	-56.6 ± 0.6	-56.1 ± 4.3	-49.2 ± 5.8	-62.2 ± 3.0	-52.3 ± 0.0	-48.5 ± 5.6	-51.1 ± 1.2
$HCrO_4^-$	-57.3 ± 4.9	-61.3 ± 2.0	-63.0 ± 2.9	-51.2 ± 0.6	-56.6 ± 3.2	-61.0 ± 3.1	-64.1 ± 3.0	-62.3 ± 4.6
OH^-	-55.4 ± 4.0	-41.7 ± 1.0	-29.2 ± 0.8	-36.8 ± 0.9	-57.1 ± 4.8	-34.9 ± 0.8	-47.4 ± 3.1	-44.9 ± 0.3
Br^-	-53.7 ± 2.1	-56.2 ± 1.8	-54.0 ± 0.7	-44.9 ± 1.8	-61.3 ± 2.3	-47.5 ± 1.6	-59.9 ± 6.0	-45.2 ± 1.4
Cl^-	-56.5 ± 4.0	-56.8 ± 1.9	-57.6 ± 5.5	-61.4 ± 3.1	-61.9 ± 0.0	-55.9 ± 5.9	-58.2 ± 4.5	-59.4 ± 7.3
$Fe(CN)_6^{4-}$	-16.6 ± 1.3	-16.2 ± 1.0	-14.9 ± 0.8	-18.7 ± 3.7	-21.0 ± 1.3	-16.5 ± 0.4	-12.6 ± 3.5	-18.5 ± 1.8
SO_4^{2-}	-20.9 ± 0.6	-25.2 ± 4.4	-32.3 ± 0.3	-37.0 ± 0.7	-34.0 ± 3.3	-33.5 ± 2.0	-33.9 ± 1.7	-31.4 ± 5.9

The majority of tested electrodes produced a Nernstian or near-Nernstian response during the potentiometric measurements with the exception of experiments ran for the determination of perchlorate ions for [MS⁻] and [MO⁻] plasticised membranes. Such super Nernstian behaviour was observed for these two membranes only.

On the contrary to [Cl⁻] based ISEs, all [TFMS⁻] based membranes exhibited more selective response towards SO_4^{2-} and OH^- and Br^- ions that to the Cl^- anions. The enhanced selectivity towards chloride ions was expected for the sensing membranes loaded with Cl^- ions prior the measurements as their high concentration dictates the response characteristics of these ISEs. Even though, the ion exchange at the sample-membrane interface will result in the presence of other, interfering ions in the membrane, their concentration will be significantly lower than that of the chloride ions. This will either result in the mixed potential response as both interfering and primary (Cl^-) ions will be present in the membrane bulk and contribute to the phase boundary potential or it will produce a response that is characteristic to the chloride ions only. This may imply that IL based membranes containing the same anion as the ion that is being detected have the potential to exhibit high selectivity towards that ion. Furthermore, with the addition of a selective ionophore, sensing properties of these membranes may be improved to produce the characteristic response even in the presence of interfering ions in the investigated sample. The same membrane became less selective towards the chloride ions when half of the [Cl⁻] ionic liquid was replaced with DOS as demonstrated in Figure 3.9 and Table 3.5 The addition of this traditional plasticiser reduced the total concentration of Cl^- ions in the membrane bulk and therefore minimised their contribution towards the overall chloride selectivity. Again, this illustrates that selective response of ISEs can be tuned by preparing mixtures of plasticisers used for membrane preparation.[53]

The selectivity of the studied polymeric membranes could be expected to become less dependent on the ion lipophilicity as the high concentration of polar groups (ILs) within the membrane matrix would result in a more pronounced presence of Coulombic

interactions between sample ions and charged IL moieties. The presence of more hydrophilic IL groups can also facilitate the diffusion of water from the sample into the membrane bulk affecting the overall polarity of the ISEs and therefore their selectivity.[52]

3.3.5 Selectivity of membranes plasticised with the mixtures of DOS and IL at 1:1 ratio

Each of the ionic liquids used in this study was later mixed with a traditional plasticiser – DOS at 1:1 ratio (33% of DOS and 33% IL) to prepare a new set of ion selective membranes. The same protocols were used as described in the experimental section. After conditioning in a 0.1 M solution of calcium chloride overnight the response characteristics of each ion exchange membranes were evaluated using a potentiometric setup. This solution was chosen to avoid membrane contact with primary ions and therefore obtain unbiased selectivity coefficients.[40] The selectivity coefficient values determined for each membrane are demonstrated in Figure 3.9 and Table 3.5.
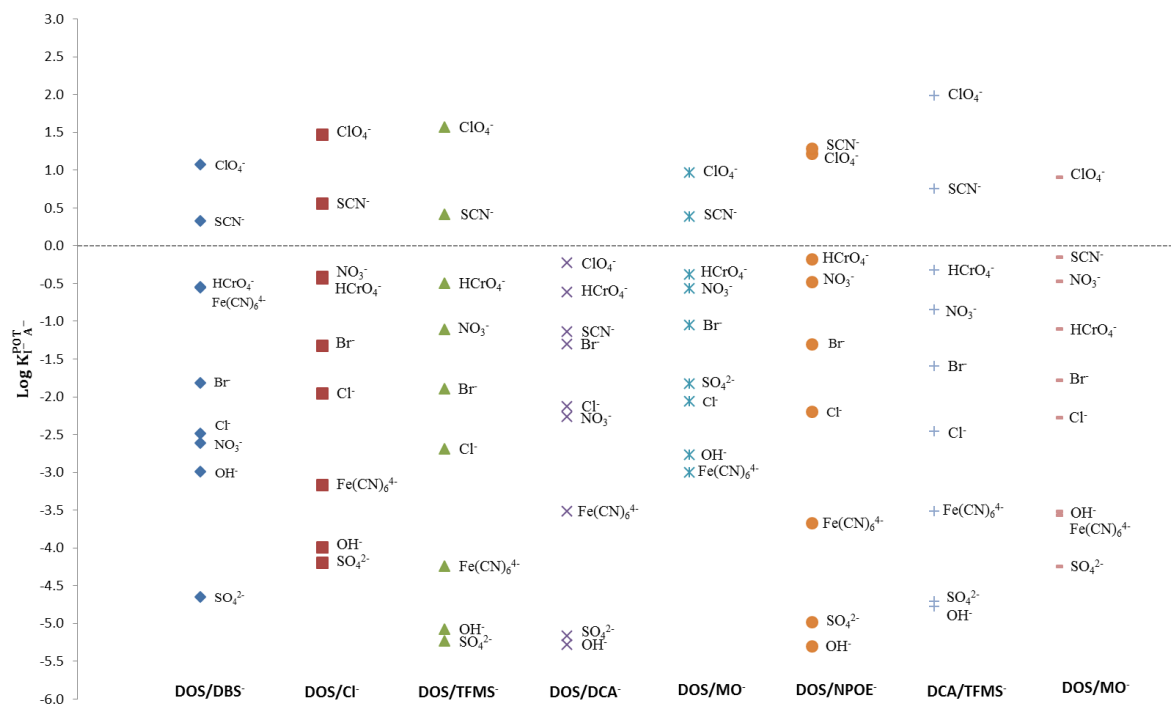
Figure 3.9 Selectivity coefficients obtained for the tested ion-exchange membranes. The dotted line corresponds to log K^{POT} equal to zero.

On many occasions, similar selectivity patterns were observed for membranes containing mixtures of DOS and ILs at 1:1 ratio as to ion exchange membranes entirely plasticised with ILs or traditional plasticisers. However, some other small deviations in the selectivity pattern could be noticed when a more lipophilic plasticiser was introduced into the membrane bulk. Ion selective membranes plasticised with mixtures of DOS and [DBS⁻] or DOS and [TFMS⁻] started producing responses that reflected the Hofmeister sequence (more lipophilic ions are preferentially extracted into the membrane). This in-part was expected as the overall lipophilicity of the membrane was increased upon the addition of more lipophilic plasticiser such as DOS. Similar observations were made for membranes plasticised with [MO⁻] ionic liquids where not only the selectivity sequence had changed but also the magnitude of the response was altered. Again, this could be explained by the reduced hydrophilicity of the membrane, which resulted in less preferential extraction of

ions such as chloride or hydroxide. This illustrates that the response characteristics of ion selective membranes plasticised with ILs can be partially controlled and modified with the addition of plasticisers of known polarity (such as DOS) and therefore the effects of such combinations can somehow be predicted.

Table 3.5 Selectivity coefficients values (log K^{POT}) calculated for the ion selective membranes containing 1:1 mixtures of ILs with DOS as plasticisers.

Anion / Type	[DBS⁻]	[Cl⁻]	[TFMS⁻]	[DCA⁻]	[MO⁻]	NPOE	[MS⁻]
ClO_4^-	1.080 ± 0.05	1.473 ± 0.00	1.574 ± 0.08	-0.229 ± 0.01	0.969 ± 0.06	1.223 ± 0.11	0.909 ± 0.08
SCN^-	0.331 ± 0.06	0.564 ± 0.01	0.418 ± 0.01	-1.138 ± 0.01	0.391 ± 0.01	1.293 ± 0.03	-0.142 ± 0.02
NO_3^-	-2.615 ± 0.03	-0.405 ± 0.01	-1.107 ± 0.01	-2.263 ± 0.02	-0.564 ± 0.02	-0.481 ± 0.03	-0.469 ± 0.07
$HCrO_4^-$	-0.547 ± 0.04	-0.426 ± 0.03	-0.495 ± 0.02	-0.613 ± 0.09	-0.384 ± 0.06	-0.180 ± 0.09	-1.102 ± 0.09
OH^-	-2.993 ± 0.07	-3.988 ± 0.03	-5.074 ± 0.32	-5.281 ± 0.01	-2.769 ± 0.02	-5.294 ± 0.11	-3.513 ± 0.03
Br^-	-1.815 ± 0.25	-1.321 ± 0.06	-1.896 ± 0.00	-1.303 ± 0.04	-1.045 ± 0.07	-1.297 ± 0.01	-1.776 ± 0.02
Cl^-	-2.488 ± 0.07	-1.951 ± 0.17	-2.689 ± 0.28	-2.129 ± 0.52	-2.057 ± 0.06	-2.192 ± 0.04	-2.273 ± 0.01
$Fe(CN)_6^{4-}$	-0.551 ± 0.04	-3.159 ± 0.04	-4.240 ± 0.01	-3.514 ± 0.03	-2.995 ± 0.02	-3.670 ± 0.17	-3.560 ± 0.00
SO_4^{2-}	-4.648 ± 0.12	-4.193 ± 0.12	-5.229 ± 0.03	-5.167 ± 0.08	-1.828 ± 0.01	-4.976 ± 0.03	-4.239 ± 0.01

Table 3.6 Experimental slopes (mV/decade) obtained during potentiometric measurements for ion selective membranes plasticised with ILs and traditional plasticisers at 1:1 ratio.

Anion / Type	[DBS⁻]	[Cl⁻]	[TFMS⁻]	[DCA⁻]	[MO⁻]	NPOE	[MS⁻]
ClO_4^-	-53.5 ± 4.2	-86.8 ± 2.1	-71.0 ± 5.1	-77.7 ± 9.5	-68.6 ± 3.6	-64.2 ± 2.6	-60.6 ± 6.4
SCN^-	-65.1 ± 3.0	-69.0 ± 3.6	-63.3 ± 2.9	-73.0 ± 1.0	-61.4 ± 4.4	-68.8 ± 1.1	-67.2 ± 6.6
I^-	-60.2 ± 1.6	-61.0 ± 6.7	-62.5 ± 3.2	-61.5 ± 5.1	-57.7 ± 2.9	-59.4 ± 3.4	-63.6 ± 4.6
NO_3^-	-50.3 ± 5.9	-61.6 ± 9.2	-52.8 ± 3.6	-56.5 ± 1.5	-62.1 ± 3.0	-57.6 ± 2.5	-61.1 ± 3.6
$HCrO_4^-$	-54.5 ± 0.4	-63.3 ± 2.6	-56.0 ± 3.9	-55.4 ± 5.3	-57.3 ± 4.4	-58.6 ± 2.6	-60.7 ± 1.3
OH^-	-52.2 ± 2.2	-49.8 ± 1.7	-54.3 ± 4.2	-42.9 ± 1.8	-48.0 ± 17.3	-47.9 ± 3.7	-46.4 ± 1.5
Br^-	-57.2 ± 5.3	-52.6 ± 3.0	-55.1 ± 3.8	-53.5 ± 3.1	-56.4 ± 5.0	-57.3 ± 4.8	-60.6 ± 2.6
Cl^-	-54.8 ± 3.6	-59.5 ± 8.2	-54.6 ± 3.0	-55.9 ± 2.0	-56.3 ± 2.8	-55.0 ± 4.0	-56.9 ± 4.2
$Fe(CN)_6^{4-}$	-15.2 ± 4.2	-16.5 ± 1.9	-15.5 ± 1.2	-15.4 ± 1.7	-12.5 ± 0.5	-14.8 ± 2.0	-14.9 ± 4.8
SO_4^{2-}	-30.7 ± 1.0	-34.9 ± 2.3	-27.6 ± 1.3	3-4.7 ± 3.4	-33.3 ± 2.2	-31.4 ± 3.6	-33.3 ± 3.8

3.3.6 Study of aqueous water layer

It was observed that the low frequency data on the Nyquist plot (Figure 3.5 - $[P_{6,6,6,14}][DBS^-]$ plasticised membranes – closed circles) approaches the real impedance axis indicating very small contact resistance between the polymeric membrane and the gold electrode. It is well known that water layer formation is a common issue encountered during the preparation of solid contact electrodes (SCEs) as it enhances mass diffusion across the membrane resulting in sub-optimal detection limits (SCEs exhibit similar behaviour to liquid contact electrodes with inner filling solution).[54] The application of IL based membranes may reduce the subsequent ion fluxes as the water layer formed at the electrode/membrane interface may diffuse into the membrane bulk due to the increased

polarity of the polymeric membranes. It could be speculated that the water uptake from both sample solution and the interface between the solid contact and sensing membrane can influence the selectivity of ISEs (dielectric constant of water = 80.4). However, the EIS measurements revealed that only very small changes in the dielectric constants were observed over the 24 h period for the [DBS$^-$] plasticised ISEs (ε before the exposure to water – 40.03 ± 1.7, ε after 24 h – 40.05 ± 1.3) suggesting that water uptake has minimal or no effect on the overall selectivity of that membrane. Even though, the influence of water uptake on the selectivity of IL based electrodes was measured only for one type of sensing membrane, it is expected that the same trend will be observed for all tested electrodes. It can be hypothesised that the high dielectric constant of the ion selective membranes that were entirely plasticised with ILs would overpower the effects of absorbed water on the overall polarity of the ISEs. Note that the results presented in here are indicative of the observed effects and therefore further examination, for instance by using neutron reflectometry[55] would be required.

3.4 Conclusions

The selectivity of ion exchange membranes is an important parameter that defines the applicability of these sensors for measurements in both clinical and environmental samples since these specimens often exhibit highly complex characteristics (presence of many interfering ions). Membrane matrices composed of plasticised polymers are one of the key factors that dictate the selectivity of ionophore-free ion exchanger-based sensors. RTILs based on trihexyl(tetradecyl)phosphonium $[P_{6,6,6,14}]$ cation have shown the capability to influence the extraction of sample ions into the membrane illustrated by the change of potentiometric selectivity coefficient. The modification was particularly significant for hydrophilic ions since for some ions the order in Hofmeister series was altered. This finding is in accordance with higher dielectric constant of RTIL-based membranes. It has been also demonstrated that the variations in selectivity can be fine-tuned by the addition of molecular plasticisers to RTIL-based membranes. Finally, it was shown that the water uptake by relatively polar RTIL-based membrane does not influence its selectivity characteristics. Overall, this study demonstrates that RTILs can be successfully utilised as plasticisers in ion exchanger-based membranes, which can be used to finely tune their selectivity.

References

(1)   Chatterjee, S.; Bryan, S. A.; Seliskar, C. J.; Heineman, W. R. *Rev. Anal. Chem.* **2013**, *32* (3).

(2)   Heineman, W. R.; Seliskar, C. J.; Morris, L. K.; Bryan, S. A. Zamboni, R., Kajzar, F., Szep, A. A., Eds.; 2012; p 854509.

(3)   Schroll, C. A.; Chatterjee, S.; Heineman, W. R.; Bryan, S. A. *Anal. Chem.* **2011**, *83* (11), 4214–4219.

(4)   Wan, H.; Ha, D.; Zhang, W.; Zhao, H.; Wang, X.; Sun, Q.; Wang, P. *Sens. Actuators B Chem.* **2014**, *192*, 755–761.

(5)   Shioya, T.; Nishizawa, S.; Teramae, N. *J. Am. Chem. Soc.* **1998**, *120* (44), 11534–11535.

(6)   Bakker, E.; Bühlmann, P.; Pretsch, E. *Electroanalysis* **1999**, *11* (13), 915–933.

(7)   Koryta, J. *Anal. Chim. Acta* **1972**, *61* (3), 329–411.

(8)   Bakker, E.; Bühlmann, P.; Pretsch, E. *Chem. Rev.* **1997**, *97* (8), 3083–3132.

(9)   Coll, C.; Labrador, R. H.; Mañez, R. M.; Soto, J.; Sancenón, F.; Seguí, M.-J.; Sanchez, E. *Chem. Commun.* **2005**, No. 24, 3033.

(10)   Hofmeister, F. *Arch. Für Exp. Pathol. Pharmakol.* **1888**, *25* (1), 1–30.

(11)   Bühlmann, P.; Chen, L. D. In *Supramolecular Chemistry*; Gale, P. A., Steed, J. W., Eds.; John Wiley & Sons, Ltd: Chichester, UK, 2012.

(12)   Roundhill, D. M. *Extraction of Metals from Soils and Waters*; Springer US: Boston, MA, 2001.

(13)   Marsh, K. N.; Deev, A.; Wu, A. C.-T.; Tran, E.; Klamt, A. *Korean J. Chem. Eng.* *19* (3), 357–362.

(14)   Armand, M.; Endres, F.; MacFarlane, D. R.; Ohno, H.; Scrosati, B. *Nat. Mater.* **2009**, *8* (8), 621–629.

(15)   Ghandi, K. *Green Sustain. Chem.* **2014**, *04* (01), 44–53.

(16)   Thuy Pham, T. P.; Cho, C.-W.; Yun, Y.-S. *Water Res.* **2010**, *44* (2), 352–372.

(17)   *Ionic liquids in synthesis*; Wasserscheid, P., Ed.; Wiley-VCH: Weinheim, 2008.

(18)   Jain, N.; Kumar, A.; Chauhan, S.; Chauhan, S. M. S. *Tetrahedron* **2005**, *61* (5), 1015–1060.

(19)   van Rantwijk, F.; Madeira Lau, R.; Sheldon, R. A. *Trends Biotechnol.* **2003**, *21* (3), 131–138.

(20)   Buzzeo, M. C.; Evans, R. G.; Compton, R. G. *Chemphyschem Eur. J. Chem. Phys. Phys. Chem.* **2004**, *5* (8), 1106–1120.

(21)   Endres, F.; Zein El Abedin, S. *Phys. Chem. Chem. Phys.* **2006**, *8* (18), 2101.

(22)   Ho, T. D.; Zhang, C.; Hantao, L. W.; Anderson, J. L. *Anal. Chem.* **2014**, *86* (1), 262–285.

(23)   Pandey, S. *Anal. Chim. Acta* **2006**, *556* (1), 38–45.

(24)   Ahrens, S.; Peritz, A.; Strassner, T. *Angew. Chem. Int. Ed.* **2009**, *48* (42), 7908–7910.

(25)   Dias, A. M. A.; Marceneiro, S.; Braga, M. E. M.; Coelho, J. F. J.; Ferreira, A. G. M.; Simões, P. N.; Veiga, H. I. M.; Tomé, L. C.; Marrucho, I. M.; Esperança, J. M. S. S.; Matias, A. A.; Duarte, C. M. M.; Rebelo, L. P. N.; de Sousa, H. C. *Acta Biomater.* **2012**, *8* (3), 1366–1379.

(26)   Wanigasekara, E.; Perera, S.; Crank, J. A.; Sidisky, L.; Shirey, R.; Berthod, A.; Armstrong, D. W. *Anal. Bioanal. Chem.* **2010**, *396* (1), 511–524.

(27)   Wang, Y.; Tian, M.; Bi, W.; Row, K. H. *Int. J. Mol. Sci.* **2009**, *10* (6), 2591–2610.

(28)   Huddleston, J. G.; Willauer, H. D.; Swatloski, R. P.; Visser, A. E.; Rogers, R. D. *Chem Commun* **1998**, No. 16, 1765–1766.

(29)   Sathyapalan, A.; Zhou, A.; Kar, T.; Zhou, F.; Su, H. *Chem Commun* **2009**, No. 3, 325–327.

(30)   Wardak, C.; Lenik, J.; Marczewska, B. **2008**, *82* (1-2), 223–233.

(31)   Wardak, C. *Electroanalysis* **2014**, *26* (4), 864–872.

(32)   Shvedene, N. V.; Chernyshov, D. V.; Khrenova, M. G.; Formanovsky, A. A.; Baulin, V. E.; Pletnev, I. V. *Electroanalysis* **2006**, *18* (13-14), 1416–1421.

(33)   Wardak, C.; Lenik, J. *Sens. Actuators B Chem.* **2013**, *189*, 52–59.

(34)   Fraser, K. J.; MacFarlane, D. R. *Aust. J. Chem.* **2009**, *62* (4), 309.

(35)   Rahman, M.; Brazel, C. S. *Polym. Degrad. Stab.* **2006**, *91* (12), 3371–3382.

(36)   Weingärtner, H. *J. Mol. Liq.* **2014**, *192*, 185–190.

(37)   Prete, A.; Paragliola, R. M.; Corsello, S. M. *Int. J. Endocrinol.* **2015**, *2015*, 1–8.

(38)   Radu, A.; Anastasova-Ivanova, S.; Paczosa-Bator, B.; Danielewski, M.; Bobacka, J.; Lewenstam, A.; Diamond, D. *Anal. Methods* **2010**, *2* (10), 1490.

(39)   O'Rourke, M.; Duffy, N.; Marco, R. D.; Potter, I. *Membranes* **2011**, *1* (2), 132–148.

(40)   Bakker, E. *Anal. Chem.* **1997**, *69* (6), 1061–1069.

(41)   Brinkman, U. A. T.; Bruno, A. E.; Burlingame, A. L. *TRAC Volume 10.*; Elsevier Science, 2013.

(42)   Malon, A.; Radu, A.; Qin, W.; Qin, Y.; Ceresa, A.; Maj-Zurawska, M.; Bakker, E.; Pretsch, E. *Anal. Chem.* **2003**, *75* (15), 3865–3871.

(43)   Qin, Y.; Bakker, E. *Anal. Chem.* **2002**, *74* (13), 3134–3141.

(44)   Buck, R. P.; Lindner, E. *Pure Appl. Chem.* **1994**, *66* (12).

(45)   Ma, Y.; Han, F.; Li, Z.; Xia, C. *ACS Sustain. Chem. Eng.* **2016**, *4* (2), 633–639.

(46)   Cheng, D. C. .; Gulari, E. *J. Colloid Interface Sci.* **1982**, *90* (2), 410–423.

(47)   Dorbritz, S.; Ruth, W.; Kragl, U. *Adv. Synth. Catal.* **2005**, *347* (9), 1273–1279.

(48)   Singh, T.; Kumar, A. *J. Phys. Chem. B* **2007**, *111* (27), 7843–7851.

(49)   Blesic, M.; Marques, M. H.; Plechkova, N. V.; Seddon, K. R.; Rebelo, L. P. N.; Lopes, A. *Green Chem.* **2007**, *9* (5), 481.

(50)   Freire, M. G.; Neves, C. M. S. S.; Canongia Lopes, J. N.; Marrucho, I. M.; Coutinho, J. A. P.; Rebelo, L. P. N. *J. Phys. Chem. B* **2012**, *116* (26), 7660–7668.

(51)   Schaller, U.; Bakker, E.; Spichiger, U. E.; Pretsch, E. *Anal. Chem.* **1994**, *66* (3), 391–398.

(52)   Grygolowicz-Pawlak, E.; Crespo, G. A.; Ghahraman Afshar, M.; Mistlberger, G.; Bakker, E. *Anal. Chem.* **2013**, *85* (13), 6208–6212.

(53)   de los A. Arada Pérez, M.; Marín, L. P.; Quintana, J. C.; Yazdani-Pedram, M. *Sens. Actuators B Chem.* **2003**, *89* (3), 262–268.

(54)   Fibbioli, M.; Morf, W. E.; Badertscher, M.; de Rooij, N. F.; Pretsch, E. *Electroanalysis* **2000**, *12* (16), 1286–1292.

(55)   Cooper, J. M.; Cubitt, R.; Dalgliesh, R. M.; Gadegaard, N.; Glidle, A.; Hillman, A. R.; Mortimer, R. J.; Ryder, K. S.; Smith, E. L. *J. Am. Chem. Soc.* **2004**, *126* (47), 15362–15363.

CHAPTER 4   Simple, robust, and plasticiser-free iodide-selective sensor based on copolymerised triazole based ionic liquid.

4.1 Introduction

Chemical sensors with their primary response being governed by extraction and molecular recognition processes are a well-studied and understood class of sensing devices.[1] Previous chapters successfully showed the application of potentiometric sensors in a variety of fields such as clinical analysis,[2] process control[3] and environmental monitoring.[4] ISEs are typically composed of plasticised polymers, ion exchange salts, and ionophores where each constituent plays a specific role in the proper functioning of these membrane based ISEs.[5] As it was described in Chapter 1, ideally the polymer matrix should provide a homogenous medium in which all active components can move freely. This strongly resembles the composition of liquid membrane electrodes since their sensing components were simply dissolved in an organic medium. However, the performance of polymer-based membranes can be drastically reduced if such sensors are used for the measurements of ions within more lipophilic environment for example in biological samples including undiluted whole blood. The cross contamination of chemical sensors coupled with leaching of the sensing components from the ion selective membrane into the sample fundamentally limited the applications of ISEs as a robust analytical tool for long-term trace level analysis.[6]

Over the years, a number of approaches have been developed to minimise the extent to which the active components diffuse out of the membrane bulk and therefore to improve

the response characteristics of ISEs. The most logical step involved chemical modifications of sensing components including addition of long alkyl chains to parent molecules in order to increase their overall lipophilicity.[7] However, changes in the solubility of the functionalised species may result in their macroscopic phase separation from the polymeric matrix. One promising approach that increases the stability of a homogenous sensing layer is the covalent attachment of all sensing components to the polymer backbone.

In recent years, the use of ISEs based on plasticiser-free membrane has been studied and the response characteristics of such membranes were evaluated in terms of their selectivity towards various cations and anions. Methacrylic-acrylic copolymers synthesised via free radical polymerisation are particularly attractive candidates as their physical and mechanical properties can be finely tuned by simply choosing either different combinations of monomers, polymerisation routes, or both.[8,9] The pioneering work on the development of self-plasticised copolymers was carried out by Heng and Hall at the beginning of XXI century in order to demonstrate if they can be used as alternative components in ISEs. They prepared a large number of methacrylate-based copolymers and evaluated their application as polymeric matrix for ISEs.[8] They also successfully demonstrated that self-plasticised copolymers doped with ion selective ionophore (e.g. valinomycin) and lipophilic ionic sites can produce potentiometric response to potassium ions. Interestingly, methacrylate or acrylate based copolymers with high T_g showed very erratic behaviour, long equilibration time and limited response to the analyte of interest. This could be explained by the hard/crystalline nature of synthesised copolymers that is characteristic to polymers exhibiting high T_g. As a result, overall reduction in the mobility of sensing components in the bulk of the membrane is expected leading to slow membrane

response and ionophore inactivity. If the same copolymers were loaded with a suitable plasticiser, significant improvements in the functionality of such ion selective membranes were observed. However, their potentiometric performance can be diminished over time due to the plasticiser exudation that often occurs in and limits the application of PVC based membranes.[10,11] Therefore, the synthesis of self-plasticised polymers/copolymers with lower glass transition temperature (can be theoretically predicted by equation 3 – Chapter 1 – Polymeric matrix) is recommended if such components are utilised in ISEs. Few years later, Bakker's group reported that sensing membranes composed of self-plasticised methyl methacrylate and decyl methacrylate (MMA-DMA) copolymer are suitable for the detection of Li^+, Na^+, K^+, Ca^{2+}, and Mg^{2+} ions.[12,13] Moreover, the formation of a water layer in between the solid contact and the ion selective membrane can be suppressed/eliminated if more hydrophobic methacrylate-based are used in combination with a conductive polymer e.g. POT.[14] This strategy was applied to produce ISEs for trace level analysis of Ag^+, Pb^{2+}, I^-.[15] Recently, Mensah et al (2014) applied the same combination of transducer layer and sensing membrane onto the filter paper modified with single-walled carbon nanotubes (SWCNTs) to produce a paper based ISEs with nanomolar detection limits for Ag^+, Cd^{2+} and K^+.[16] Furthermore, the findings from Chapter 2 demonstrate that methacrylate based membranes are also excellent candidates for the trace-level analysis of carbonate ions.[17]

Moreover, the covalent attachment of ionophore was recognised as a viable strategy to develop ion selective membranes with significantly improved lower limits of detection.[18] It has been shown that such modifications reduce the zero current transmembrane ion fluxes producing ISEs with nanomolar detection limits.[19] Bachas and Daunert (1990)

demonstrated that covalent attachment of chemically modified benzo-15-crown-5 ionophore to carboxylated PVC yields K^+ selective electrodes with good detection limits and improved lifetime.[20] The observed improvements were attributed to the reduced leaching rate of the hydrophilic ionophore from the sensing membrane to sample solution. This also opened several avenues to employ hydrophilic molecules as sensing components which high solubility in aqueous phase previously prevented their application in ion sensing devices.

Recently, several attempts were undertaken to attach cation and anion exchangers to the polymeric matrix of the sensing material. Reinhoudt et al (1994) already attached tetraphenylborate (TPB^-) anion to the polysiloxanemembrane[10]; however an unsubstituted TPB^- anion can undergo irreversible decomposition in the presence of acids, oxidants and light.[21,22] Qin and Bakker (2003) successfully polymerised a C-derivative of the closo-dodecacarborane anion with MMA-DMA monomers to produce a plasticiser-free membrane with cation-exchange properties and significantly reduced rate of leaching of ionic sites.[23] Kimura et al (1996) reported on the covalent immobilisation of anionic lipophilic salts (tetradecyldimethyl(3-trimethoxysilylpropyl)ammonium chloride) into sol-gel based membranes.[24] Abbas et al (2015) attached phthalocyanine ionophore to poly(butyl methacrylate-co-do-decyl methacrylate polymer backbone to produce ClO_4^- sensing membrane with detection limits approaching 1.0×10^{-9} M.[25] Even though, large improvements in lower detection limits were observed, the lifetime of these ISEs would be dictated by leaching of the cationic lipophilic salts that were added to the membrane during its preparation. However, only a limited number of studies have examined the functionality

of ion selective membranes containing both ionophore and lipophilic salts covalently attached to the polymer backbone.

Other attempts to improve the robustness and sensing properties of ISEs were aimed towards finding appropriate replacement to the conventional plasticisers such as dioctyl sebacate (DOS) or 2-nitrophenyl octyl ether (NPOE) since it has been established that the nature of the plasticiser plays a pivotal role in the analytical performance of polymer based sensors.[26] In that study, the authors have used polymeric plasticiser (polyester sebacate (PES)) and demonstrated that the polymeric nature of the plasticiser increases retention of membrane components thus resulting in robust membranes exhibiting significantly longer life-times relative to traditional ones.

Recently, RTILs have been proposed as alternative materials to traditionally used sensing components. As it was demonstrated in the previous chapter when incorporated in an ion exchange membrane, IL can strongly influence their response characteristics for instance via changing the selectivity of the sensing phase.[27,28] Furthermore, even more studies focused on the use of RTIL as ion chelators have been reported.[29] Versatility of ILs is exhibited in a large variety of cations and anions forming IL and the possibility to chemically modify each ionic component in order to tune the properties of ILs towards specific application. In ISEs, this means that one of the constituent ions (e.g. cation) can be modified to allow its polymerisation and/or covalent attachment to the polymer backbone. If the counter-ion of IL selected for the preparation of ISEs is the same as the targeted ion (primary ion), it could be considered that such membrane would inherently contain the primary ion thus eliminating the need for conditioning. Moreover, due to the preservation

of charge balance in the membrane, an outward diffusion of the counter-ion (primary ion) would be severely suppressed thus reducing outward fluxes. Therefore, utilisation of polymerised ILs as membrane component could allow the development of very simple, one component sensing film that does not require conditioning.

However, as the growing interest in the development of ISEs based on the presence of imidazolium[30,31] and phosphonium[32,33] based ionic liquids emerged, only a very small number of reports describing the application of other RTILs for the preparation of ion selective membranes is available. The discrepancy in the popularity of using other than above-mentioned groups of ILs (imidazolium[34] and phosphonium[35]) for the development of ISEs could be attributed to their limited commercial availability.

Even though, phosphonium and imidazolium ILs started receiving considerable attention in analytical chemistry, in the field of organic synthesis they were recently identified as less 'ideal' due to the formation of N-heterocyclic carbenes under very basic experimental conditions.[36] This may result in the presence of unwanted side-reactions that could affect, for instance, the purification process of targeted molecule.[36] Therefore, further synthetic attempts were focused on the development of new, even more inert RTILs that could be successfully utilised across many scientific fields. 1,2,3-Triazolium salts have been suggested as suitable alternatives as they do not have an acidic-ring carbon surrounded by two nitrogen atoms.[37] Even though, 1,2,3-triazolium salts had been reported as early as in XIX century,[38] their IL properties were not investigated until recently. Several synthetic routes for the formation of triazole based ILs have been already proposed in the literature in which two main steps can be distinguished: a) construction of the triazole ring system;

b) and then its N-alkylation.[39] This is usually performed via Huisgen-Meldal-Sharpless copper (I) mediated cycloaddition of azides with alkynes (click reaction), where the Cu catalysis provides the appropriate regioselectivity and improves the rate of reaction if compared to non-catalysed reactions.[40] The resulting 1,4-disubstituted 1,2,3-triazoles are then further N-alkylated (using alkyl halides or tosylates) to produce 1,2,4-trisubstituted 1,2,3-triazolium based RTILs.[36] 1,2,3-Triazolium salts, similarly to phosphonium and imidazolium based ionic liquids can be subjected to metathesis procedures to prepare various RTILs with exchanged anions. The variety of synthetic pathways led to the commercialisation of triazole based ILs and therefore opened new avenues for their implementation in ISEs.

Recently, several colourimetric and electrical sensors based on the presence of triazole ring have been reported.[41–47] 1,2,3-triazole moieties can be either directly involved in binding of the target analyte, act as a linker between the ionophore and for instance fluorophore or contribute further to the reporter dye as part of the conjugated fluorophore.[48] For instance, Chen et al (2013) demonstrated that triazole functionalised gold nano-particles can be used for the determination of Cr^{3+} ions in lake water samples with almost no interference from related metal ions.[49] Similarly, Kumar and Pandey (2009) designed a 1,2,3-triazole based sensor that exhibits high selectivity and good detection limits for mercury (II) ions.[50] Interestingly, the same research group prepared silver nano-particles based on the presence of triazole ligands for dual colourimetric sensing of iodide and mercury.[51] This was explained by the formation of nanoparticle aggregates upon the addition of targeted ions due to the presence of Ag-Hg amalgams or adsorption of iodide onto the surface of nano-particles. If the concentration of measured ions was increased in the sample, more

aggregates would be formed resulting in the change in optical signal that could be further quantified using UV/Vis spectroscopy. Moreover, chemosensors containing triazole moieties and their derivatives were recognised as potential halide chelators where anion binding properties of 1,2,3-triazoles were attributed to the highly polar nature of C-H bond.[43,45] Even though, several triazole based potentiometric and colourimetric sensors for the detection of iodide have been recently reported, to the best of the author's knowledge there are no studies utilising 1,2,3-triazole based ILs as anion sensing components for the preparation of ISEs.[52,41]

Herein, it was attempted to develop a hybrid material that utilises strong electrostatics interactions between the triazole moiety and halide anion e.g. iodide. The inherent presence of [triazole][iodide] ion pair was used to explore the concept of producing a single component, conditioning-free sensing film. In principle, triazole functional group could be chemically modified to allow its covalent attachment to the polymer backbone thus producing iodide selective membrane with improved robustness (no leaching of sensing components). The response mechanism of this system could be understood in analogy to plasticiser-free polymer membrane-based ISEs based on charged ionophore where triazole moiety serves as charged ionophore to iodide.

4.1.1 Iodide in clinical analysis

Routine monitoring of urinary iodide (UI) is an excellent example where iodide-selective electrode can make the most significant impact. Dietary iodine insufficiency significantly impairs psycho-physiological growth and metabolism and can result in iodine deficiency

disorders (IDD) such as hypothyroidism, goitre, cretinism, mental retardation etc. Approximately 1.6 billion people (mostly in developing countries) are currently at risk of IDD.[53,54] In most circumstances, the determination of UI provides little useful information of the long-term iodine status of an individual, since the results obtained merely reflect recent dietary iodine intake. Measuring UI in a representative cohort of individuals from a specific population provides a useful index of the iodine level endemic to that region.[55] The proposed values of average urinary iodine levels as a guide for a region's IDD status are: <20 µg/L (severe); 20 - 49 µg/L (moderate); 50 - 100 µg/L (mild) and > 100 µg/L (normal).[56]

Currently, UI is measured by Sandell and Kolthoff (SK) method which is based on the catalytic effect of iodide in the redox reaction between yellow cerium (IV) and arsenic (III), to yield the colourless cerium (III) and arsenic (V).[57] SK method requires some sample pre-treatment to remove compounds in urine that interfere with the above-mentioned reaction. Typically, the pre-treatment requires wet digestion techniques using chloric acid or perchloric acid.[58,59] Since the wet digestion is lengthy (hours) and used acids are potentially explosive, many modifications of SK were previously proposed in the literature.[58,60] Moreover, several analytical techniques including ion chromatography,[61] electrochemistry,[62] inductively coupled plasma mass spectroscopy,[63] organic chromophores and fluorophores[64] have been used for determination of iodide in environmental and clinical samples. However, these methods often require complex experimental setup, suffer from long examination time and have a high cost per sample/measurement.

4.2 Experimental

4.2.1 Materials

Methacryloyl chloride (MACl), 2,2'-azobis(2-methylpropionitrile) (AIBN), lauryl methacrylate (LMA), propargyl alcohol (PgOH), bis(2-ethylhexyl)sebacate (DOS), tridodecylmethylammonium iodide (TDMAI), poly(3-octylthiophene) (POT) and sodium ascorbate (NaASC) were purchased from Sigma-Aldrich. Poly(vinyl chloride) (PVC), tridodecylmethylammonium chloride (TDACl) and tetrahydrofuran (THF) were obtained from Fluka. Triethylamine was distilled from calcium hydroxide immediately prior to use and 1-azidobutane (AzBu) was recrystallised from cold methanol. All other reagents were of the highest commercially available purity and were used as received. Solutions of metal ions were prepared in ultra-pure water obtained from a Pico Pure 3 water system. Working solutions of different activities were prepared by serial dilutions of a 1 M stock solution. DropSens Dual Carbon Screen-printed Electrodes (C1110) were purchased from Metrohm, USA.

4.2.2 Preparation of iodide-selective electrodes

For potentiometric measurements a solution of POT (1.0×10^{-3} M of monomer in chloroform) was drop cast onto the top of screen-printed electrodes and left at room temperature to dry. Iodide selective electrodes were prepared by dissolving 100 mg of IL based copolymer in THF (0.5 ml). After the complete dissolution of the copolymer an aliquot (~20 µL) was drop cast onto the top of the solid contact electrodes (SCEs) and left at room temperature to dry overnight. If not otherwise stated, the electrodes were placed directly in the solution used for potentiometric measurements.

4.2.3 Preparation of ionophore-free membranes containing TDMAI

Ionophore-free membranes were prepared by dissolving the desired amount of TDMAI and PVC and DOS totalling 100 mg in 0.5 mL of THF. After the complete dissolution of all components the aliquot was drop cast onto the top of the POT layer and left at room temperature to dry overnight. The following day, the ionophore-free membranes were placed in 1.0×10^{-3} M solution of potassium iodide for 24 h.

4.2.4 Potentiometric measurements

Potentiometric responses of all electrodes were recorded using Lawson Labs Inc. 16-channel EMF-16 interface (3217 Phoenixville Pike Malvern, PA 19355, USA) in a stirred solution against a double-junction Ag/AgCl reference electrode with a 1 M LiOAc bridge electrolyte (Fluka). Non-conditioned ISEs were immersed in sample solution (ultra-pure water, artificial urine or human urine as indicated) followed by addition of aliquots of known concentration of KI. The pH of the solution was monitored using a glass VWR symphony 14002-780 Ag/AgCl pH electrode. All the measurements were performed in ultra-pure water unless stated otherwise.

4.2.5 Preparation of artificial urine

The composition of human urine is highly variable due to the diet, the level of activity and the overall state of health of an individual. This inevitably leads to wide variation in composition of artificial urine (AU). The AU used in this work contained the following: 14.1g NaCl, 2.8g KCl, 17.3g Urea, 1.9 ml 25% w/v NH_3, 0.6g $CaCl_2$, and 0.43g $MgSO_4$.[65] All the excipients were dissolved in one litre of distilled water and the pH was adjusted to 4 with 0.1 M nitric acid.

4.2.6 Human urine testing

In order to perform the analysis of human urine, information and consent letter were given to one individual. Furthermore, urine samples were collected from a volunteer over the period of two days. After collection, the samples were instantly used for the iodide determination (50 ml) using ISEs without any sample pre-treatment (pH = 7). The remaining samples were then refrigerated for no longer than two days before being disposed. Full anonymity was adhered to throughout the sample collection and testing phases. Ethical approval for this study was obtained from Research Ethics Committee at Keele University. (Approval code: ERP369).

4.2.7 Iodide measurements using FI-ICP-MS

Human urine samples prior their analysis on flow injection-inductively coupled plasma mass spectrometry (FI-ICP-MS) were centrifuged at 5000 rpm for 10 min and then 7 mL of each sample was transferred into 10 mL autosampler tubes (PerkinElmer). The resulting urine solutions were either analysed directly or with extra dilution if high matrix concentrations were encountered. The instrument used for the analysis was Waters Alliance 2695 coupled to NexION 300D (PerkinElmer). Instrumental operating parameters are demonstrated in Table 4.1 and 4.2. All measurements were done in standard mode. Calibration standards ranging from 1.0×10^{-5} M to 1.0×10^{-7} M were prepared from potassium iodide dissolved in 5% (v/v) HNO_3 and used to produce a calibration curve (Figure 4.1). In between each measurement (including iodide standards and urine samples), a sample blank was analysed to reduce/eliminate the memory effect.
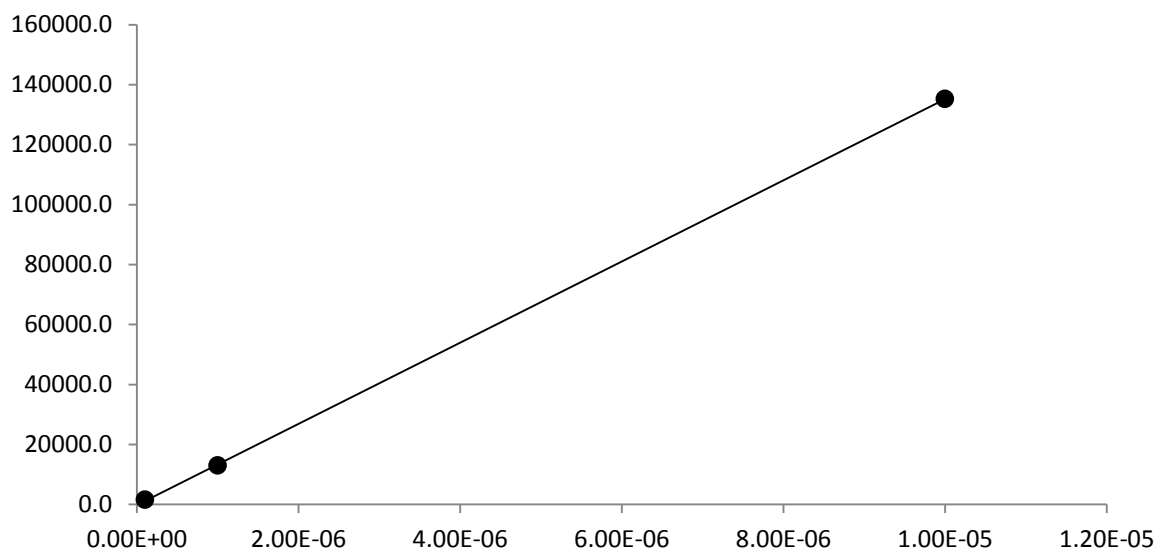
Figure 4.1 Three point calibration line obtained for iodide standards during FI-ICP-MS measurements ($R^2 = 1$).

Table 4.1 FI-ICP-MS instrumental conditions.

Sample uptake rate	0.5 ml/min
Nebuliser	Micromist 149597
Spray chamber	Cyclonic
RF power	1600 W
Plasma gas flow (L/min)	18
Auxiliary gas flow (L/min)	1.2
Nebulizer gas flow (L/min)	1.14
Sample run time	2 min
Masses monitored	126.90

Table 4.2 Flow injection high performance liquid chromatography (FI-HPLC) instrumental conditions.

Mobile phase	A: 1% (v/v) HNO_3 B: MeOH + 1% (v/v) HNO_3
Seal wash	80% H_2O 20% MeOH
Instrument	Waters Alliance 2695
Sample compartment temperature	4˚C
Mobile phase composition	90% A 10% B
Flow rate	0.5 mL/min
Injection volume	5 µL
Sample run time	2.5 min
Needle wash	1 : 1 : 1 H_2O : MeOH : propan-2-ol

4.2.8 Selectivity measurements

Iodide selective electrodes were prepared and applied onto the electrodes according to the protocol described in 'Preparation of iodide-selective membranes'. Each electrode was left at room temperature to dry overnight. The following day, the iodide selective membranes were conditioned in the 0.1 M $CaCl_2$ solution (to avoid contact with primary ions) and responses towards all ions were recorded according to separate solution method as described by Bakker.[66]
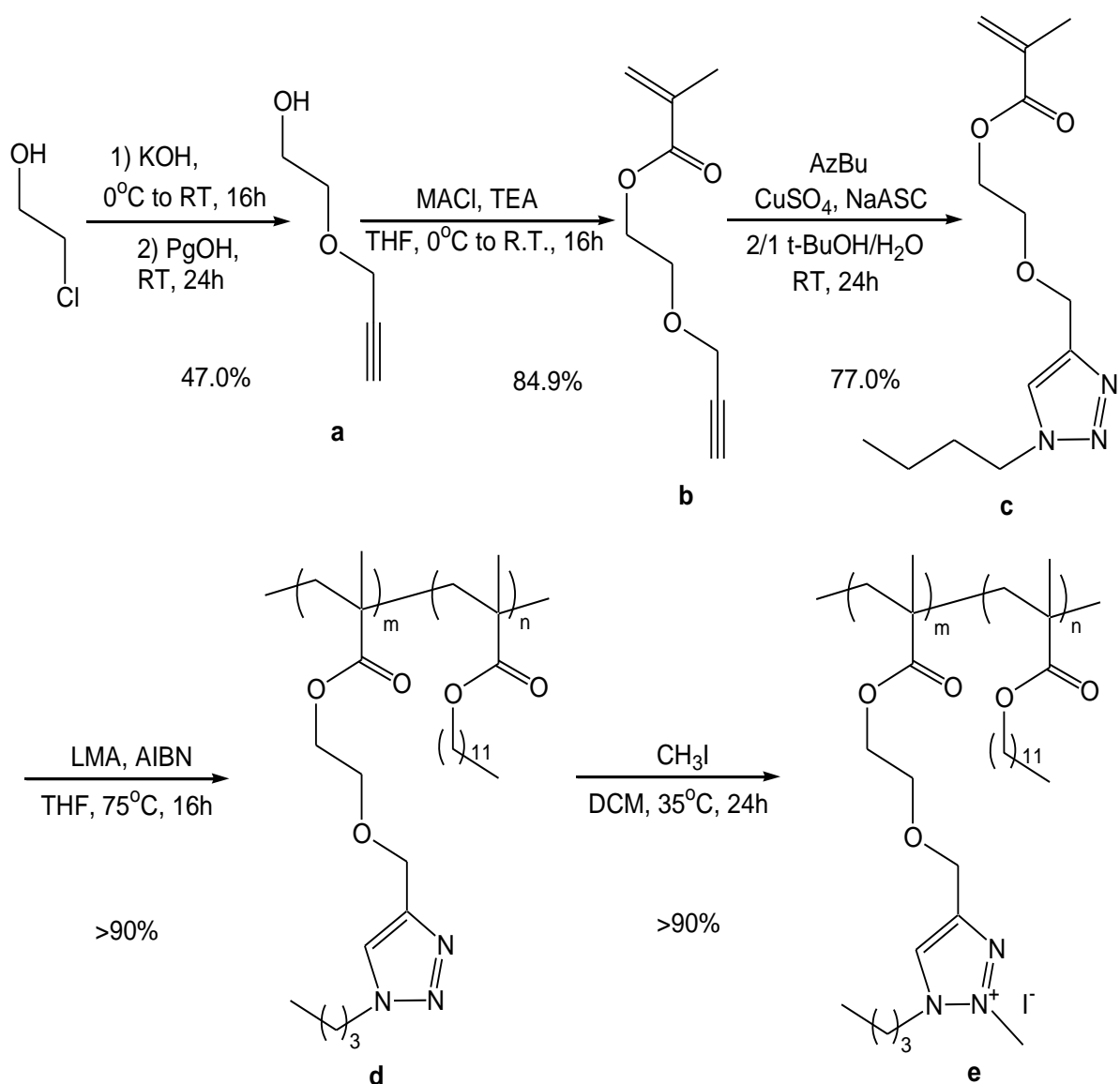
Scheme 4.1 Experimental synthetic pathway to produce random IL-LMA copolymer.

4.2.9   Synthesis of 2-(prop-2-ynyloxy)ethanol (a)

In a round-bottomed flask, propargyl alcohol (5.6 g, 100 mmol) was cooled in an ice-water

bath. Finely pulverised KOH (6.2g, 110 mmol) powder was added under vigorous stirring.

After adding the KOH, the mixture was allowed to warm to room temperature and stirred

for 16 hours. Then 2-chloroethanol (8.9g, 110 mmol) was added dropwise and the mixture

was stirred for 24 hours. The suspended solid was removed by filtration on a sintered-glass

funnel and the filtrate was extracted with diethyl ether (3 × 30 ml). The resulting organic phases were combined and washed with water (3 × 30 ml). The mixture was then dried with $MgSO_4$ and filtered. The volatiles were removed under reduced pressure. The resulting yellow oil was subjected to vacuum distillation and the product was collected at 52°C/0.1 Torr as a colorless liquid (4.7g, 47.0 mmol, 47.0%). ^{1}H NMR (200 MHz, $CDCl_3$, δ): δ 4.14 (d, J = 2.42 Hz, 2H, $CH_2C≡C$), 3.68 (b, 2H, CH_2OH), 3.57 (t, J = 4.69 Hz, 2H, CH_2OC), 2.84 (s, 1H, OH), 2.43 (t, J = 2.39 Hz, 1H, C≡CH).

4.2.10 Butyl azide synthesis

Sodium azide (19.7 g, 303 mmol), 1-bromobutane (13.8g, 100 mmol) and deionised water (100 ml) were added to 250 mL round-bottom flask. The reaction mixture was refluxed for 72 h at 100°C. After cooling, the organic layer was separated and the aqueous phase was extracted with dichloromethane (DCM) (4 x 25 ml). The combined organic layer was then dried over magnesium sulphate. The solid was filtered and the solvent was removed via rotatory evaporation to give butyl azide at 72% yield. ^{1}H NMR (200 MHz, $CDCl_3$, δ): δ 3.21 (t, J = 6.80, 2H, CH_2N_3), 1.52 (m, 2H, $CH_2CH_2N_3$), 1.36 (m, 2H, CH_3CH_2), 0.90 (t, J = 7.08 Hz, 3H, CH_3).

4.2.11 Synthesis of 2-(prop-2-ynyloxy)ethyl 2-methylacrylate (b)

In a flamed-dried, argon-purged, round-bottomed flask, compound (a) (4.7 g, 47.0 mmol) was mixed with anhydrous THF (100 ml) and triethylamine (5.7 g, 56.3 mmol) and cooled in an ice bath. Methacryloyl chloride (5.9 g, 56.3 mmol) was added dropwise while the mixture was constantly stirred. After addition, the mixture was warmed to room temperature and stirred for an additional 16 h. The precipitate was removed by filtration and the filtrate was concentrated by rotary evaporation in a room-temperature water bath.

The resulting yellow oil was diluted with diethyl ether (30 ml) and washed with water (3 ×
20 ml). Then the solvent was removed by rotary evaporation to yield the product (6.7 g,
39.9 mmols, 84.9%). ^{1}H NMR (200 MHz, CDCl$_3$, δ): δ 6.11 (s, 1H, CH$_2$=C), 5.55 (s, 1H,
CH$_2$=C), 4.28 (t, J = 4.82 Hz, 2H, COOCH$_2$), 4.16 (d, J = 2.38 Hz, 2H, CH$_2$C≡C), 3.75 (t, J
= 4.83 Hz, 2H, CH$_2$O), 2.42 (t, J = 2.37 Hz, 1H, C≡CH), 1.91 (m, 3H, CH$_3$).

4.2.12 Synthesis of 2-{[1-(butyl)-1H-1,2,3-triazole-4-yl]methoxy}ethyl 2-methylacrylate (c)

In a round-bottom flask, compound (b) (12.6 g, 75 mmol), butyl azide (10.1 g, 102 mmol),
and CuSO$_4$ solution (1 M aq., 4.0 ml, 4.0 mmol) were added into a mixture of tert-butanol
and H$_2$O (2:1 v:v, 150 ml) in an ice bath. The flask was sealed with a rubber septum and
degassed by bubbling argon through the solution for 20 minutes. Sodium ascorbate (4.5 g,
22.5 mmol) in water (5 ml) was injected into the flask. After half an hour, the mixture was
warmed to room temperature and stirred for an additional 16 h. The resulting green
solution was diluted with water (50 ml) and extracted with diethyl ether (3 × 25 ml). The
combined organic phases were washed with NH$_4$OH solution (5% aq., 3 × 45 ml), HCl
solution (5% aq., 40 ml), NaHCO$_3$ solution (5% aq., 40 ml), and brine (3 ×40 ml)
successively and dried over Na$_2$SO$_4$. The solvent was removed by rotary evaporation to
yield compound (c) (15.4 g, 58 mmol, 77.0%). ^{1}H NMR (200 MHz, CDCl$_3$, δ): δ 7.57 (s,
1H, NCH=C), 6.13 (s, 1H, CH$_2$=C), 5.59 (s, 1H, CH$_2$=C), 4.70 (s, 2H, OCH$_2$C=C), 4.34 (t,
J = 4.93 Hz, 2H, COOCH$_2$), 3.80 (t, J = 4.58, 2H, CH$_2$CH$_2$O), 3.48 (q, J = 6.94, 2H,
CH$_2$N), 1.37 (m, 2H, CH$_2$CH$_2$N), 1.22 (m, 2H, CH$_2$CH$_3$), 0.96 (t, J = 7.30, 3H, CH$_3$).

4.2.13 General synthesis procedure for copolymer (d)

All copolymers were synthesised via thermally initiated free radical solution polymerisation. Calculated amounts of 2-{[1-(butyl)-1H-1,2,3-triazole-4-yl]methoxy}ethyl 2-methylacrylate and lauryl methacrylate were added to anhydrous THF (5 ml) before addition of AIBN (1% wt). The homogenous solution was purged with a stream of nitrogen for 25 min. Polymerisation was then carried out at 75°C under vigorous stirring for 16 h. After the reaction was completed, the excess solvent was removed using rotatory evaporation and a yellow precipitate was collected. The residue obtained was dissolved in DCM and reprecipitated by excess cold methanol. The same procedure was repeated three times and the resultant copolymer was dried under ambient laboratory conditions. The peak intensities for LMA and product (c) obtained from ^{1}H NMR spectroscopy were used to calculate final concentrations of each monomer in a copolymer. ^{1}H NMR (200 MHz, CDCl$_3$, δ): δ 7.76 (br, 1H, NCH=C), 4.67 (br, 2H, OCH$_2$C=C), 4.39 (br, 2H, COOCH$_2$), 4.14 (br, CH$_2$N), 3.93 (br, 2H, COOCH$_2$), 3.76 (br, 2H, CH$_2$CH$_2$O), 1.92 − 0.96 (m, COOCH$_2$(CH$_2$)$_{10}$CH$_3$; CH$_2$CH$_2$N; NCH$_2$CH$_2$CH$_2$CH$_3$; NCH$_2$CH$_2$CH$_2$CH$_3$).

4.2.14 General synthesis procedure for ionic liquid copolymer (e)

The above solid (1 equiv.) was dissolved in DCM (30 ml) and methyl iodide (3 equiv.) were added to the reaction vessel. The mixture was then heated to 35°C and stirred for 24 h. The resulting IL was isolated by removing all volatile products under vacuum (yield > 90%).^{1}H NMR (200 MHz, CDCl$_3$, δ): δ 9.30 (br, 1H, NCH=C), 5.16 (br, 3H, NCH$_3$), 4.70 (br, 2H, OCH$_2$C=C), 4.46 (br, 2H, COOCH$_2$), 4.15 (br, CH$_2$N), 3.91 (br, 2H, COOCH$_2$), 3.73 (br, 2H, CH$_2$CH$_2$O), 1.88 − 0.86 (m, COOCH$_2$(CH$_2$)$_{10}$CH$_3$; CH$_2$CH$_2$N; NCH$_2$CH$_2$CH$_2$CH$_3$; NCH$_2$CH$_2$CH$_2$CH$_3$).

4.2.15 Preparation of ionic liquid copolymer containing nitrate as counter-ion

100 mg of the ionic liquid copolymer was dissolved in 1 mL of THF and the resulting solution was cast into 90 mm in diameter Teflon plate. After overnight THF evaporation, a membrane of approximately 100 μm thickness remained. 10 ml of potassium nitrate solution (2 M) was poured over the polymeric film and then the Teflon plate was sealed and placed in the oven for 12 h at 50ºC. The resulting polymer was washed 5 times with ultra-pure water and then dried in a vacuum oven at room temperature. ^{1}H NMR (200 MHz, CDCl$_3$, δ): δ 9.10 (br, 1H, NCH=C), 4.97 (br, 3H, NCH$_3$), 4.63 (br, 2H, OCH$_2$C=C), 4.38 (br, 2H, COOCH$_2$), 4.11 (br, CH$_2$N), 3.89 (br, 2H, COOCH$_2$), 3.70 (br, 2H, CH$_2$CH$_2$O), 1.99 – 0.83 (m, COOCH$_2$(CH$_2$)$_{10}$CH$_3$; CH$_2$CH$_2$N; NCH$_2$CH$_2$CH$_2$CH$_3$; NCH$_2$CH$_2$CH$_2$CH$_3$).

4.2.16 Preparation of triazole based ISEs with nitrate serving as counter-ion

Ion selective electrodes were prepared according to the protocol described in 'Preparation of iodide selective electrodes'. However, on this occasion a newly synthesised random copolymer with exchanged anion (nitrate) was used.

4.3 Results and discussion

1,2,3-Triazole based compounds have been recently recognised as weakly coordinating metal ion ligands for sensing of biologically relevant molecules.[52,67] Therefore, these compounds have promising application prospects as sensing materials for the fabrication of ISEs. Their ionic liquid derivatives are particularly attractive as they exhibit versatile chemical functionality and their properties can be even further modified by exchanging their anionic moieties for example by salt methatesis.[68] With the goal of finding a good candidate material for selective iodide sensing a 2-{[1-(butyl)-1H-1,2,3-triazole-4-yl]methoxy}ethyl 2-methylacrylate (LMA) poly-ionic liquid with iodide serving as a counter ion (Figure 4.2) was used for the preparation of ion selective membrane. Poor interactions between covalently immobilised cationic moieties and the 'free' moving anions permit their ion exchange when in contact with other anionic species in aqueous solutions. Since this newly synthesised compound was already preloaded with iodide (during the formation of poly-ionic liquid - polyIL), it was expected that the selectivity of this molecule towards I⁻ would be significantly enhanced. Even though, ILs are composed of two weakly coordinating species, the affinity of the positively charged copolymer to the preloaded iodide is expected to be much higher than towards any other competing species. This would ensure high selectivity of a sensor during potentiometric experiments and such factors have been a driving force in the development of ionic liquid based sensors.
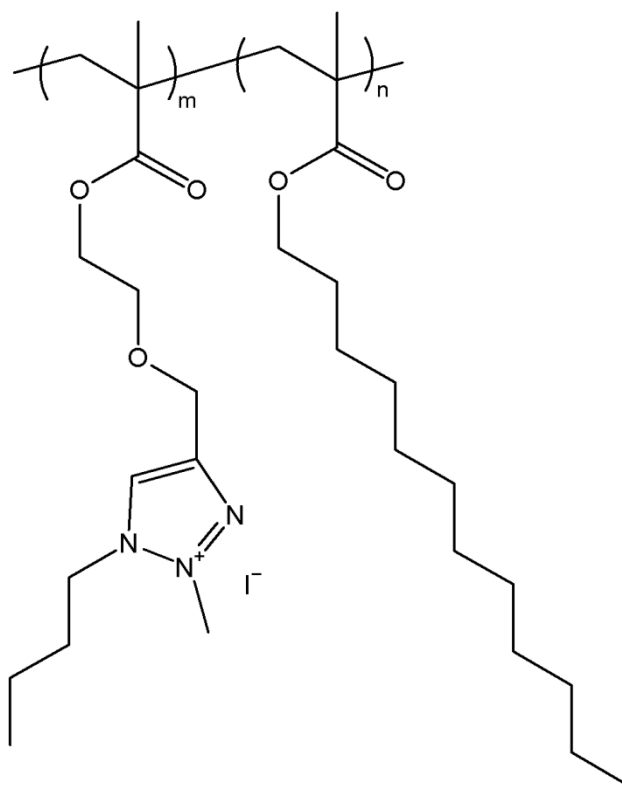
Figure 4.2 Structure formula of the synthesised random copolymer.

In this study, a positively charged ionophore mechanism[1,5] was attributed to the ion selective membranes made up of a single element - LMA-IL copolymer. Most of the membranes under study exhibited good signal stability and Nernstian response (-56.1 ± 2.1 mV/decade) towards iodide ion with the concentration range spanning from 6.31 x 10^{-8} to 1.0 x 10^{-3} M as illustrated in Figure 4.3.

Figure 4.3 Response curve of I⁻ selective electrode made of copolymerised 1,2,3-triazole moieties and immersed directly into sample solution (conditioning step omitted).

Interestingly, the same potentiometric behaviour was observed for membranes conditioned in the solution of primary ions (1.0×10^{-5} M) prior to the experiment as well as for membranes that were immediately immersed in the investigated sample solution. On each occasion, both lower detection limits (LDLs) and selectivity of either conditioned or non-conditioned ion selective membranes remained the same. Such phenomenon could be attributed to the intrinsic nature of the newly synthesised copolymer as iodide ion serves a function of a charged delocalised anion that contributes to the formation of the above-mentioned ionic liquid. Since each sensing membrane is already "preloaded" with the anion of interest, it can be hypothesised that local equilibrium is reached a soon as the casting solvent evaporates. These findings have remarkable implications for the

172

development of new class of ion selective sensors where the need for long, complex and repeated conditioning is a significant burden, for example, in single-use disposable sensors for field biological and environmental applications. One could easily imagine development of sensors based on copolymerised ionic liquids where the counter ion is the charged species of interest.

However, this idea comes with a caveat; the copolymerised cation component of ionic liquid (in this case triazole moiety) may exhibit certain selectivity to counter-ions. For instance, Bachas et al (2010) have recently demonstrated that molecules based on C-H hydrogen bonding from 1,2,3-triazole moieties with a pre-organised central cavity (also known as triazolophanes) exhibit excellent selectivity towards halide ions.[44,45] Hua and Flood (2010) later demonstrated using advanced computational models that triazole units exhibit the highest binding energy towards chloride ions: $- 13$ kcal mol^{-1} with respect to N-phenylenes (-5 kcal mol^{-1}) and C-phenylenes (-4 kcal mol^{-1}).[69] Furthermore, structural changes that occur upon binding of targeted anion to triazolophenes could be quantified structurally and quantitatively using ^{1}H NMR spectroscopy. However, it has to be noted that such theoretical models apply to the structures with pre-organised triazole moieties and do not directly describe the behaviour of proposed polyIL. The above-mentioned experimental procedures used to determine and quantify the binding strength of formed complexes were applied for molecules studied in solutions (e.g. ionophore-ligand complexes). As the synthesised polyIL contains covalently immobilised triazole moieties, the same reasoning cannot be directly used to describe the binding mechanism of the polyIL. It could be further hypothesised that the distribution of 1,2,3-triazoles within the synthesised copolymer represent partially organised domains that could potentially provide

size based selectivity towards iodide. However, these conclusions are purely speculative and would require further confirmation e.g. using appropriate computational models.

To validate the concept that the proposed polyIL demonstrates selectivity to I^- (via experimental methods), another triazole-based copolymer containing NO_3^- as counter ion was prepared and its potentiometric response to iodide relative to iodide-containing copolymer was recorded. These findings are presented in Figure 4.4.
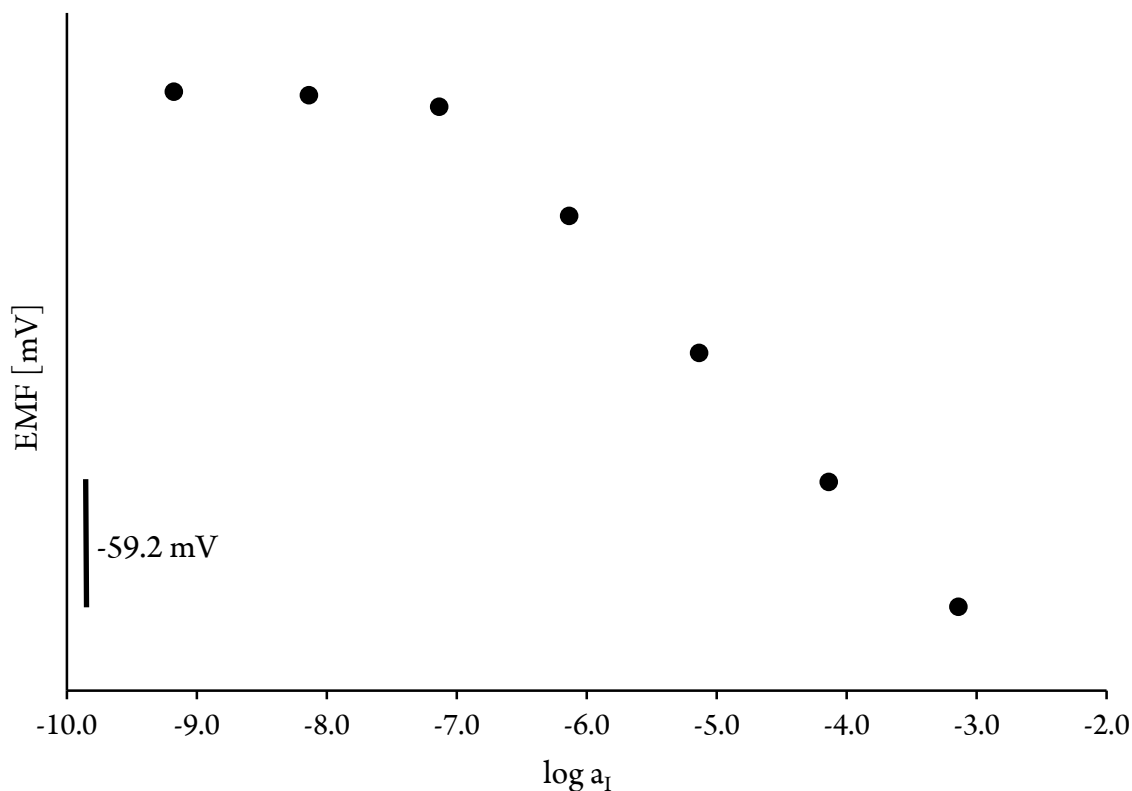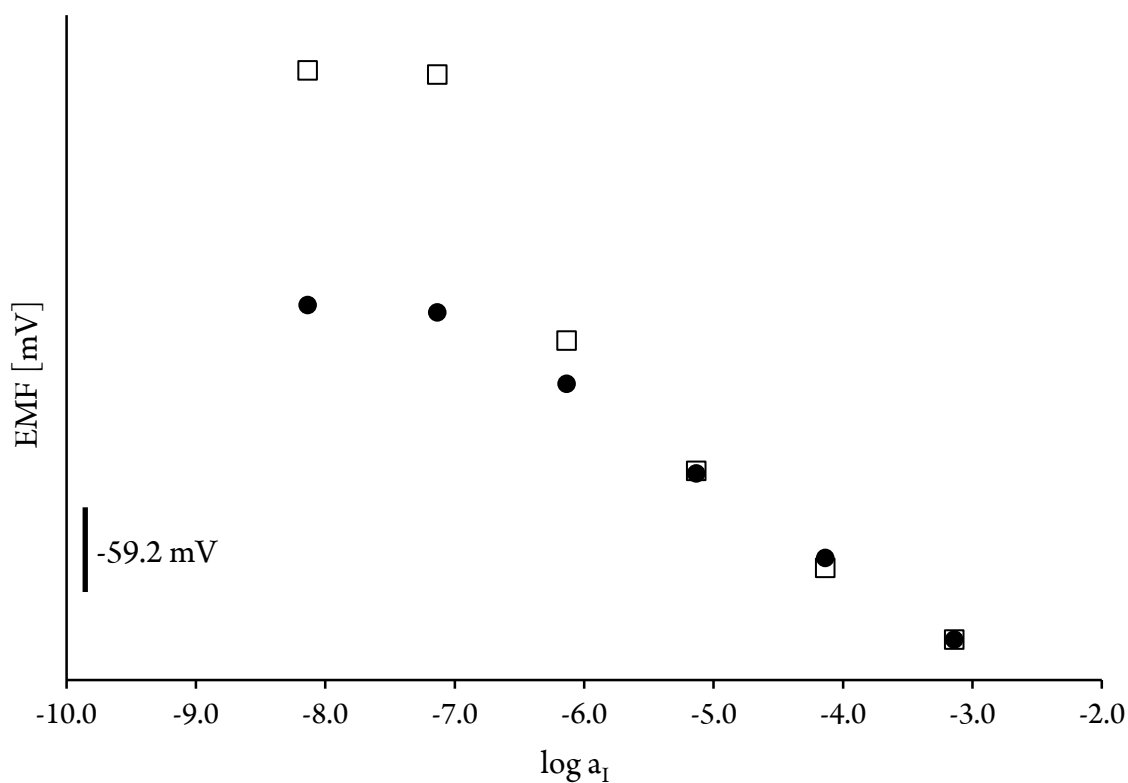

Figure 4.4 Closed circles: potentiometric response of I^- selective electrode made of copolymerised 1,2,3-triazole moieties and immersed directly into sample solution (conditioning step was omitted). Open squares: the same copolymer containing NO_3^- as counter ion.

It is apparent that nitrate-containing copolymer exhibited strong super-Nernstian response indicating the exchange of nitrate to iodide ions. Observation of the super-Nernstian response indicates strong membrane uptake of iodide ions most likely because of stronger preference of triazole moiety to iodide versus nitrate. Uptake of iodide ions creates inward ion fluxes resulting in super-Nernstian response as reported in the literature.[70,71] Furthermore, the polyIL with exchanged anion exhibited significantly higher selectivity to iodide than to other interfering ions such as NO_3^-, Br^-, Cl^- and SO_4^{2-} as illustrated in Figure 4.5 and Table 4.3. This supports the findings from previous experiments and demonstrates that the copolymerised triazole unit exhibits high binding affinity to iodide. Interestingly, Wardak (2014, 2015) has also observed super-Nernstian response slopes in the cases when free, not covalently attached ionic liquids (phosphonium- and imidazolium-based) are clearly utilised as non-specific ion exchanger.[29,72] However, the origin of this super-Nernstian response is not clear and more work is needed in order to shed light on exact function of ILs in polymer membrane based ion-selective electrodes.

Table 4.3 Selectivity coefficients and experimental slopes for the copolymer based ISEs with exchanged anion (I^- slope = -59.9 ± 3.1 mV/decade).

Anion	Cl^-	Br^-	NO_3^-	SO_4^{2-}
$\log K^{POT}$	-4.6 ± 0.1	-2.9 ± 0.2	-3.3 ± 0.2	-5.2 ± 0.1
Slope [mV/decade]	-40.8 ± 1.6	-59.5 ± 0.5	-47.4 ± 1.1	-28.4 ± 2.5
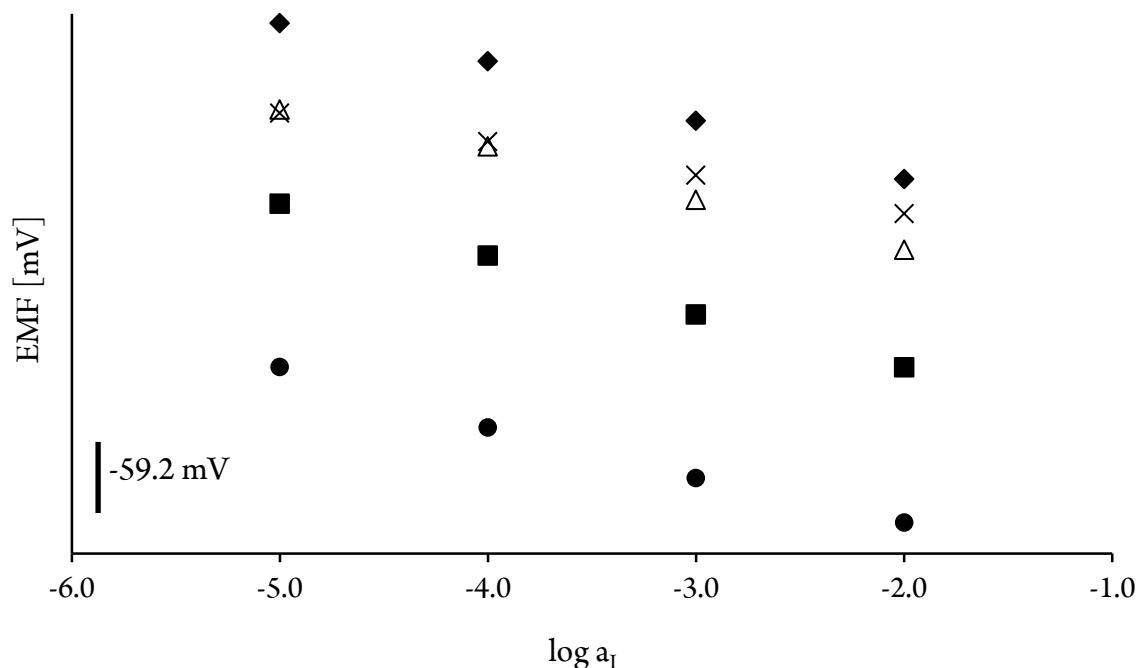
Figure 4.5 Potentiometric response of ionic liquid based ion selective electrodes with exchanged anion for various anions: I^- (circles), NO_3^- (open triangles), Cl^- (diamonds), SO_4^{2-} (crosses) and Br^- (squares).

4.3.1 Selectivity

Selectivity is an extremely important characteristic of a chemical sensor. It quantifies the preference for the chosen analyte over the other potentially interfering ions and therefore defines the practical functionality of ISEs for sensing purposes. Only interfering ions that are relevant to applications in clinical analysis such as nitrate, sulphate, chloride and bromide ions were used in this study. Especially for practical determination of iodide ions in biological sample such as human urine, it is important that the proposed sensor exhibits high selectivity over chloride ions. Note that the concentration of Cl^- is strongly influenced by the dietary intake of that salt by a healthy individual and therefore the effective chloride concentration can span from 10 to 25 mmol/L.[60] This indicates that the proposed sensor should exhibit sufficient selectivity to discriminate against Cl^- ions. Previous selectivity

176

experiments successfully demonstrated that the potentiometric response of proposed sensor does not depend on the nature of the counter-ion in the polyIL. However, such electrodes need to be conditioned prior the measurements in order to eliminate the occurrence of super-Nernstian responses at lower concentration of primary ions.

In this study, the proposed polyIL with I^- serving as counter-ion exhibited high selectivity towards iodide when tested against above-mentioned interfering anions. Importantly, this electrode exhibited higher selectivity for I^- over Cl^- than any previously reported ionophore based iodide selective electrodes (log K^{POT} = -4.5 ± 0.2).[73,74] The log K^{POT} values calculated in this study for the copolymer-based membranes are listed in Table 4.4 along with the experimental slopes (Figure 4.6) obtained for each interfering ion during potentiometric experiments. Note that these ISEs exhibited excellent selectivity to iodide over sulphate, chloride and nitrate ions but when measured against bromide only limited selectivity was achieved (log K^{POT} = -2.3 ± 0.1). This could be partially attributed to the relatively high lipophilicity of that ion and similar electrochemical properties as to iodide that would further favour the extraction and stabilisation of Br^- by the positively charged triazole moiety. Even though, only limited selectivity to Br^- was recorded, it is important to note that bromide urinary levels usually do not approach concentrations at which successful iodide determination would be compromised.[75] Interestingly, a polyIL preloaded with NO_3^- (counter-ion) is more selective to Br^- over I^- than the initially proposed iodide selective copolymer. Despite the improvements in selectivity of NO_3^- containing polyIL, such polymeric architecture has not been selected for further studies due to the requirement for conditioning prior to their practical application.

Observation of near-Nernstian slopes for all interfering ions for ISEs preloaded with primary ions (iodide) may seem to contradict traditional knowledge. However, it should be noted that in this study iodide is the counter-ion to covalently attached triazole moiety. Its diffusion towards the membrane phase boundary is therefore significantly limited thus minimising membrane ion fluxes. Furthermore, due to the inherent preference of triazole moiety towards iodide none of the studied ions could displace iodide thus further minimising ion fluxes. As a consequence, no outward fluxes of iodide are created enabling observation of near-Nernstian slopes for all ions and calculations of unbiased selectivity coefficients despite the fact that primary ion is present in the membrane prior to their determination. To further explore the functionality of the proposed polyIL, the selectivity coefficients of simple ion-exchange membrane based on TDMAI (results shown in Table 4.5) were determined. Drastically smaller selectivity coefficients of TDMAI-based membranes compared to polyIL-based further indicate specificity of triazole moiety to iodide ions. It is also important to point out that response slopes for all interfering ions are near-Nernstian indicating the preference of the triazole-based moiety for iodide. None of the studied ions can displace iodide as the counter-ion to triazole-based cation. This is a very important finding in terms of the robustness and practical application of polyIL-based electrodes. The presence of primary ions in the membrane does not affect the membrane performance and more importantly it significantly reduces the need for membrane preparation and optimisation. Encouraged by these results, and upon confirmation of suitable selectivity to several major interfering ions, the polyIL based ISEs were tested in a complex artificial urine media (see Determination of iodide in artificial urine).

Table 4.4 Selectivity coefficients and experimental slopes for the copolymer based ISEs (I^- slope = -57.3 ± 0.1 mV/decade).

Anion	Cl^-	Br^-	NO_3^-	SO_4^{2-}
log K^{POT}	-4.5 ± 0.2	-2.3 ± 0.1	-3.6 ± 0.1	-5.2 ± 0.1
Slope [mV/decade]	-53.8 ± 1.3	-55.1 ± 1.7	-48.2 ± 2.7	-29.8 ± 2.0
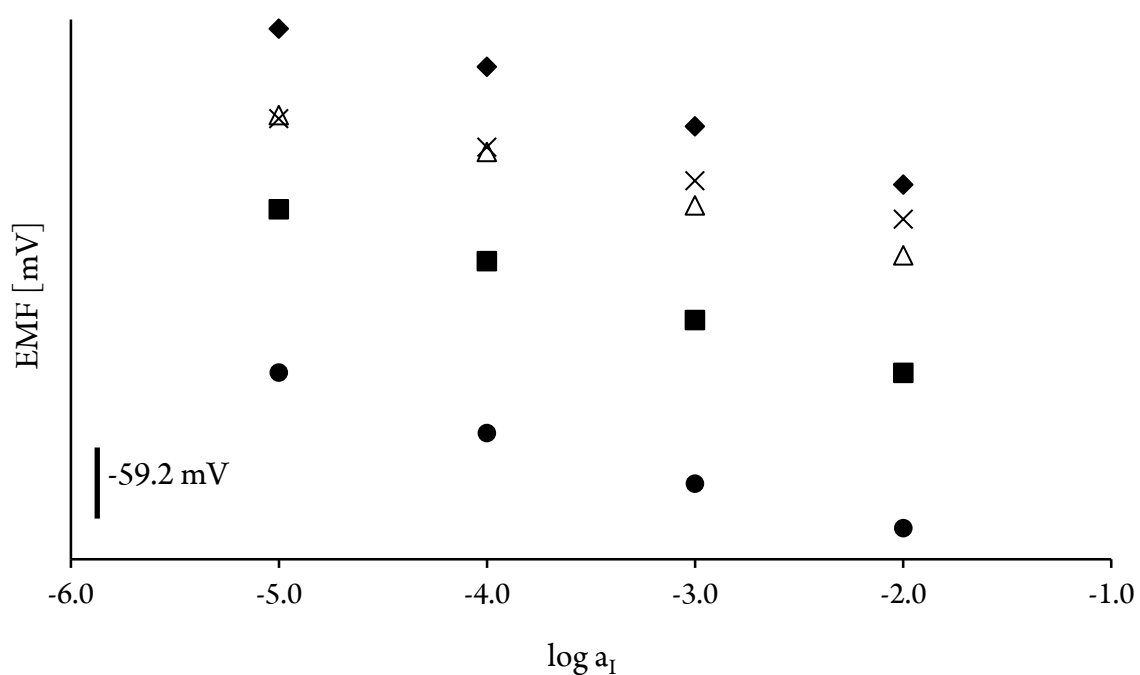
Figure 4.6 Potentiometric response of ionic liquid based ion selective electrodes for various anions: I^- (circles), NO_3^- (open triangles), Cl^- (diamonds), SO_4^{2-} (crosses) and Br^- (squares).

Table 4.5 Selectivity coefficients and experimental slopes for the ionophore free membrane doped with TDMAI ionic sites (I^- slope = -55.2 ± 0.3 mV/decade).

Anion	Cl^-	Br^-	NO_3^-	SO_4^{2-}
$\log K^{POT}$	-1.9 ± 0.01	-1.9 ± 0.02	-1.3 ± 0.01	-3.2 ± 0.01
Slope [mV/decade]	-55.6 ± 1.7	-48.6 ± 0.2	-52.8 ± 2.2	-23.1 ± 0.3

To further confirm the functionality of synthesised random copolymer and whether it can perform function of the ionophore in sensing membranes, 2% wt of the compound along with 1% TDMACl were added to 33% PVC and 66% DOS and dissolved in minimum amount of THF. The following cocktail mixture was applied according to the previously described method and the resulting membrane was used directly for the determination of iodide. Herein, a hypothesis that the proposed polyIL behaves as pre-formed primary ion-ionophore complex (in the form of triazole moiety as charged ionophore and iodide as primary ion) was tested. Lipophilic ionic salts were added to the ISEs to fully mimic traditional selective membranes. On each occasion, the following electrodes were run alongside [9]mercuracarborand-3 (MC-3) based electrodes to see if significant deviation in the response characteristic between these sensors would occur. Both electrodes exhibited near-Nernstian behaviour to iodide ions over similar concentration range as illustrated in Figure 4.7. MC-3 ionophore was selected in this study as it has been previously recognised as an excellent halide ion chelator.[76] However, strong interference from hydroxide and some other halide ions often renders it unsuitable for the analysis of iodide when no sample pre-treatment is desired or when high halide concentrations are encountered (biological samples). For instance, very low detection limits for MC-3 based ISEs were previously achieved in potentiometric measurements in water. However, limited selectivity

of such membranes towards iodide over chloride anions rendered it unsuitable for measurements of iodide in urine. The proposed molecule even when introduced as ionophore without any further optimisation displayed almost identical behaviour to MC-3 based membranes. The most apparent change in the potentiometric performance of these sensors was found at their lower detection limit. In both cases, detection limits shifted towards higher-concentration end of the calibration curve. Such behaviour could be somehow predicted for MC-3 based membranes as measurements were run at pH = 6 implying that strong hydroxide activity hindered detection of iodide (sample acidification would be required). Worsening of the detection limits for the copolymer based ISEs could be attributed to the non-optimal ionophore-ionic sites ratio and the nature of the lipophilic salt itself. For instance, TDMACl ionic site comprises of a bulky trimethyl-tetradecyl ammonium cation and chloride anion resulting in the mixture of iodide and chloride ions in the membrane bulk. Since, the copolymer based ISEs were not conditioned in the primary ion solution prior the experiments, upon first contact with the sample, abrupt ion exchange would take place (in the direction of the membrane) causing large potential jump also referred as super-Nernstian response. The occurrence of such response (see Figure 4.4) confirms previous hypothesis that the observed worsening of detection limits is predominantly caused by the ionophore-ionic sites imbalance and therefore can be corrected by further adjustments. Additionally, it was recently demonstrated that added ionic sites could be used to optimise the response of ISEs based on charged ionophores. However, this avenue has not yet been explored as the main purpose of this study is to show the functionality of newly prepared copolymer as ion sensing membrane without any pre-treatment. This proof of concept experiments demonstrate that the proposed molecule when introduced into other more traditional polymeric matrixes can exhibits ion-binding

properties and with additional optimisation carry a big potential to develop highly sensitive and selective iodide specific ISEs.
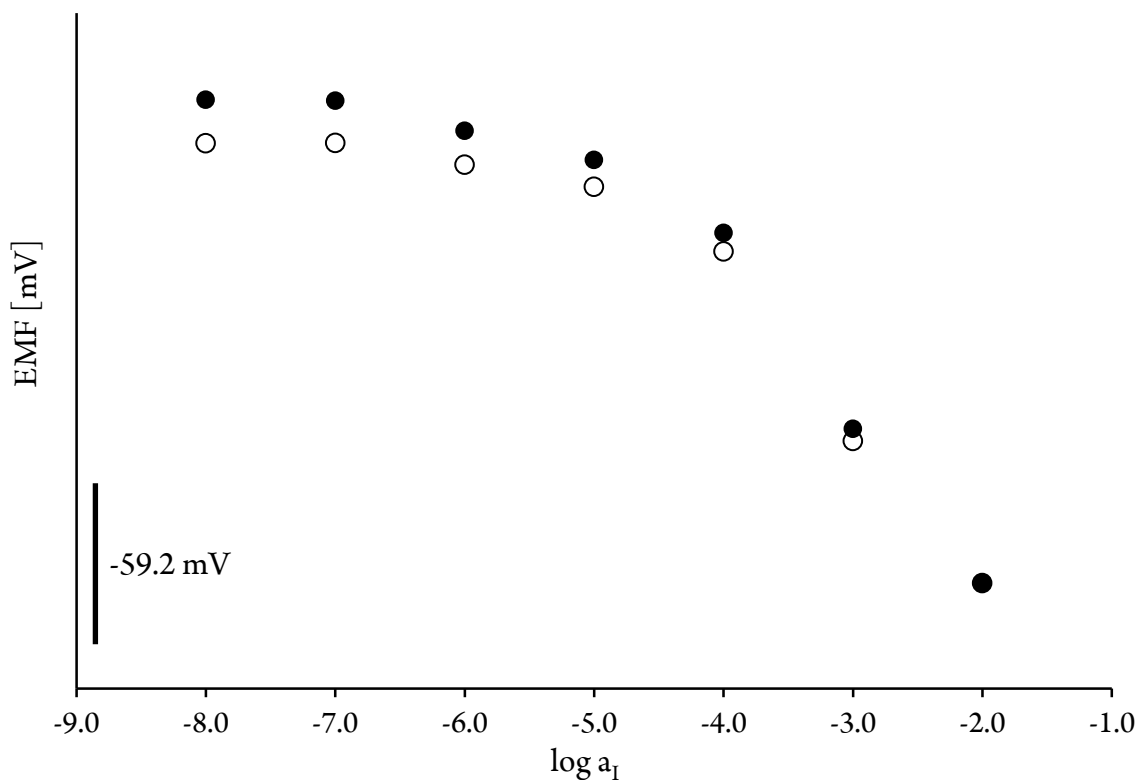
Figure 4.7 Response characteristics of iodide selective electrodes containing MC-3 as ionophore (open circles; slope = -59.7 mV/decade), and using the proposed polyIL (closed circles). In the case of the latter the slope was -56.1 mV/decade with $R^2 = 0.99$.

4.3.2   pH stability

The influence of pH on the potentiometric response of iodide selective electrodes based on the presence of 1,2,3-triazole ILs moieties was elucidated by recording the change in response of ISEs as a result of adding aliquots of either orthophosphoric acid (H_3PO_4) or NaOH to ultra-pure water as it is demonstrated in Figure 4.8. For the self-plasticised polyIL, the electrode potential was relatively independent of pH in a range spanning from 3 to 10. The potentiometric response of ISEs at more alkaline pH (> 10) can be explained

as a response to hydroxide ions, which is demonstrated by the gradual decrease in the potential with increasing pH. The potential changes observed for pH < 3 are likely due to increasing concentration of hydrogen ions. In contrast to ISEs loaded with MC-3 ionophore, the proposed polyIL is suitable for iodide determination in samples at the physiological pH (approximately 7.4) without the need of acidifying the sample.
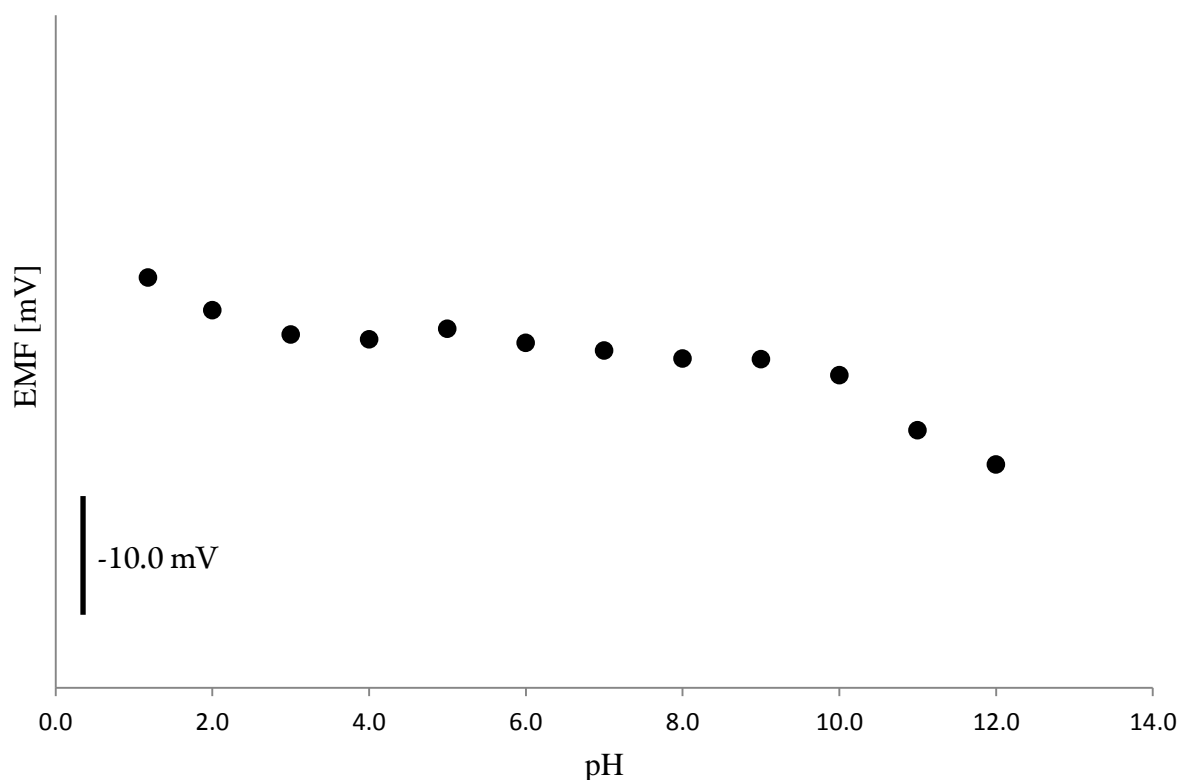
Figure 4.8 Effect of pH on the potentiometric response of triazole based self-plasticised copolymer.

4.3.3   Robustness

Even though, recent improvements in the sensing field yielded a wide range of chemical sensors demonstrating required selectivity and sensitivity towards the analyte of interest, their overall performance was only limited to short measurements due to their poor long-

term stability. It is relatively well understood that the lifetime of ISEs can be considered as a function of chemical stability and lipophilicity of components that are used to prepare ion selective membranes. Therefore, limited robustness of ISEs was usually associated with the leaching of membrane components from the hydrophobic matrix into the sample solution, especially when more polar plasticisers such as NPOE were used for the preparation of sensing devices. In the case of ISEs based on the presence of neutral ionophore, leaching of the ion ligand would reduce the amount of free ionophore available for binding ultimately causing an imbalance in the L:R ratio. As the concentration of ionophore in the membrane decreases, the ISEs start exhibiting a response that resembles the one of ionophore-free membranes ultimately becoming unresponsive to changing concentrations of primary ions. However, for ion selective membranes based on the presence of charged ionophore in order to fulfil the electroneutrality requirement, the loss of charged ionophore must be accompanied either by co-extraction (opposite charged species diffuse into the sample) or ion exchange processes (transfer of ions of the same charge into the membrane).[77] In this study, a plasticiser free IL-LMA copolymer with covalently attached ionophore was synthesised to prevent mass diffusion of such species and also to fully eliminate the risk of plasticiser exudation and therefore to improve overall durability of iodide selective electrodes. Potentiometric responses of iodide selective ISEs were recorded over the period of two weeks to assess their practicality as applied chemical sensor. Each electrode was prepared on the same day using only freshly made cocktail. In addition, each electrode was only used once (during initial measurement) and then stored in the distilled water and re-used. Since, it was demonstrated that the presence of iodide ions within the membrane is sufficient enough to establish thermodynamic equilibrium, no sample pre-treatment (conditioning) was carried out. Note that the full possible response

range was not recorded for these electrodes. Rather, the focus was placed on the smaller response range in order to monitor the reproducibility and robustness. Table 4.6 contains the response characteristics (slope and response range) of at least four randomly selected electrodes from the larger dataset (over 50 electrodes). Near-Nernstian behaviour at the measured response range was observed in all cases. Note that no worsening of potentiometric response of freshly prepared ISEs and those stored in the distilled water for either a week or two weeks were observed. The same observations were made with the regards to their signal stability as even after two weeks of storing, no significant signal drift was observed. Retention of the slope, signal stability and measured detection limits especially in the cases of used ISEs that were stored for extensive period of time is an extremely important finding in terms of practical, *in field* application.

Table 4.6 Response range and slopes of selected ISEs.

Electrode category	Fresh	1 week old	2 weeks old
Measured range	$10^{-5} - 10^{-2}$ M		
Slope [mV/decade]	-53.3 ± 0.5	-50.0 ± 1.7	-58.9 ± 1.3

In Table 4.6 the iodide selective electrodes were divided into three main categories: a) fresh electrodes representing the ISEs that were instantly used for potentiometric measurements without prior conditioning; b) 1 week old electrodes that were used once for iodide determination in aqueous sample and then they were stored in distilled water for one week before their next set of potentiometric responses was obtained; c) already used ion

selective membranes that were utilised to record at least one calibration curve followed by the recording of responses after storage in water for 2 weeks.

4.3.4 Determination of iodide in artificial urine

To further investigate the utility of polyIL-based ISEs, such sensors were used to determine the activity of iodide ions in the solution of artificial urine. Note that the composition of human urine is strongly influenced by the diet, activity and overall health of an individual. Therefore, numerous ways to prepare artificial urine sample were proposed in the literature. In this study, the composition of AU was selected to resemble physiological human urine as mentioned in the experimental section – Chapter 4; Preparation of artificial urine. No metabolites, hormones and proteins were introduced into the buffer solution as their influence on the potentiometric response of iodide selective electrodes was later evaluated in real human urine. During the measurements, tested electrodes exhibited near-Nernstian behaviour (-63.2 mV/decade) over a large concentration range with lower detection limits found at $10^{-6.1}$ M (see Figure 4.9). It is apparent that high concentration of background (interfering) ions lead to slightly increased lower detection limit compared to the one observed under no interference conditions (see Figure 4.3). Nevertheless, typical urinary iodide concentrations range from 3.0 x 10^{-7} (38 ppb) to 6.0 x 10^{-6} (760 ppb).[78] Note that proposed values of average urinary iodine levels as a guide for a region's IDD status are: < 1.6 x 10^{-7} M (20 ppb) is classed as severe deficiency; levels between 1.6 x 10^{-7} M (20 ppb) and – 4.0 x 10^{-7} M (50 ppb) are classed as moderate deficiency while levels 4.0 x 10^{-7} M (50 ppb) – 8.0 x 10^{-7} M (100 ppb) are considered as mild deficiency. Levels of UI above 8.0 x 10^{-7} M (100 ppb) are considered normal[56] This demonstrates that the proposed sensor could be potentially applied for the

quantification of iodide in human urine and therefore it could be used as an indicative test for iodide related disorders.
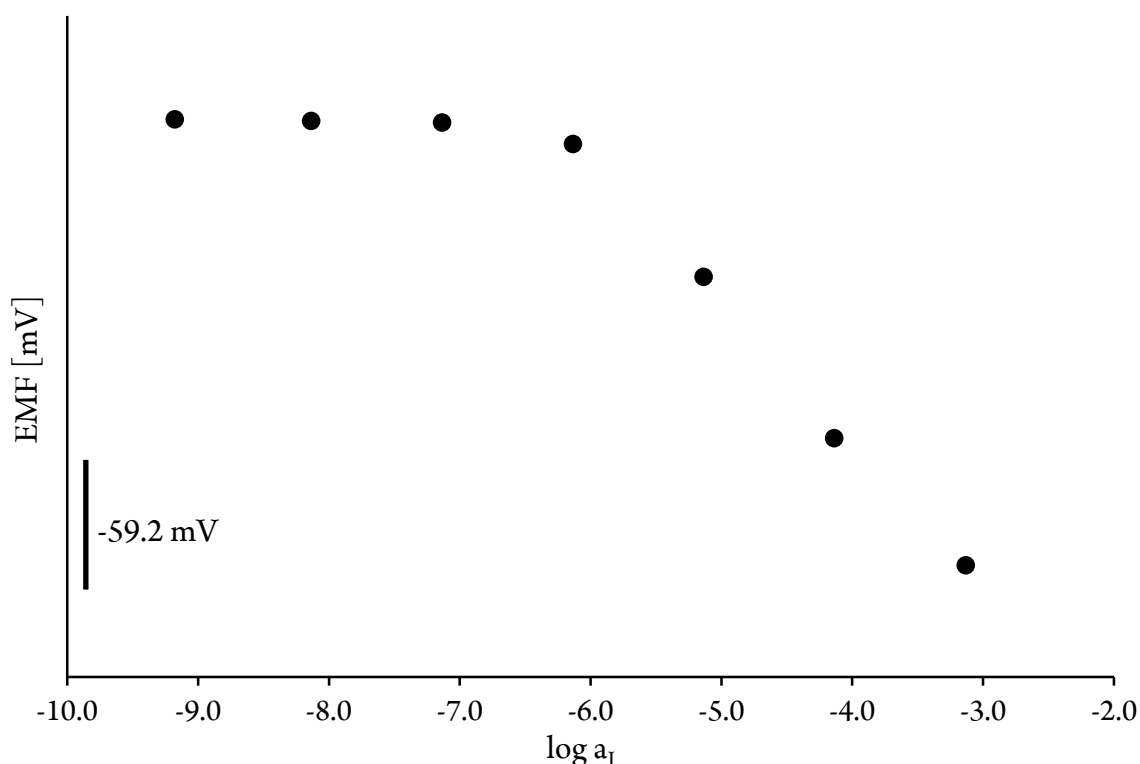
Figure 4.9 Potentiometric response of the self-plasticised copolymer based ion selective membrane for the determination of iodide in artificial urine. Note that none of the electrodes were conditioned in the solution of primary ions prior to the experiment.

4.3.5 Iodide determination in a real urine sample

Encouraged by the promising results obtained from artificial urine measurements, the proposed polyIL membrane was used for the determination of iodide in human urine sample. Figure 4.10 depicts the response of non-conditioned polyIL-based electrodes obtained in a real urine sample. Iodide level in this sample using ISEs was estimated as 3.16×10^{-6} M (0.40 ppm). This result was evaluated using ICP-MS and the iodide level of 1.35×10^{-6} M (0.17 ppm) was determined. The results obtained with the two techniques

agree reasonably well which is very encouraging for further application of polyIL-based iodide selective electrodes in real-life urine samples.
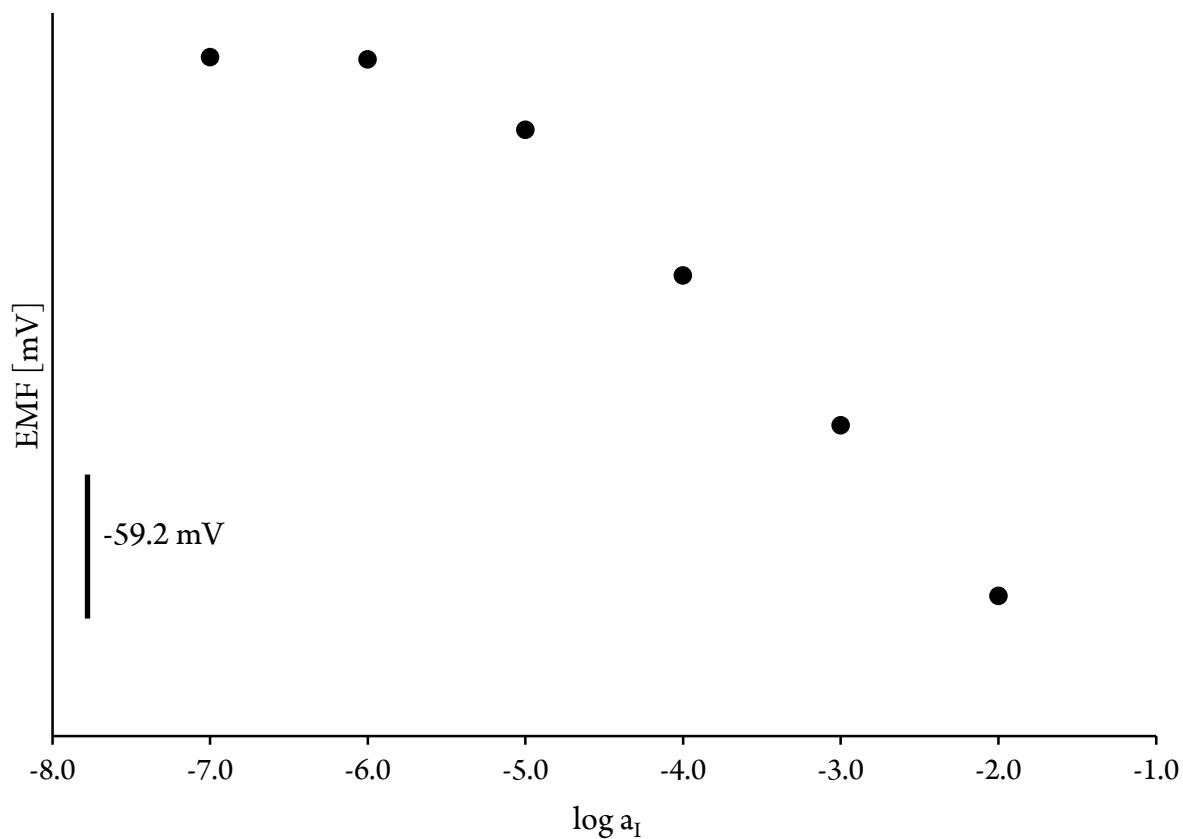
Figure 4.10 Response of the non-conditioned iodide selective membrane prepared from a single-component polyIL. Human urine sample was used as background solution to determine if the resulting electrodes can be used for iodide sensing in more complex sample.

4.4 Conclusions

Novel solid contact iodide selective electrodes based on covalently attached 1,2,3 triazole ionic liquid (IL) were prepared and investigated in this chapter. Triazole-based IL moieties were synthesised using click chemistry and were further copolymerised with lauryl methacrylate via a simple one step free radical polymerisation to yield a "self-plasticised" copolymer. The mechanical properties of the copolymer were found to be suitable for the fabrication of plasticiser-free ion-selective membrane electrodes. It has been demonstrated that covalently attached IL moieties provide adequate functionality to the ion selective membrane. This study also demonstrates that the presence of iodide as the counter-ion to the triazole moiety has direct influence on membrane's selectivity. Potentiometric experiments revealed that each electrode displayed high selectivity towards iodide anions over a number of inorganic anions. Moreover, the inherent presence of iodide in the membrane reduces the need for conditioning. The electrodes exhibited a near Nernstian behaviour with a theoretical slope of -56.1 mV per decade across large concentration range with lower detection limits found at approximately 6.31×10^{-8} M (8 ppb). The same all solid state sensors were later utilised for the determination of iodide in human urine sample demonstrating a close match with the results obtained from ICP-MS analysis. Furthermore, the non-conditioned ISEs showed excellent robustness and durability when stored for two weeks. Therefore, this study demonstrates an excellent potential of self-plasticised copolymers as sensing materials for the development of ISEs that can be directly used for *in situ* detection of biologically relevant ions without the need for sophisticated conditioning protocols.

References

(1)   Bakker, E.; Bühlmann, P.; Pretsch, E. *Chem. Rev.* **1997**, *97* (8), 3083–3132.

(2)   Lewenstam, A.; Maj-Zurawska, M.; Hulanicki, A. *Electroanalysis* **1991**, *3* (8), 727–734.

(3)   Rocha, R. A.; Rojas, D.; Clemente, M. J.; Ruiz, A.; Devesa, V.; Vélez, D. *J. Agric. Food Chem.* **2013**, *61* (45), 10708–10713.

(4)   McGraw, C. M.; Radu, T.; Radu, A.; Diamond, D. *Electroanalysis* **2008**, *20* (3), 340–346.

(5)   Bühlmann, P.; Pretsch, E.; Bakker, E. *Chem. Rev.* **1998**, *98* (4), 1593–1688.

(6)   Telting-Diaz, M.; Bakker, E. *Anal. Chem.* **2001**, *73* (22), 5582–5589.

(7)   Gehrig, P.; Rusterholz, B.; Simon, W. *Anal. Chim. Acta* **1990**, *233*, 295–298.

(8)   Heng, L. Y.; Hall, E. A. H. *Anal. Chim. Acta* **2000**, *403* (1-2), 77–89.

(9)   Heng, L. Y.; Toth, K.; Hall, E. A. H. *Talanta* **2004**, *63* (1), 73–87.

(10)   Reinhoudt, D. N.; Engbersen, J. F. J.; Brzozka, Z.; van der Vlekkert, H. H.; Honig, G. W. N.; Holterman, H. A. J.; Verkerk, U. H. *Anal. Chem.* **1994**, *66* (21), 3618–3623.

(11)   Peper, S.; Tsagkatakis, I.; Bakker, E. *Anal. Chim. Acta* **2001**, *442* (1), 25–33.

(12)   Qin, Y.; Peper, S.; Radu, A.; Ceresa, A.; Bakker, E. *Anal. Chem.* **2003**, *75* (13), 3038–3045.

(13)   Qin, Y.; Peper, S.; Bakker, E. *Electroanalysis* **2002**, *14* (19-20), 1375–1381.

(14)   Veder, J.-P.; De Marco, R.; Clarke, G.; Chester, R.; Nelson, A.; Prince, K.; Pretsch, E.; Bakker, E. *Anal. Chem.* **2008**, *80* (17), 6731–6740.

(15)   Chumbimuni-Torres, K. Y.; Rubinova, N.; Radu, A.; Kubota, L. T.; Bakker, E. *Anal. Chem.* **2006**, *78* (4), 1318–1322.

(16)   Mensah, S. T.; Gonzalez, Y.; Calvo-Marzal, P.; Chumbimuni-Torres, K. Y. *Anal. Chem.* **2014**, *86* (15), 7269–7273.

(17)   Mendecki, L.; Fayose, T.; Stockmal, K. A.; Wei, J.; Granados-Focil, S.; McGraw, C. M.; Radu, A. *Anal. Chem.* **2015**, *87* (15), 7515–7518.

(18)   Püntener, M.; Fibbioli, M.; Bakker, E.; Pretsch, E. *Electroanalysis* **2002**, *14* (19-20), 1329–1338.

(19)   Radu, A.; Peper, S.; Bakker, E.; Diamond, D. *Electroanalysis* **2007**, *19* (2-3), 144–154.

(20)   Daunert, S.; Bachas, L. G. *Anal. Chem.* **1990**, *62* (14), 1428–1431.

(21)   Nishida, H.; Takada, N.; Yoshimura, M.; Sonoda, T.; Kobayashi, H. *Bull. Chem. Soc. Jpn.* **1984**, *57* (9), 2600–2604.

(22)   Rosatzin, T.; Bakker, E.; Suzuki, K.; Simon, W. *Anal. Chim. Acta* **1993**, *280* (2), 197–208.

(23)   Qin, Y.; Bakker, E. *Anal. Chem.* **2003**, *75* (21), 6002–6010.

(24)   Kimura, K.; Sunagawa, T.; Yajima, S.; Miyake, S.; Yokoyama, M. *Anal. Chem.* **1998**, *70* (20), 4309–4313.

(25)   Abbas, M. N.; Radwan, A. L. A.; Bühlmann, P.; Ghaffar, M. A. A. E. *Am. J. Anal. Chem.* **2011**, *02* (07), 820–831.

(26)   Zahran, E. M.; New, A.; Gavalas, V.; Bachas, L. G. *The Analyst* **2014**, *139* (4), 757–763.

(27)   Coll, C.; Labrador, R. H.; Mañez, R. M.; Soto, J.; Sancenón, F.; Seguí, M.-J.; Sanchez, E. *Chem. Commun.* **2005**, No. 24, 3033.

(28)   Safavi, A.; Maleki, N.; Honarasa, F.; Tajabadi, F.; Sedaghatpour, F. *Electroanalysis* **2007**, *19* (5), 582–586.

(29)   Wardak, C. *Electroanalysis* **2014**, *26* (4), 864–872.

(30)   Wardak, C.; Lenik, J.; Marczewska, B. **2008**, *82* (1-2), 223–233.

(31)   Cicmil, D.; Anastasova, S.; Kavanagh, A.; Diamond, D.; Mattinen, U.; Bobacka, J.; Lewenstam, A.; Radu, A. *Electroanalysis* **2011**, *23* (8), 1881–1890.

(32)   Kavanagh, A.; Byrne, R.; Diamond, D.; Radu, A. *The Analyst* **2011**, *136* (2), 348– 353.

(33)   Gourishetty, R.; Crabtree, A. M.; Sanderson, W. M.; Johnson, R. D. *Anal. Bioanal. Chem.* **2011**, *400* (9), 3025–3033.

(34)   Green, M. D.; Long, T. E. *Polym. Rev.* **2009**, *49* (4), 291–314.

(35)   Atefi, F.; Garcia, M. T.; Singer, R. D.; Scammells, P. J. *Green Chem.* **2009**, *11* (10), 1595.

(36)   Yacob, Z.; Liebscher, J. In *Ionic Liquids - Classes and Properties*; Handy, S., Ed.; InTech, 2011.

(37)   Hanelt, S.; Liebscher, J. *Synlett* **2008**, *2008* (7), 1058–1060.

(38)   Zincke, T.; Th. Lawson, A. *Berichte Dtsch. Chem. Ges.* **1887**, *20* (1), 1176–1183.

(39)   Martinelli, M.; Milcent, T.; Ongeri, S.; Crousse, B. *Beilstein J. Org. Chem.* **2008**, *4*.

(40)   Tornøe, C. W.; Christensen, C.; Meldal, M. *J. Org. Chem.* **2002**, *67* (9), 3057– 3064.

(41)   Lee, I.-L.; Sung, Y.-M.; Wu, C.-H.; Wu, S.-P. *Microchim. Acta* **2014**, *181* (5-6), 573–579.

(42)   Karagollu, O.; Gorur, M.; Gode, F.; Sennik, B.; Yilmaz, F. *Sens. Actuators B Chem.* **2014**, *193*, 788–798.

(43)   Bandyopadhyay, I.; Raghavachari, K.; Flood, A. H. *Chemphyschem Eur. J. Chem. Phys. Phys. Chem.* **2009**, *10* (14), 2535–2540.

(44)   Li, Y.; Flood, A. H. *Angew. Chem.* **2008**, *120* (14), 2689–2692.

(45)   Zahran, E. M.; Hua, Y.; Li, Y.; Flood, A. H.; Bachas, L. G. *Anal. Chem.* **2010**, *82* (1), 368–375.

(46)   Li, Y.; Pink, M.; Karty, J. A.; Flood, A. H. *J. Am. Chem. Soc.* **2008**, *130* (51), 17293–17295.

(47)   Kim, S. H.; Choi, H. S.; Kim, J.; Lee, S. J.; Quang, D. T.; Kim, J. S. *Org. Lett.* **2010**, *12* (3), 560–563.

(48)   Lau, Y. H.; Rutledge, P. J.; Watkinson, M.; Todd, M. H. *Chem. Soc. Rev.* **2011**, *40* (5), 2848.

(49)   Chen, Y.-C.; Lee, I.-L.; Sung, Y.-M.; Wu, S.-P. *Sens. Actuators B Chem.* **2013**, *188*, 354–359.

(50)   Kumar, A.; Pandey, P. S. *Tetrahedron Lett.* **2009**, *50* (42), 5842–5845.

(51)   Kuo, S.-Y.; Li, H.-H.; Wu, P.-J.; Chen, C.-P.; Huang, Y.-C.; Chan, Y.-H. *Anal. Chem.* **2015**, *87* (9), 4765–4771.

(52)   Zhou, W.; Chai, Y.; Yuan, R.; Wu, X.; Guo, J. *Electroanalysis* **2008**, *20* (13), 1434–1439.

(53)   Hetzel, B. S.; Dunn, J. T. *Annu. Rev. Nutr.* **1989**, *9* (1), 21–38.

(54)   Delange, F.; de Benoist, B.; Pretell, E.; Dunn, J. T. *Thyroid Off. J. Am. Thyroid Assoc.* **2001**, *11* (5), 437–447.

(55)   Dunn, J. T. *J. Clin. Endocrinol. Metab.* **1998**, *83* (10), 3398–3400.

(56)   Abraham, G. E.; Flechas, J. D.; Hakala, J. C. *Orig. Internist* **2004**, *11* (4), 19–32.

(57)   Sandell, E. B.; Kolthoff, I. M. *J. Am. Chem. Soc.* **1934**, *56* (6), 1426–1426.

(58)   Dunn, J. T.; Crutchfield, H. E.; Gutekunst, R.; Dunn, A. D. *Thyroid* **1993**, *3* (2), 119–123.

(59)   Mantel, M. *Clin. Chim. Acta* **1971**, *33* (1), 39–44.

(60)   Zhang, W.; Mnatsakanov, A.; Hower, R.; Cantor, H.; Wang, Y. *Front. Biosci. J. Virtual Libr.* **2005**, *10*, 88–93.

(61)   Michalke, B.; Witte, H. *J. Trace Elem. Med. Biol. Organ Soc. Miner. Trace Elem. GMS* **2015**, *29*, 63–68.

(62)   Yang, L.; Zou, L.; Li, G.; Ye, B. *Talanta* **2016**, *147*, 634–640.

(63)   Lee, J. H.; Ji, O. J.; Song, M. J.; Park, H. D.; Kim, H. K.; Kim, S. W.; Chung, J. H.; Lee, S. Y. *Korean J. Lab. Med.* **2010**, *30* (4), 351–356.

(64)   Yang, W.; Shao, J.; Xu, Y.; Zhou, W.; Xie, J. *J. Photochem. Photobiol. Chem.* **2014**, *292*, 49–55.

(65)   Brooks, T.; Keevil, C. W. *Lett. Appl. Microbiol.* **1997**, *24* (3), 203–206.

(66)   Bakker, E. *Anal. Chem.* **1997**, *69* (6), 1061–1069.

(67)   Schibli, R; Struthers, H; Mindt, T L; Spingler, B. **2008**.

(68)   Khan, S.; Hanelt, S.; Liebscher, J. *Arkivoc* **2009**, *2009* (12), 193–208.

(69)   Hua, Y.; Flood, A. H. *Chem. Soc. Rev.* **2010**, *39* (4), 1262.

(70)   Ceresa, A.; Bakker, E.; Hattendorf, B.; Günther, D.; Pretsch, E. *Anal. Chem.* **2001**, *73* (2), 343–351.

(71)   Sokalski, T.; Ceresa, A.; Fibbioli, M.; Zwickl, T.; Bakker, E.; Pretsch, E. *Anal. Chem.* **1999**, *71* (6), 1210–1214.

(72)   Wardak, C. *Sens. Actuators B Chem.* **2015**, *209*, 131–137.

(73)   Shahrokhian, S.; Taghani, A.; Moattar, F. *Electroanalysis* **2002**, *14* (23), 1621–1628.

(74)   Jalali, F.; Rajabi, M. J.; Bahrami, G.; Shamsipur, M. *Anal. Sci. Int. J. Jpn. Soc. Anal. Chem.* **2005**, *21* (12), 1533–1535.

(75)   Cuenca, R. E.; Pories, W. J.; Bray, J. *Biol. Trace Elem. Res.* **1988**, *16* (2), 151–154.

(76)   Radu, A.; Bakker, E. *Chem. Anal.* **2005**, *50* (1), 71–83.

(77)   Buhlmann, P.; Umezawa, Y.; Rondinini, S.; Vertova, A.; Pigliucci, A.; Bertesago, L. *Anal. Chem.* **2000**, *72* (8), 1843–1852.

(78)   Toh, H. S.; Tschulik, K.; Batchelor-McAuley, C.; Compton, R. G. *The Analyst* **2014**, *139* (16), 3986–3990.

CHAPTER 5   Lumogallion-based fluorescent optical sensor for the determination of aluminium (III) with ultra-low detection limits.

5.1   Introduction

Previous chapters successfully demonstrated that the performance of ion selective electrodes can be improved either by modifications of well-established protocols that are employed during the preparation of sensing membranes or via the synthesis of new materials including new ion receptors and self-plasticised polymeric architectures. The response of previously proposed sensing devices is strictly governed by the changes in electrical potential at the phase boundary between the ion selective membrane and aqueous solution that can be further quantified using a potentiometric setup (see Chapter 1). However, all ISEs need to be connected to an external voltmeter and therefore if miniaturised, a precise delivery instrumentation (e.g. micromanipulator) is required to minimise the effect of background noise that is generated by the movement of the electrode or to reduce any external electrical interferences. Therefore, alternative approaches based on the host-guest chemistry are explored in this chapter in order to develop a sensor that would exhibit excellent selectivity and sensitivity towards targeted ions as previously demonstrated with ISEs.

In recent years, several staining methodologies have been suggested for the detection of metal ions in environmental and clinical samples.[1–5] However, on many occasions the analysed sample cannot be recovered for further testing (destructive measurement) limiting

their application to the measurements in which only high amount of sample is available. Additionally, staining protocols require that the investigated sample must be collected and often processed in the laboratory prior to their analysis thus the vast majority of these techniques are not suitable for real-time or *in situ* measurements.[6,7] This is a significant issue as the presence of heavy metal ions can have a big impact on the surrounding environment and human life. For example, aluminium, copper, zinc and iron have been previously recognised as 'toxic' agents that can influence the formation of amyloid fibrils in the brain tissue, therefore, increasing the risk of developing Alzheimer disease.[7–9] Moreover, the presence of aluminium can successfully point to whether or not the corrosion processes of aluminium based alloys are taking place.[10] In agriculture, Al^{3+} toxicity has been identified as a major factor that inhibits the growth of roots in plants in acidic soils.[11,12] However, very limited solubility of aluminium in natural waters (10 - 400 ug/L in fresh water and 0.5 − 10 ug/L in sea water) creates a need for the development of ultra-sensitive analytical procedures that would allow the unequivocal determination of this ion.

Fluorescent techniques, which rely on the complex formation between targeted ion and the fluorophore, have been receiving considerable attention as they often exhibit superb sensitivity, selectivity, rapidity and portability (Chapter 1 – Optodes).[13] Morin is a well-studied type of a fluorophore that is predominantly used for the detection of aluminium in solutions[14,15] with recent attempts focused on the chemical modifications for sensing purposes.[16,17] However, resulting sensors often did not yield the required sensitivity and selectivity towards Al^{3+} as such dyes readily bind other metal ions that are commonly encountered in physiological samples such as magnesium or calcium.[12,18] Furthermore,

small binding affinity for Al^{3+} at circumneutral pH (pH range: 6.5 – 7.5) makes it unsuitable for real-time clinical measurements.[19] Other fluorescent probes based on the presence of coumarin,[20] 5-[{(2-Hydroxynaphthalen-1-yl)methylene}amino]pyrmidine-2,4(1H,3H)-dione,[21] thiophene-2-carboxylic acid hydrazide,[22] piperidine carboxylic acid dithiocarbamate[23] amongst many others have been reported. However, new analytical methodology is required if we are to develop very sensitive and robust sensors for aluminium determination.

Fluorometric detection of Al^{3+} based on the presence of lumogallion has gained a widespread acceptance as such technique offers good sensitivity and selectivity to Al^{3+}.[24] Lumogallion has been already routinely employed in separation science as a pre-column derivatisation dye[25] or in plant chemistry[26] as aluminium tracing agent. Moreover, recent studies carried out by Mold et al (2014) reported the first use of lumogallion for the unequivocal determination of aluminium adjuvants in monocytic T helper 1 (THP-1) cell line.[27] Lumogallion is an azo dye known to form 1:1 stoichiometric complexes with the soluble Al^{3+} fraction and if irradiated with the wavelength of 500 nm it produces fluorescence with the emission signal found at 590 nm (orange fluorescence).[28,29] Despite its excellent properties as a staining agent in solutions, there has been only limited number of studies involving the use of lumogallion for the development of optical probes.[30] This could be attributed to the poor solubility of the dye in various organic solvents required for the preparation of optodes as well as to its predominantly hydrophilic character that would cause the diffusion of lumogallion from the more hydrophobic polymeric membrane into the aqueous solution. These significantly would lessen the lifetime of resulting probes and

limit their practical application to samples that could undergo contamination upon leaching of the fluorescence dye.[31]

Over several years, large advancements in analytical and organic chemistry offered a vast number of approaches to minimise the extent to which the active components diffuse out of the sensing layer and consequently to improve the overall performance of the polymer based chemical sensors.[32] The most logical and intuitive approach involved chemical modifications of sensing components such as addition of long alkyl chains in order to improve the overall hydrophobicity of studied molecules.[33] However, resulting changes in the solubility of the derivatised molecules may often result in the phase separation within the polymeric matrix permanently reducing the performance of sensing devices. Moreover, depending on the type of chemical modifications (changes in the lipophilicity), the resulting fluorophore/ionophore may still partition out of the hydrophobic bulk into sample solution limiting the robustness and application of designed sensors. As it was discussed in the previous chapters, a permanent attachment of sensing components to the polymer backbone can significantly improve the stability of a homogenous sensing layer.[34] This may also significantly reduce or even fully eliminate leaching of sensing components out of the polymeric optical film. Permanent immobilisation of fluorescent moieties also prevents the formation of aggregates by reducing the intermolecular interactions and can improve emission signal intensity by eliminating collisions of a fluorophore with the solution molecules.[35]

The range of monomers carrying fluorescent properties that have already been reported in the literature is very extensive and includes all commonly employed classes of dyes.[36] This includes polycyclic aromatic hydrocarbons, azo dyes, coumarins, fluorescein, cyanine dyes and rhodamines where all of the derivatives are fully compatible with commonly applied polymerisation techniques such as free radical polymerisation, atom transfer radical polymerisation (ATRP),[37] reversible addition–fragmentation chain transfer (RAFT) polymerisation,[38] living anionic and cationic polymerisation and ring opening metathesis polymerisation.[39] In recent years, several optical sensors based on plasticiser-free membrane have been investigated and the response behaviour of such films was evaluated in terms of their selectivity, sensitivity and robustness towards various physiologically relevant cations and anions. As described in previous chapters, methacrylic-acrylic random copolymers synthesised via free radical polymerisation gain widespread popularity as polymeric architectures in sensing as several synthetic routes can be chosen for their preparation.[40] Furthermore, Chapters 2 and 4 demonstrated that self-plasticised ion selective electrodes based on the methacrylic-acrylic polymer backbone are suitable for trace analysis of ionic species.[41]

In this study a new polymerisable lumogallion based derivative that has been covalently attached to a hydrophobic self-plasticised polymer backbone is described for practical applications in ion optical sensors. In this study, the first single element copolymer for the detection of aluminium (III) ions with ultra-low sensitivity (pM concentrations) and superior selectivity over various biologically relevant ions is reported demonstrating its great potential as a sensor for environmental or *in vivo* and *in vitro* measurements.

5.2 Experimental

5.2.1 Materials

Methacryloyl chloride, 2,2'-azobis(2-methylpropionitrile) (AIBN), sodium tetrakis[3,5-bis(trifluoromethyl)phenyl]borate (NaTFPB), poly(ethylene glycol) methacrylate (PEGMA), lauryl methacrylate (LMA), polyethylene glycol methyl ether methacrylate (PEGMEM), methyl methacrylate (MMA), Brij L23 and tetrahydrofuran (THF) were purchased from Sigma-Aldrich. 2,2',4'-Trihydroxy-5-chloroazobenzene-3-sulfonic acid (lumogallion) was obtained from TCI Chemicals. DropSens Dual Carbon Screen-printed Electrodes (C1110) were purchased from Metrohm USA. AIBN was re-crystallised from cold methanol prior to use and each monomer was passed through neutral alumina column to remove the inhibitor and then was stored in the freezer under N_2 atmosphere until further use. All other reagents were of the highest commercially available purity and were used as received. Solutions of metal ions were prepared in ultra-pure water obtained from a Pico Pure 3 water system. Working solutions of different activities were prepared by serial dilutions of a 1 M stock solution.

5.2.2 Synthesis of lumogallion methacrylate (LuMA)

In a flamed-dried, argon-purged, round-bottomed flask, lumogallion (200 mg, 0.58 mmol) was mixed with anhydrous dimethylformamide (5 mL DMF), caesium carbonate (284 mg, 0.87 mmol) and triethylamine (58.7 mg, 0.58 mmol). The following reaction mixture was stirred for 2 h and then cooled in an ice bath. Methacryloyl chloride (60.6 mg, 0.58 mmol) was added dropwise while the mixture was constantly stirred. After addition, the mixture was warmed to room temperature and stirred for an additional 16 h. The volatiles were then removed under reduced pressure and the obtained reaction mixture was dried under

the high vacuum. The resulting precipitate was added to the heterogeneous mixture of ethyl acetate (5 mL) and dilute hydrochloric acid (5%, 5 mL). The organic phase was then washed with water (3 x 10 mL) and the organic solvent was removed via rotatory evaporation to yield the product (34%). ^{1}H NMR (200 MHz, DMSO, δ): δ 7.95 (d, J = 0.93 Hz, 1H, CN-CH-CCl), 7.67 (dd, J = 0.37, J = 0.18, 1H, CH-*CH*-CN), 7.48 (d, J = 0.61 Hz, 1H, CCl-CH-CSO$_3$H), 6.50 (m, 1H, COH-*CH*-CH), 6.32 (t, J = 9.53, 1H, COH-*CH*-COH), 5.97 (s, 1H, C=CH$_2$), 5.61 (s, 1H, C=CH$_2$).

5.2.3   General copolymer synthesis procedure

All copolymers were synthesised via thermally initiated free radical solution polymerisation. Calculated amounts of lumogallion methacrylate (LuMA), methyl methacrylate and either polyethylene glycol methyl ether methacrylate or poly(ethylene) glycol methacrylate were added to the anhydrous mixture of THF (3 mL) and DMF (2 ml) before addition of AIBN (1% wt). The homogenous solution was purged with a stream of nitrogen for 25 min. Polymerisation was then carried out at 75˚C under vigorous stirring for 24 h. After the reaction was completed, the excess of solvent was removed using rotatory evaporation, dried under the high vacuum and the dark coloured precipitate was collected. The residue obtained was dissolved in dichloromethane (DCM) and reprecipitated by excess cold methanol. The same procedure was repeated three times and the resultant copolymer was dried under ambient laboratory conditions. ^{1}H NMR (200 MHz, DMSO, δ): δ 7.96 (br, 1H, CN-CH-CCl), 7.64 (br, 1H, CH-*CH*-CN), 7.42 (br, 1H, CCl-CH-CSO$_3$H), 6.61 (m, 1H, COH-*CH*-CH), 6.31 (br, 1H, COH-*CH*-COH), 4.03 (br, COO-*CH$_2$*-CH$_2$), 3.55 (br, 3H, O-CH$_3$), 3.37 (s, 3H, CH$_2$-O*CH$_3$*), 1.82-0.75 (m, -[*CH$_2$*]$_n$-).

5.2.4 UV/Vis and fluorescence measurements

Ultraviolet-visible (UV/Vis) spectra were recorded using a Unicam UV500 double beam spectrophotometer (Unicam Instruments Ltd, UK) and fluorescence measurements were collected using a Cary Eclipse Fluorescent Spectrophotometer (Agilent Technologies, USA) with 1000 W xenon lamp and a photomultiplier tube (PMT) set at the voltage of 600 V. Quartz 1 cm x 1 cm x 4.5 cm cuvettes were used for all cuvettes measurements. The excitation wavelength was determined from UV/Vis measurements (the absorption maxima after the complex formation between aluminium and lumogallion based copolymer) and set at 485 nm while the emission wavelengths were monitored from 510 nm to 900 nm. All measurements were carried out at ambient temperature

5.2.5 Preparation of lumogallion-based optical membranes

Each glass slides were prepared by cutting standard microscope slides into dimensions of 1.3 cm x 3.0 cm using a diamond cutter. The resulting slides were then rinsed with ultra-pure water and acetone and then dried under nitrogen gas. Optode membranes were prepared by dissolving 100 mg of lumogallion-based copolymer in 0.5 mL of THF. After the complete dissolution of the copolymer the aliquot was spread out onto each glass slide by using a spin coater at 2000 rpm for 30 sec to yield membranes with the approximate thickness of 50 ± 2.5 μm and then each membrane was left at room temperature to dry overnight. Subsequently, prepared optode membranes were immersed in the acidified solutions of Al^{3+} ions (pH 3.5, to ensure that only free aluminium (III) ions are present) for 30 min, mounted into the customised quartz cuvette suitable for fluorescence measurements and then the fluorescence characteristics of prepared membranes were determined.

5.2.6 Fabrication of the optical nano-particles

Fabrication of polymeric particles via a solvent displacement method was adapted and modified from Bychkona and Shvarev (2009).[42] 100 mg of PEGMA-MMA-LuMA based copolymer was dissolved in 1:1 heterogeneous mixture of ethylene glycol and THF (total volume – 1 ml). A small glass container (10 mL) was filled with a 0.02% solution of the surfactant (Brij L23) in ultra-pure water. The resulting solution was stirred for 10 min at approximately 150 rpm. A small aliquot (500 µL) of the copolymer solution was drawn into a disposable syringe with an attached needle. The syringe was held approximately 5 mm above the surface of the liquid and the copolymer solution was rapidly injected into the vial. Precipitation of the polymer was observed within seconds after the injection of the mixture into the surfactant solution. The resulting nano-beads were directly transferred onto new glass slide and were instantly subjected to microscopic examination.

5.2.7 Preparation of ISEs based on copolymerised lumogallion

For the preparation of lumogallion based ISEs a solution of POT (1.0×10^{-3} M of monomer in chloroform) was drop cast onto the top of screen-printed electrodes and left at room temperature to dry overnight. Aluminium selective membranes were prepared by dissolving 100 mg of synthesised copolymer in THF (0.5 ml) with varying amounts of ionic sites (20 mmol/kg^{-1}, 10 mmol/kg^{-1} and 5 mmol/kg^{-1}) (NaTFPB). After the complete dissolution of the copolymer an aliquot (~20 µL) was drop cast onto the top of screen printed electrodes and left at room temperature to dry overnight. The prepared membranes were then equilibrated for 24 h in 1.0×10^{-9} M solution of aluminium nitrate.

5.2.8 Fluorescence microscopy

Lumogallion based nano-beads were analysed using an Olympus BX50 fluorescence microscope with a BX-FLA reflected light fluorescence attachment, equipped with a mercury burner and a vertical illuminator. For lumogallion imaging a U-MNIB3 fluorescence filter cube was used (bandpass excitation filter: 470 – 495 nm, dichromatic mirror: 505 nm, longpass emission filter: 510 nm) (both from Olympus, UK). All images of copolymer based nano-particles were recorded at $\times$ 40 magnification using a $\times$ 100 Plan-Fluorite oil immersion objective (Olympus, UK) in combination with low auto-fluorescence immersion oil (Olympus immersion oil type-F). The exposure settings for the lumogallion analyses were fixed at 1 s with fixed light transmission values. Digital images were obtained using the Cell^D software package (Olympus, Soft Imaging Solutions, GmbH).

5.2.9 Particle size analysis

Size of prepared nano-particles and the resulting size distribution were determined by laser light scattering with particle size analyser (90 Plus, Brookhaven Inst, Huntsville, NY, USA) at a fixed angle of 90° at 25 °C. The dried nano-particles were suspended in ultra-pure water and then sonicated to prevent particle aggregation and to form uniform dispersion of nano-particles.

5.2.10 EMF measurements

All potentiometric measurements were performed using a Lawson Labs Inc. 16-channel EMF-16 interface (3217 Phoenixville Pike Malvern, PA 19355, USA) in a stirred solution against a double-junction Ag|AgCl|sat. KCl|1M LiOAc reference electrode (Fluka).

5.3   Results and discussion

Dissolved lumogallion has been already recognised as very sensitive optical ligand for the detection of aluminium with the lower detection limits (LDLs) reaching µg/L levels.[29] Even though, lumogallion has been identified as an excellent dye for Al^{3+} determination its very low solubility in organic solvents typically used for the preparation of optical films and ISEs limits its application as a sensing component in hydrophobic polymeric membranes. It should be noted that a small fraction of this fluorescence dye (< 1% wt) can be successfully dissolved in the mixture of PVC and DOS (33% wt, and 66% wt respectively) in THF carrying a promise for its application as optical sensor. However, upon the contact of the sensing film with the aqueous phase, almost instantaneous diffusion of lumogallion from the sensing membrane in the direction of sample took place rendering this sensor unsuitable for further testing.

Similarly, lumogallion has been introduced into the polymeric matrix composed of the copolymerised MMA-LMA moieties (copolymer D – see Chapter 2, Experimental). Recently, self-plasticised membranes have been recognised as excellent substituents to traditionally plasticised PVC membranes as their performance was not impaired by the exudation of the plasticiser from the membrane matrix into the sample.[40] Moreover, it was already reported that such membranes display lower diffusion coefficient if compared to predominantly used plasticised PVC membranes.[43] This could potentially reduce the extent to which lumogallion diffuses out of the polymeric membrane. However, upon contact with an aqueous phase, severe leaching of the fluorescence dye has occurred. This calls for further advancements in the development of lumogallion-based optical sensors.

Therefore, the most intuitive approach was to chemically modify lumogallion either by adding long alkyl chains or modifying already existing functional groups to reduce the overall polarity of this molecule. In this study, one component optical sensor based on the presence of lumogallion, which can form fluorescent complexes with aluminium (III) ions, has been proposed. This derivative contains a methacrylate moiety instead of the hydroxyl group at the para position relative to the azo group to allow simple attachment to the polymer backbone. Methacrylate based monomers were selected to yield plasticiser free copolymers with varying degree of hydrophilicity to find the best candidate for the Al^{3+} determination. This would ensure high robustness of a sensor during spectroscopic experiments and such factor has been a driving force in the development of lumogallion-based sensors. The synthesis procedure of lumogallion-based fluorescence sensor is illustrated in Scheme 5.1.
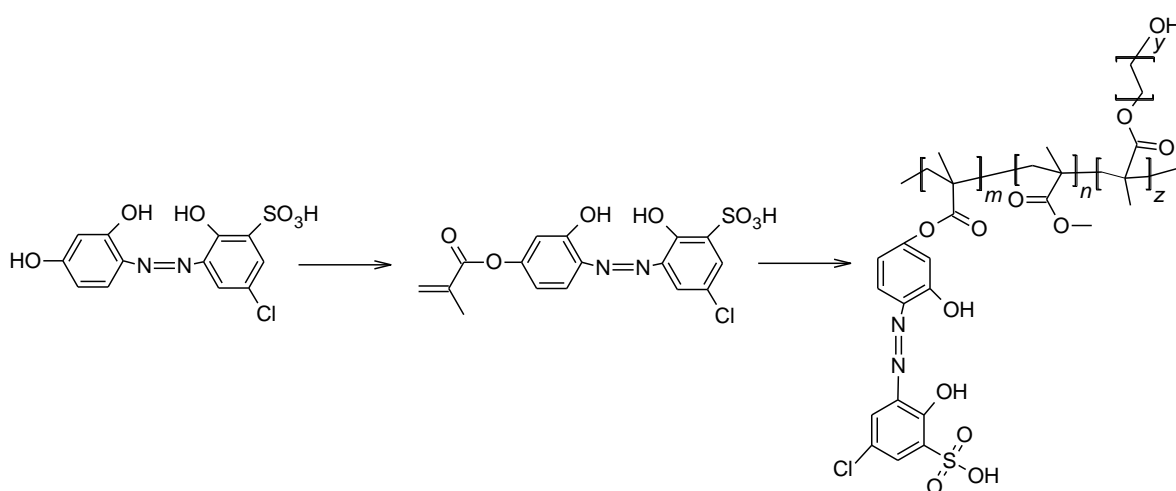
Reagents and conditions: (i) Lumogallion, C_4H_5ClO, Cs_2CO_3, DMF, 85°C, 24 h (ii) Lumogallion methacrylate, PEGMA, MMA, AIBN, DMF, 75°C, 24 h

Scheme 5.1 Experimental pathway for the synthesis of the copolymer consisting of methyl methacrylate, poly(ethylene glycol) methyl methacrylate and lumogallion methacrylate moieties.

5.3.1 Sensitivity

The excitation and emission wavelengths of the resulting copolymer were found at 485 nm and 580 nm respectively. The small hypsochromic shift from the values reported in the literature (excitation wavelength at 500 nm for dissolved lumogallion in water) could be attributed to structural modifications introduced during the synthetic process. The synthetic pathway for the formation of lumogallion-based copolymers is illustrated in Scheme 5.1. Another factor that may contribute towards a small shift in emission and excitation wavelengths is the solvatochromic character of this fluorescent dye. Azo dyes have been already reported as molecules that can exhibit either bathochromic (red, longer wavelength) or hypsochromic (blue, shorter wavelength) shift upon the interactions with solvents of different polarity.[44,45] Interestingly, the excitation and emission wavelengths of the copolymerised fluorescent dye remain the same when exposed to solvents of different polarities. This phenomenon is likely to arise from the presence of methacrylate based polymer backbone that also serves a function of the solvating matrix for the azo dye and therefore defines its spectral properties. Furthermore, the same copolymerised optical films were exposed to several solutions of different Al^{3+} concentrations in order to establish lower detection limits (LDLs) and spectral behaviour of this covalently attached dye.
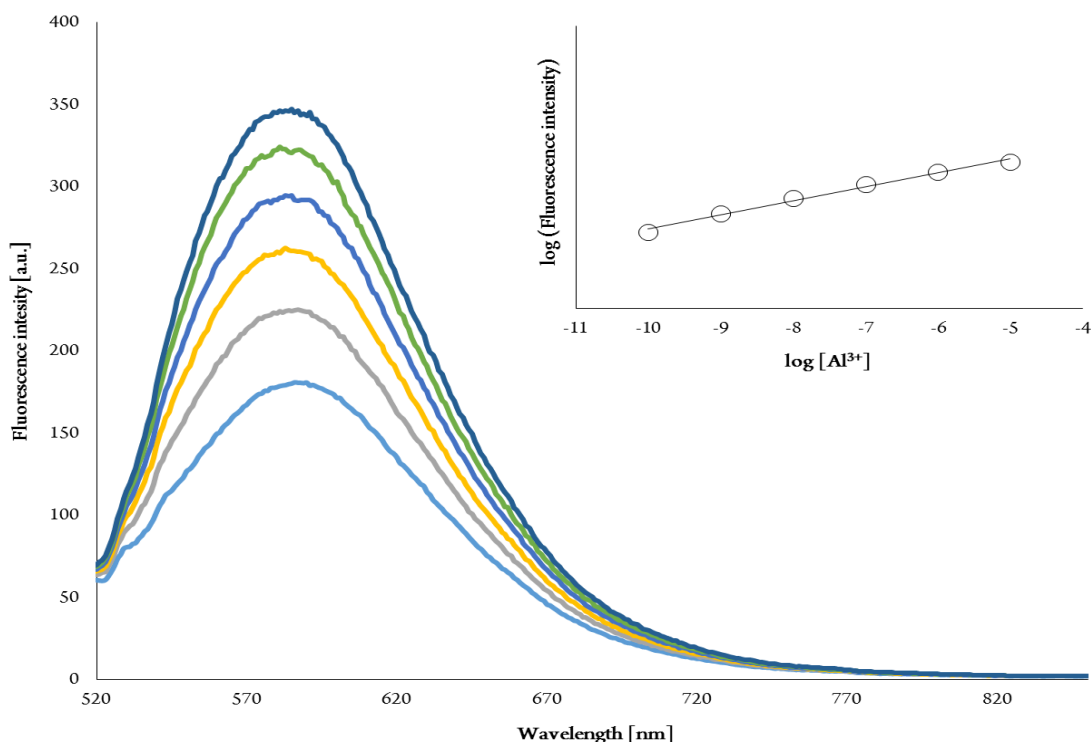
Figure 5.1 Response of the lumogallion-based optical sensor to aluminium (III) ions. The data are represent as the fluorescence intensity with the excitation wavelength of 485 nm and emission equal to 580 nm. The inset demonstrates the linear response range with R^2 equal to 0.99 for varying Al^{3+} concentrations.

More detailed investigation of spectral properties showed that the lumogallion based copolymer emits fluorescence that increases linearly with increasing Al^{3+} concentration (between 1.0×10^{-10} M and 1.0×10^{-5} M) making it suitable for sensing applications in biological samples (Figure 5.1). In this study, the minimum concentration of aluminium (III) ions that could be successfully measured was 4.8×10^{-12} M (S/N = 3) (see inset Figure 5.1). LDLs found in this study exceed those reported for other optical sensors based either on the use of lumogallion (2.0×10^{-7} M) or morin (3.7×10^{-7} M) fluorophores.[30,46] This demonstrates that the presence of copolymerised lumogallion significantly enhances the sensitivity of the developed optical sensor. In this case, permanent immobilisation of lumogallion protects the fluorophores from quenching by non-radiative processes for

example via collisions with solution molecules. This results in the improvements of the emission intensity and increased sensitivity. Also, it can be hypothesised that covalent attachment of lumogallion suppresses intermolecular interactions between adjacent dye molecules and therefore prevents further lumogallion stack formation thus increasing signal intensity.

Moreover, it should be noted that overall lipophilicity of lumogallion could be also increased by the addition of alkyl chains, for instance at the para position to the azide bond via a nucleophilic substitution reaction of primary alcohols with alkyl halides. However, it could be hypothesised that molecules similar to dodecylbenzenesulfonate anion (DBS$^-$) used in Chapter 2 may form micellar aggregates within polymer matrix. This could be explained by the relatively polar character of the lumogallion 'core' that if introduced in more hydrophobic matrix would start forming reversed micelles in which long alkyl chains would ultimately shield the more hydrophilic 'core' of the fluorophore. This could reduce the overall number of available binding sites on the fluorophore thus limiting its sensitivity towards the analyte of interest. Therefore, only chemical modifications allowing the attachment of lumogallion molecule to the polymer backbone were performed in this study.

5.3.2 Reversibility

Furthermore, the reversibility of the lumogallion-based copolymer was examined by firstly exposing the membrane to 1.0×10^{-2} M solution of aluminium (III) ions and then regenerating the optode with 0.1 M HNO$_3$ in order to protonate hydroxyl groups (involved in binding) and consequently to release Al^{3+} back into the aqueous solution. The same

procedure was repeated for three consecutive cycles. However, it was noticed that when the same optical film was placed directly into the aqueous solution containing the analyte of interest (after acid washing step), no ion binding was observed. This could be due to the limited affinity of hydroxyl groups towards Al^{3+} in the presence of high concentration of hydrogen ions (pH < 1.5). This could be overcome by washing the polymeric membrane with slightly more alkaline solution such as sodium hydroxide (0.1 M) and then rinsing the same sensor with ultra-pure water to remove any excess base that would ultimately cause a precipitation of aluminium hydroxide upon contact of Al^{3+} with a very alkaline medium. The findings from this study are demonstrated in Figure 5.2.
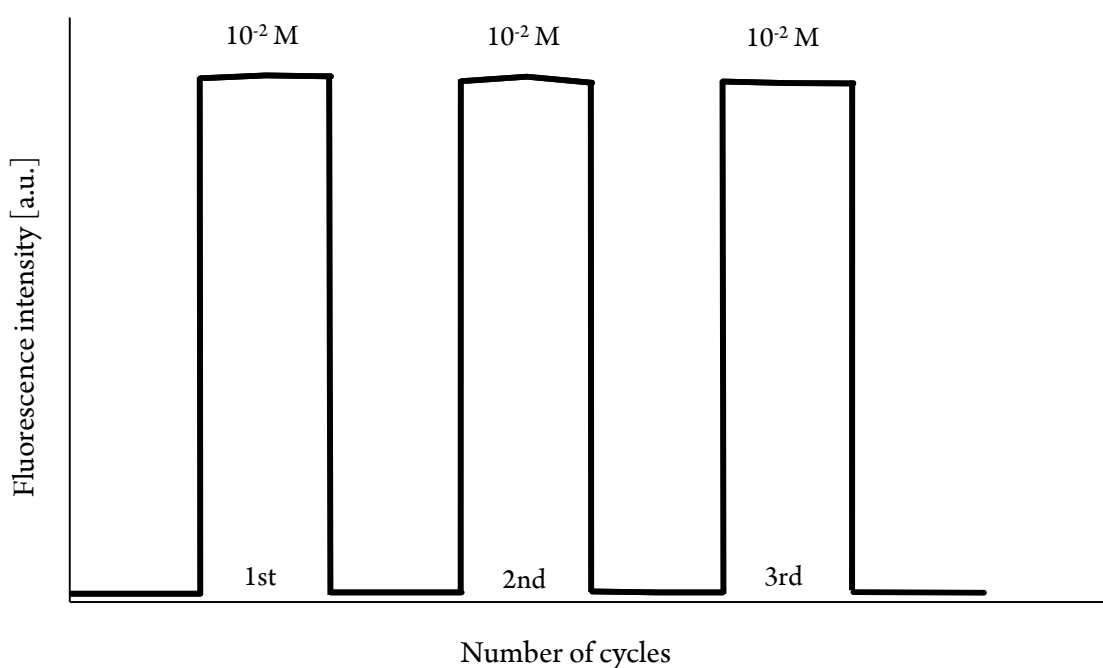
Figure 5.2 Reversible optical response of the proposed sensor after exposure to 1.0×10^{-2} M Al^{3+} and the regeneration with 0.1 M HNO_3 and 0.1 M NaOH.

Even though, the complex formation between lumogallion and aluminium (III) ion is fully reversible, further attempts should be undertaken to shorten the number of steps required to regenerate the optical sensors and therefore to make it fully operational for practical

applications. This could involve: a) using different types of acid (e.g. citric acid) at varying concentrations; b) placing the sensor in very high concentrations of interfering ions (e.g. 3 M) to cause dissociation of Al^{3+}-lumogallion complexes or c) introducing other Al^{3+} complexing agents at high concentrations which would compete with the proposed copolymer for the targeted ion.

On some occasions this relatively disadvantageous property of the optode (requirement for acid wash) may be utilised for other purposes than its intended primary application as an aluminium sensing device. It was observed that the same optical film when exposed to 0.1 M HNO_3 solution that was used to regenerate the sensor causes a release of Al^{3+} into the aqueous solution. This is an interesting observation as such device could be potentially applied for the selective ion extraction and controlled Al^{3+} release with the possibility to monitor in real time the efficiency of such process by looking at changes in the fluorescent signal of bound and unbound forms of the dye. However, this was not the primary scope of the chapter and any further examination regarding aluminium (III) ion extraction has not been carried out.

5.3.3   Response time

Another important characteristic that defines the functionality of optical sensors is their response time towards the analytes of interest. Since the response of traditional optical films result from a complete ion exchange in the bulk of the polymeric membrane, mass diffusion through the membrane bulk limits the response time making it much slower when compared to ISEs. In this research, several lumogallion-based copolymers with different monomer feeds were prepared and analysed to find the most optimal Al^{3+} optical sensor. In

order to ensure that any observed differences arise specifically from the presence of various monomers and their feeds, optical films were spin coated onto a glass substrate to produce polymeric membranes with reproducible thicknesses equal to 50 ± 2.5 μm. The reported response time was defined as 95% of the time required to reach steady state.

Independent of the type of monomer used for membrane preparation, each polymeric film displayed similar LDLs when exposed to aluminium (III) ions – approximately 4.8 x 10^{-12} M. However, large differences in the response time between analysed copolymers were observed as demonstrated in Table 5.1. Optical films composed of LuMA (1%) copolymerised with LMA-MMA (40% wt and 59% wt respectively) exhibited the longest response times when exposed to Al^{3+} ions (up to 36 h). As the MMA content of the copolymer decreased, softer self-plasticised membranes were obtained (70% wt of LMA, 29% wt of MMA and 1% LuMA) and the response time of a resulting optode was shorten by 12 h. However, analysed copolymers with high LMA content had poor adhesive properties and were less mechanically stable. Moreover, very long response time of the synthesised copolymers rendered these sensors unsuitable for practical applications and further experiments involving the use of such membranes were not carried out. These poor response characteristics were attributed to the overall hardness of the membrane as self-plasticised copolymers often exhibit reduced diffusion coefficients if compared to traditionally used PVC and DOS membranes.[43] Additionally, a predominantly hydrophobic (apolar) character of methyl methacrylate, lauryl methacrylate and lumogallion methacrylate based (MMA-LMA-LuMA) copolymer could further limit the diffusion of relatively hydrophilic Al^{3+} ions from the aqueous solution into the bulk of the membrane slowing sensor's response time.

In order to shorten the response time of lumogallion based copolymer while retaining suitable mechanical properties for sensor manufacture, only LMA moieties were replaced with monomers of varying polarity. Initially, LMA was replaced with PEGMEM moiety to produce more hydrophilic self-plasticised copolymers (MMA-PEGMEM-LuMA). Such modifications instantly resulted in shortening the response time of the prepared optical films down to 50 min. When the PEGMEM building block was replaced with even more polar PEGMA monomer, the response time was even further reduced (composition of resulting copolymer – MMA-PEGMA-LuMA). The findings of this study are summarised in Table 5.1.

Observed improvement in the response time of synthesised copolymers could be due to a combination of factors such as: a) increase in overall polarity of the membrane and b) water uptake by the membrane c) combination of both above-mentioned processes. As the hydrophilicity of the membrane increased, a diffusion of Al^{3+} ions from the aqueous solution into the membrane became more energetically favourable improving significantly the response characteristics of such sensors. Moreover, it can be hypothesised that the increase in polarity of the sensor also facilitated a water uptake by the membrane resulting in an enhanced extraction of relatively hydrophilic aluminium (III) ions and shortened response time. Such a phenomenon may also explain the very poor/slow behaviour of lumogallion based membranes composed of LMA and MMA moieties as their more hydrophobic character repels water more readily from the membrane bulk and therefore produces sensors with longer response time. On many occasions, water uptake can be considered as an issue in the case of traditionally prepared optical sensors or ISEs. As the

water content increases in such membranes, exudation of the plasticiser from its bulk into the aqueous solution is facilitated. This not only carries the risk of deteriorating mechanical stability of ISEs/optodes but it may also promote the diffusion of sensing components such as ionophore or ionic sites in the direction of the sample. If sufficiently exposed, these membranes may be rendered inactive for practical applications. However, one component membranes that were used in this study were expected to exhibit much improved robustness as covalent linkage of the fluorescent dye to the polymer backbone would prevent its leaching upon contact with the aqueous solution. This hypothesis was further tested and the findings of this study are described in more detail in this chapter under the heading Robustness.

Table 5.1 Response time of synthesised lumogallion based copolymers. Lumogallion methacrylate monomer (LuMA) contributed 1% towards the overall polymer yield.

Copolymer composition	LMA + MMA (40% and 59%)	LMA + MMA (70% and 29%)	PEGMEM + MMA (40% and 59%)	PEGMA + MMA (40% and 59%)
Response time	36 h	24 h	50 min	15 min

5.3.4 Selectivity

Even though, lumogallion can form strong complexes with other ions such as gallium and indium,[47,48] such interactions do not pose a significant issue for instance in corrosion sensing as the presence of other metal ions would also contribute to the overall corrosion rate. Similarly, biologically available fractions of both Ga^{3+} and In^{3+} in human body are

only present at very low levels and therefore the determination of Al^{3+} in e.g. Alzheimer studies should not be impaired.[49] In addition, dissolved lumogallion has been reported to bind aluminium selectively even in the presence of several biologically relevant ions such as Mg^{2+}, Ca^{2+}, Zn^{2+}.[27] Herein, the selectivity of resulting copolymer was measured against above-mentioned cations as well as Na^+, K^+ and Fe^{3+} ions in order to demonstrate the potential of the synthesised copolymer for the *in vivo* and *in vitro* Al^{3+} determination. In each case, prepared lumogallion based membranes were exposed to 0.1 M of interfering ions for 24 h and then their fluorometric responses were measured. The data obtained from selectivity experiments is summarised in Figure 5.3. It is apparent that only membranes preconditioned in the Al^{3+} solution produced fluorescence response while no emission was recorded for other interfering ions. These findings demonstrate that chemically modified lumogallion retains its excellent selectivity towards Al^{3+} and can be potentially used for its determination in very complex matrixes such as cellular environment.
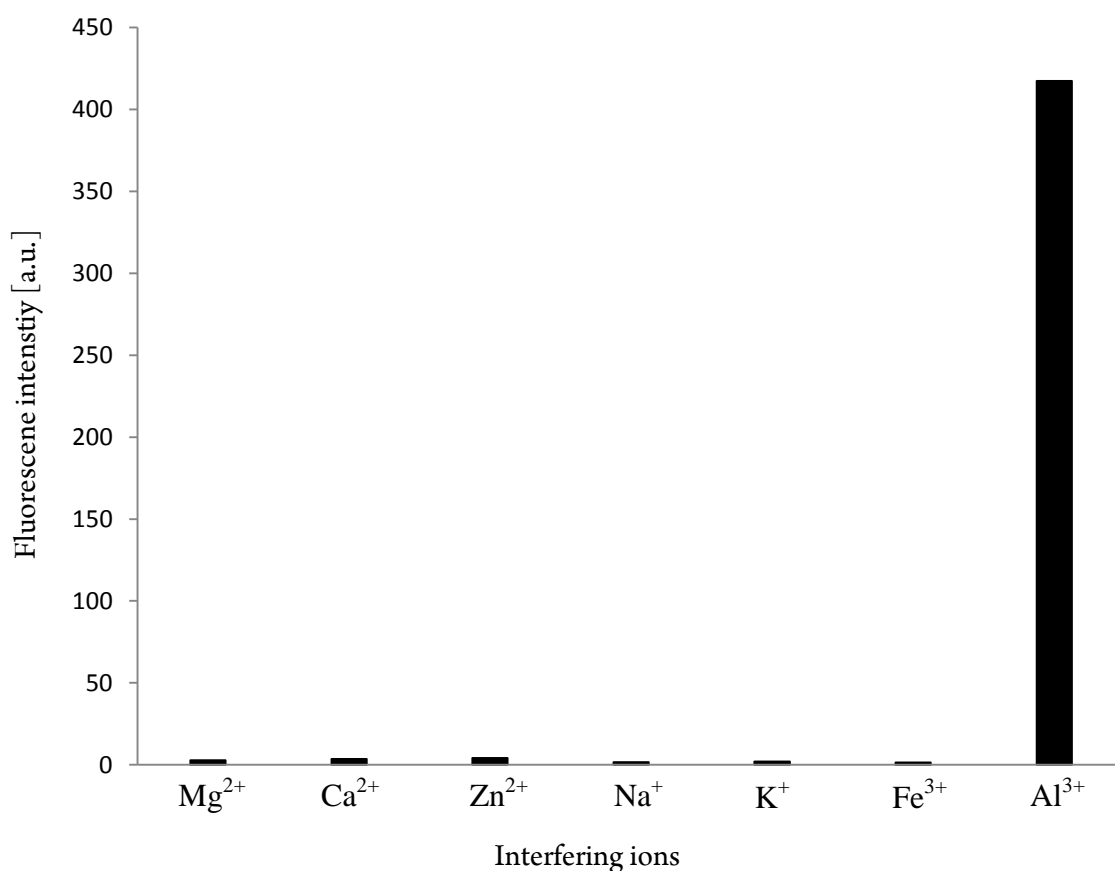
Figure 5.3 Selectivity of the proposed optical sensor for aluminium determination. Individual bars represent the fluorescence intensity recorded for various metal cations. Each polymeric membrane was placed in 1.0 x 10^{-1} M solution of interfering ions for 24 h in order to compensate for the variations in the response time between different cations. The concentration of aluminium (III) ions at which the measurements were performed was set at 1.0 x 10^{-5} M.

5.3.5 Robustness

Despite recent improvements in the sensing field that yielded a wide range of chemical sensors with excellent selectivity and sensitivity towards many analytes of interest, their overall performance has been limited to short measurements due to their poor long-term stability. This was usually associated with the leaching of membrane components from the sensing matrix into the sample solution. This phenomenon does not only limit the overall

performance of the sensor but may also result in the contamination of the analysed sample and therefore can carry serious consequences especially when medical/forensic samples are being analysed. To examine robustness of newly synthesised optical sensors, each polymeric membrane was exposed to the aqueous solutions of Al^{3+} ions (1.0×10^{-5} M) for one day, one week and two weeks respectively. After specified exposure time, fluorescence measurements of the aqueous phase (pipetted into a quartz fluorescence cuvette) were taken and the sensing membranes were placed back into the same sample solution, sealed and left until other optical measurements were performed. No fluorescence signal was recorded for the aqueous solution that was exposed to the lumogallion-based copolymer at any specified time point. Such experiments revealed that no leaching of the fluorescence dye from the sensing membrane into the sample solution occurred and therefore this demonstrates the stability of the proposed covalent attachment to the polymer backbone.

Moreover, each newly synthesised methacrylate based copolymer exhibited high mechanical stability as no loss of coating from the glass slide was observed. Another important parameter that defines durability of ion selective optodes is their stability over a wide range of pH. This is especially important if the proposed sensor is used for a wide range of applications such as biological and environmental measurements or corrosion studies. Previously reported lumogallion based sensors were only operational in the Al^{3+} solution made up in distilled water (only solvent used) as the use of buffered solution such as acetic acid/sodium acetate buffer would cause detachment of lumogallion derivative from the glass surface. This was attributed to the salt formation upon the interaction of poly allyamine hydrochloride (PAH) layer with acetic acid.[30] Such approach to simply

attach un-derivatised lumogallion to the polymer backbone (via formation of sulfonamides) was also carried out. The preparation of the following optical film was very fast (less than 30 min) and could be performed on a variety of substrates (glass or Teflon) with predefined shapes and thicknesses (this optical film was generously donated by the group of Prof Granados-Focil, Clark University, USA). This yielded a group of sensors with quick response time as the fluorescent dye was mainly present at the surface of the sensing film thus reducing the distance and consequently time required for Al^{3+} to interact with lumogallion molecules (mass diffusion). Even though, this appears to be a very attractive approach, such polymeric films were unstable in more alkaline solutions (pH > 8) due to the hydrolysis of sulfonamide bond. Therefore, there were excluded from further examination.

5.3.6 Lumogallion-copolymer based nano-particles

PEGMA-MMA-lumogallion copolymer was selected for the fabrication of fluorescent nano-beads as previous experiments in this chapter demonstrated that this copolymer exhibited the shortest response time, ultra-low detection limits and superior selectivity to Al^{3+}. The solvent displacement method used for the preparation of nano-particles comprises of two essential steps: a) a hydrophobic polymer must be dissolved in a water miscible solvent; b) spontaneous emulsification should take place upon the contact of injected polymer solution with aqueous solution. Surfactants can be also added to further stabilise the colloidal suspension. This method is particularly attractive for the preparation of optical nano-sensors as it simply relies on the injection of dissolved polymer into the aqueous sample generating stable micro/nano-spheres within few seconds.

Initially, copolymer solution in THF was injected directly into the aqueous phase instantly yielding nano-particles with average diameter of 375 ± 11 nm. In order to record the images, a small aliquot (10 µL) was deposited on a glass slide and the solution was partially dried to increase the density of the emulsion. Under these experimental conditions, it is possible that fabricated nano-particles would aggregate on the surface of the glass slide. Microscopic examination confirmed that no aggregates were formed either in the solution or on the glass slide. The nano-spheres formed from dissolving the membrane cocktail in THF are shown in Figure 5.4.
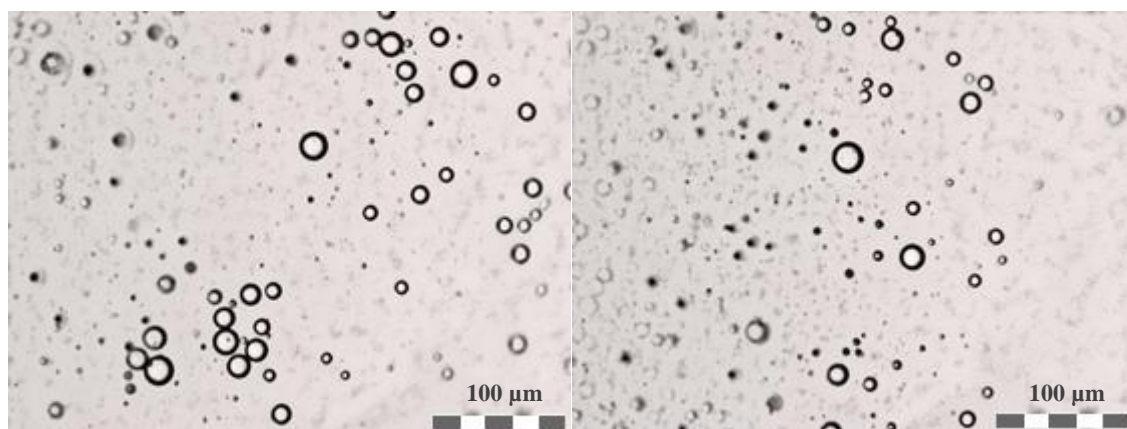

Figure 5.4 Bright field photographs of the polymeric particles fabricated via solvent displacement method from the cocktail diluted in THF. The continuous phase contains 0.02% of Brij-L23. The image was captured under x 40 magnification.

Furthermore, it has been reported that size distribution of polymeric micro/nano-particles can be controlled for instance via altering the concentration of polymer solution used for the injection or by using different organic solvents. In an attempt to fabricate nano-particles with smaller diameter, the lumogallion-based copolymer was firstly diluted in a homogenous mixture of THF and ethylene glycol (1:1 ratio) and then injected into the sample (as describe in Chapter 5 - Experimental). Note that the concentration of membrane cocktail as well as experimental conditions (for example stirring rate) were kept constant

(10 wt/vol%) therefore any changes in size of fabricated nano-beads can be attributed to the difference in solvents used for their preparation. The resulting nano-particles were significantly smaller in size (average diameter - 195 ± 11 nm) if compared to ones dissolved in THF only (Figure 5.5). This is in good agreement with findings reported in the literature showing that the nature of used solvent has indeed a strong influence on the size of micro/nano-particles. However, the primary purpose of this study was to demonstrate that the proposed copolymer could be used for the fabrication of stable nano-particles that could be potentially applied for aluminium tracing in biological/clinical samples. Nevertheless, it can be hypothesised that more thorough optimisation of experimental conditions can further yield unimodal nano-spheres with narrow size distribution.
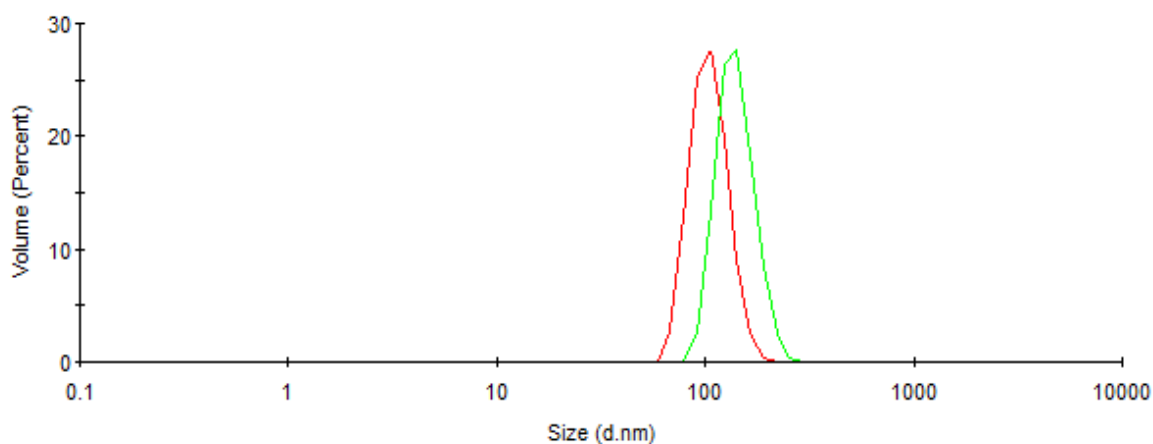
Figure 5.5 Particle size distribution of nano-particles synthesised via solvent displacement methods prepared from 1:1 THF and ethylene glycol solution (red) and from the dissolved copolymer in THF (green).

Since the nano-particles fabricated from the copolymer solution in 1:1 mixture of THF and ethylene glycol exhibited on average smaller diameter, they were subjected for further examination using fluorescence microscopy. This is demonstrated in Figure 5.6. It is

instantly apparent that generated lumogallion based nano-spheres in the absence of aluminium (III) ions exhibit none/very faint background fluorescence that can be only recorded if the exposure time exceeds 15000 ms. This is important if precise fluorescence intensity measurements are required for instance either by using microspectrophotometer or via the extraction of intensities of red, green and blue (RGB) channels from the image.[50] The latter has been recently utilised in manufacturing of portable sensing devices for point of care diagnostics.[51–54]

Figure 5.6 Bright field (left) and fluorescence images (centre) and (right) of nano-particles fabricated from the copolymer dissolved in THF and ethylene glycol. Fluorescence photographs were obtained using 510 nm emission and 470 – 495 nm excitation filters with 1000 ms (b) and 15000 ms (c) exposure time. All images were captured under x 40 magnification.

To further assess the functionality of synthesised nano-particles for aluminium detection, the same nano-beads were exposed to 1.0×10^{-6} M solution of aluminium nitrate and analysed in both bright field and fluorescence modes. There were no observed changes in the appearance of nano-spheres exposed to aluminium ions as to particles that were stored in ultra-pure water and visualised in bright field mode (Figure 5.4, and Figure 5.7 left). However, as soon as the sample was analysed in the fluorescence mode, characteristic orange emission originating from the nano-particles was observed (Figure 5.7 right). This

confirms that the proposed lumogallion-based copolymer can be used for the preparation of aluminium selective fluorescence based nano-particles.
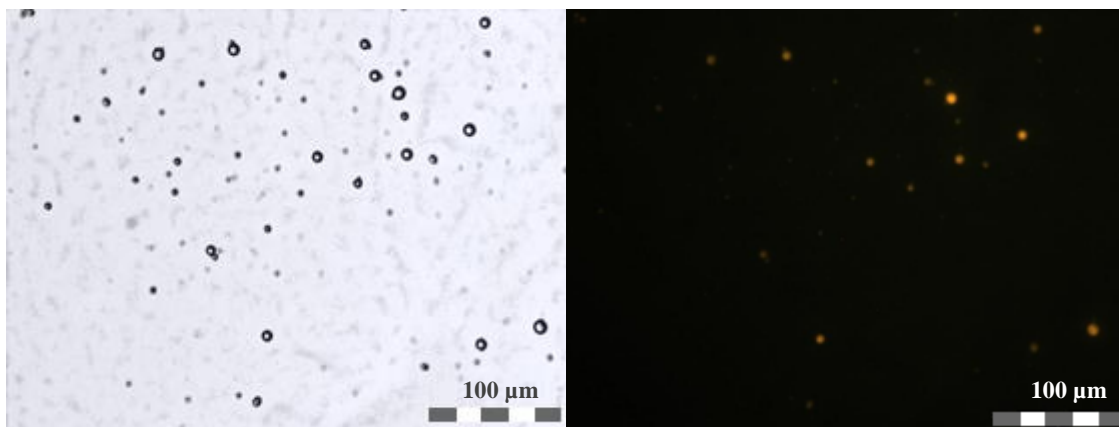

Figure 5.7 Bright field photograph (left) and fluorescence image (right) of the polymeric particles incubated for 15 min in 1.0 x 10^{-6} M solution of aluminium nitrate (exposure time 1000 ms; x 40 magnification).

5.3.7 Single element ISEs

Recent studies demonstrated that fluorescent dyes if incorporated into the polymeric matrix doped with lipophilic ionic sites could serve a dual function as an optical or potentiometric sensor depending on the selected detection mode. However, note that these two operational modes are described by different theoretical considerations. A change in optical signal is typically induced by the concentration change of a component within a thin polymeric film/nano-sphere. Moreover, to fulfil electroneutrality requirement both primary ion and its counter-ion have to be extracted from aqueous sample into the hydrophobic phase. Ideally, a complexation reaction of at least one of the two extracted ions should result in an optical response for instance due to changes in fluorescence or absorbance. On the contrary, potentiometric measurements rely on the change in the phase-boundary potential (see Chapter 1) where the concentration of ionophore and its complexes within the ion selective

membrane is kept constant providing that the electrode is exhibiting Nernstian behaviour. Therefore, it can be assumed that if lipophilic ionic sites were incorporated into the lumogallion-based copolymer, the resulting sensor could serve as ion selective electrode for aluminium (III) determination due to the increasing ion-permselectivity of a membrane. For that purpose a single piece lumogallion based copolymer was dissolved together with varying amounts of lipophilic salts, as described in the experimental part of this chapter, and its potentiometric response against changing concentrations of Al^{3+} was recorded.

On each occasion, tested ion selective membranes did not produce any response upon addition of Al^{3+} ions into the sample solution. Such behaviour has been already reported in the literature where the stability constant of the ionophore-ion complex was found to be too high to allow reversible ion exchange. Therefore, it could be hypothesised that once aluminium (III) ions enter the membrane during equilibration (conditioning) step, very strong lumogallion-Al^{3+} complexes are formed, simultaneously facilitating extraction of the ion of opposite charge from the aqueous phase. This would result in the loss of membrane permselectivity (Donnan exclusion failure) rendering this sensor unsuitable for potentiometric measurements. However, the binding constant reported for dissolved and un-derivatised lumogallion-Al^{3+} complex (log K = 7.76)[55] lies within the normal range of those reported for various other ionophores used for the preparation of ISEs indicating that some other mechanism could be potentially responsible for the limited response of a proposed sensor.[56–58] Moreover, limited response of ionophore based ISEs could be caused by the imbalance between covalently attached ionophore and incorporated ionic sites thus decreasing the overall permselectivity of such membrane.[59] This hypothesis was investigated by making several ion selective membranes with varying concentrations of

ionic sites as recommended for ISEs based on neutral ionophores with 1:1 binding stoichiometry.[60] Again, in each case the proposed ISEs were irresponsive to changing concentrations of Al^{3+} ions in the sample solution. Additionally, it can be hypothesised that relatively polar character of the ion selective membrane facilitates water uptake causing swelling of the membrane. This could subsequently facilitate leaching of the ionic sites from the membrane into the sample solution thus reducing the permselectivity of proposed ISEs. This could be potentially investigated either by means of impedance spectroscopy[61] or by doping the membrane with optically active species, which diffusion can be monitored for instance using spectroscopic techniques (e.g. their concentration in aqueous solution). However, this has not been examined in this study and further attempts need to be undertaken to validate the proposed hypothesis. Note that during all experiments an optical response could be recorded thus indicating the formation of lumogallion-Al^{3+} complex in the membrane bulk. Even though, fabricated ISEs based on the presence of copolymerised lumogallion were not suitable for potentiometric analysis, the ability to record the optical response of such sensors demonstrated their potential for direct measurements of Al^{3+} in aqueous samples.

5.4 Conclusions

Quantitative analysis of the free ion concentration within a biological sample is highly critical to the advancement of accurate disease screening and personalised medicine. Moreover, there is an ongoing demand for the development of precise analytical tools for environmental monitoring of metal ions such as Al^{3+}, Pb^{2+} and Hg^{2+}. Therefore, a single piece, colour changeable, fluorescence polymer membrane based sensor has been proposed for the highly selective and sensitive determination of aluminium (III) ions in aqueous environments. The sensing layer of the probe consists of a lumogallion derivative that is covalently attached to the methacrylate based polymer backbone. This fully eliminates the diffusion of the fluorophore from the sensing membrane into the aqueous solution that previously limited the development of optodes based on this relatively hydrophilic molecule. Such proposed optical sensors also exhibited excellent robustness over the period of two weeks as no leaching of the fluorophore was observed. The same optical film upon the contact with Al^{3+} ions produces a specific emission peak at 585 nm even for aluminium concentrations as low as 100 pM. Moreover, the performance of the resulting polymer was not inhibited by the presence of other interfering metal cations showing excellent selectivity towards Al^{3+}. These findings demonstrate an excellent potential of self-plasticised copolymers as sensing materials for the development of optical sensors that can be directly used for *in situ* detection of biologically relevant ions.

References

(1) Dash, N.; Malakar, A.; Kumar, M.; Mandal, B. B.; Krishnamoorthy, G. *Sens. Actuators B Chem.* **2014**, *202*, 1154–1163.

(2) Sui, N.; Wang, L.; Yan, T.; Liu, F.; Sui, J.; Jiang, Y.; Wan, J.; Liu, M.; Yu, W. W. *Sens. Actuators B Chem.* **2014**, *202*, 1148–1153.

(3) Choi, Y. W.; Park, G. J.; Na, Y. J.; Jo, H. Y.; Lee, S. A.; You, G. R.; Kim, C. *Sens. Actuators B Chem.* **2014**, *194*, 343–352.

(4) Long, F.; Zhu, A.; Shi, H.; Wang, H.; Liu, J. *Sci. Rep.* **2013**, *3*.

(5) McComb, J. Q.; Rogers, C.; Han, F. X.; Tchounwou, P. B. *Water. Air. Soil Pollut.* **2014**, *225* (12).

(6) Chambers, B. D.; Taylor, S. R. *Corros. Sci.* **2007**, *49* (3), 1584–1596.

(7) House, E.; Collingwood, J.; Khan, A.; Korchazkina, O.; Berthon, G.; Exley, C. *J. Alzheimers Dis. JAD* **2004**, *6* (3), 291–301.

(8) Tomljenovic, L. *J. Alzheimers Dis. JAD* **2011**, *23* (4), 567–598.

(9) Faller, P.; Hureau, C.; Berthoumieu, O. *Inorg. Chem.* **2013**, *52* (21), 12193–12206.

(10) McAdam, G. *Struct. Health Monit.* **2005**, *4* (1), 47–56.

(11) Qifu, M. A.; Rengel, Z.; Kuo, J. *Ann. Bot.* **2002**, *89* (2), 241–244.

(12) Horst, W. J.; Schmohl, N.; Kollmeier, M.; Balu ka, F. ek; Sivaguru, M. *Plant Soil* *215* (2), 163–174.

(13) Carter, K. P.; Young, A. M.; Palmer, A. E. *Chem. Rev.* **2014**, *114* (8), 4564–4601.

(14) Ahmed, M. J.; Hossan, J. *Talanta* **1995**, *42* (8), 1135–1142.

(15) Eticha, D. *J. Exp. Bot.* **2005**, *56* (415), 1351–1357.

(16) Gupta, V.; Jain, A.; Maheshwari, G. *Talanta* **2007**, *72* (4), 1469–1473.

(17) Yao, S.-Z.; Chen, X.-M.; Nie, L.-H. *Microchim. Acta 100* (5), 299–304.

(18) Lian, H.; Kang, Y.; Bi, S.; Yasin, A.; Shao, D.; Chen, Y.; Dai, L.; Tian, L. *Anal. Bioanal. Chem.* **2003**, *376* (4), 542–548.

(19) Vitorello, V. A.; Haug, A. *Plant Sci.* **1997**, *122* (1), 35–42.

(20) Guha, S.; Lohar, S.; Sahana, A.; Banerjee, A.; Safin, D. A.; Babashkina, M. G.; Mitoraj, M. P.; Bolte, M.; Garcia, Y.; Mukhopadhyay, S. K.; Das, D. *Dalton Trans.* **2013**, *42* (28), 10198.

(21) Singh, V. P.; Tiwari, K.; Mishra, M.; Srivastava, N.; Saha, S. *Sens. Actuators B Chem.* **2013**, *182*, 546–554.

(22) Tiwari, K.; Mishra, M.; Singh, V. P. *RSC Adv.* **2013**, *3* (30), 12124.

(23) Mehta, V. N.; Singhal, R. K.; Kailasa, S. K. *RSC Adv* **2015**, *5* (42), 33468–33477.

(24) Hydes, D. J.; Liss, P. S. *The Analyst* **1976**, *101* (1209), 922.

(25) Kalogria, E.; Varvaresou, A.; Papageorgiou, S.; Protopapa, E.; Tsaknis, I.; Matikas, A.; Panderi, I. *Chromatographia* **2014**, *77* (19–20), 1275–1281.

(26) Kataoka, T.; Mori, M.; Nakanishi, T. M.; Matsumoto, S.; Uchiumi, A. *J. Plant Res.* *110* (3), 305–309.

(27) Mold, M.; Eriksson, H.; Siesjö, P.; Darabi, A.; Shardlow, E.; Exley, C. *Sci. Rep.* **2014**, *4*, 6287.

(28) Wu, J.; Chao Yan Zhou; Chi, H.; Ming Keong Wong; Hian Kee Lee; Her Yam Ong; Choon Nam Ong. *J. Chromatogr. B. Biomed. Sci. App.* **1995**, *663* (2), 247–253.

(29) Ren, J. L.; Zhang, J.; Luo, J. Q.; Pei, X. K.; Jiang, Z. X. *The Analyst* **2001**, *126* (5), 698–702.

(30) Warren-Smith, S. C.; Heng, S.; Ebendorff-Heidepriem, H.; Abell, A. D.; Monro, T. M. *Langmuir* **2011**, *27* (9), 5680–5685.

(31)   Basabe-Desmonts, L.; Reinhoudt, D. N.; Crego-Calama, M. *Chem. Soc. Rev.* **2007**, *36* (6), 993.

(32)   Badini, G. E.; Grattan, K. T. V.; Tseung, A. C. C. *The Analyst* **1995**, *120* (4), 1025.

(33)   Gründler, P. *Chemical sensors an introduction for scientists and engineers*; Springer: Berlin; London, 2007.

(34)   Ayadim, M.; Habib Jiwan, J. L.; De Silva, A. P.; Soumillion, J. P. *Tetrahedron Lett.* **1996**, *37* (39), 7039–7042.

(35)   Klajn, R. *Chem Soc Rev* **2014**, *43* (1), 148–184.

(36)   Robin, M. P.; O'Reilly, R. K. *Polym. Int.* **2015**, *64* (2), 174–182.

(37)   Matyjaszewski, K. *Macromolecules* **2012**, *45* (10), 4015–4039.

(38)   Moad, G.; Rizzardo, E.; Thang, S. H. *Aust. J. Chem.* **2012**, *65* (8), 985.

(39)   Sutthasupa, S.; Shiotsuki, M.; Sanda, F. *Polym. J.* **2010**, *42* (12), 905–915.

(40)   Heng, L. Y.; Hall, E. A. H. *Anal. Chim. Acta* **2000**, *403* (1–2), 77–89.

(41)   Mendecki, L.; Fayose, T.; Stockmal, K. A.; Wei, J.; Granados-Focil, S.; McGraw, C. M.; Radu, A. *Anal. Chem.* **2015**, *87* (15), 7515–7518.

(42)   Bychkova, V.; Shvarev, A. *Anal. Chem.* **2009**, *81* (6), 2325–2331.

(43)   Heng, L. Y.; Toth, K.; Hall, E. A. H. *Talanta* **2004**, *63* (1), 73–87.

(44)   Yazdanbakhsh, M. R.; Mohammadi, A. *J. Mol. Liq.* **2009**, *148* (1), 35–39.

(45)   Zhang, L.; Cole, J. M.; Liu, X. *J. Phys. Chem. C* **2013**, *117* (49), 26316–26323.

(46)   Al-Kindy, S.; Badía, R.; Díaz-García, M. E. *Anal. Lett.* **2002**, *35* (11), 1763–1774.

(47)   Abramenkova, O. I.; Amelin, V. G.; Aleshin, N. S.; Korolev, D. S. *J. Anal. Chem.* **2011**, *66* (12), 1212–1216.

(48)   Carroll, M. K.; Bright, F. V.; Hieftje, G. M. *Anal. Chem.* **1989**, *61* (15), 1768–1772.

(49)   André, J. .; Mäcke, H. . *J. Inorg. Biochem.* **2003**, *97* (4), 315–323.

(50)   Waters, J. C. *J. Cell Biol.* **2009**, *185* (7), 1135–1148.

(51)   Shen, L.; Hagen, J. A.; Papautsky, I. *Lab. Chip* **2012**, *12* (21), 4240.

(52)   Barbosa, A. I.; Gehlot, P.; Sidapra, K.; Edwards, A. D.; Reis, N. M. *Biosens. Bioelectron.* **2015**, *70*, 5–14.

(53)   Wasson, A.; Bischof, L.; Zwart, A.; Watt, M. *J. Exp. Bot.* **2016**, *67* (4), 1033–1043.

(54)   de Villiers, C. A.; Lapsley, M. C.; Hall, E. A. H. *The Analyst* **2015**, *140* (8), 2644–2655.

(55)   Klug, B.; Specht, A.; Horst, W. J. *J. Exp. Bot.* **2011**, *62* (15), 5453–5462.

(56)   Shultz, M. M.; Stefanova, O. K.; Mokrov, S. B.; Mikhelson, K. N. *Anal. Chem.* **2002**, *74* (3), 510–517.

(57)   Miyake, M.; Chen, L. D.; Pozzi, G.; Bühlmann, P. *Anal. Chem.* **2012**, *84* (2), 1104–1111.

(58)   Boswell, P. G.; Szíjjártó, C.; Jurisch, M.; Gladysz, J. A.; Rábai, J.; Bühlmann, P. *Anal. Chem.* **2008**, *80* (6), 2084–2090.

(59)   Bakker, E.; Bühlmann, P.; Pretsch, E. *Chem. Rev.* **1997**, *97* (8), 3083–3132.

(60)   Bakker, E. *Talanta* **2004**, *63* (1), 3–20.

(61)   Veder, J.-P.; Patel, K.; Sohail, M.; Jiang, S. P.; James, M.; De Marco, R. *Electroanalysis* **2012**, *24* (1), 140–145.

CHAPTER 6   Concluding remarks

Since the implementation of ionophore as an ion-binding agent in ISEs, almost five decades ago, the research in this area has been predominantly focused on the design of new ion ligands and their application in polymeric membranes. Only recently, many analytical chemists diverted their attention towards gaining a better understanding of response mechanisms of ISEs. This for instance resulted in the discovery of transmembrane ion fluxes and thus opened new avenues for the improvements in ISEs.

Therefore, it was quickly realised that the response characteristics of ISEs such as selectivity, detection limits and long term stability can be significantly improved by the optimisation of traditionally employed sensing methodologies as well as by the use of novel materials such as new polymers and plasticisers or novel electrode designs. Despite significant progress made in ionophore-based sensors, their application in long term analysis and *in field* measurements has been limited. This calls for further improvements in the field to produce robust and durable sensing devices suitable for ion sensing in biologically and environmentally important samples.

Herein, two different avenues that could lead to significant advancements in ion selective electrodes and optical sensors were explored. Firstly, it was demonstrated that robust and ultra-sensitive ISEs can be produced by a simple alteration of the sensor's conditioning protocol. This resulted in the reduction of ion fluxes across the membrane interface

consequently lowering the LDLs of carbonate-ISEs to picomolar levels. Furthermore, it was shown that novel materials - RTILs when used as plasticisers could modify the properties (e.g. selectivity) of polymer-based membranes. Such membranes exhibited strong deviations from the well-established Hofmeister series indicating a multitude of applications for these ion-exchanging systems. The concept of using ILs as sensing materials was further expanded and utilised to develop a very simple one component sensing membranes for direct measurements of iodide in human urine samples. For this purpose, 1,2,3-triazole based IL with iodide serving as counter-ion was covalently attached to the polymer backbone to yield self-plasticised ISEs. Moreover, the need for conditioning was fully eliminated due to the inherent presence of iodide within the copolymer matrix thus significantly shortening the overall preparation time of ISEs. Similarly, single element optical sensing device for aluminium (III) ion detection was designed by attaching the water-soluble lumogallion molecule to the methacrylate backbone. This eliminated the diffusion of the fluorescent dye from the polymeric film into the aqueous phase significantly improving the robustness of optical sensors. Additionally, the proposed system could be readily miniaturised demonstrating great potential for clinical *in situ* measurements.

The results of this work provided more detailed information on how the properties of ion selective membranes and optical sensors can be altered by using new methodologies or novel materials such as ionic liquids and whether their implementation would benefit in achieving more sensitive, selective and cost effective sensors.

Appendix   Ethical approval letterV

Ref: ERP369

16th March 2016

Mr Lukasz Mendecki
School of Physical and Geographical Sciences
Lennard-Jones Building
Keele University

Dear Lukasz,

Re: Using ion-selective electrodes for measurement of iodide in human urine

Thank you for submitting your revised application for review.

I am pleased to inform you that your application has been approved by the Ethics Review Panel. The following documents have been reviewed and approved by the panel as follows:

Document(s)	Version Number	Date
Example Recruitment Poster	2	16-03-2016
Example Recruitment Email	2	16-03-2016
Invitation/Information Sheet	2	16-03-2016
Consent Form	1	28-12-2015

If the fieldwork goes beyond the date stated in your application (30th January 2017), you must notify the Ethical Review Panel via the ERP administrator at research.erps@keele.ac.uk stating ERP3 in the subject line of the e-mail.
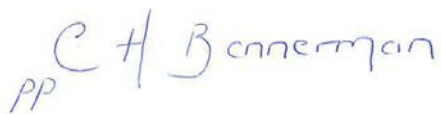
If there are any other amendments to your study you must submit an 'application to amend study' form to the ERP administrator stating ERP3 in the subject line of the e-mail. This form is available via http://www.keele.ac.uk/researchsupport/researchethics/.

If you have any queries, please do not hesitate to contact me via the ERP administrator on research.erps@keele.ac.uk stating ERP3 in the subject line of the e-mail.

Yours sincerely

pp C H Bannerman

Mrs Val Ball
Chair – Ethical Review Panel

CC   RI Manager
         Supervisor